NASA CR-66728-2

Master
[illegible]

FINAL SUMMARY REPORT

STUDY OF A SOFT LANDER/SUPPORT MODULE FOR MARS MISSIONS

VOLUME II - SUBSYSTEMS STUDIES

By Ramond S. Wiltshire, Michael Kardos, Melvin W. Kuethe,
Ralph H. Dergance, Roger T. Schappell, Stephen G. Homic,
Dean A. Schneebeck, and Theodore F. Morey

Distribution of this report is provided in the interest of information exchange. Responsibility for the contents resides in the author or organization that prepared it.

Prepared under Contract No. NAS1-7976 by
MARTIN MARIETTA CORPORATION
Denver, Colorado

for

NATIONAL AERONAUTICS AND SPACE ADMINISTRATION

FOREWORD

This Final Summary Report for the Soft Lander/ Support Module study, a supplement to the "Study of Direct Versus Orbital Entry for Mars Missions" (NASA Contract NAS1-7976), is provided in accordance with Part III A.6 of the contract schedule as amended. This Final Summary Report is in three volumes as follows:

NASA CR-66728-1 Volume I, Summary;

NASA CR-66728-2 Volume II, Subsystem Studies;

NASA CR-66728-3 Volume III, Appendixes.

CONTENTS

Page

FOREWORD ii
CONTENTS . . . . iii thru vii
SUMMARY 1
SYMBOLS AND ABBREVIATIONS 2
SUBSYSTEMS 4
1. Science Subsystem Studies 4
2. Structures and Mechanisms 73
3. Propulsion 83
4. Guidance and Control System 99
5. Telecommunications 139
6. Power and Pyrotechnic Subsystems 173
7. Thermal Control 190
REFERENCES . . . . 217 and 218

Figure
1 Soil Sampler Tentative Design 12
2 Soil Sampler Details 13
3 Soil Sampler with Three Degrees of Freedom . . . 16
4 Subsurface Probe 20
5 Penetration vs Force for Loose Soil 24
6 Penetration vs Force for Compacted Soil 25
7 Laboratory Apparatus for Penetration Tests . . . 26
8 Thermal Conductivity and Diffusivity vs Soil Moisture Content 28
9 Variation of Thermal Conductivity with Moisture Content 29
10 Variations of Thermal Conductivity with Dry Density 30
11 Diagram of Thermal Conductivity for Sandy Soils 31
12 Variations of Specific Heat with Mean Temperature 32
13 Relationship of Specific Heat of Soil-Water Mixtures and Moisture Content 33
14 Soil Temperature vs Time 34
15 Gulliver IV, *In Situ* Model 42
16 Support Equipment for *In Situ* Gulliver IV . . . 43
17 Gulliver IV *In Situ* Single Chamber Module . . . 44

18 Gulliver IV Deployment 45
19 Development Program Flow Diagram for Gulliver IV Qualification 51
20 Multiple Experiment Life Detection System . . . 52
21 $C^{14}O_2$ Evolved by Chlorella Pyrenoidosa in Response to Light and Dark Growth Cycles 58
22 Development Program Flow Diagram for MELDS Qualification 61
23 Radiation Environment for Biology Instrument . . 63
24 Isotope Heaters 64
25 Power Profile, Science Subsystem 71
26 Integration Sketch, Autonomous Capsule/Support Module (All Sterilized) 74
27 All-Sterilized Autonomous Capsule and Support Module 75
28 Six Major Assemblies and Associated Subsystems . 77
29 Autonomous Capsule/Support Module (Alternative Configuration) Configuration Modes 78
30 Walter Kidde 300-lb_f Monopropellant Engine . . . 85
31 Minuteman III TCV Valve 87
32 Mars Lander Valve 88
33 Flow Rate vs Pressure Drop 89
34 Valve Bode Plot 91
35 Midcourse/Deflection/ACS Engine 92
36 Propulsion Subsystem Preferred Design 94
37 Cruise Attitude Control System 95
38 Support Module Spin Rocket 97
39 Throttle Valve/Engine Test Program 98
40 Guidance and Control System Block Diagram . . . 99
41 Errors Due to Tipoff Rate and Spinup 104
42 Denutation of Support Module with Pendulum Damper from Time = 6 to 100 sec 105
43 Pendulum Damper Schematic 106
44 Terminal Descent Axial Control Plan 109
45 Guidance and Control Hardware Configuration . . 112
46 Sun Sensor Assemblies 113
47 LM Radar Electronics and Antenna Assembly . . . 128
48 LM Radar Antenna Assembly 129
49 Recommended Beam Pattern for the LM Radar . . . 132
50 VDA Inputs and Outputs 134
51 Cone Angle and Communication Range 140
52 Low-Gain Antenna Radiation Pattern 142
53 Telecommunications Performance Predictions, Interplanetary Cruise 144
54 Nominal Entry Geometry 158

55 Capsule Antenna Aspect Angle Dispersions 159
56 Support Module Antenna Aspect Angle Dispersions 160
57 Communication Range Dispersions 161
58 Definition of Angle Convention and Trajectory Parameters 162
59 Nominal Communication Profile 164
60 Communication Profile (Dispersion from Nominal) 165
61 Telecommunication Block Diagram 169
62 Power Subsystem Block Diagram 174
63 Cruise Solar Array Output 176
64 Support Module Load Profile 177
65 Lander Power Profile, Encounter through Landing + 3 Days 179
66 Extended Mission Power Profile and Solar Array Power 182
67 Lander Solar Panel Performance 183
68 Available Battery Energy Profile 185
69 Simplified Block Diagram, Lander Pyrotechnic Subsystem 188
70 Equipment Heat Output after Landing 192
71 Cruise Mode Thermal Control System 194
72 Capsule Postseparation, Thermal Control System . 196
73 Support Module Postseparation, Thermal Control System 198
74 Mars Surface Thermal Control System 199
75 Capsule Nodal Diagram 201
76 Capsule Transient Temperatures 204
77 Support Module Nodal Diagram 207
78 Support Module Transient Temperatures 209
79 Lander Temperature, Hot Environment 210
80 Thermal Switch 213
81 Sterilized Support Module Thermal Control . . . 216

Table

1 Percent Water on a Oven Dry Basis under Various Conditions 36
2 The Resistance (Ohms) of Nylon Blocks Equilibrated above Water at 20°C, Wetted and then Dried at 20 mm Hg 37
3 Resistance (Ohms) of Nylon Blocks Imbedded in Wet Soil Material at 16 mm Hg 37
4 Resistance (Ohms) of LiCℓ Treated Nylon Blocks Air Dry, at 100% Relative Humidity, and in Air Dry Kaolinite and at 20 mm Hg 38

5 Resistance (Ohms) of Mg or Li Montmorillonite Treated Blocks at 100 Relative Humidity and in Air Dry Kaolinite at 20 mm Hg 39
6 Resistance (Ohms) of Mg or Li Montmorillonite Impregnated Nylon Blocks at 100% Relative Humidity and in Kaolinite Initially Dried at 16 mm Hg 39
7 Resistance (Ohms) of Mg or Li Montmorillonite Impregnated Nylon Blocks from Table 6 Place Above Water 39
8 Reistance (Ohms) of Mg or Li Montmorillonite Impregnated Nylon Blocks Equilibrated at 100% Relative Humidity and Place in Kaolinite Dried at 105°C in a Vessel at 16 mm Hg Pressure . . . 39
9 Resistance (Ohms) of Mg or Li Montmorillonite Impregnated Nylon Blocks Equilibrated at 100% Relative Humidity and Placed in Vessel at 10 mm Hg Pressure 39
10 Gulliver IV Engineering and Science Data (Feasibility Model) 46
11 Gulliver IV Operational Sequence 48
12 MELDS Engineering and Science Data 53
13 MELDS Operational Sequence (after Landing on Mars) 54
14 Isotope Heater Radiation Effects 65
15 Science Package Radiation Levels 66
16 Entry Science Data Return 68
17 Surface Science Data Collection 69
18 Engine Manufacturer Survey 83
19 Comparison of Three-Engine and Four-Engine Configurations 84
20 Pressure Drop and Flow Rate 86
21 System Weights 90
22 Guidance and Control Performance Requirements . 100
23 Guidance and Control System Component Sources . 110
24 Canopus Tracker Performance Summary 115
25 IMU Requirements 117
26 Gyroscope Comparison 119
27 Candidate Accelerometers 120
28 Candidate Digital Computers 123
29 AMR-1 Radar Altimeter Characteristics 124
30 Honeywell Micro-Min Radar Altimeter 126
31 Westinghouse Altimeter Parameters 127
32 LM Radar Specified Accuracies 130
33 Recommended LM Radar Modifications 131

FINAL SUMMARY REPORT

STUDY OF A SOFT LANDER/SUPPORT MODULE FOR MARS MISSION

VOLUME II - SUBSYSTEM STUDIES

By Ramond S. Wiltshire, Michael Kardos, Melvin W. Kuethe, Ralph H. Dergance, Roger T. Schappell, Stephen G. Homic, Dean A. Schneebeck, and Theodore F. Morey

SUMMARY

This report presents the results of all the subsystem trade studies and analyses performed during the study. The alternative configuration effect, where applicable, is discussed.

The science section describes sample acquisition, subsurface temperature and moisture probe, moisture detection, biology instrumentation, and radioisotope heater environmental effects.

The totally sterilized soft lander/support module configuration is discussed in the structures and mechanisms section. The major differences between this and the preferred configuration results from the separation of both the forward and aft portions of the sterilization canister by the time of trans-Mars injection.

Walter Kidde engine and the LTV valve is discussed in the propulsion section. All the propulsion components and their parameters are presented.

The justification of the suggested lunar module (LM) radar changes is given in the guidance and control section. Additional data are provided on the applicability of current components in the guidance and control subsystem.

Performance predictions for each of the links is given in the telecommunications section. The data return under both adverse and favorable conditions is shown. A single telemetry system has been selected to perform all the telemetry processing and formatting functions required during all mission phases.

The power and pyrotechnic section provides the total power requirements for each phase of the mission and a description of the hardware implementation.

The final section presents the thermal control computer program and the temperature results it provided. The environments for each mission phase are given and the thermal control system performance shown.

SYMBOLS AND ABBREVIATIONS

ACS	attitude control system
AMR-1	high-altitude radar altimeter
AMR-2	low-altitude radar altimeter
au	astronomical units
B_E	entry ballistic coefficient, M/C_DA, slugs/foot^2
bps	bits per second
CST	combined system test
C_3	Earth departure energy, (kilometers/second)^2
DAU	data automation unit
DLA	declination of departure asymptote, degrees
DSIF	Deep Space Instrumentation Facility
DSS	Deep Space Station
FSK	frequency shift keying
G&C	guidance and control
GC-MS	gas chromatograph - mass spectrometer
h_P	periapsis altitude, kilometers
IMU	inertial measurement unit
LM	Lunar Module
ODP	orbit determination period
PCM	pulse code modulation
PSK	phase shift heying
R&D	research and development

S/C	spacecraft
TDLR	terminal descent and landing radar
T/M	telemetry
TWTA	traveling wave tube amplifier
VDA	Valve drive amplifiers
V_E	entry velocity, kilometers/second
V_{HE}	Mars approach energy, kilometers/second
α	absorptivity
α_c	lander antenna aspect angle, degrees
$\alpha_{S/M}$	relay antenna aspect angle, degrees
ΔV	velocity increment, meters/second
γ_E	inertial entry flightpath angle, degrees
ϵ	emissivity
σ	standard deviation
τ_{EJ}	deflection angle, degrees

SUBSYSTEMS

1. SCIENCE SUBSYSTEM STUDIES

The science subsystem design activity reported in this volume, covers five main areas. These are: a study of the soil sampling; the subsurface probe; direct biology; environmental considerations; and science data return.

The soil sampling study and portions of the subsurface probe study consist principally of work conducted for Martin Marietta by Dr. Ronald F. Scott on a consulting basis. Dr. Scott is a member of the faculty at the California Institute of Technology and was Principle Investigator on the Surveyor lunar soil mechanics experiment. The objectives of the soil sampling study were to develop the reasoning on which to base the design of a Mars soil sampler, to produce a tentative concept for such a device, to assess the design features, and to suggest a sequence of steps leading to development of a sampling device suitable for a Mars lander. The suggested development sequence was to be based to the greatest extent possible on experience gained from the Surveyor program.

The objectives of the subsurface probe study were to identify and evaluate the requirements and constraints for a probe to measure the Mars subsurface soil temperature and moisture and appraise the probe.

The moisture sensor portion of the subsurface probe study consists principally of work conducted for Martin Marietta by Dr. A. E. Erickson on a consulting basis. Dr. Erickson is a member of the faculty at Michigan State University and an internationally recognized expert in the area of agricultural soil sciences. He was assisted by Dr. M. M. Mortland, a faculty member at Michigan State University. The objectives of this study were to evaluate the detection threshold of several widely used soil moisture cells and assess the feasibility of using these devices to detect moisture in the soil around a Mars lander.

The biology study consists of work conducted for Martin Marietta by Dr. Gilbert V. Levin on a consulting basis. Dr. Levin has been involved with the development of instrumentation for planetary direct biology measurements since the beginning of interest in this field. He is codeveloper of the Gulliver life detection experiment and has developed and field-tested several Gulliver breadboard instruments during his association with Hazleton Laboratories, Inc. Dr. Levin is presently associated with Biospherics, Inc. where he is involved with hardware development under NASA contract for an advanced multicell detection instrument.

The work reported here was carried out to support an estimate of the cost for developing and producing qualified instruments for direct biology experiments on Mars. Selecting the level of instrument complexity and planning the flow of development effort were governed by the requirement that hardware be available for Titan/Mars '73 mission (ref. 1).

Two types of instruments were considered, encompassing the range of sizes recommended by the Space Science Board as a result of their study of planetary exploration in the 1968-75 time period (ref. 2). For one end of the range a simple, low-weight instrument weighing less than 1 lb was selected. The specific device chosen was the Gulliver IV metabolism detector. At the other end of the size range a complex, higher-weight instrument (10 lb) was considered. For study purposes a conceptual instrument capable of detecting turbidity, fluorimetry, and metabolism effects (Wolftrap, Multivator, and Gulliver experiments, respectively) was used. These instrument selections offer a realistic basis for cost estimating since a history of breadboard hardware and operational testing exists for Wolftrap, Multivator, and Gulliver devices.

Soil Sampling

Nature of the Martian Surface.- The report on the Mariner Mars 1964 Project by Leighton et al. (ref. 3) discusses the possible nature of the Martian surface on the basis of previous earth-based observations and the photographic results of the Mariner flyby. The photographs taken by the Mariner IV spacecraft showed a cratered Martian surface, in which the crater density per unit area was only slightly less than that observed in lunar highland areas. However, the craters on Mars appeared more subdued than on the moon and relatively few sharply-outlined craters (usually interpreted as "fresh-appearing") were observed. The authors interpreted this to indicate that surface-modifying processes at work on Mars are relatively more effective than modifying processes on the moon, but less effective than on the earth.

Although direct evidence is lacking, it is assumed that the craters on Mars, as on the moon, are formed by meteorite impacts. Since it is estimated that the meteoroidal flux at Mars is from 4 to 25 times that at the moon, the lower incidence of craters observed on Mars reinforces the inference that crater modification and subsequent elimination have occurred at a faster rate on Mars than on the moon.

With meteorite impact as the crater-forming agent, a Mars surface model is suggested analogous to that observed by the Surveyor spacecraft (ref. 4) on the moon. The surface to a depth of at least 10 m, but varying from place to place, consists of a granular material with a wide range of sizes, but possessing a substantial proportion (possibly greater than 50%) of fine material in the tens of microns size range. On the moon (ref. 4) the surface soil possesses a small but effective amount of cohesion between the particles and Scott and Roberson have interpreted this as being possibly due to the presence of Van DerWaals forces between the relatively clean grains. The existence of a significant atmosphere on Mars, compared to the moon, would imply that the surfaces of mineral grains would become contaminated on breaking up of the parent rocks. It might therefore be expected that cohesion between grains of Martian soil would be lacking, unless other forms of cementation are present.

Yellow "clouds" have frequently been observed on Mars both visually and photographically. Observation of the properties of these clouds suggest that they may be composed of windborne fine mineral particles (ref. 3). Thus, Leighton et al. (ref. 3) conclude that deposition of these clouds of particles would mantle and soften the outlines of craters. They also consider that the craters might be modified by thermal and vibrational creep of the granular material on slopes.

Consequently, if this is correct, blankets of relatively uniformly fine-grained soil may cover areas of Mars. With the experience developed by lunar surface investigations, and considering the low probability that Martian soil is cohesive, there is little likelihood that these fine-grained deposits will be extremely loose or highly porous. As Leighton et al. point out, an exception to this model may occur in those areas, if such exist, where permafrost exists at the surface. Temperatures favorable for the production of permanently frozen water in the soil (permafrost) if the water supply is sufficient, only occur between latitudes of 40 to 50°N and S and the poles. Only near-equatorial sites are now being considered for spacecraft landings. In this region, temperatures exceed 0°C daily for 10 Martian months. It is therefore considered that there is essentially no possibility of encountering permafrost at the spacecraft's landing site.

In summary, the surface existing at a Martian equatorial landing site has a high probability of consisting of fine-grained cohesionless mineral particles, with a density of around 1.5 gm/cc (terrestrial basis) and a porosity in the neighborhood of 50%. Larger particles in the millimeter to centimeter or larger range may be encountered, although there is a high probability that some fine-grained soil can be reached.

Sample acquisition.- With a Martian soil model as outlined above, a sampling device does not need a rock-coring, sampling, or grinding capability. Considering the soil analysis requirement, there are two possible approaches to the experiment: deploying the soil analysis equipment from the spacecraft to the Martian surface; or bringing a soil sample to an analytical device mounted on the spacecraft. Each of these approached will be discussed. Certain problems, such as sterilization, launch, flight, and landing survival arise with both approaches.

Analysis at surface: In this case, it is visualized that an experiment similar to the alpha-scattering experiment of Surveyor spacecraft will perform the required analysis of the Martian soil composition. An attachment will be necessary to determine the water content of the soil. With this technique a sensor head will be lowered or extended to the surface to obtain the appropriate measurements. The soil's mechanical properties do not affect such a deployment technique. The advantages and disadvantages of this technique will be listed here. This approach has essentially one degree of freedom in sampling. The advantages are:

1) Requires no imagery of test area (although such imagery might be useful for interpreting the results of the experiment);

2) Deployment has minimal power requirements;

3) Automatic on receipt of deployment signal;

4) Operation and performance of test have minimum interaction with other devices;

5) Type of surface (rock, soil) relatively unimportant for compositional analysis.

The disadvantages of the analysis at surface technique are:

1) One-shot test;
2) Sample cannot be selected;
3) Deployment failure cancels test;
4) Shape of surface (large rock) may tip sensor or otherwise render test ineffective;
5) Sensor head requires mounting bracket, interface harness, etc.

Soil sample retrieval: This approach, in general, has the following advantages:

1) Degree of flexibility in sample selection (if imaging capability present);
2) Gain in other information, such as strength, physical composition of Martian soil, variability with depth, etc;
3) Chemical compositional experiment remains fixed to spacecraft;
4) Analysis of more than one sample facilitated (depth variation).

The disadvantages of the retrieval approach are:

1) Power requirements;
2) Weight may be somewhat greater than deployment mechanism for composition experiment alone;
3) Failure leads to no compositional analysis;
4) Imaging desired;
5) Command complexity;
6) Location on spacecraft restricted with respect to both the imaging system and the analysis experiment;
7) Analysis experiment requires sample receiver.

In the sample retrieval approach, there are three classes of mechanism that may obtain a sample of Martian soil for delivery to an onboard sensing device -- automatic, manual, and semiautomatic.

The automatic device would be preprogramed to extend until an obstacle (presumably the surface) was encountered by a force or motor current sensor. This sensor would activate a sample bucket or scoop to retrieve a sample. The sampler would then be withdrawn from the surface and the program would initiate motions to cause the soil sample to be placed in the analysis apparatus. No earth commands, except for initiation, are required in this operation.

The advantages and disadvantages of this approach are almost the same as those for deployment of the chemical compositional equipment itself, except that a sample may be retrieved further from the spacecraft and the sample site may be arranged to appear in the imaging system's field of view. This equipment would also have one degree of freedom in obtaining a sample.

The manual retrieval device is the type of surface sampler used on Surveyor lunar spacecraft (ref. 4). The advantages in sample selection and manipulation are obvious, and additional information may be obtained by rock and soil manipulation. However, on Mars, there are considerable disadvantages in using such a device. Many pictures of the sampler and the area of operation are required so that, although power requirements for the device itself may be low, more work is required of the imaging system. The time delay for signals to and from Mars makes such an operation extremely time-consuming because of the decisions required. A command system is required. An apparatus of this kind would possess at least three degrees of freedom in movement.

A semiautomatic device is visualized as a surface sampling device that would be preprogramed as with the automatic system, to obtain a soil sample and deposit it in the analytical experiment. However, operations could be interrupted on earth command to permit certain simple decisions. Two degrees of freedom would be required in the apparatus to make the response to decisions meaningful. All the disadvantages associated with the sample retrieval function are inherent in this approach, but there are a number of advantages over the other techniques suggested. The probability of sample retrieval is good, almost regardless of the nature of the surface. Multiple samples might be possible with suitable design and the analytical sensor. Additional information on the physical nature of the surface would be obtained. Below-surface samples might be possible. One, or at most two pictures from the imaging system, would be sufficient for the operation.

Tentative Conclusion.- A fully manually-controlled sample-acquiring mechanism is not considered feasible for the proposed Mars landing spacecraft. The alternatives are deployment of the soil analysis sensor or sensors to the surface or some form of automatic sample retrieval. If the sample retrieval is to be fully automatic (i.e., no earth command or decision-making involved except for initiating a sequence), there appear to be few advantages in providing a separate sample-retrieval device over simply deploying the compositional analyzer to the surface. A fully automatic sample retriever is therefore not recommended. There are distinct advantages in some form of sampling device, however, over the deployment of an analyzer to the surface, as indicated above. It is suggested that a semiautomatic sampling device be considered. One approach to designing such a piece of equipment is given in the following subsection.

Tentative design of semiautomatic sampler.- The design will consist of an extendible device, such as a furlable tube, possessing a sample retrieval container at its extremity. The entire sequence of desired operations will be performed by an onboard program. The sample container will be designed to open when the apparatus is being extended, and close when it is retracted. On receipt of an extension command the retrieval container will extend an inch or two, during which it opens and extension continues. On receiving a retraction command, the container will first retract about ½ in. before it closes and retraction continues.

The apparatus will be mounted on the spacecraft and oriented so that the elevation of the extension device is fixed. Its elevation altitude will be established before flight so that intersection of the sampling device with the nominal Martian surface occurs when extension is approximately two-thirds of the maximum possible. At this distance the contact with the Martian surface will be within the field of view of the imaging system of the spacecraft. The device will be automatically rotated in aximuth by an electric motor or other means. However, it may be stopped on earth command at an azimuth position stored in the onboard program. When this direction has been entered in the sampler command sequence, power on and execute commands to the sampling device will cause it to rotate to the selected azimuth position and extend to the surface until a force-limiting device stops its extension (in the Martian soil). It will then retract (closing the soil container) and rotate to the position required for the sample to be placed in the soil composition apparatus. At this time it will be given an extend command so that the container will open and the soil sample be ejected in the composition apparatus. The device will return to its starting point and switch off. It is desirable to reactivate the device, with a different stored azimuth angle to perform the whole sequence again.

A tentative design is shown in figure 1. Furlable tubes are described in references 5 and 6. The weight of the sampling device alone may be in the range of 3 to 4 lb. Electric motors working on 20 to 30 Vdc are used to move the device; it is expected that they will require $\frac{1}{4}$ to $\frac{1}{2}$ A of current during the operating cycle. The entire sampling cycle should occupy a few minutes of time.

Design features.- Soil mechanics and machine design considerations were incorporated and two designs were examined: one with two degrees of freedom and the second with three degrees of freedom.

To reduce the weight and power requirements as much as possible, only one electric motor was included in the design of the two-degree-of-freedom extendible tube device shown in figure 1. In the principal views of this figure, the axis of the sampler operation is essentially horizontal and approximately parallel to the hinge-axis of the left-hand leg in the figure. In the alternative view the axis of the sampler is almost vertical. Consequently, the first horizontal position gives surface samples located along a radial line at various distances from the spacecraft, while the alternative arrangement will obtain samples along an arc at points whose distance from the spacecraft varies (the variation depends on the degree of tilt of the sampler axis from the vertical). Intermediate axis positions between these two are possible. The choice lies between the sampling capabilities desired and the location of the sample collection apertures on the spacecraft.

The arm rotation and extension drives are located coaxially for any of the sampling device positions considered above, as shown in figure 2. As shown schematically in figure 2(a), a reversible motor drives a planetary gear system, whose operation is controlled by a solenoid switched, spring-held brake. This brake is operated to hold either the inner or the outer drum stationary on command. If the inner drum is held, the motor (which is stationary) rotates the entire mechanism, including the sampling arm about the axis. If the outer drum is held fixed, the motor drives the arm reel (on which is wound the furlable tube) to extend or retract the sampling tube.

Note: 1. One motor required.
2. One axis rotation.
3. One axis extension only.

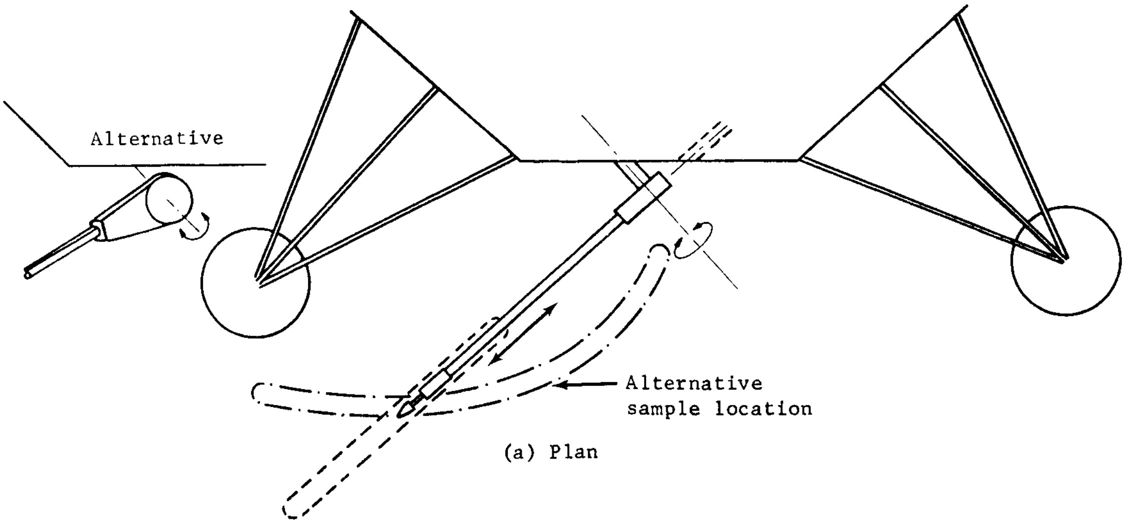
Alternative
Alternative sample location

(a) Plan

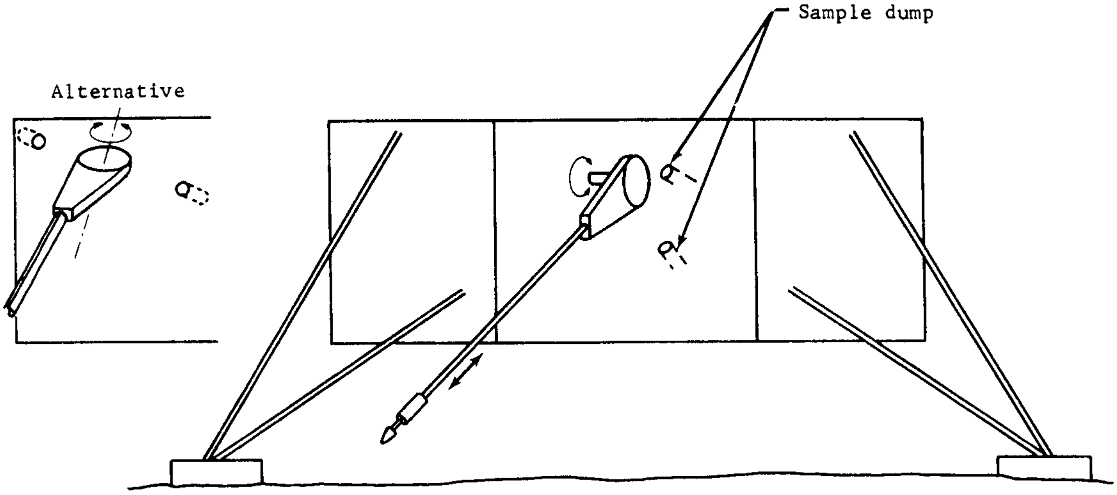
Sample dump
Alternative

(b) Front elevation

Figure 1.- Soil Sampler Tentative Design

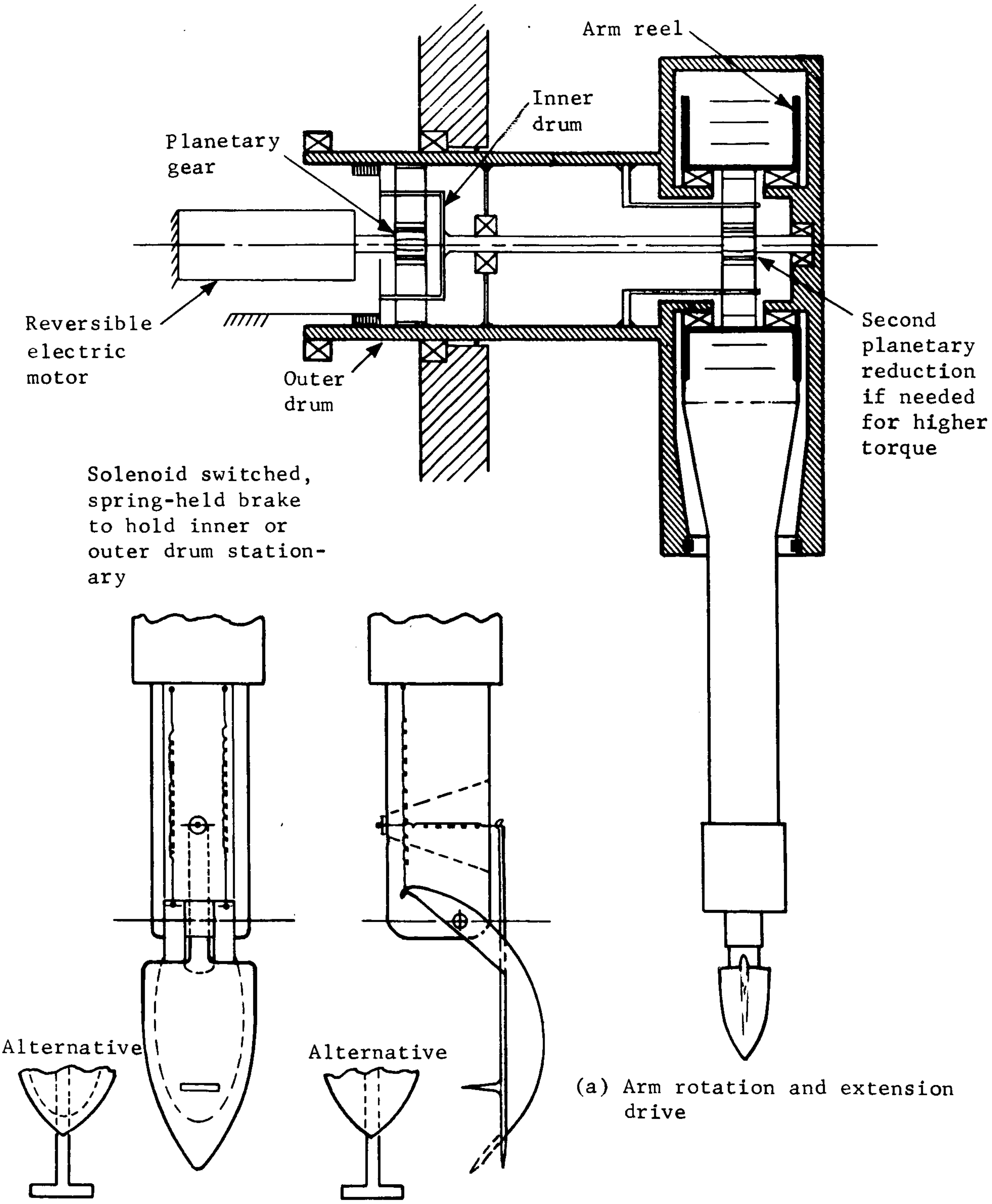

Arm reel
Inner drum
Planetary gear
Reversible electric motor
Outer drum
Second planetary reduction if needed for higher torque
Solenoid switched, spring-held brake to hold inner or outer drum stationary
Alternative
Alternative

(a) Arm rotation and extension drive

(b) Scoop detail

Figure 2.- Soil Sampler Details

Thus, for a sampling operation, the following sequence of events will occur:

1) A picture of the sampling area is obtained and a desirable sample location is identified in spacecraft and sampler coordinates;
2) A signal is sent to the spacecraft for onboard storage to identify the running or operating times of the solenoid brake and the motor so that, on being actuated, the system will locate the sampling bucket at the preselected sample position. The sample dump positions are already stored in the sampling command auxiliary;
3) Power-on and execute commands are transmitted to the sampler mechanism, which will go through the sequence of rotating from its flight position to the selected angle (inner drum braked), and then extending (outer drum braked) to the Martian surface. The extension distance can either be part of the preselected storage or may be controlled by a switching device at the sampler bucket, actuated by contact with the soil.

In figure 2(a) seals are shown at both the motor and the sampler ends of the extension drive housing, together with a collar around the end of the extension arm itself. Retraction against the extension arm seal protects the drive system during launch, flight, and landing.

An entirely mechanical, contact-actuated scoop-opening mechanism is shown in figure 2(b). It is visualized that the axis of scoop opening lies in a plane vertical to the Martian surface so that the opening of the scoop itself will not be hindered by contact with the surface. The scoop can be asymmetrical as shown, or may have two symmetrical doors opened by the plunger system shown in the alternative sketch of figure 2(b). This plunger operates the scoop doors through a scissors mechanism similar to that of figure 2(b).

There are a number of advantages and disadvantages to the mechanism shown, in any of its possible variants. The advantages are:

1) Simplicity;
2) No electrical devices on scoop tip that require wires along the furlable tube;

3) No command logic required.

The disadvantages of the mechanism are:

1) May not sample soil adequately or at all;
2) May jam;
3) May lose soil after retrieval, before dumping in collectors;
4) Design against launch vibration may be difficult.

The disadvantages can only be overcome by testing various scoop doors and mechanisms in a variety of soils. An electrically operated (solenoid or motor) scoop door should be given attention because of its very definite superiority in sample retrieval over the passive devices of figure 2(b). If an electrical approach is taken, the motor or solenoid must operate the door or doors through a spring, so that the doors will tend to close when retrieved soil falls from the bucket on retraction.

An outline of the mechanism that might be used to give more degrees of freedom in sampling is shown in figure 3. Two electrical motors are required (apart from bucket-design considerations). In the arrangement of figure 3 with the furlable tube, a soil sample can be retrieved from a selected accurate rectangular area on the Martian surface.

Development program.- The program will be initiated with a functional specification written by NASA or its agent, or by the principal investigator (if one is selected). This specification will outline the overall requirements to be satisfied by the sampling device:

1) Total extension distance;
2) Extension distance below nominal Martian surface;
3) Rate of extension;
4) Maximum force applied to the soil;
5) Volume of sample required;
6) Number of sample repetitions;
7) Capacity and accuracy of any sensors (force, displacement, etc, required);

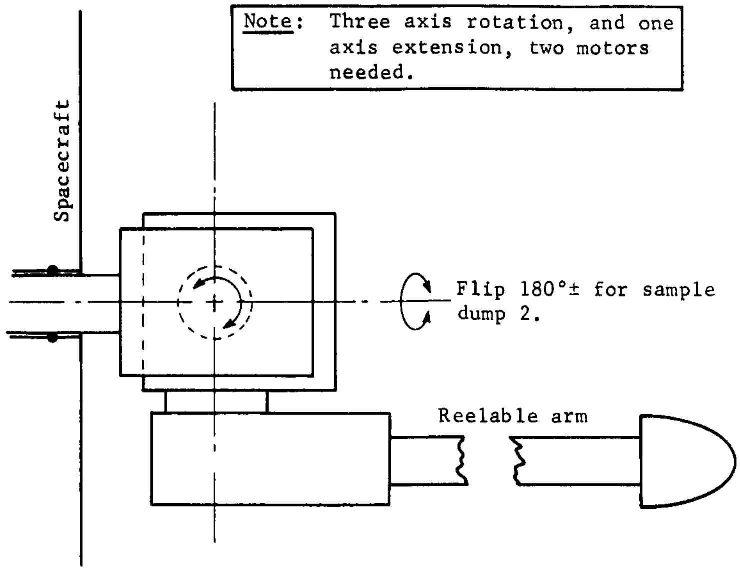

Note: Three axis rotation, and one axis extension, two motors needed.

Spacecraft
Flip 180°± for sample dump 2.
Reelable arm

(a) Plan

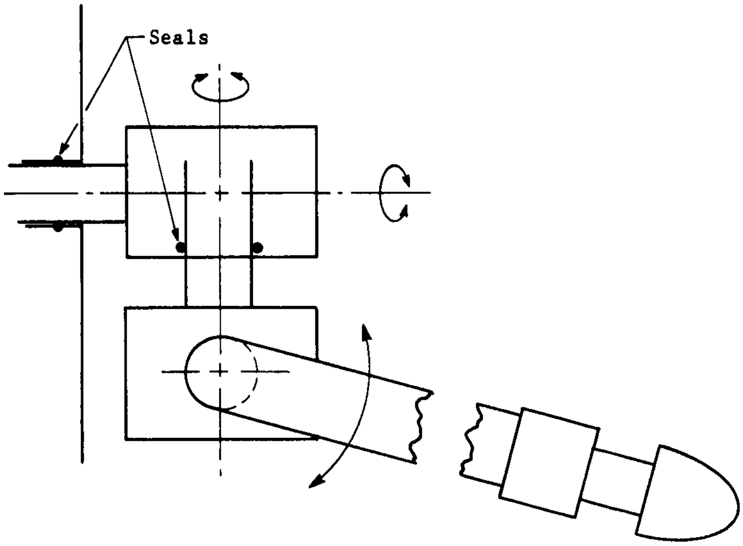

(b) Side elevation

Figure 3.- Soil Sampler with Three Degrees of Freedom

8) Time for which motor can be stalled;
9) Position accuracy required by sample compartment or collector.

NASA must also establish the engineering requirements to which the device must comply, such as various test specifications. These specifications attempt to duplicate (in excess) the conditions to which the apparatus will be subjected in launch, flight, landing, and operation. Some of the requirements are:

1) Environmental -
    a) Shock in stowed position,
    b) Vibration in stowed position,
    c) Temperature, nonoperating,
    d) Temperature, operating,
    e) Steady-state acceleration and deceleration,
    f) Vacuum or pressure (with temperature),
    g) Soil particle or dust environment;
2) Spacecraft interface -
    a) Force limitations,
    b) Magnetic field,
    c) Lifetime,
    d) Reliability,
    e) Command requirements,
    f) Communication requirements,
    g) Voltage,
    h) Power;
3) Experimental interfaces -
    a) Spacing, distance,
    b) Sample requirements,
    c) Electrical, etc.

To produce an apparatus that will meet these requirements and specifications, the following stages of development are needed.

Stage 1 - Preliminary development includes:

1) Prepare design specification;
2) Outline preliminary design or designs;
3) Procure and test components;
4) Construct breadboard models;
5) Carry out operational studies and error analyses of breadboard models;
6) Evaluate test results, select design.

Stage 2 - Prototype design includes:

1) Prepare prototype (sampler and electronics auxiliary) design drawings;
2) Carry out stress and thermal analyses;
3) Prepare detail drawings.

Stage 3 - Prototype manufacture includes:

1) Make parts according to detail drawings (for two or three prototype units);
2) Obtain components and subassemblies from subcontractors;
3) Test parts and components individually.

Stage 4 - Prototype performance and test includes:

1) Assemble prototype sampling device and auxiliary and evaluate functional performance with respect to functional and engineering requirements;
2) Modify parts, components, and subassemblies and drawings as required;
3) Carry out interface compatibility (with spacecraft and other experiments), and viewability (imaging system) tests.

Stage 5 - Final engineering model development includes:

1) Fabricate and assemble engineering models;

2) Perform type approval tests* to ensure that all requirements are met;

3) Revise model as required.

Stage 6 - Flight units development includes:

1) Manufacture and assemble flight units;

2) Perform flight acceptance tests.†

In parallel with these stages, two other phases of development are required as support for the sampler unit. In Stage 7 testing and calibration equipment is designed, constructed, and assembled. Stage 8 includes design, construction, assembly, and test of mission ground support equipment.

Subsurface Probe

It is desirable to obtain temperature measurements at more than one location below the Martian surface, because multiple measurements can be used for soil thermal property evaluation. Because the measurements will be of principal value if soil exists at the landing site (many of the measurements are predicted on the presence of soil) the tentative design incorporates thermal sensors in a probe of the shape and arrangement shown in figure 4. This shape of probe offers certain advantages in penetrating a soil, or soil-rock mixture, and in stowage and operation from the spacecraft. If, in addition, a heating element is suitable installed along the axis of a portion of the probe, an active thermal diffusivity experiment may be performed (ref. 7). A soil moisture sensor or sensors can be incorporated in another section of the probe. Some of the items in the design of such a probe are considered below.

---

*Type of approval tests are performed on prototype units to prove the adequacy of the design under more severe environmental conditions than are expected during the mission.

†Flight acceptance tests are carried out on flight units to confirm that workmanship and assembly are acceptable under anticipated mission environment.

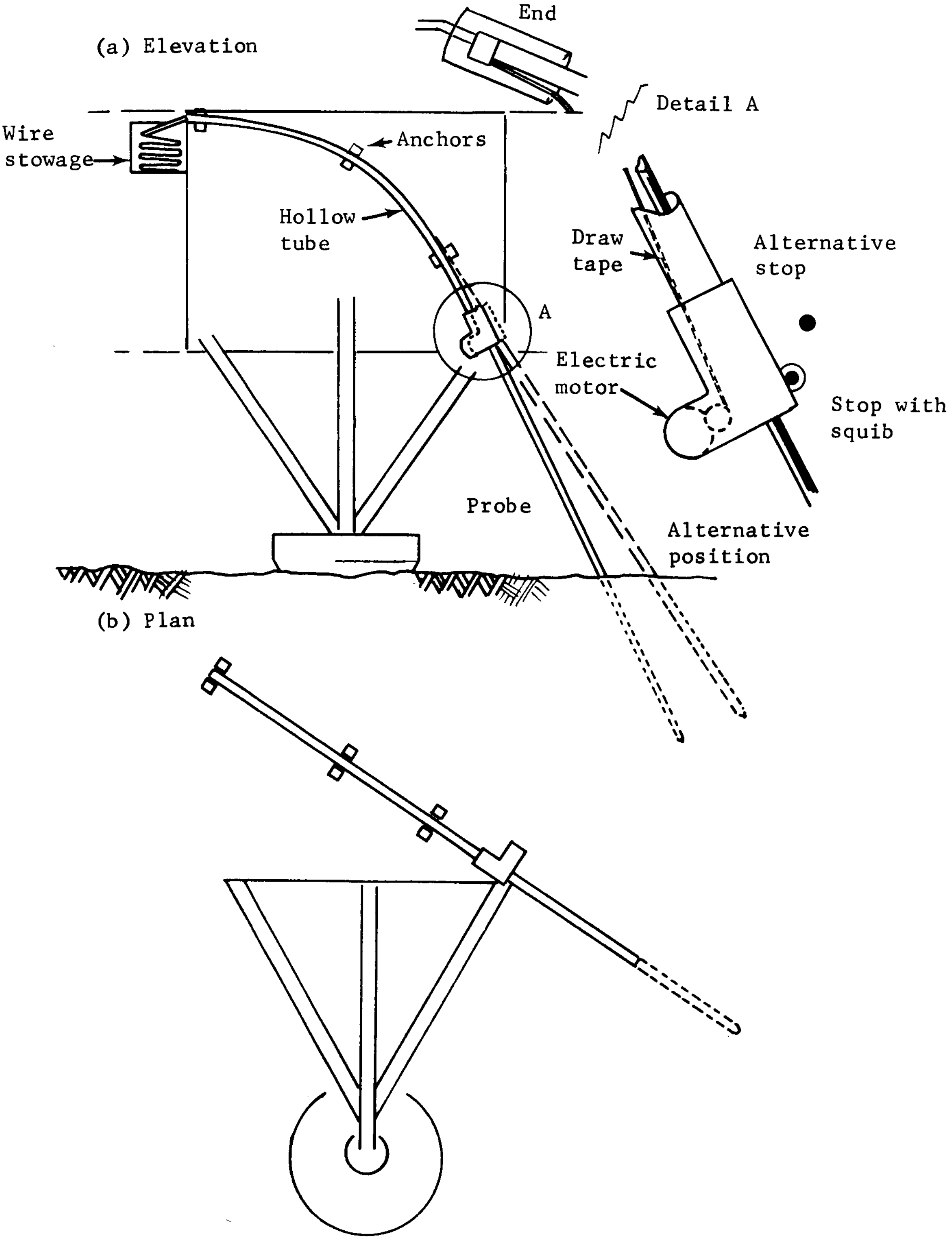
(a) Elevation

(b) Plan

End
Detail A
Wire stowage
Anchors
Hollow tube
Draw tape
Alternative stop
A
Electric motor
Stop with squib
Probe
Alternative position

Figure 4.- Subsurface Probe

The operation of the probe involves the selection of a suitable penetration point from a preliminary photograph of the Martian surface. The probe may be deployed at its original position [fig. 4(a) and detail] or in the alternative position by activating an explosive (or solenoid-operated) pin, which acts as a stop for the probe guide. The probe is expelled from a curved guide tube, possibly by an electric motor and draw-tape as shown. A potentiometer or contact switch could indicate full or partial deployment. The probe itself should be distinctively striped, so that its penetration can be measured from postdeployment pictures. This, together with a knowledge of the torque characteristics of the deployment motor, will give useful information on the mechanical properties of the Martian soil, as well as aiding interpretation of the subsurface thermal data.

Mechanical design considerations.- Elastic bending of the probe tube: Two tubes to carry the thermal sensors will be considered: (1) 0.05-in. mean radius, 0.02-in. wall thickness; and (2) 0.10-in. mean radius, 0.04-in. wall thickness. Their moments of inertia, I, are 8.1×10^{-6} in.^{4} and 130×10^{-6} in.^{4}, respectively. Assuming the depth of the spacecraft to be 18 in., it will be necessary to stow the tube in a guide whose radius of curvature is somewhat greater than 18 in. Assume the minimum radius to be 24 in. The extreme fiber stress, σ, in the probe under this condition is

$$\sigma = \frac{E(r + t/2)}{R} \tag{1}$$

where r is the tube radius, t its thickness, E the modulus of elasticity, and R the radius. The extreme stresses become, in a steel tube, $E = 30 \times 10^6$ psi:

1) 75 000 psi;
2) 150 000 psi.

To this must be added the compressional stress due to expelling the tube; however, the latter is of the order of 2000 psi. Either of the two stresses are achievable with a suitable choice of steel, but the smaller tube gives a more desirable value. The effect of the spacecraft temperature extremes on the material behavior should be evaluated. It is also possible that a small aluminum tube would perform suitably. The material selection will also depend on thermal considerations.

Buckling of the tube on soil penetration: At the moment of soil penetration, the probe can be considered fixed at the top, and hinged at the soil entry point. If the spacecraft shock absorbers are fully extended, the free length, ℓ, of the probe at this stage will be about 20 in. The critical buckling load, P_c is given by the expression

$$P_c = \frac{20.2\ EI}{\ell^2} \tag{2}$$

For the two tubes, P_c = 12 lb and = 200 lb, respectively. The penetration resistance of the soil (see below) increases with depth, so that a later stage in penetration may be considered where ℓ = 25 in., say, and the probe is considered to be fixed at both ends. In this case

$$P_c = \frac{4\pi^2 EI}{\ell^2} \tag{3}$$

For the small probe (1) only, this gives P_c = 15.6 lb; the force for the larger probe is very large.

Soil penetration: It is preferable to estimate the axial load required to force each size of probe into a soil experimentally rather than to attempt a calculation. Accordingly, a series of tests was carried out as follows.

Since the gravitational acceleration on Mars is 0.4 times that of the earth, tests on dry cohesionless (the Martian model) soil on earth will give too high a penetration resistance. However, if the soil is submerged in water, the buoyant unit weight of the soil will be quite close to that of a dry Martian soil on Mars. It has been found that water does not substantially alter the frictional properties of mineral grains in such a test. If the probe is pushed in slowly pore water pressure effects will also be absent.

Ottawa sand (a silica sand) was tested with two diameters of solid probe, 0.105 in. and 0.200 in., respectively. Two soil densities were used, corresponding approximately to unit weights of 90 (loose) and 110 (dense) lb/ft^3 in air. Submerged, the effective buoyant weights of the two soils are about 60 and 69 lb/ft^3, respectively. If these latter two values are considered to represent unit weights of dry Martian soils, they would be equivalent to terrestrial soils weighing $\frac{1.0}{0.4} \times 60 = 150$ and 172 lb/ft^3, respectively. The latter figures are on the low side, but the test results may be taken as a first approximation to the penetration problem. Three tests of each probe were performed in each of the two (dense and loose) soils under water. The force versus penetration depth is shown in figure 5 (loose) and figure 6 (dense), respectively. The laboratory apparatus is shown in figure 7.

A reasonable effort was made to keep the soil density homogeneous in each test, but, in view of the preliminary nature of the tests, all of the control that might be applied in a precise test was not used. Scatter is always apparent in soil tests, and uniformly loose material is more difficult to prepare than uniformly dense. The effect of the presence of rocks in the soil could be investigated by similar tests.

With these provisions it is seen that the small rod may be pushed to the depth of 12 in. in the loose soil with a force of 0.5 to 0.7 lb maximum. The same rod may be pushed into the dense soil to a depth of 12 in. with a force of about 10 lb maximum. The larger rod requires substantially higher forces in both cases.

Conclusions and recommendations: Putting the previous results together it appears feasible to use a 0.1-in. diam. steel tube as a Martian soil probe in the manner suggested in figure 4. The yield stress of a steel or possibly aluminum tube would not be exceeded in stowage or deployment. A small electric motor with suitable gearing can develop the force necessary to penetrate a Martian soil of the type assumed to a depth of about 12 in., and the probe will not buckle on being pushed into the soil. The ability of the probe to penetrate frozen soil will depend on the moisture (ice) content of the soil. The 12-in. depth was selected as being a desirable goal from thermal considerations (discussed in the following subsection.

Thermal experiment considerations.- On earth, the daily soil surface temperature fluctuation is attenuated to an amplitude of a few degrees at depths of about a foot in soils. Since the Martian day is about the same length as the earth day, the same consideration should apply. A maximum depth of probe penetration of about 12 in. will therefore give a useful amount of thermal information, and will also probably be limiting in terms of possible temperature discrimination.

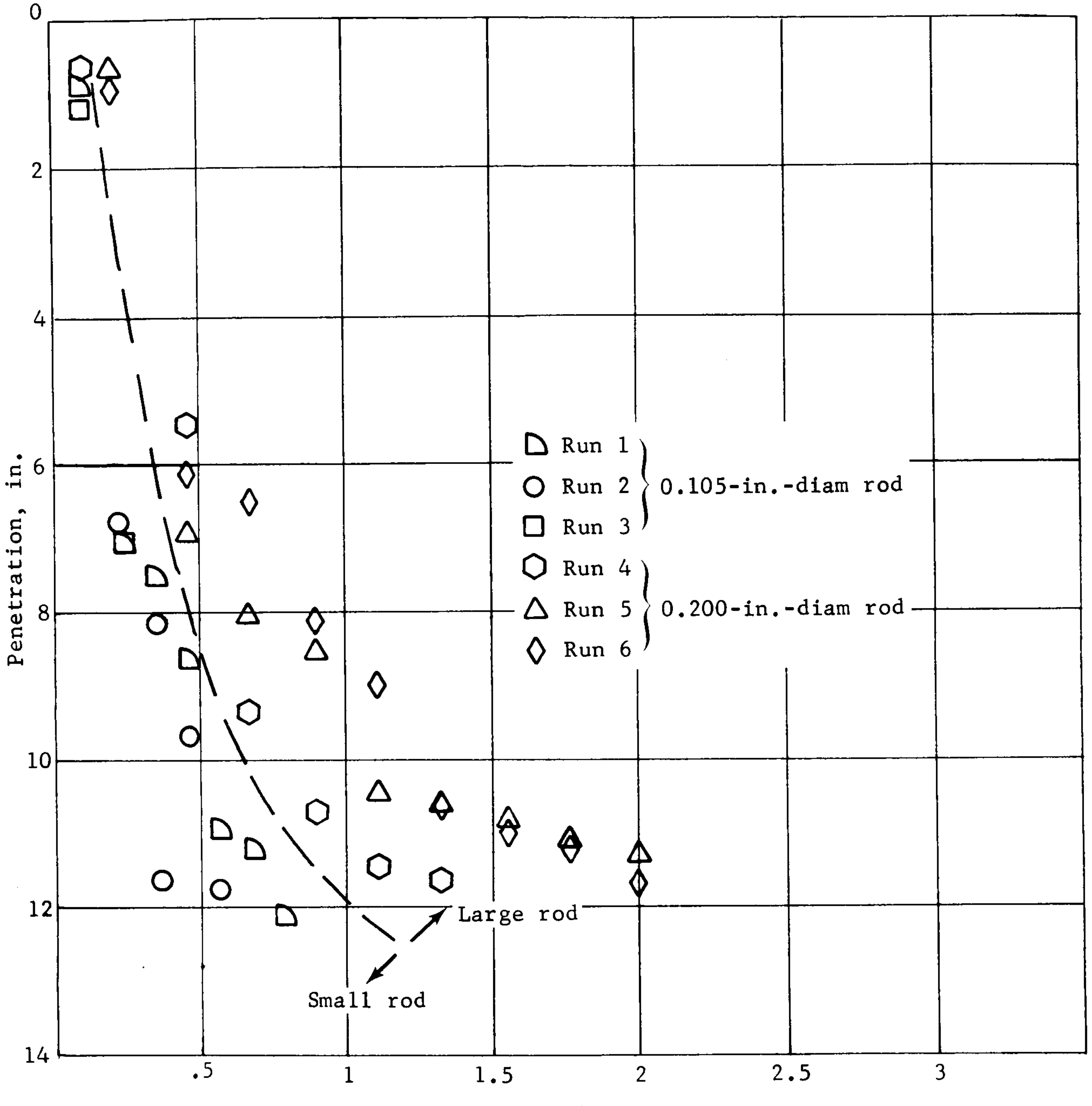

Figure 5.- Penetration vs Force for Loose Soil

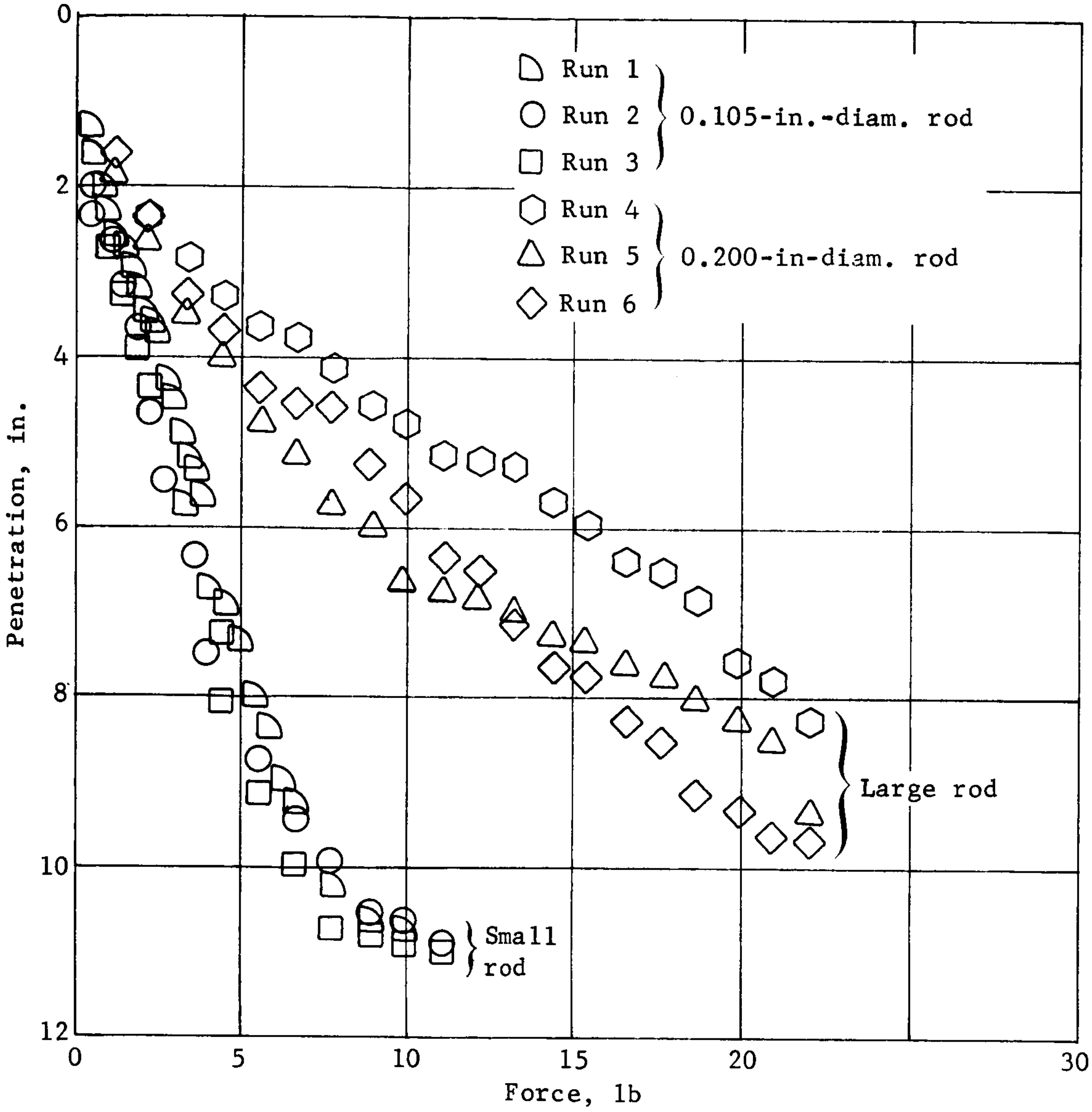

Figure 6.- Penetration vs Force for Compacted Soil

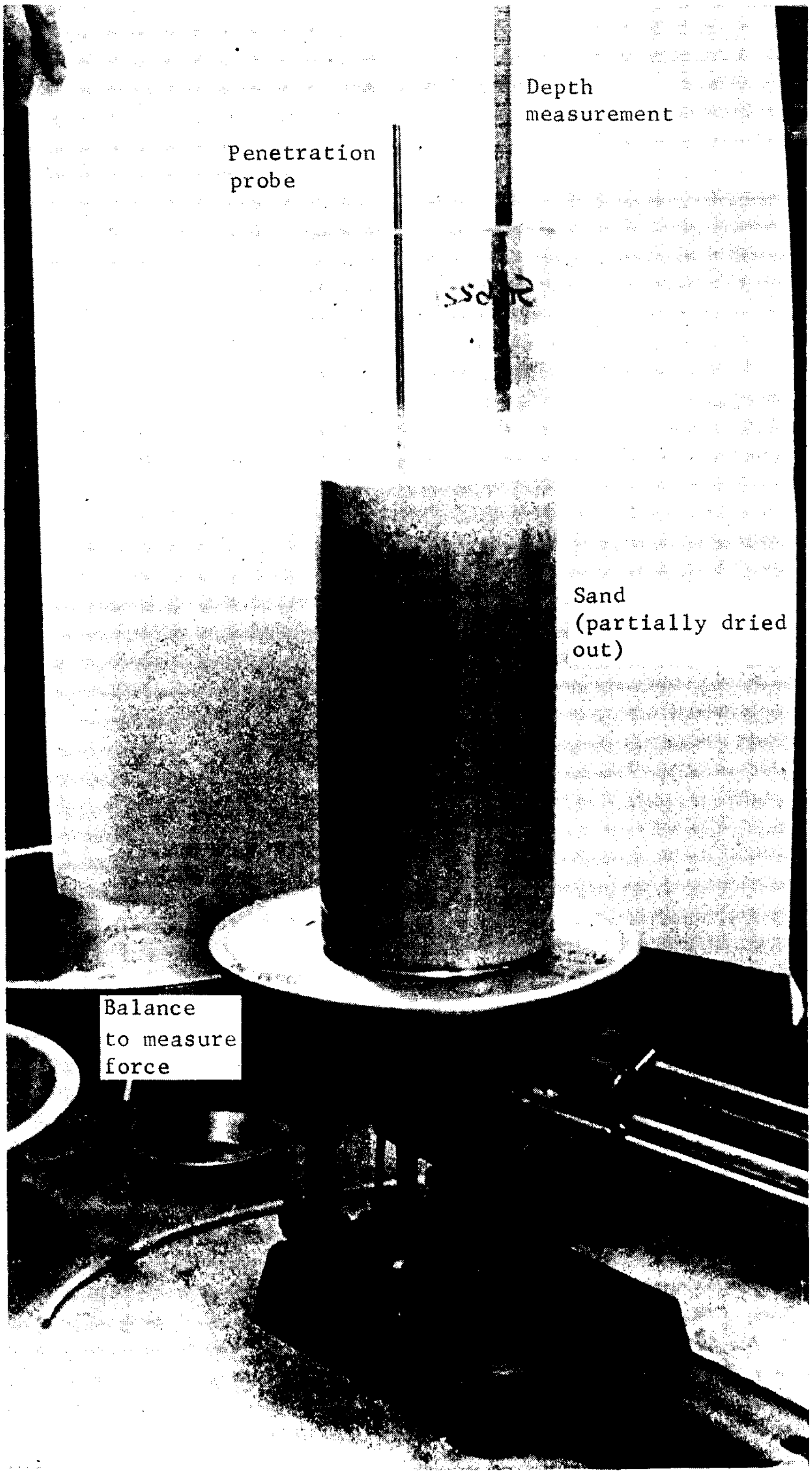
Depth measurement
Penetration probe
Sand (partially dried out)
Balance to measure force

Figure 7.- Laboratory Apparatus for Penetration Tests

Soil thermal properties: The variation of soil thermal properties with moisture content and unit weight on earth was investigated by Kersten (ref. 8). The results are reproduced as figures 8 thru 13. It is seen from figures 8 thru 11 that the soil thermal conductivity is very sensitive to moisture content and less so to its unit weight. The specific heat varies to a lesser extent with moisture content (fig. 13), so that the thermal diffusivity of the soil (added to fig. 8) changes considerably with water content. Calculation of the thermal diffusivity or conductivity of the Martian soil would lead to an estimation of limits on its water content. It is found that the data of figures 8 thru 13 hold good for soils of a wide range of mineral content.

Martian thermal properties from soil probe: In figure 14(b) the theoretical curves of temperature versus time are shown at different depths in a terrestrial soil over an annual sinusoidal temperature cycle always above freezing. The soil physical properties were a unit weight of 120 lb/cu ft, moisture content of 10% (of dry weight of soil), and thermal properties of conductivity of 1.2 Btu ft/ft^2 °F hr, and volumetric specific heat of 24 Btu/ft^3 °F. The fluctuation of daily temperatures in soil to a depth of a few inches from a daily surface sinusoidal fluctuation is similar. (This yearly fluctuation was chosen to compare the curves with those of figure 14(a) and only yearly data were available on temperature fluctuations when freezing was involved. Daily temperature calculations can readily be carried out when required.)

The ratios of the amplitudes of temperature fluctuations at different depths, and, separately, the phase lags of temperatures at various depths can both be used to calculate the thermal diffusivity of the soil (ref. 9). If the Martian soil density or unit weight can be estimated from the behavior of the spacecraft's footpads on landing, and the observations of both the sampling device and the thermal probe, the specific heat can be estimated and the conductivity calculated from the temperature measurements via the diffusivity. This then may give a bound to, or confirmatory data for water contents.

Soil freezing and thawing: When the soil freezes and thaws because of its moisture content during a thermal cycle, the nature of the temperature fluctuation with depth changes characteristically. An example of the behavior is shown in figure 14(a). The same soil was involved in both of figures 14(a) and (b), but in figure 14(a) a latent heat of soil moisture (10% water content) of 1500 Btu/ft^3 was included. The diffusivity can no longer be calculated directly but the properties may perhaps be obtained by simulation studies.

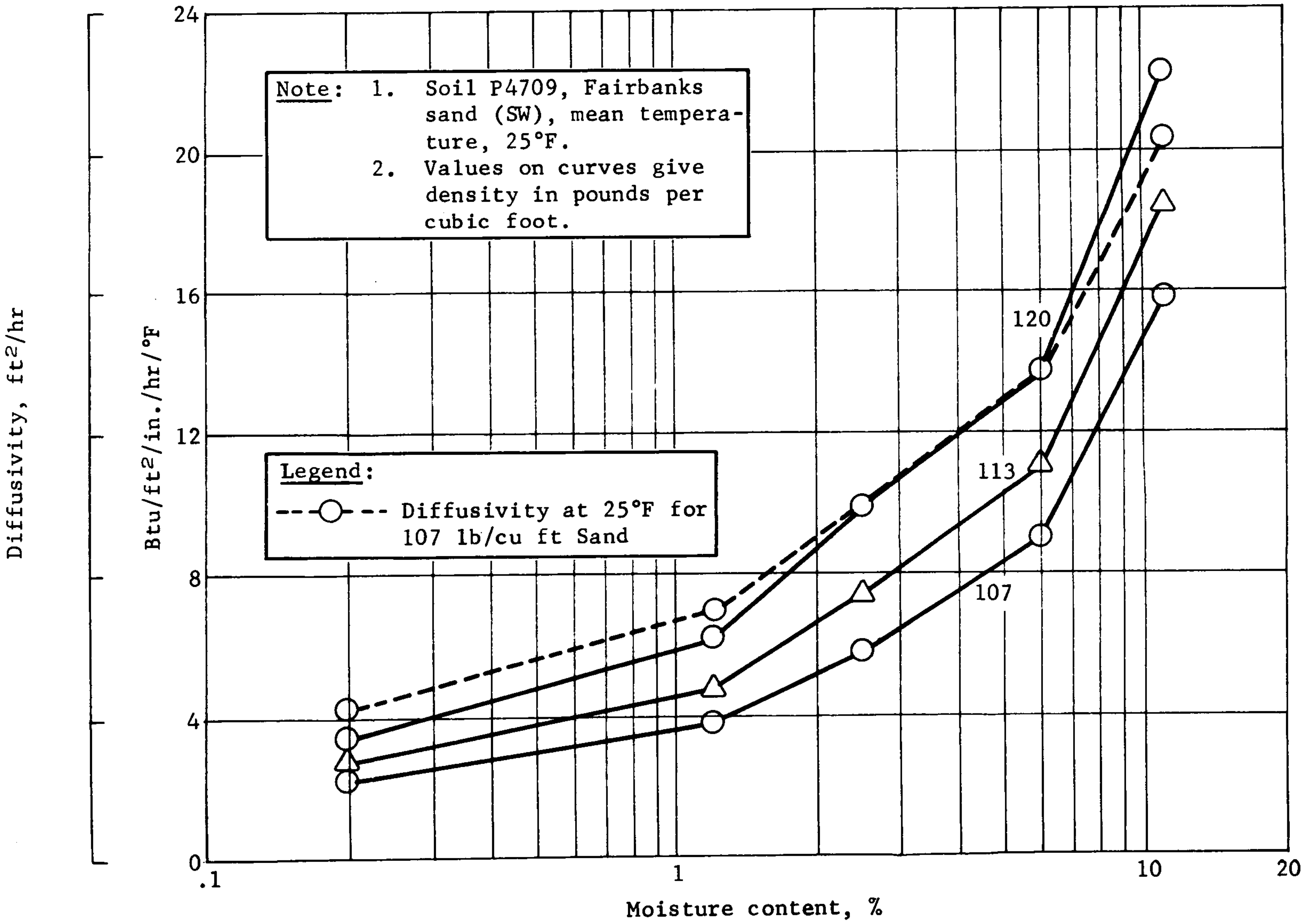

Figure 8.- Thermal Conductivity and Diffusivity vs Soil Moisture Content

Note: 1. Soil P4709, Fairbanks sand (SW), mean temperature, 25°F.
2. Values on curves give density in pounds per cubic foot.

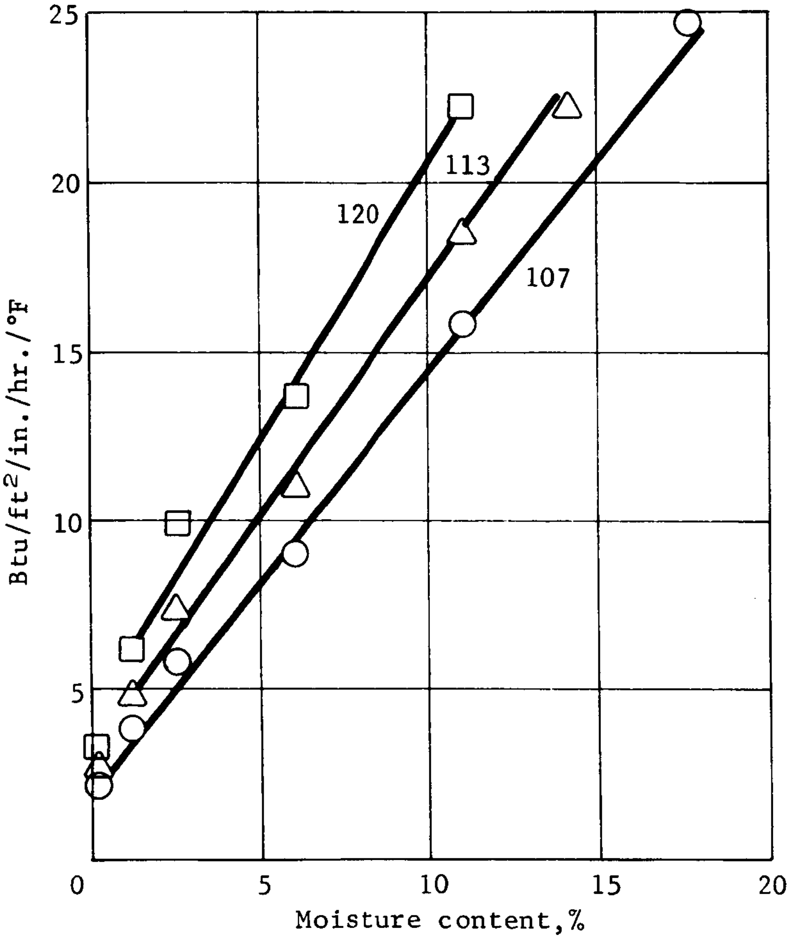

Figure 9.- Variation of Thermal Conductivity with Moisture Content

Note: 1. Soil P4701, graded Ottawa sand (SP), mean temperature, 40°F.
2. Values on curves give constant moisture content.

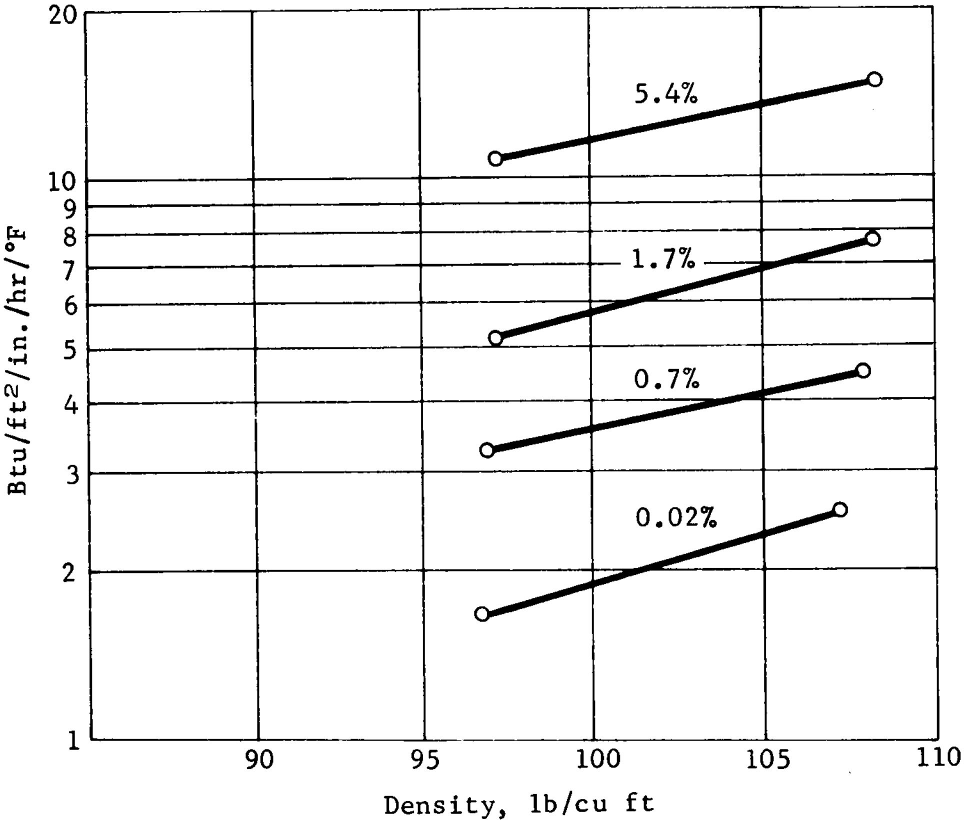

Figure 10.- Variations of Thermal Conductivity with Dry Density

Note: Unfrozen, mean temperature 40°F.
Degree of accuracy = 25%.

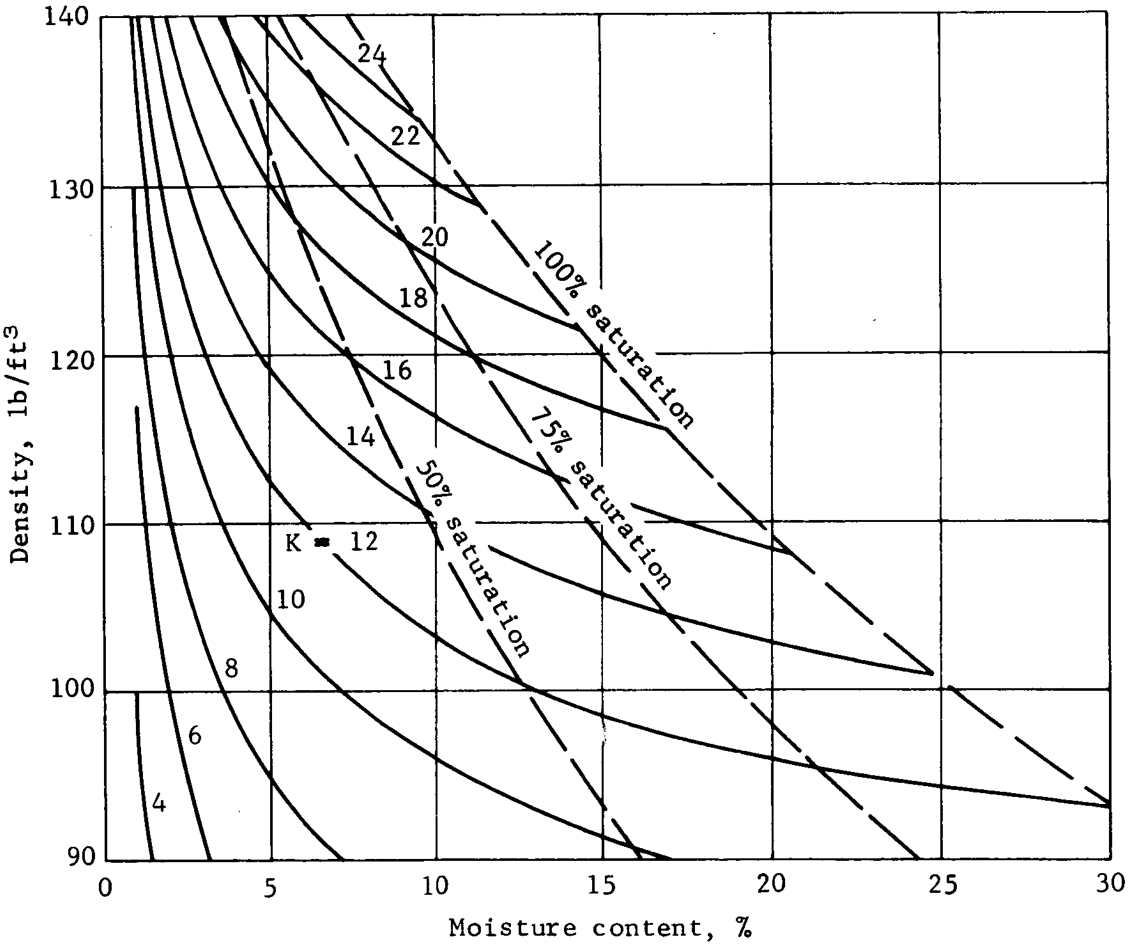

Figure 11.- Diagram of Thermal Conductivity for Sandy Soils

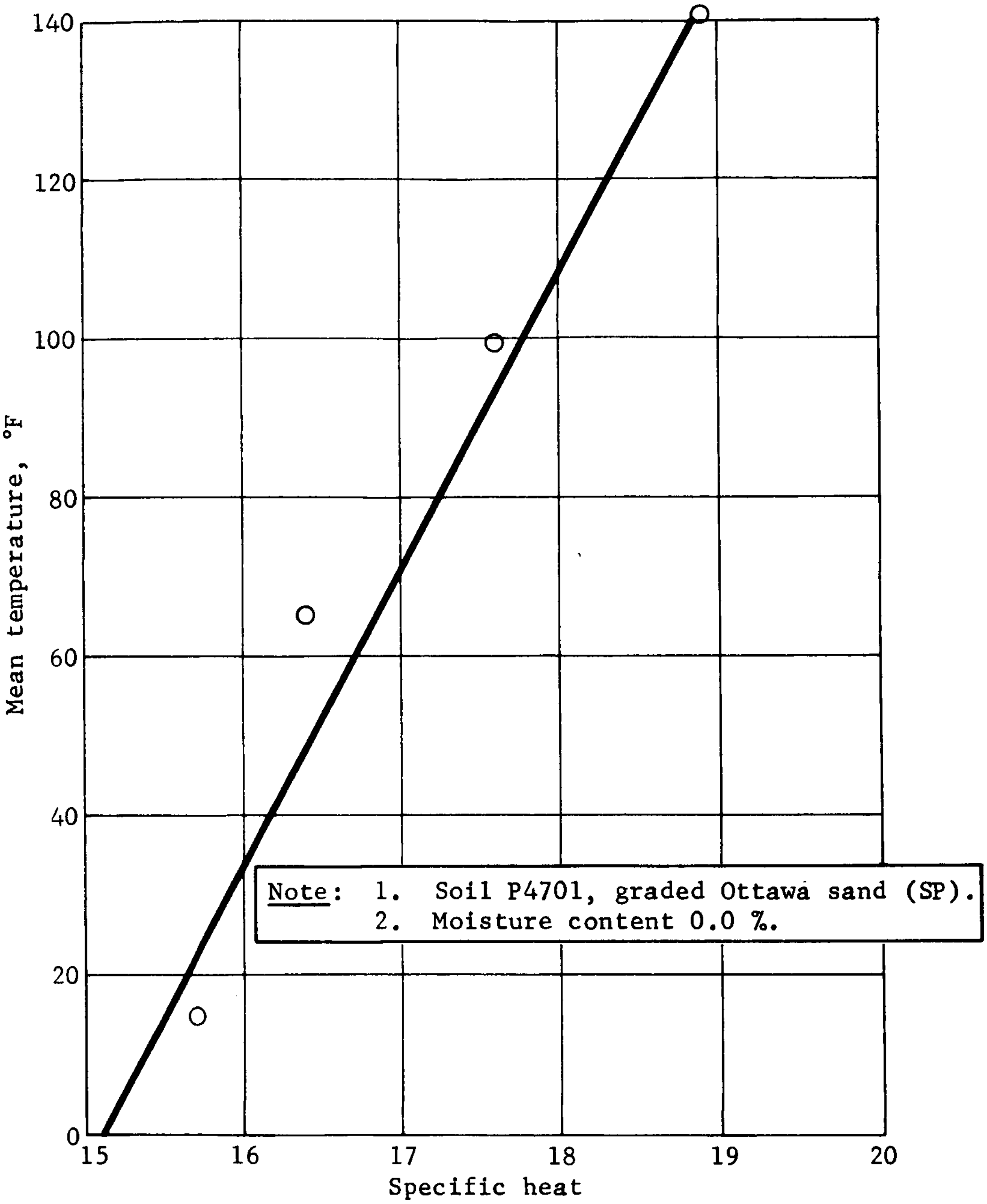

Figure 12.- Variations of Specific Heat with Mean Temperature

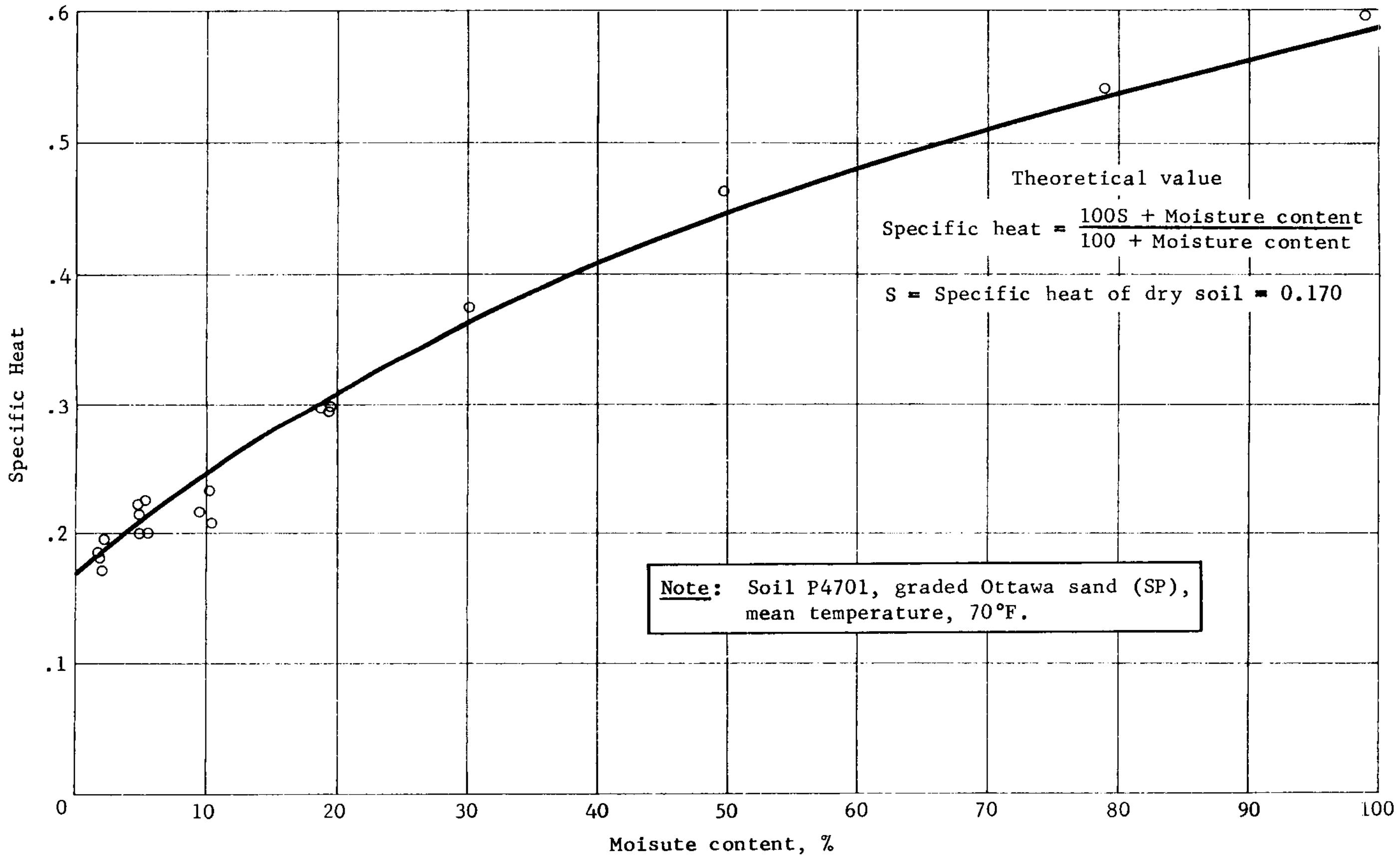

Figure 13.- Relationship of Specific Heat of Soil-Water Mixturesand Moisture Content

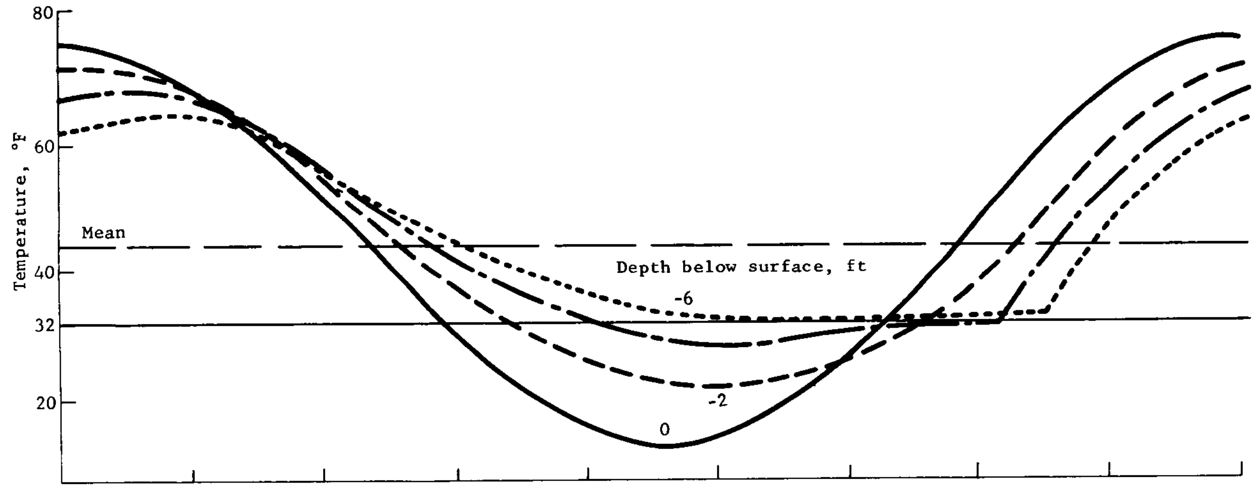

(a) Soil moisture freezes

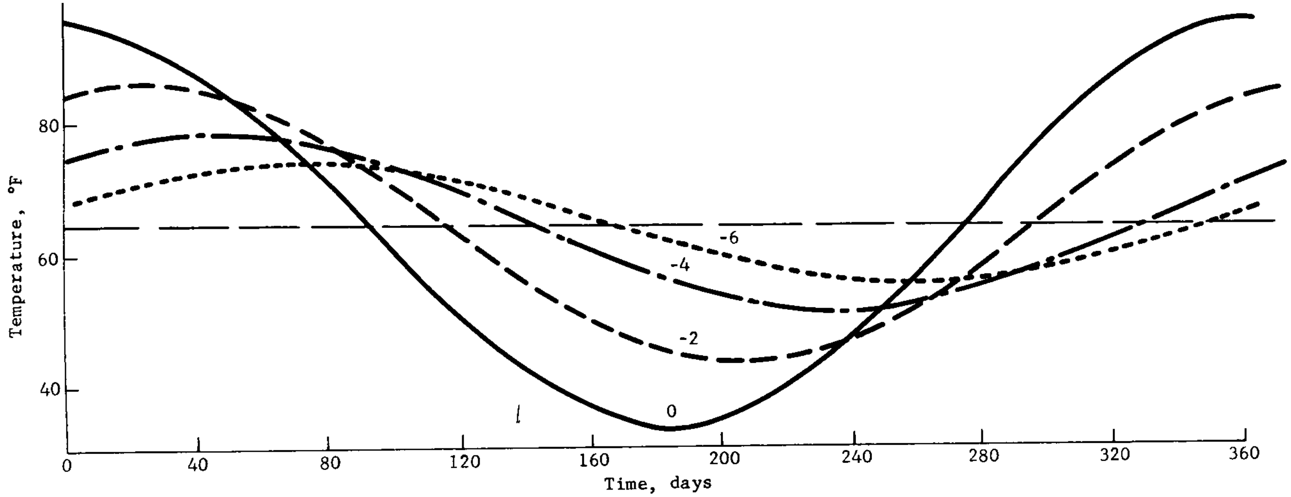

(b) No freezing of soil moisture

Figure 14.- Soil Temperature vs Time

However, the different appearance of the curves would indicate that a change of state was occurring, in itself, a significant conclusion.

Note that at the actual landing site the surface temperature fluctuation at the probe will not vary sinusoidally because of the different nature of the heat flow during day (short wave incoming, long wave incoming and outgoing) and night (long wave incoming and outgoing), and possibly evaporation and condensation processes, in addition to spacecraft shading effects.

The use of an active thermal diffusivity experiment (ref. 7) beside supplying thermal properties, may also be of value in enabling the probe to penetrate soil if it is frozen. If the probe does not initially penetrate to the fullest possible extent, the effect of heating the soil with the diffusivity heater element and reactivating the probe drive might be informative.

Moisture Sensor.- A series of laboratory experiments was conducted to determine the detection threshold of several widely used soil moisture cells. The feasibility of using these devices to detect moisture in the soil around a Mars lander was assessed. A number of cells were modified in an attempt to extend their detection threshold to the extremely dry conditions expected on Mars. The measurement of soil gases is discussed in references 10 thru 13.

Materials and methods: The blocks used were manufactured by the Industrial Instruments Company following the design of Dr. George Bouyoucos. They consist of nylon cloth between and around two stainless steel screen electrodes 1 1/8 in. square encased in a coarse stainless steel mesh, giving an overall dimension approximately 1 1/2x1 1/4x1/8 in. The resistance between the electrodes is measured with an AC Wheatstone bridge circuit with 1000 Hz bridge oscillation similar to the Bouyoucos Model C moisture bridge now sold by Beckman Instruments, Cedar Grove Operations.

The experimental atmosphere apparatus consisted of a vacuum pump, large vacuum desiccators with mercury manometer for pressure measurement, and a glass stopcock for pressure adjustment.

Two soil-like materials were used in the experiment -- Kaolinite and quartz. A Kaolinite sample consists primarily of coarse material 1 to 10 μ in size. This is one of the least reactive of the clay minerals available and would be a conservative approximation for unweathered clay size material. The quartz silt was a ground quartz sand passing a 325 mesh and would be less than 47μ in size. Table 1 shows recorded soil water percentages on an oven dry basis (oven at 105°C) for these materials under different conditions and also a Miami subsoil sample for comparison. Note that these materials are extremely dry at low atmospheric pressures and that the Kaolinite and quartz silt have very low water content compared to the dry Miami subsoil that contains some organic matter and more reactive clays than Kaolinite.

TABLE 1.- PERCENT WATER ON AN OVEN DRY BASIS[a]
UNDER VARIOUS CONDITIONS

Material	Air dry	After 4 hr, 16 mm Hg	Wet 42 hr at 16 mm Hg[b]	16 mm Hg[c]	Oven dry 2 hr at 16 mm Hg[d]
Kaolinite clay	0.43	0.279	0.17	0.165	0.0010
< 47μ quartz	0.042	0.070	0.043	----	----
Miami subsoil	3.08	1.86	----	----	----

[a] Oven at 105°C

[b] Final moisture, Table 3

[c] Final moisture, Table 6

[d] Final moisture, Table 8.

Experimental results and discussion: The untreated nylon blocks were first equilibrated over water in a desiccator, they were then wetted and dried at 20 mm Hg (Table 2). After 2½ hr the blocks became so dry that they had a resistance over 5 500 000 ohms, which was the maximum for the bridge. These blocks were placed in wet Kaolinite and wet quartz silt and placed in the low-pressure system (table 3). As the soil materials dried out the resistance increased to the end of the experiment. Once the resistance goes above 2 000 000 ohms it is difficult to determine the resistance of these blocks with any precision. At the end of this experiment the soil material was quite dry but probably not as dry as will be expected. These blocks therefore, did not meet the requirements for a moisture sensor.

TABLE 2.- THE RESISTANCE (OHMS) OF NYLON BLOCKS EQUILIBRATED ABOVE WATER AT 20°C, WETTED AND THEN DRIED AT 20 mm Hg

Block number	Above H_2O	Wet	Wet after 2 days	At 20 mm Hg		
				½ hr	1 hr	2½ hr
1	90×10^3	220	180	190	190	5.5×10^6
2	100×10^3	140	190	210	5500	5.5×10^6

TABLE 3.- RESISTANCE (OHMS) OF NYLON BLOCKS IMBEDDED IN WET SOIL MATERIAL AT 16 mm Hg

Material	Time after pumping								
	0	15 min	1.5 hr	3.5 hr	6 hr	8.5 hr	18.5 hr	24 hr	42 hr
Kaolinite	180	180	700	600	45×10^3	140×10^3	275×10^3	500×10^3	2.5×10^6
Quartz silt	15 000	19 000	28 000	31 000	33×10^3	38×10^3	190×10^3	950×10^3	5.5×10^6

The nylon blocks were treated with lithium chloride to determine if this hygroscopic salt would improve the characteristics of the blocks by lowering their resistance, especially in the dry region. The treatment consisted of soaking the blocks in 0.1 molar $LiC\ell$ and allowing them to air dry for 24 hr. The blocks were then equilibrated in a water-saturated atmosphere, then placed in contact with air dry Kaolinite and after a day were put under reduced pressure (Table 4). The $LiC\ell$ did reduce the resistance, but because the blocks did rapidly go above 2 000 000 ohms in the reduced atmosphere even when in contact with air dry Kaolinite, they were eliminated as possible sensors. The fact that $LiC\ell$ impregnated blocks in contact with moist soil could rapidly loose their salt to the soil and change resistance characteristics is also detrimental. It was decided to try a treatment with a lithium-saturated montmorillonite clay that would overcome the possible loss of salt and perhaps also improve the resistance characteristics.

TABLE 4.- RESISTANCE (OHMS) OF LiCℓ TREATED NYLON BLOCKS AIR DRY, AT 100% RELATIVE HUMIDITY, AND IN AIR DRY KAOLINITE AND AT 20 mm Hg

Block number	Air dry	Above H_2O	In air dry Kaolinite at time				1 hr after 20 mm Hg
			0	0.5 hr	1 hr	23 hr	
1	1000	50	100	500	700	6×10^3	3×10^6
2	160	50	100	300	500	10	4.5

The Li-montmorillonite treatment was made by dipping the washed and dried nylon blocks into a dilute clay suspension and allowing them to air dry. Because magnesium clays also have what was thought to be favorable water characteristics, another block was treated with Mg-saturated montmorillonite in a similar way. Results of placing these clay film treated blocks in a water-saturated atmosphere and then in contact with air dry Kaolinite in reduced atmosphere are recorded in table 5. These blocks, especially the Li-montmorillonite, showed enough promise that a series of experiements were performed to test them further, including experiments where the Kaolinite was at equilibrium with an atmospheric pressure of 16 mm Hg (table 6), a rehydration above water (table 7), where kaolinite was dried at 105°C (table 8), and alone at an atmospheric pressure of 10 mm Hg (table 9).

The Mg-montmorillonite-treated blocks had too high a resistance when they dried. This could be caused by the discontinuities that appeared in this film. The Li-montmorillonite-treated block seemed to perform better and would go from the hydrated condition (equilibrium over water) to the dry condition in 1 to 2 hr, which is probably the most extreme change. The final resistance was always less than 1 MΩ, which was encouraging. However, a reading of 650 000 ohms for 0.165% H_2O (table 6) and 450 000 ohms at 0.001% H_2O (table 8) shows that this block was not sensitive to the moisture conditions in the Kaolinite, or the resistance-moisture curve of the block if it existed, changed with time.

The development of the Li-montmorillonite-impregnated block did achieve a block that operates in the resistance and moisture range desired. However, considerable development would be necessary before an operational device could be assured. It appears that the blocks used here had considerable lag because of the amount of water associated with the films. This could no doubt be modified. To start with blocks could be used in an oven-dry condition and the loss in resistance measured when in contact with the reduced atmosphere or relatively dry soil. However, it was felt that dry films would be too fragile for this application.

TABLE 5.- RESISTANCE (OHMS) OF Mg OR Li MONTMORILLONITE TREATED BLOCKS AT 100 RELATIVE HUMIDITY AND IN AIR DRY KAOLINITE AT 20 mm Hg

Treatment	Above H_2O	In air dry Kaolinite at 20 mm Hg					
		10 min	20 min	45 min	1.75 hr	4 hr	26 hr
Li montmorillonite	----	160	960	30 x 10^3	350 x 10^3	500 x 10^3	1 x 10^6
Mg montmorillonite	----	1000	5500	550 x 10^3	1000 x 10^3	1500 x 10^3	5.5 x 10^6

TABLE 6.- RESISTANCE (OHMS) OF Mg OR Li MONTMORILLONITE IMPREGNATED NYLON BLOCKS AT 100% RELATIVE HUMIDITY AND IN KAOLINITE INITIALLY DRIED AT 16 mm Hg

Treatment	Over H_2O	Time in Kaolinite									
		0	3 min	5 min	10 min	15 min	25 min	45 min	1 hr	1.5 hr	2 hr
Li montmorillonite	100	170	----	2 900	11 x 10^3	27 x 10^3	120 x 10^3	500 x 10^3	550 x 10^3	650 x 10^3	650 x 10^3
Mg montmorillonite	260	560	15 000	33 000	550 x 10^3	1750 x 10^3	5500 x 10^3	5500 x 10^3	5500 x 10^3	5500 x 10^3	5500 x 10^3

TABLE 7.- RESISTANCE (OHMS) OF Mg OR Li MONTMORILLONITE IMPREGNATED NYLON BLOCKS FROM TABLE 6 PLACED ABOVE WATER

Treatment	Time above water						
	0	15 min	23 min	30 min	45 min	1 hr	8 hr
Li montmorillonite	650 x 10^3	3 x 10^3	1600	940	640	500	120
Mg montmorillonite	5500 x 10^3	13 x 10^3	8000	5000	26000	1900	300

TABLE 8.- RESISTANCE (OHMS) OF Mg OR Li MONTMORILLONITE-IMPREGNATED NYLON BLOCKS EQUILIBRATED AT 100% RELATIVE HUMIDITY AND PLACED IN KAOLINITE DRIED AT 105°C IN A VESSEL AT 16 mm Hg PRESSURE

Treatment	Time after burial									
	2 min	3 min	5 min	7.5 min	10 min	15 min	30 min	60 min	1.5 hr	2 hr
Li montmorillonite	300	----	3.5 x 10^3	9 x 10^3	18 x 10^3	29 x 10^3	150 x 10^3	340 x 10^3	450 x 10^3	450 x 10^3
Mg montmorillonite	----	25 000	100 x 10^3	250 x 10^3	600 x 10^3	750 x 10^3	1000 x 10^3	1500 x 10^3	2000 x 10^3	2000 x 10^3

TABLE 9.- RESISTANCE (OHMS) OF Mg OR Li MONTMORILLONITE IMPREGNATED NYLON BLOCKS EQUILIBRATED AT 100% RELATIVE HUMIDITY AND PLACED IN VESSEL AT 10 mm Hg PRESSURE

Treatment	Time after burial								
	0	2 min	5 min	10 min	15 min	30 min	45 min	1 hr	1½ hr
Li montmorillonite	120	220	1 x 10^3	25 x 10^3	55 x 10^3	350 x 10^3	450 x 10^3	550 x 10^3	550 x 10^3
Mg montmorillonite	200	1000	150 x 10^3	900 x 10^3	1500 x 10^3	1800 x 10^3	2000 x 10^3	2000 x 10^3	2000 x 10^3

Conclusions: The use of nylon soil moisture blocks in the range of soil moistures found at 10 mb is not feasible. Impregnating the blocks with lithium montmorillonite did improve the resistance range for the dry moisture conditions in this atmosphere but does not seem very promising. At these very dry conditions the resistance block method is quite insensitive and is outside the operating range of the method.

Alternatives would be to use the neutron scatter method, but at these low water contents this method would also be insensitive. The only alternative that seems promising would be the determination of water by a chemical method, especially one that could produce a gas that would give a relatively easy measurement of volume and/or pressure.

Direct Biology

Simple, low-weight instrument (1 lb).-

Physical description of the instrument: The only direct biology life detection instrument meeting the 1-lb restriction that has been developed and tested is the Guilliver IV (ref. 14). On the basis of its relatively advanced status and scientific evaluation, it is proposed for this purpose. The instrument operates on the in situ principle, which offers the following advantages:

1) The problems of sample acquisition are eliminated;
2) The sample is an undisturbed section of the planetary surface;
3) The sample cross-section is extended below the surface layer that might be subject to intense ultraviolet irradiation;
4) The planetary material may act as a chromatographic bed to effect composition and concentration gradients of the applied microbiological medium, thereby increasing the opportunity for the organisms to find some favorable formulation and concentration;
5) A significant decrease in real time to complete the experiment has been demonstrated for this method.

The instrument as constructed (fig. 15) is a cylinder 65 mm by 30 mm in diameter and, with the exception of the umbilical cord, weighs 81 grams. The unit contains all of the components required for the experiment including preliminary data processing of the electrical signals. The primary power source is supplied through the umbilical cord by the spacecraft capsule. The data are sent to the support equipment through this same link. The support equipment is shown in figure 16 and includes the ejection mechanism as well as the signal conditioning circuitry.

An exploded view of the instrument is shown in figure 17. The instrument is shown in stored and deployed modes in figure 18. Table 10 presents the physical characteristics of the instrument.

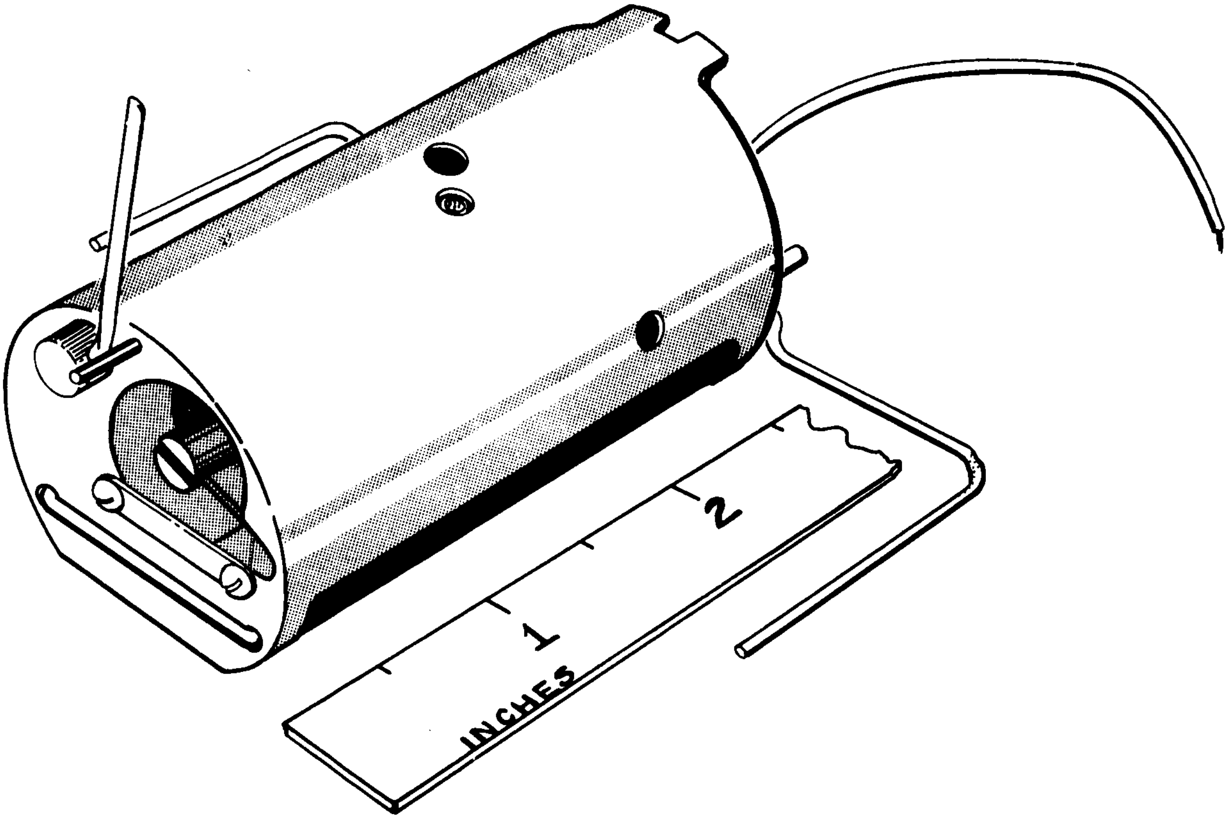

Figure 15.- Gulliver IV, In Situ Model (ref. 14)

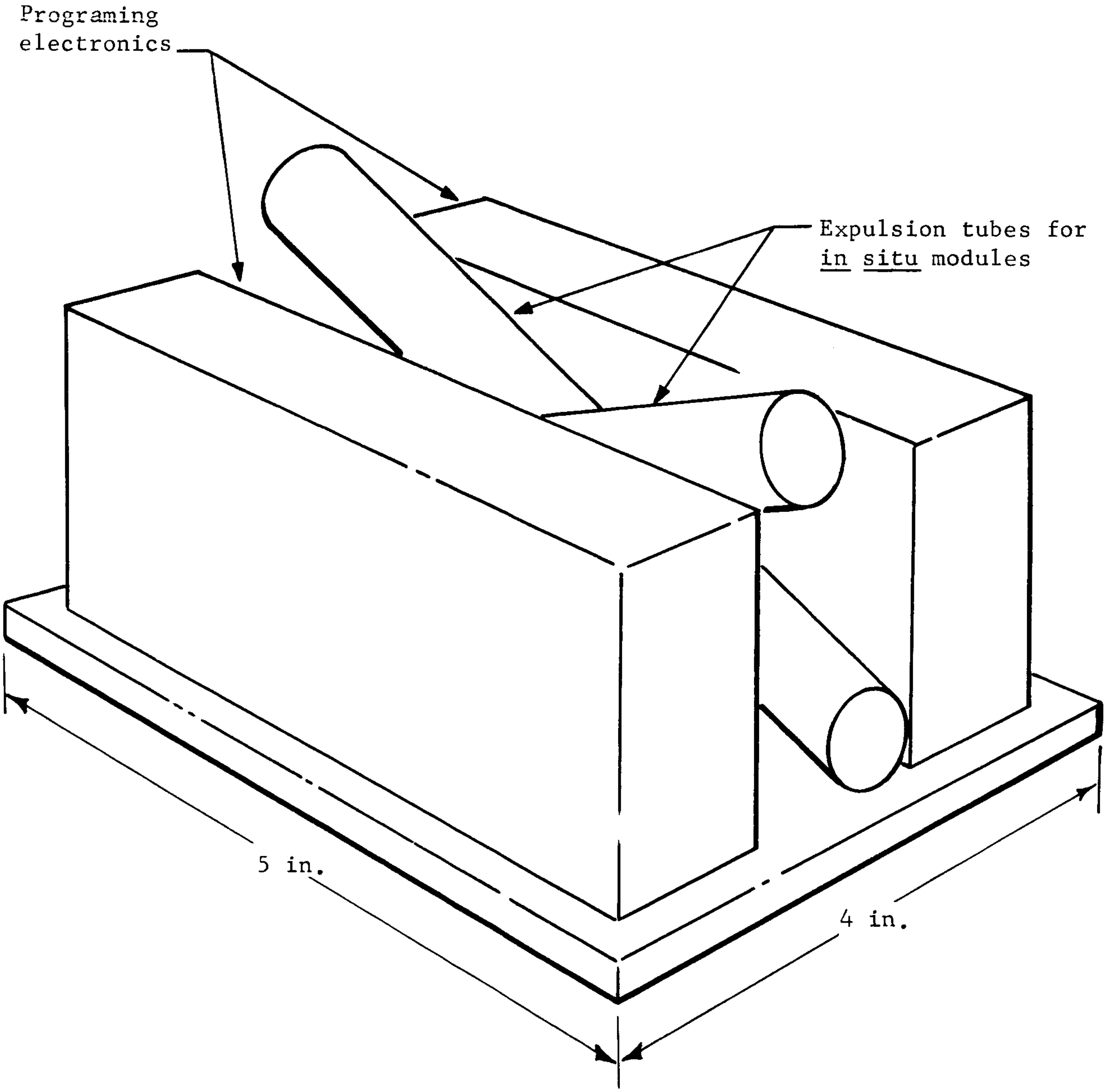
Programing electronics
Expulsion tubes for in situ modules
5 in.
4 in.

Figure 16.- Support Equipment for In Situ Gulliver IV

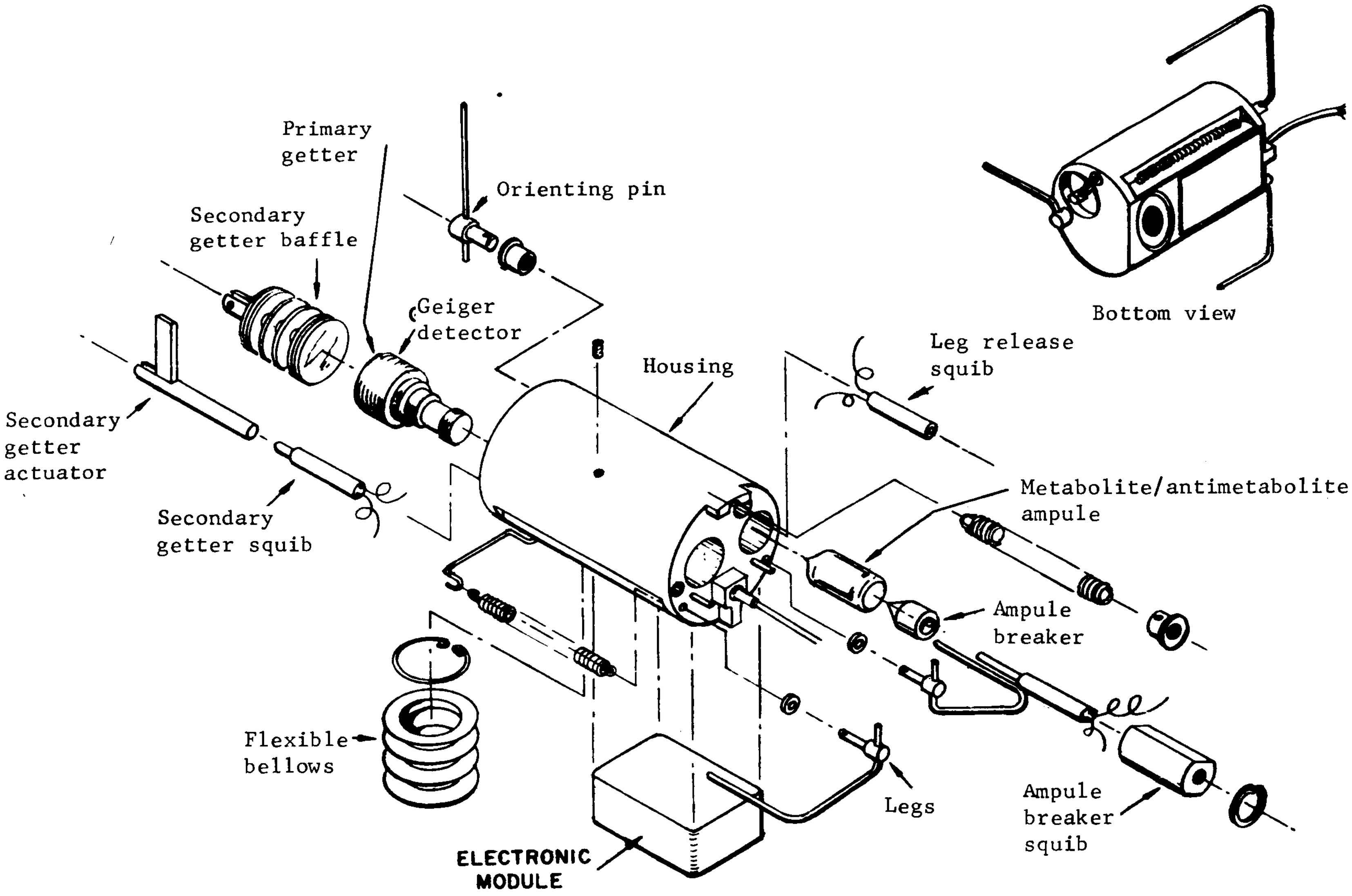
Primary getter
Orienting pin
Secondary getter baffle
Geiger detector
Bottom view
Housing
Leg release squib
Secondary getter actuator
Secondary getter squib
Metabolite/antimetabolite ampule
Ampule breaker
Flexible bellows
Legs
Ampule breaker squib
ELECTRONIC MODULE

Figure 17.- Gulliver IV In Situ Single Chamber Module (ref. 14)

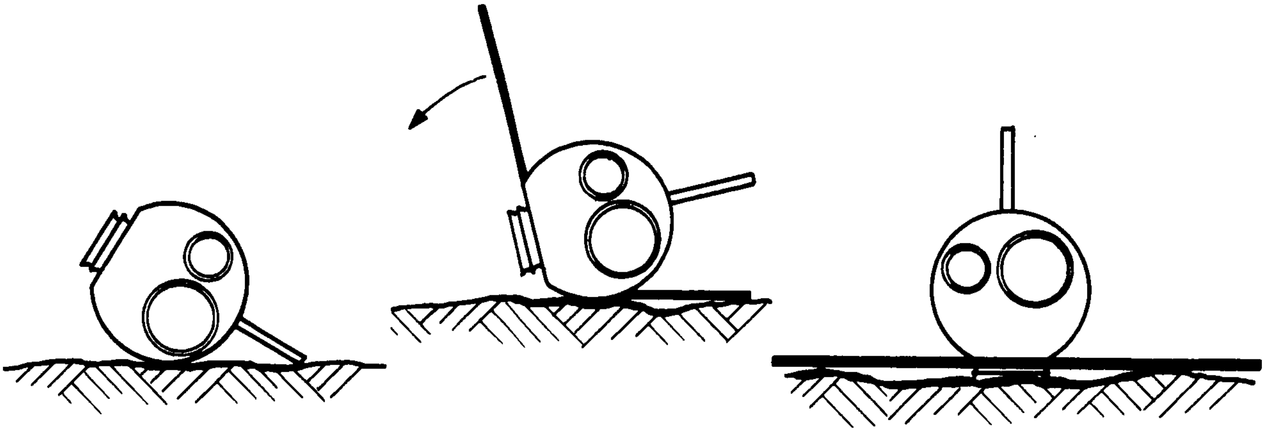

Orientation sequence

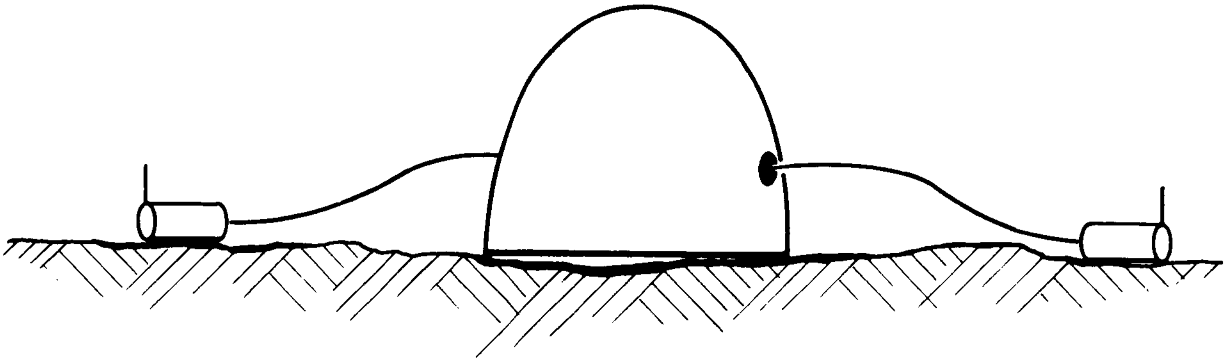

Deployed experiment

Figure 18.- Gulliver IV Deployment

TABLE 10.- GULLIVER IV ENGINEERING AND SCIENCE DATA (FEASIBILITY MODEL)

A. In situ module (2 required)

Size: 1.187 in. diam., 2.250 in. long
Weight: 81 grams
Instrument power: 24 Vdc @ 57 mA (operating)
Signal: 2 V pulse, 5 μsec wide for each GM response
Average power: 1.4 W for instrument, 5 W maximum for temperature control to prevent sample field from freezing.

B. Support equipment (expulsion of modules, program activation and readout, and data interface)

Size: 5 in. long, 4 in. wide, and 4 in. high.
Weight: 300 grams with 5 ft of umbilical cord to each module
Power: 24 Vdc @ 100 mA (operating) 2.4 W
Peak power: 24 V @ 1 A
Readout sequence: One minute integrated readings taken at: background, 0, 1, 2, 4, 8, 16, 32, 64 (1:04 hr), 128 (2:08 hr), 256 (4:16 hr), 512 (8:32 hr), 1024 (17:04 hr), 2048 (34:08 hr), and 4096 (68:16 hr) minutes.

Output signal: Voltage proportional to log of counts-per-minute (cpm) covering five decades: 1 cpm = 0 V, 10 cpm = 2 V, 100 cpm = 4 V, 1000 cpm = 6 V, 10 000 cpm = 8 V, 100 000 cpm = 10 V. Analog voltage signal is supplied for conversion by capsule's central data processor and ADC to 10 bit data. Fifteen readout cycles include the background measurement for each module for a total of 30 cycles (two modules) with a total of 300 bits required for the data, not including programer readout. Programer may be included for less than 700 total bits.

Programer: Provides entire program: expulsion, module, orientation, ampule material release, getter positioning, and all readout cycles shown above.

Operational description: After the capsule comes to rest on the planetary surface, the two Gulliver IV instruments will be ejected from the capsule and land on the planetary surface. Ejection will be in opposite directions to avoid entangling of the umbilical cords. As the instruments leave the ejection cylinders, spring-loaded orienting pins will pop out to prevent them from landing directly on their backs. After each instrument stops rolling, the first squib fires to release the self-erecting legs and complete the orientation of the module so that the bellows come in contact with the planetary surface to form the reaction chamber. A background radiation measurement will then be made to serve as a baseline. The second squib will then fire, breaking the ampule containing, in the case of the test unit, the medium, and, in the case of the control unit, the medium-antimetabolite mixture. These liquids will now be conducted to the surface through wicks. After application of the radioactive liquid, a 4-min period will be permitted for the secondary getter to collect the nonmetabolic $C^{14}O_2$ which might have evolved in the medium during the 8-month space journey. When the 4-min period expires, the third squib will fire and cause the secondary getter to slide out of the reaction chamber, removing it from view of the Geiger tube exposed by this same action. The exposure of the Geiger tube presents the primary getter surface, which is a thin layer on the tube window, to the chamber for the collection of metabolically evolved $C^{14}O_2$. As soon as the primary getter is exposed, a zero-time reading will be made to serve as a reference point for the experiment. During the course of the experiment, heating units will be used to ensure against freezing of the surface in the growth chamber. The temperature control will be mediated by a thermister that will not call for heat when the ambient temperature is such that the liquid will not freeze. Readouts of both instruments will be made on a binary time sequence. The readings, 1 min in duration, will be taken at the following minutes after initiation of the experiment: 1, 2, 4, 8, 16, 32, 64, 128, 256, 512, 1024, 2048, and 4096.

Evidence for life would consist of a rising level of radioactivity readings with time, preferably at an exponential rate. This evidence would be confirmed by a comparison between the test and control units if the latter showed inhibition caused by the antimetabolite.

Developmental plan and effort leading to the mission-qualified instrument:

Present state of instrument development: The Mark IV Gulliver has been developed to the point where a full-scale, functional breadboard instrument has been designed, fabricated, and briefly tested after being placed on the soil surface. The performance of the flight-configuration unit was good, but some design changes could improve the instrument.

The operational sequence is shown in table 11.

TABLE 11.- GULLIVER IV OPERATIONAL SEQUENCE

1. Capsule lands on surface of Mars and comes to rest.
2. The two in situ modules are ejected in opposite directions, 5 ft from the capsule.
3. When the modules stop rolling, the orienting pin prevents the module from coming to rest with the bellows directly up.
4. The first squib releases the legs and orients the module so that the bellows now are in contact with the soil and seal the reaction chamber from the Mars atmosphere.
5. A 1-min background radiation measurement is made.
6. The second squib breaks the metabolite/antimetabolite ampule, allowing the medium to diffuse to the soil through a wick.
7. The secondary getter is allowed to collect the nonmetabolic $C^{14}O_2$ for 4 min after which time the third squib moves this getter so that the primary getter is exposed.
8. The zero time 1-min reading is made.
9. Readout of one minute integrals are continued at 1, 2, 4, 8, 16, 32, 64, 128, 256, 512, 1024, 2048, and 4096 min.

Design development effort: The principal recommended design change is the enlargement of the growth chamber. This can be accomplished by using a larger diameter bellows. A heating system must be incorporated to prevent freezing of the liquid medium during the test. The design will include the latest technological developments, particularly from the standpoint of materials selection. The instrument must be designed to withstand the terminal heat sterilization cycle.

A rapid sequential development of two or three breadboards is recommended to maximize the benefit of breadboard experience. It is necessary to construct one, then carefully analyze it, and incorporate apparent improvements into the next breadboard. The actuation and readout techniques should also be optimized. Each breadboard will be tested biologically and environmentally.

Each breadboard model will be placed through a complete field test requiring the operation of all electromechanical and electronic components. The sensitivity of the units will be measured against laboratory procedures using the same soil and medium. The efficiency of the unit from the standpoint of the total system will be determined in this manner. Data will thus be developed to define the necessary tradeoff between sensitivity and operation.

Prototype unit: Following final development of the breadboard model, ten prototype units should be fabricated simultaneously.

Two of the prototype units will be used to conduct expulsion and landing tests. These tests will permit a statistical determination of the reliability of the instrument in ejection and self-orientation.

Four of the units, two as test and two as controls, will be used to determine the constancy, accuracy, and reliability of data that are obtained. Biological tests will be conducted in the laboratory and field with carefully prepared pure and mixed cultures. Comparisons will also be made with the laboratory Gulliver procedure.

Four units will be used in the environmental testing program. These tests are to simulate capsule launch, space transit, Mars landing, exposure to the Mars environment, and long-term storage in the spacecraft environment. The latter study should be conducted using accelerated storage techniques.

Qualification units (mission qualification): It is recommended that, following successful prototype development and testing, a subcontract be negotiated for the manufacture of 16 qualification units. The subcontract should be to a firm experienced in the fabrication of spacecraft qualification instruments with experience in biological as well as physical quality control.

The qualification units should be placed through the same series of tests as was described for the prototype units.

The sequence of events for the entire developmental program presented here is described in the flow diagram shown in figure 19.

Complex, higher-weight instrument (10 lb).-

Physical description of the instrument: A Multiple-Experiment Detection System (MELDS) can be developed for the proposed 1973 Mars mission. This system would be comprised of a Wolf trap, a multivator, and an hν Gulliver. Figure 20 shows the major components of the instrument that integrates these experiments into a single system. Details are presented in table 12.

Basically, the MELDS consists of two growth chambers which are physically and optically isolated from each other. Each chamber is filled with 20 ml of growth media to which 2 cm^3 of Mars "soil" are added. The temperature of the media is monitored with a thermistor probe and is controlled to prevent freezing in the chambers. One of the chambers is used as a control and contains the same ingredients as the test chamber except an antimetabolite is also included. The MELDS is a self-contained instrument and accepts soil from the soil sampling and distributing equipment.

After receiving the soil, the MELDS seals itself from the Mars atmosphere and is pressurized to a few hundred torr so that the liquid in the growth medium will not boil or evaporate. The experiments are cycled automatically through the light and dark cycles with one data point being taken for each experiment during each cycle.

Wolf trap: The Wolf trap is described thoroughly in several recent articles (refs. 15 and 16). The MELDS monitors the changes in turbidity and acidity in each growth medium.

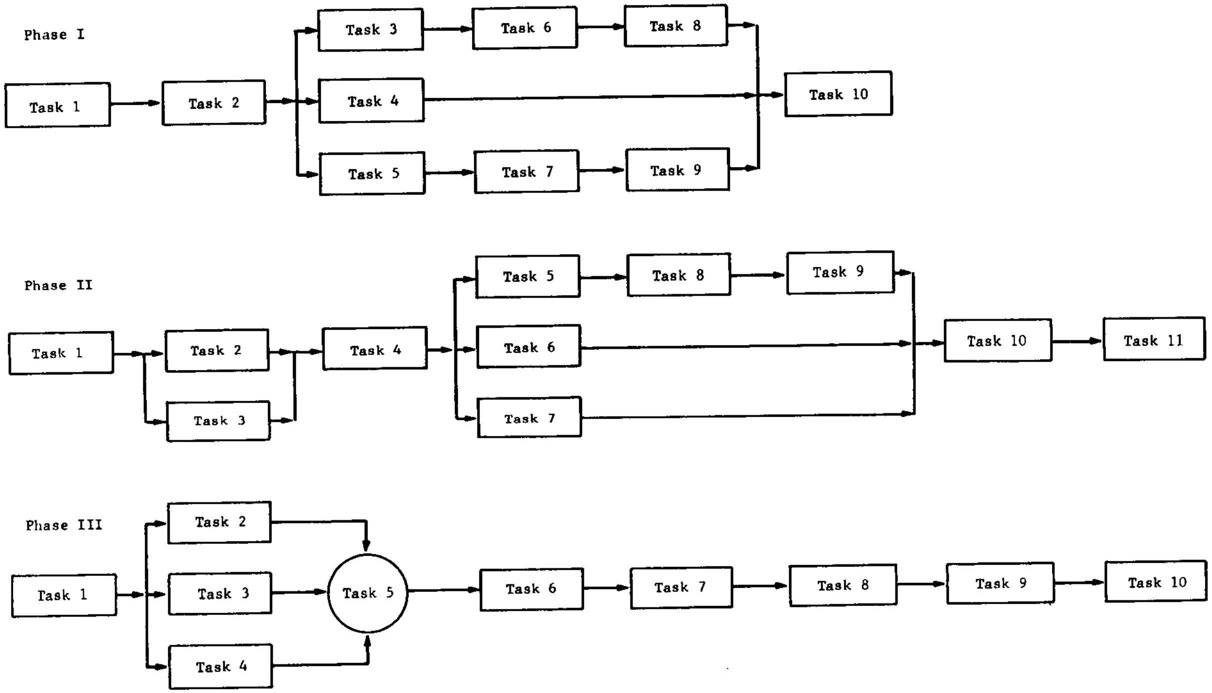
Phase I
Task 1
Task 2
Task 3
Task 4
Task 5
Task 6
Task 7
Task 8
Task 9
Task 10
Phase II
Task 1
Task 2
Task 3
Task 4
Task 5
Task 6
Task 7
Task 8
Task 9
Task 10
Task 11
Phase III
Task 1
Task 2
Task 3
Task 4
Task 5
Task 6
Task 7
Task 8
Task 9
Task 10

Phase I - Demonstrate and evaluate techniques

Tasks
1 Establish Mars mission profile
2 Establish instrument performance requirements
3 Design breadboard to incorporate latest technology
4 Perform biochemistry verification of method
5 Design support equipment and signal conditioning
6 Test for biology verification
7 Construct breadboard
8 Test for environmental parameters
9 Test breadboard
10 Technical review of entire system

Phase II - Prototype development

Tasks
1 Define design constraints
2 Perform instrument system analysis
3 Design testing and evaluation program
4 Incorporate latest parameter to prototype design
5 Construct prototype modules
6 Construct prototype support equipment
7 Establish latest biochemistry operating parameters
8 Test module launch system and environment
9 Test data recovery technique and repeatability
10 Perform environmental testing of system
11 Technical review of prototype design

Phase III - Qualification unit development

Tasks
1 Incorporate latest technology in design
2 Release modules to manufacturing
3 Release support equipment to manufacturing
4 Release data output specification to prime contractor
5 Assemble system
6 Perform acceptance tests
7 Perform calibration tests
8 Life testing program
9 Qualification design review
10 Final report preparation

Figure 19.- Development Program Flow Diagram for Gulliver IV Qualification

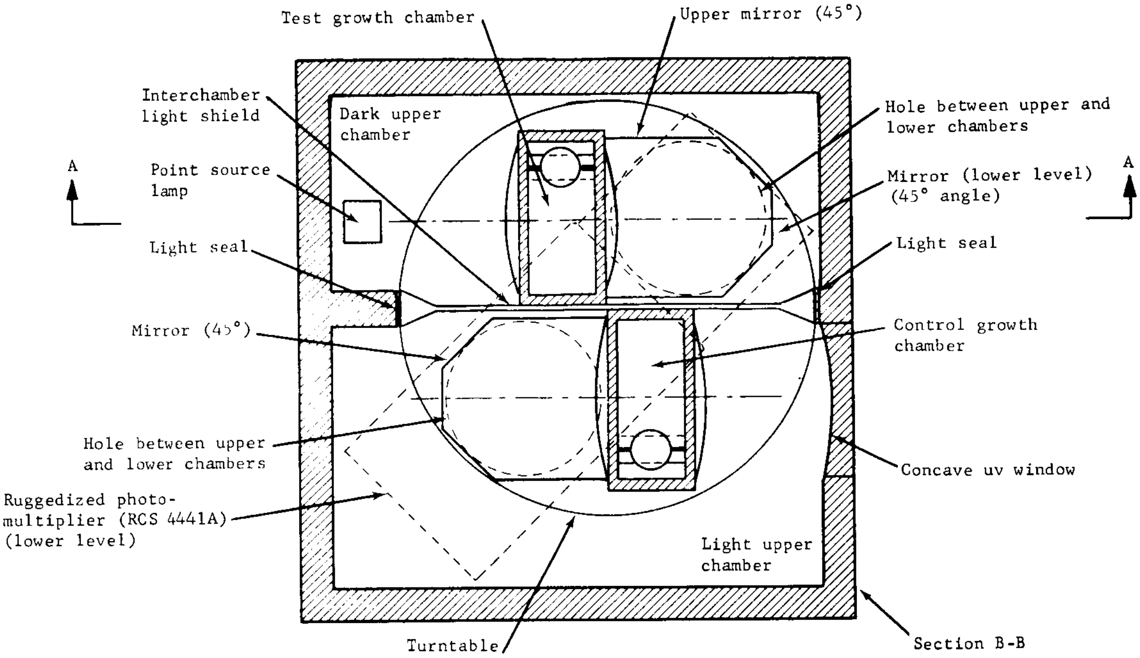
Test growth chamber
Upper mirror (45°)
Interchamber light shield
Dark upper chamber
Hole between upper and lower chambers
A
Point source lamp
Mirror (lower level) (45° angle)
A
Light seal
Light seal
Mirror (45°)
Control growth chamber
Hole between upper and lower chambers
Concave uv window
Ruggedized photo-multiplier (RCS 4441A) (lower level)
Light upper chamber
Turntable
Section B-B

(a) Top view

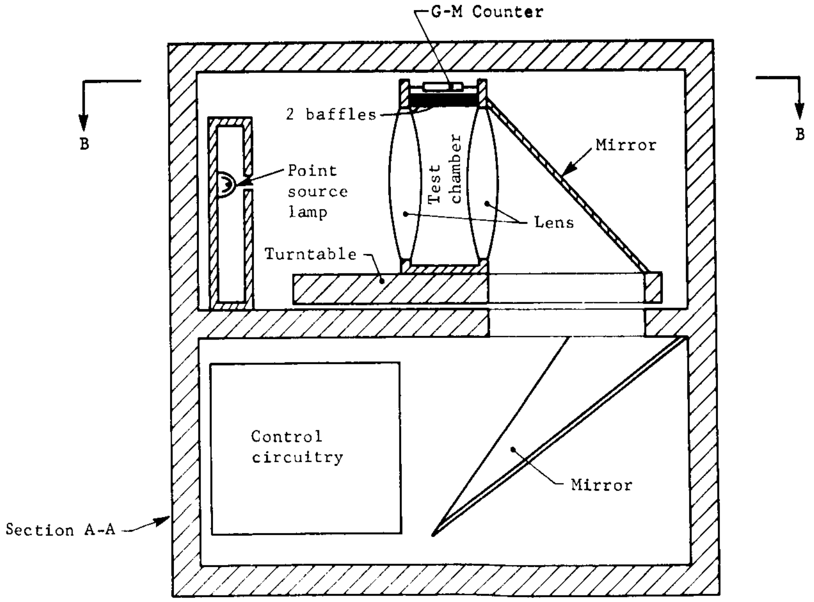
G-M Counter
2 baffles
B
B
Mirror
Point source lamp
Test chamber
Lens
Turntable
Control circuitry
Mirror
Section A-A

(b) Cross-sectional view

Figure 20.- Multiple Experiment Life Detection System

TABLE 12.- MELDS ENGINEERING AND SCIENCE DATA

Size: 5 in. long, 5 in. wide, 5 in. high

Weight: Less than 10 lb

Power: Average power is less than 10 W from 24 Vdc.
Peak current is less than 2 A for turntable motor.

Temperature Control: Maintains growth chamber medium above freezing.

Output Signals: Voltage pulse with amplitude proportional to the measurement. Pulse width is adjustable to accommodate requirements of capsule's central data processer and ADC. The measurement is:

Wolf trap signal:
1) Voltage of lamp excitation;
2) Voltage proportional to medium temperature;
3) Voltage proportional to medium pH.

Multivator signal: Voltage proportional to log of fluorescence (photoanode current). 10^{-10} A=0 V, 10^{-9} A=2 V, 10^{-8} A=4 V, 10^{-7} A=6 V, 10^{-6} A=8 V, 10^{-5} A=10 V.

hν Gulliver: Voltage proportional to log of counts-per-minute covering five decades: 1 cmp=0 V, 10 cmp=2 V, 100 cmp=4 V, 1k cmp=6 V, 10k cmp=8 V, 100k cmp=10 V.

ADC should be at least 6 bits of data and preferably 7 or 8 bits. Since there are about 250 data points, a 6-bit convertor would yield 1500 bits for the total 3-day experiment, not including identification codes or programer status of the operation, which may be included for an additional 1000 bits. Also, an integrated light flux for the photosynthesis experiment may be included for an additional 200 bits.

Programer: Provides entire programing: soil inclusion, media transfer, pressurization of instrument, rotation of chamber turntable (for light and dark cycling), readout of GM counters, programing of light sources, readout of photomultiplier, and providing necessary analog signal conditioning.

Readout sequence: See table 13.

TABLE 13.- MELDS OPERATIONAL SEQUENCE (AFTER LANDING ON MARS)

Step no.	Chamber	Time required	Total time lapse	Operation description
1	Test	1 min	0:01	Background radiation and temperature measurement
2	Control	1 min	0:02	Background radiation and temperature measurement
3	Test	5 min	0:07	Add soil and metabolite
4	Control	5 min	0:12	Add soil and metabolite and seal experiment (200 torr)
5	Test	1 min	0:13	2nd background radiation measurement
6	Control	1 min	0:14	2nd background radiation measurement
7	Test	½ min	0:14.5	Turbidity measurement (with temperature and pH)
8	Test	½ min	0:15	Fluorescent measurement
9	----	1 min	0:16	Rotate chambers
10	Control	½ min	0:16.5	Turbidity measurement (T + pH)
11	Control	½ min	0:17	Fluorescence measurement
12	Test	½ hr	0:47	Photosynthesis from ambient light
13	Test	1 min	0:48	Radiation measurement
14	Control	1 min	0:49	Radiation measurement
15	Control	½ min	0:49.5	Turbidity measurement (T + pH)
16	Control	½ min	0:50	Fluorescence measurement
17	----	1 min	0:51	Rotate chambers
18	Test	½ min	0:53	Turbidity measurement (T + pH)
19	Test	½ min	0:54	Fluorescence measurement
20	Control	½ hr	1:24	Photosynthesis from ambient light
21	Test	1 min	1:25	Radiation measurement
22	Control	1 min	1:26	Radiation measurement
23	Test	½ min	1:26.5	Turbidity measurement (T + pH)
24	Test	½ min	1:27	Fluorescence measurement
25	----	1 min	1:28	Rotate chamber
26	Control	½ min	1:28.5	Turbidity measurement (T + pH)
27	Control	½ min	1:29	Fluorescence measurement
28	Test	½ hr	1:59	Photosynthesis for ambient light

TABLE 13.- MELDS OPERATIONAL SEQUENCE (AFTER LANDING ON MARS)-Concluded

Step no.	Chamber	Time required	Total time lapse	Operation description
29	Test	1 min	2:00	Radiation measurement
30	Control	1 min	2:01	Radiation measurement
31	Control	½ min	2:01.5	Turbidity measurement (T + pH)
32	Control	½ min	2:02	Fluorescence measurement
33	----	1 min	2:03	Rotate chambers
34	Test	½ min	2:03.5	Turbidity measurement (T + pH)
35	Test	½ min	2:04	Fluorescence measurement
36	Control	½ min	2:34	Photosynthesis from ambient light
37	Test	1 min	2:35	Radiation measurement
38	Control	1 min	2:36	Radiation measurement
39	Test	½ min	2:36.5	Turbidity measurement (T + pH)
40	Test	½ min	2:37	Fluorescence measurement
41	----	1 min	2:38	Rotate chambers
42	Control	½ min	2:38.5	Turbidity measurement (T + pH)
43	Control	½ min	2:39	Fluorescence measurement
44	Test	1 hr	3:39	Photosynthesis from ambient light
45 to 75	----		7:00	Repeat steps 13 to 43 except photosynthesis time is increased to 1 hr
76	Test	2 hr	9:00	Photosynthesis from ambient light
77 to 107	----		15:21	Repeat steps 13 to 43 except photosynthesis time is increased to 2 hr
108	Test	4 hr	19:21	Photosynthesis from ambient light
109 to 139			31:42	Repeat steps 13 to 43 except photosynthesis time is increased to 4 hr
140	Test	4 hr	35:42	Photosynthesis from ambient light
141 to 171			48:03	Repeat steps 109 to 139
172	Test	4 hr	52:03	Photosynthesis from ambient light
173 to 203			64:24	Repeat steps 109 to 139
204		4 hr	68:24	Photosynthesis from ambient light
205 to 220			72:36	Repeat steps 109 to 124

Turbidity is measured with scattering of a parallel light beam as it passes through the growth chambers. The optics are so designed that, when no scattering elements are present, all the light is focused on a small (0.2 in.) occulting disc that is positioned at the center of the photocathode. As light scattering commences and increases the medium, the control circuitry for the light source reduces the light intensity so that the luminous flux impinging on the photocathode is kept at a constant value. In this manner, the lamp power signal is then a direct measurement of the turbidity.

The acidity of the medium is measured with a sturdy pH detector and is monitored sequentially with the turbidity measurement.

Multivator: The multivator experiment proposed for the MELDS is the detection of the enzyme phosphatase by fluorimetry. Several recent articles describe this experiment (refs. 17 and 18).

The MELDS measures enzymatic dephosphorylation of a complex included in the growth medium. The complex is labeled so that the liberated phosphate portion becomes fluorescent. The appearance of this fluorescent material is evidence for the enzymatic reaction. This measurement is made by illuminating the medium with ultraviolet radiation and measuring the reemitted fluorescent radiation with a photomultiplier. The quantity of fluorescence is determined once during each cycle and for both the control and test chambers.

The $h\nu$ Gulliver: The $h\nu$ Gulliver is a combination of the Gulliver III and the heterotrophic-photosynthesis experiment. These experiments have been described in several articles (refs. 14, 19, and 20).

In this experiment, radioactive carbon labeled substrates has been included in the aqueous growth media. As organisms consume the substrates, labeled carbon dioxide is evolved from the medium and is collected on a getter surface of a Geiger-Mueller counter tube. The radioactivity thus accumulated is periodically monitored as evidence for heterotrophic life. The growth chambers are alternately exposed to light and dark. If photosynthetic life forms are present, they will release $C^{14}O_2$ in the dark and fix it in the light. These changes will be reflected in the measurements of the cumulative radioactive levels on the getters.

The increments of activity accumulated in the light are indicative of heterotropic metabolism, and any increase in the rate occuring in the dark is attributed to the endogenous respiratory release of fixed $C^{14}O_2$ by photosynthetic organisms. The data are compared to those from the inhibited controls. Figure 21 shows a typical response of this experiment.

Operational description: After the capsule comes to rest on the surface of Mars, the MELDS must wait to receive soil from the sampler. During this waiting period, the instrument is programed to take background radiation and temperature measurements to establish baselines for the experiments.

On receipt of the soil sample, the MELDS measures out a 2 cm^3 portion that is added, along with 20 ml of medium, to each growth chamber. An antimetabolite is included in the control chamber so that the experiments will have a reference point for each measurement.

After the soil sample has been brought into the instrument, all openings are sealed from the Mars atmosphere and the entire instrument is pressurized to a few hundred torr. This must be done so that the vapor pressure of the fluid in the medium will not be significant and interfere with the instrument's operation.

When the MELDS growth chambers have been loaded, the experimental measurements begin (as shown in table 12) with another measurement of the radiation background. This will help to determine if any radioactive substances were added to the MELDS interior during soil sampling.

As the experimental measurements continue, the various detectors are read out sequentially for each experiment. The test and control growth chamber are alternately exposed to the sunlight. Sunlight is brought into the MELDS through a concave window. A turntable allows the chambers to be positioned either in the sunlight or in the dark where the turbidity and fluorescence measurements are made.

At the end of each data cycle, an analog signal is sent to the capsule's central data processer for analog-to-digital conversion. The analog data may be temporarily stored in a sample-and-hold circuit if necessary.

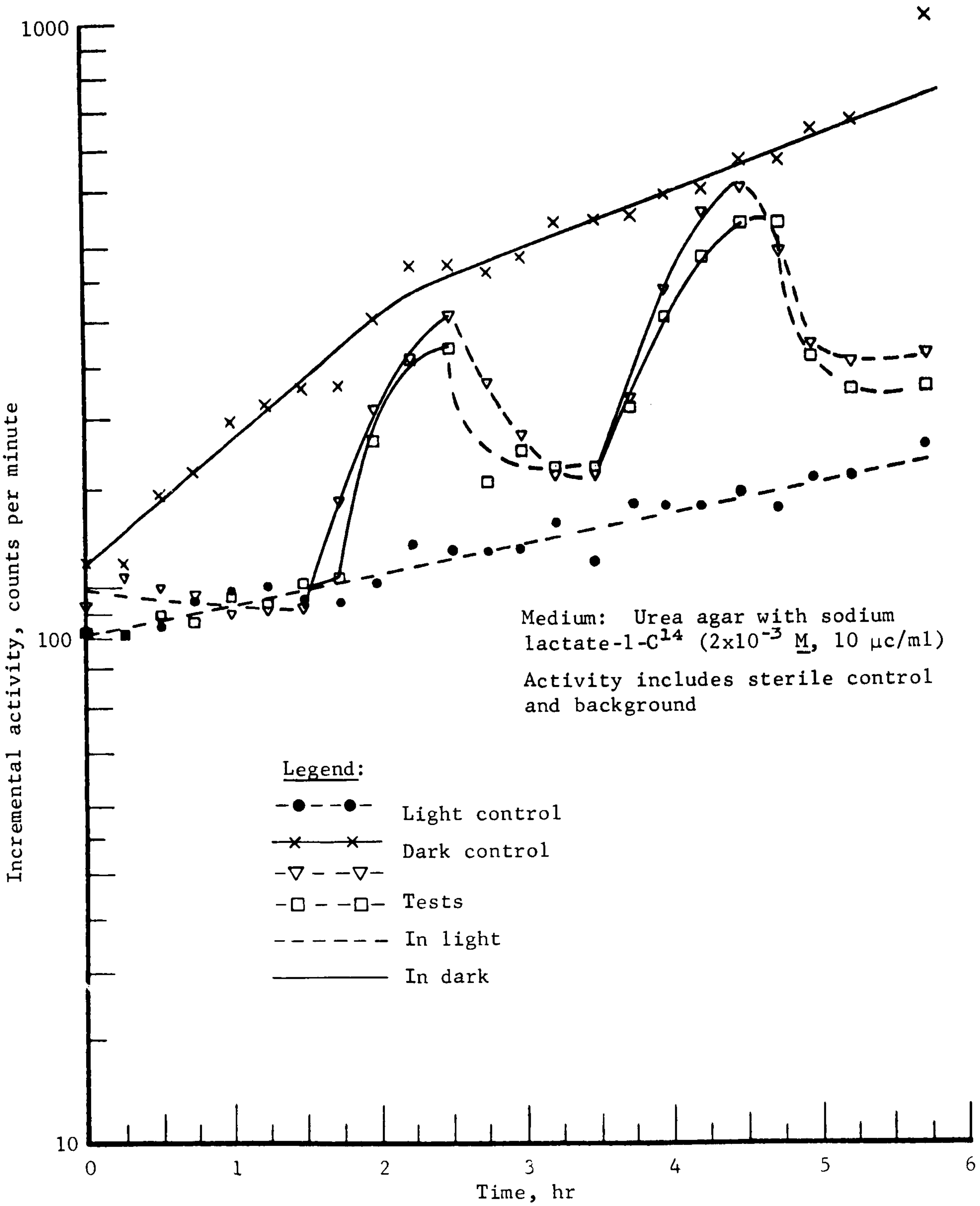

Figure 21.- $C^{14}O_2$ Evolved by Chlorella Pyrenoidosa in Response to Light and Dark Growth Cycles (from ref. 20)

The bite size of the ADC is critical in that a 6-bit bite will give only a 20% accuracy on the five-decade log readout experiments. A 7-bit bite size will result in a 10% accuracy and an 8-bit bite, 5%. The bite size is critical if limitations are made on the total number of data bits from the MELDS. A 6-bit bite size with 250 data points yields 1500 bits of data for the experimental measurements only. This does not include any identification codes or programer monitoring.

It is recommended that 3000 bits of data be allowed in this experiment.

Developmental plan and effort leading to mission qualified instrument:

Present state of instrument development: The higher-weight instrument described in this report is a new concept integrating several experiments that have been under development. However, no breadboard or other instrumentation of this combined unit has yet been attempted. Hardware for the individual experiments has been developed to varying degrees.

The sample-acquiring Gulliver Mark III has been breadboarded and successfully field tested under a wide variety of conditions.

The photosynthetic or hν experiment has been developed and tested in the laboratory. In addition, a rudimentary breadboard of this instrument was built using a grain of wheat lamp as the light source. However, this instrument has not been field tested.

The Wolf trap experiment has gone through two generations of breadboard instrumentation. Considerable laboratory testing has been done using this technique and one of the breadboards has been field tested under a wide variety of conditions. Initial steps have been taken toward the development of a miniature Wolf trap that may weigh as little as 1 lb.

The multivator experiment has also gone through two generations of breadboard development. Extensive laboratory efforts have been made to define the specific experiments to be performed by the unit. The principle candidate experiment is the one in which extraterrestrial phosphatase would be detected through fluorescence that appears in one of the molecular fractions of an ester after it is split by the enzyme.

Some problems with the experiment remain to be solved and no field tests of the instrument have been made.

Design development effort: Concerted scientific work and engineering efforts are required to develop the desired aspects of the experiments and instrument to an acceptable point.

If time permits, as many as three breadboard models of the instrument will be serially developed as described for the low-weight instrument.

The test program will include operational, biological, and environmental tests of the instrument as well as of the programing and data systems.

Prototype units: Five prototype units will be constructed for this phase.

One of the prototype units will be used for testing the interface with the planetary surface to evaluate sample acquisition. Two of the units, one test and one control, will be used in a series of experiments designed to test the reliability, accuracy, and repeatability of the measurements. Two other units will go through the environmental testing program as described for the low-weight instrument.

Qualification units (mission qualification): Eight qualification units should be constructed under subcontract to be let in similar fashion to that described for the low-weight instrument.

Five units should be put through the same test described for the prototype units. The remaining three units should be held in reserve for contingency problems that might arise.

The flow sheet in figure 22 depicts the entire developmental plan.

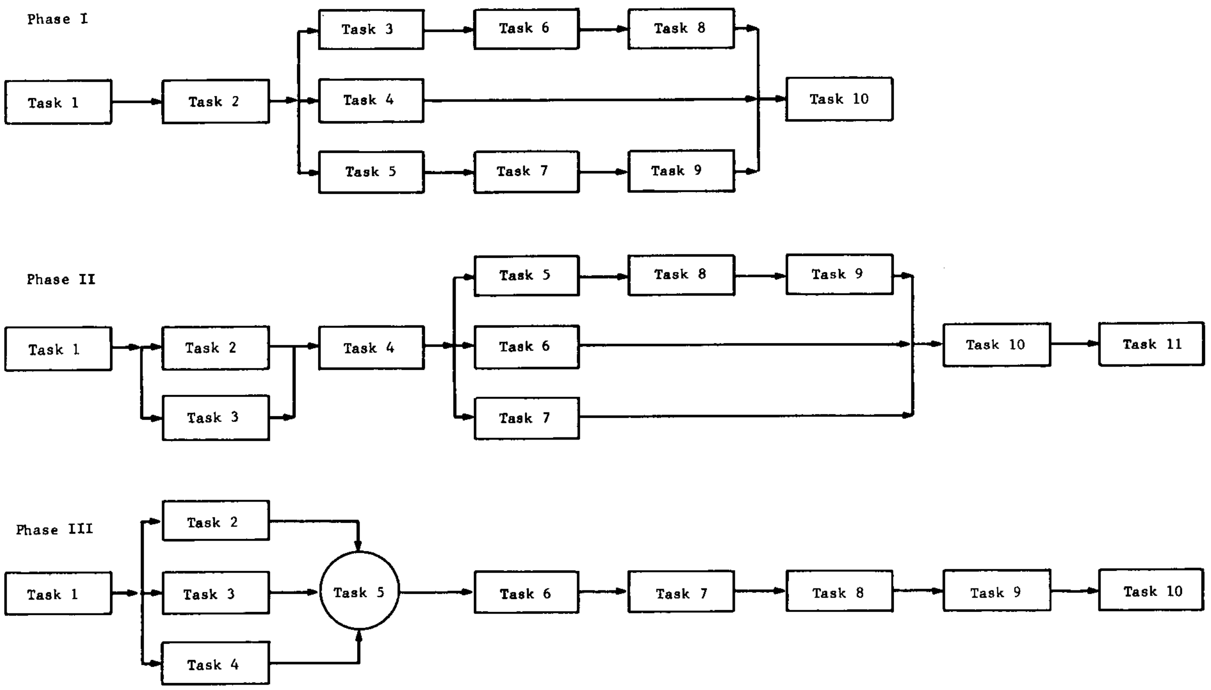
Phase I
Task 1
Task 2
Task 3
Task 4
Task 5
Task 6
Task 7
Task 8
Task 9
Task 10
Phase II
Task 1
Task 2
Task 3
Task 4
Task 5
Task 6
Task 7
Task 8
Task 9
Task 10
Task 11
Phase III
Task 1
Task 2
Task 3
Task 4
Task 5
Task 6
Task 7
Task 8
Task 9
Task 10

Phase I - Demonstrate and evaluate techniques

Tasks
1 Establish Mars mission profile
2 Establish instrument performance requirements
3 Design breadboard to combine experiments
4 Perform biochemistry to verify combined operation
5 Design support system
6 Test for biology verification
7 Construct breadboard
8 Test for environmental parameters
9 Test breadboard
10 Technical review of entire system

Phase II - Prototype development

Tasks
1 Define design constraints
2 Perform instrument system analysis
3 Design testing and evaluation program
4 Incorporate latest parameter to prototype design
5 Construct prototype MELDS chambers and readout
6 Construct prototype MELDS support system
7 Test design of soil/medium transfer system
8 Test combined MELDS components
9 Test data recovery technique and repeatability
10 Perform environmental testing of system
11 Technical review of prototype design

Phase III - Qualification unit development

Tasks
1 Incorporate latest technology in design
2 Release mechanical hardware to manufacturing
3 Release readout and programing design to manufacturing
4 Release data output specification to prime contractor
5 Assemble system
6 Perform acceptance tests
7 Perform calibration tests
8 Life testing program
9 Qualification design review
10 Final report preparation

Figure 22.- Development Program Flow Diagram for MELDS Qualification

Environmental Considerations

The expected environmental effects of the radioisotope heaters were studied in reference 21.

The following radiation limits obtained from Dr. C. R. Weston* are used as a criterion for judging the severity of radiation levels from radioisotope heaters onboard the lander.

Phase of mission	Estimated upper limit of tolerable radiation
During flight. Limits are based on photodiodes in the Wolf trap instrument.	10^{13} neutron/cm^2. 10^7 Roentgen gamma
During operation of biology instrument after landing. Limits are based on biological considerations.	10^6 neutron/cm^2 10^3 Roentgen gamma

The curves in figure 23 show the neutron and gamma ray environments due to the four 50 W isotope heaters (fig. 24) assuming $Pu^{238}O_2$ as the fuel. The doses shown were calculated assuming a $1/R^2$ dependence of particle flux with distance, a good assumption at the distances involved. Doses due to the four heaters were superimposed. Inflight doses are considerably under the criteria of 10^{13} n/cm^2 and 10^7r. The landed gamma criteria of 10^3r is likewise no problem. However, the landed criteria of 10^6 n/cm^2 is exceeded after 1 day of operation, provided the standard $PU^{238}O_2$ fuel is used. If, however, the O^{17} and O^{18} isotopes are removed from the fuel a factor of 11 reduction in neutron fluence is obtained, as shown. These isotopes produce most of the neutrons through (α,n) reactions. An additional factor of 10 reduction is possible using a shield consisting of about 6.5 in. of LiH.

Table 14 assesses the allowable radiation levels and the primary effects on several of the principal science instruments. Table 15 summarizes the primary effects.

---

*Professor of Biology, San Fernando Valley State College, formerly with the University of Rochester.

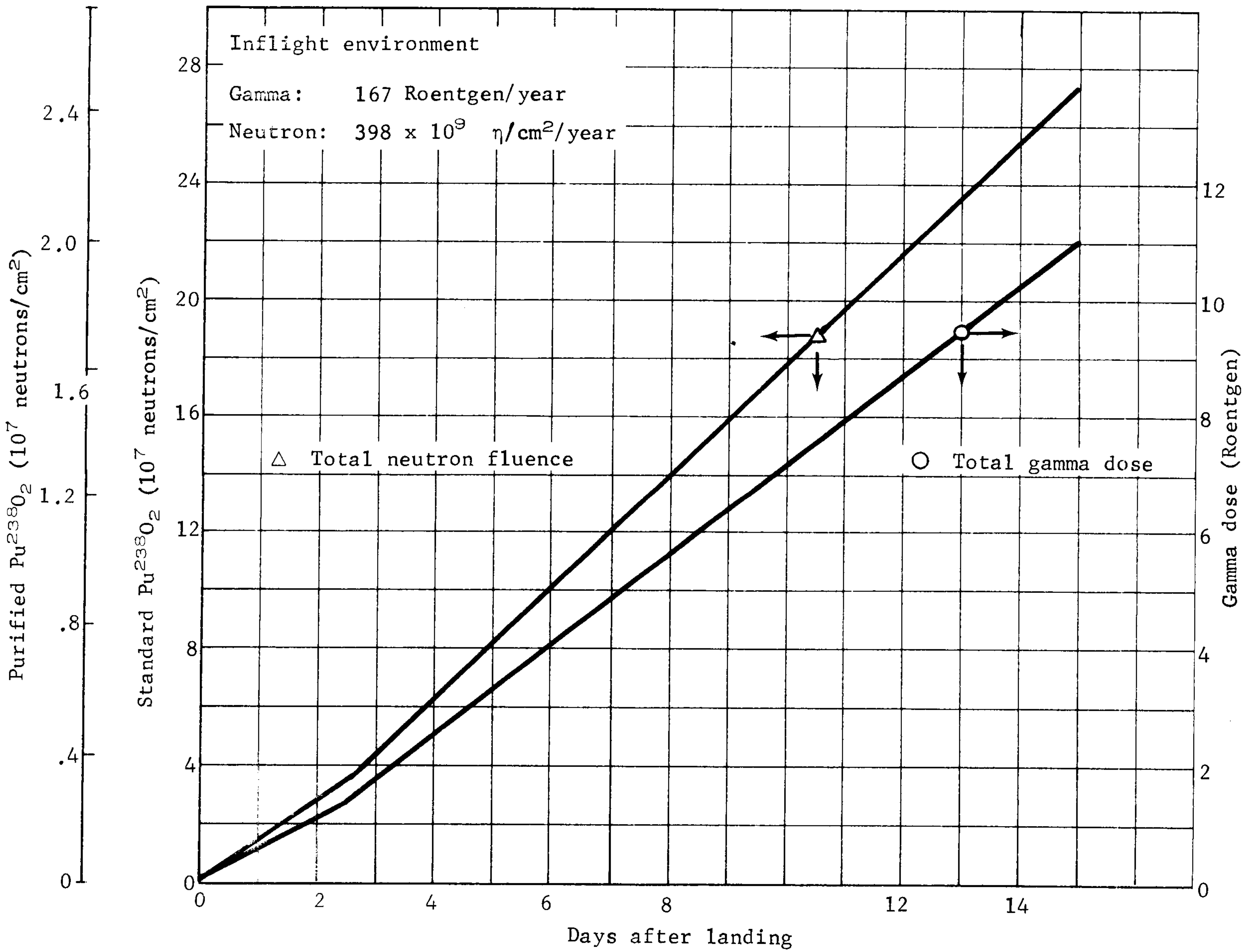

Figure 23.- Radiation Environment of Biology Instrument

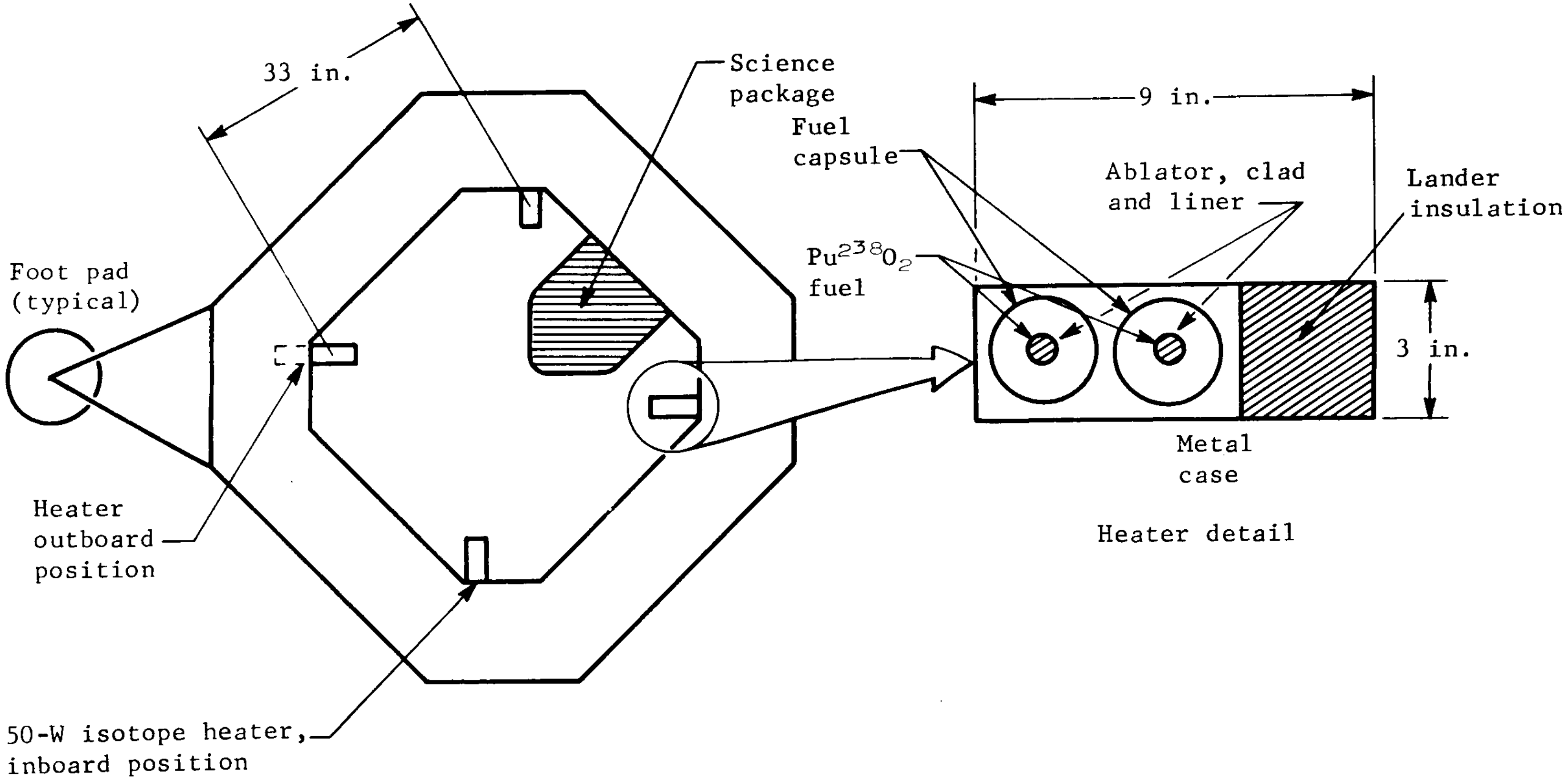
33 in.
Science package
Fuel capsule
9 in.
Ablator, clad and liner
Lander insulation
Pu^{238}O$_2$ fuel
3 in.
Foot pad (typical)
Metal case
Heater detail
Heater outboard position
50-W isotope heater, inboard position

Figure 24.- Isotope Heaters

TABLE 14.- ISOTOPE HEATER RADIATION EFFECTS

Instrument	Primary radiation effects	Approximate allowable levels	Comments
Facsimile camera	Photodetector parameters changes (dose effect)	10^{11} n/cm^2 (fast) 10^5 rads (gamma)	Heater radiation levels are well below the allowable levels
Biology experiments			
(1) Turbidity experiments (Wolf Trap)	Photodetector parameter changes (dose effect)	10^{12} n/cm^2 (fast), 10^6 rad (gamma)	Heater radiation levels are well below the allowable levels
(2) Counting experiments (Gulliver)	Spurious counts in Geiger counter or solid-state detector (dose rate effect)	50 counts/minute	Direct counts due to compton electrons generated by 8-rays in geiger tube are <1 count/min. Indirect counts due to externally generated electrons are <10 counts/min.
Mass spectrometer	Ionization of gas in device causing spurious current. Direct emission of electrons from dynodes by γ-rays. Noise generation in electrometer circuit (dose rate effect)	10^{-12} A maximum spurious current 10% noise in electrometer at 10^{-11} A	$<10^{-12}$ A current due to ionization and electron emission from heaters due to small ambient density, very little ionization-induced noise in electrometer may be expected. Testing recommended
Semiconductor devices (General)	Atomic displacement defects and resulting parameter changes (dose effect)	10^{11} to 10^{13} n/cm^2, depending on device 10^5 to 10^8 rads, depending on device	Heater radiation levels are well below the allowable levels

TABLE 15.- SCIENCE PACKAGE RADIATION LEVELS[a]

Gamma ray dose rate -	0.1 Roentgen/day = 2200 photons/cm^2-sec
Neutron flux -	3.7 x 10^7 n/cm^2-day = 4.3 x 10^2 n/cm^2-sec

Six-month inflight doses:

Gamma rays 8.9 rad (Si)
Neutrons 3.4 x 10^9 n/cm^2

Average gamma ray energy, 1 Mev

Average neutron energy, 2 Mev

At 3 ft, radiation from one 50 w heater in one week is less than recommended weekly maximum human dose. Microorganisms are orders or magnitude less sensitive than humans.

---

[a] In plane of heaters. Values are for 4 heaters

Science Data Return and Power Profile

The entry and landed science subsytem experiments are summarized in Volume I of this report. The science data return and subsystem power profile is tabulated in this subsection.

Table 16 lists the total data samples by experiment as well as the total bits of data. Table 17 is a tabulation of surface data collected in terms of data bits per day over the first four-day mission period. The table also references the daily transmission of data bits in terms of imagery data and stored science and engineering data. As noted at the end of the table, in excess of 10.5 x 10^6 bits of imagery data and 8.0 x 10^5 bits of stored science and engineering data are transmitted. After the first three days the data collection and transmission rate are reduced basically to a weather station mission.

The low rate of data transmission after the first three days after landing is based on minimum mission conditions (22° adverse slope). With more favorable landed conditions, a greater data return capability is possible and will be used for transmission of additional imaging data periodically throughout the 90-day period. Extended data transmission capabilities, are discussed in the Telecommunications section.

Figure 25 presents the instrument power sequencing over the first three-day period. After the third day the science data handling equipment is turned off and the science data, including weather data, subsurface probe data, and the biology data are read out by the telemetry subsystem.

TABLE 16.- ENTRY SCIENCE DATA RETURN

Science instrument	Bits per sample	Sample per second	Total samples						Total bits	
			Minimum			Maximum			Minimum	Maximum
			Ballistic phase	Descent phase	Vernier phase	Ballistic phase	Descent phase	Vernier phase		
			139 sec	26 sec	43 sec	336 sec	50 sec	50 sec		
Accelerometer triad[a]										
Longitudinal axis	8	15	2085	390	645	5040	750	750	24 960	52 320
Range, longitudinal axis	2	15	2085	390	645	5040	750	750	6 240	13 080
Lateral axis	8	15	2085	390	645	5040	750	750	24 960	52 320
Vertical axis	8	15	2085	390	645	5040	750	750	24 960	52 320
Temperature, accelerometer[b]	8	15	2085	390	645	5040	750	750	24 960	52 320
IMU accelerometer[c]										
Longitudinal axis	8	5	695	130	215	1680	250	250	8 320	17 440
Lateral axis	8	5	695	130	215	1680	250	250	8 320	17 440
Longitudinal axis	8	5	695	130	215	1680	250	250	8 320	17 440
Stagnation pressure	8	1	139	----	----	336	----	----	1 112	2 688
Temperature, stagnation pressure[b]	8	1	139	----	----	336	----	----	1 112	2 688
Total temperature[d]	8	1	139	----	----	336	----	----	1 112	2 688
Temperature, total temperature[b]	8	1	139	----	----	336	----	----	1 112	2 688
Hygrometer	8	1	----	26	43	----	50	50	552	800
Temperature, hygrometer[b]	8	1	----	26	43	----	50	50	552	800
Ambient temperature	8	1	----	26	43	----	50	50	552	800
Temperature, ambient temperature[b]	8	1	----	26	43	----	50	50	552	800
Ambient pressure	8	1	----	26	43	----	50	50	552	800
Temperature, ambient pressure[b]	8	1	----	26	43	----	50	50	552	800
Mass spectrometer	1000	0.33	----	8	13	----	16	16	21 000	32 000
Temperature, mass spectrometer[b]	8	1	----	8	13	----	16	16	168	256
Voltage, mass spectrometer[b]	8	1	----	8	13	----	16	16	168	256
Radar altimeter	10	1	139	26	43	336	50	50	2 080	4 360
Total data bits									162 216	327 104

[a] Mounted at center of gravity of entry capsule.

[b] Calibration measurement.

[c] Part of guidance and control subsystem.

[d] Deployed after blackout period.

TABLE 17.- SURFACE SCIENCE DATA COLLECTION

Instrument	Time		Data collection	Data bits
	T + hr	M + min		
Postlanded data transmission period				
Landing	0	0		
Meteorology Pressure Temperature Hygrometer Anemometer	0	0.5	Sampled 10 times/sec for initial 30-sec postlanded period (10 x 30 x 8 x 4)	9 600
Facsimile camera	0	1.0	Landing site survey, 90° azimuth by 25° elevation at 0.1° resolution; imaging period: 10 min	1 400 000
Meteorology data Pressure Temperature Hygrometer Anemometer	0	11.0	Sampled 10 sps per measurement for 10 sec (10 x 10 x 8 x 4)	3 200
			Total data transmitted during postlanding period	1 412 800
Data collection and storage period, day one				
Mass spectrometer	1	0	Double focus mass spectrometer, atmospheric data; two scans of 10 to 90 amu data plus calibration data	2 000
Meteorology Pressure Temperature Hygrometer Anemometer	2	0	Five data samples per measurement are taken over a 10-sec period; data readings are repeated every 2 hr for a total of 12 readings over a 24-hr period (5 x 8 x 12 x 4)	1 920 (per 24 hr)
Mass spectrometer	9	0	Double focus mass spectrometer, atmospheric data; two scans of 10 to 90 amu data plus calibration data.	2 000
Mass spectrometer	17	0	Double focus mass spectrometer, atmospheric data; two scans of 10 to 90 amu data plus calibration data	2 000
Soil sampler	18	0	Deploy and operate surface soil sampler; acquire soil sample and deposit in soil hopper.	1 000
Sample processor and distribution	18	15	Process soil sample and distribute sample to the pyrolysis unit and direct biology experiment	500
Pyrolysis and gas chromatograph-mass spectrometer (GC-MS)	18	30	Pyrolyze soil sample no. 1; perform GC-MS composition analysis of the pyrolyzed sample gases	12 000
Direct biology	19	0	Direct biology experiment is started; the experiment continues for a period of 3 days minimum	1 000 (per 24 hr)
Subsurface probe	19	0	Subsurface probe deployed to the planet surface; subsurface moisture and temperature data are measured once every 2 hr (5 x 8 x 12 x 3)	1 440 (per 24 hr)
	16	50	Direct link data communication period, day one (2.62 hr at 353 bps)	
			Imaging data transmission (353 bps for 2.4 hr)	3 060 130
			Stored data transmission, sync and engineering data (353 bps for 0.22 hr)	267 390

TABLE 17.- SURFACE SCIENCE DATA COLLECTION - Continued

Instrument	Time		Data collection	Data bits
	T + hr	M + min		
Data collection and storage period, day two				
Meteorology Pressure Temperature Hygrometer Anemometer	24	0	Five data samples per measurement and taken over a 10-sec period; data readings are repeated every 2 hr over a 24-hr period for a total of 12 data readings per day (5 x 8 x 12 x 4)	1 920 (per 24 hr)
Subsurface probe	24	0	Five data samples per measurement are taken over a 10-sec period; data readings are repeated every 2 hr over a 24-hr period for a total of 12 data readings per day (5 x 8 x 12 x 3)	1 440 (per 24 hr)
Pyrolysis and GC-MS	27	0	Pyrolyze soil sample no. 2; perform GC-MS composition of the pyrolyzed sample gases	12 000
Pyrolysis and GC-MS	35	0	Pyrolyze soil sample no. 3; perform GC-MS composition of the pyrolyzed sample gases	12 000
Direct biology			Data are taken periodically throughout the experiment period	1 000 (per 24 hr)
	41	30	Direct link data communication period, day two (2.62 hr at 353 bps)	
			Imaging data transmission (353 bps for 2.4 hr)	3 060 130
			Stored data transmission, sync and engineering data (353 bps for 0.22 hr)	267 390
Data collection and storage period, day three				
Meteorology Pressure Temperature Hygrometer Anemometer	48	0	Five data samples per measurement are taken over a 10-sec period; data readings are repeated every 2 hr over a 24-hr period for a total of 12 data readings per day (5 x 8 x 12 x 4)	1 920 (per 24 hr)
Subsurface probe Moisture (1) Temperature (2)	48	0	Five data samples per measurement are taken over a 10-sec period; data readings are repeated every 2 hr over a 24-hr period for a total of 12 data readings per day (5 x 8 x 13 x 3)	1 440 (per 24 hr)
Direct biology			Data are taken periodically throughout the experiment period	1 000 (per 24 hr)
	66	0	Direct link data communication period, day three (2.62 hr at 353 bps)	
			Imaging data transmission (353 bps for 2.4 hr)	3 060 130
			Stored data transmission, sync and engineering data (353 bps for 0.14 hr)	267 390

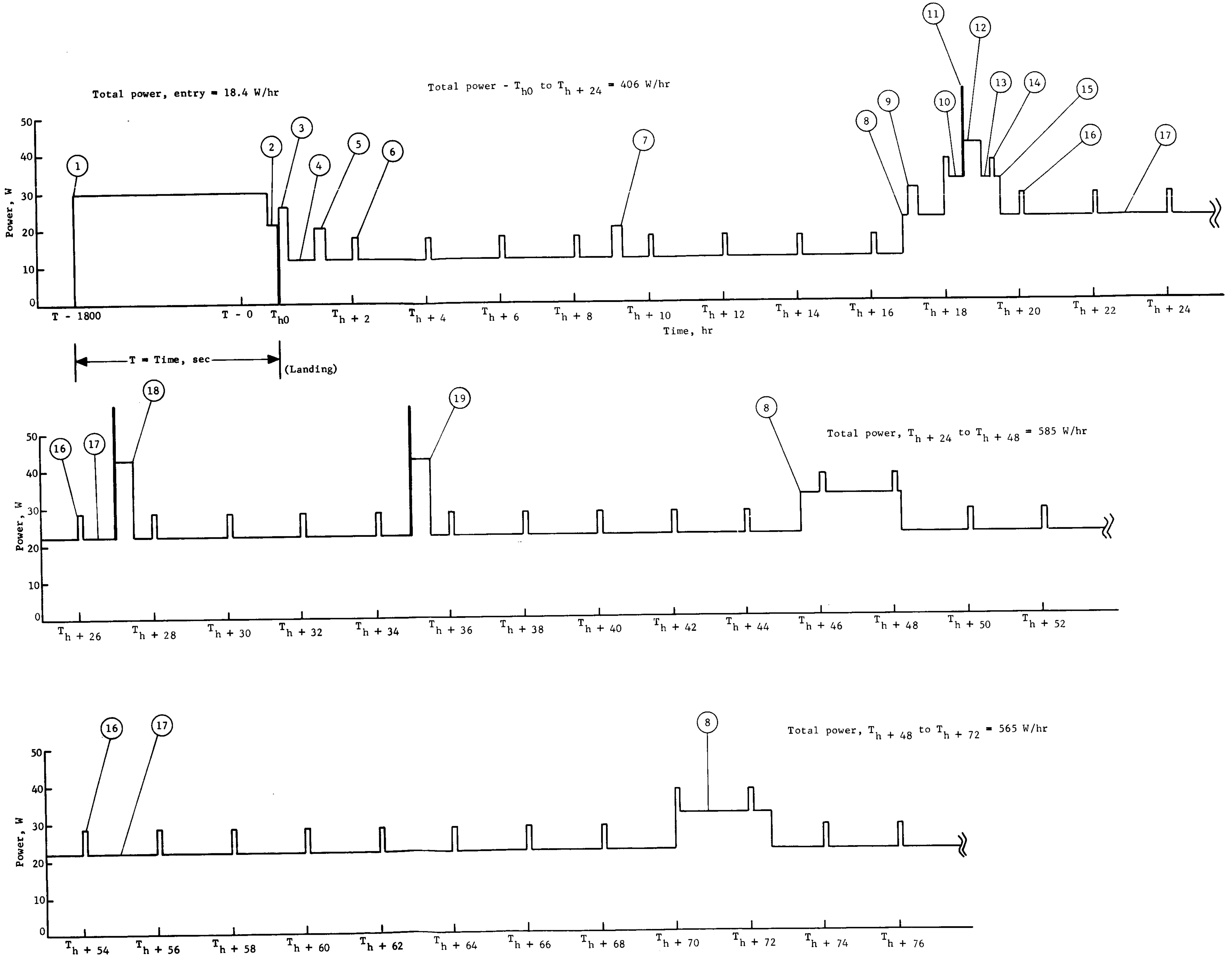

Legend:

① All entry science instruments are turned on for warmup. Following warmup, engineering and calibration data are taken at T_o sec at 800 x 10^3-ft altitude.

② At approximately 10 000 ft altitude, the parachute is deployed and the aeroshell (A/S), including the A/S-mounted instruments, are separated and terminal descent data, including mass spectrometer, hygrometer, pressure, and temperature, are taken. These data continue until T_h = 0, landing.

③ Postlanded science instruments, including facsimile camera, and meteorology instruments, including the anemometer, hygrometer, pressure transducer, and temperature sensor, are deployed and operating. The immediate postlanded data are transmitted for a minimum of 10 min at 2400 bps over the relay link uhf transmitter.

④ Data automation unit operates continuously for the first 3 days of the mission.

⑤ Double focus mass spectrometer data are taken of atmospheric samples in accordance with a preprogramed schedule.

⑥ Meteorology data are taken once every 2 hr in accordance with a preprogramed schedule.

⑦ Double focus mass spectrometer data are taken of atmospheric samples in accordance with a preprogramed schedule.

⑧ Facsimile camera is operated, and preprogramed imagery data are transmitted in real time over the direct link S-band transmitter. Stored science data are also transmitted at this time -- interlaced between photographic images.

⑨ The final preprogramed operation of the double focus mass spectrometer analysis of atmospheric samples is performed.

⑩ The soil sample acquisition, processing, and sample distribution units are operated; soil samples are distributed to the biology experiment and the gas chromatograph-mass spectrometer (GC-MS) pyrolysis unit.

⑪ Pyrolysis of soil sample 1.

⑫ The GC-MS unit is operated.

⑬ The direct biology experiment is started and operates for a minimum of 3 days.

⑭ The subsurface probe is operated and deployed to the planet surface.

⑮ The facsimile camera is turned off at the end of the direct link communication period.

⑯ Meteorology and subsurface probe data are taken once every 2 hr in accordance with a preprogramed schedule.

⑰ Continued operation of the data automation unit and the direct biology experiment.

⑱ Pyrolysis and GC-MS analysis of soil sample 2 in accordance with a preprogramed schedule.

⑲ Pyrolysis and GC-MS analysis of soil sample 3 in accordance with a preprogramed schedule.

Figure SIX.- Power Profile, Science Subsystem

2. STRUCTURES AND MECHANISMS

All Sterilized Autonomous Capsule/Support Module

In addition to the preferred configuration, a study was made of a totally sterilized spacecraft. This configuration is shown on the launch vehicle in figure 26. A general arrangement layout is presented in figure 27.

The six major assemblies that comprise the spacecraft are shown in figure 28 with a listing of the equipment contained in each. They are assembled and function in the following configuration modes: launch, cruise, entry, parachute, and touchdown (fig. 29).

Launch mode.- In the launch mode all assemblies are present.

Cruise mode.- The forward canister is separated in earth orbit and the canister/adapter stays with the transtage after trans-Mars injection. The remaining assemblies comprise the cruise configuration.

Entry mode.- In the vicinity of Mars the support module is separated leaving the entry configuration.

Parachute mode.- After entry (less than Mach 2.0) the parachute is deployed and the aeroshell is released shortly thereafter. The remaining elements comprise the parachute configuration mode.

Touchdown mode.- At an altitude of approximately 5300 ft the aerodecelerator/cruise module is separated, thus achieving the touchdown mode.

Functional description.- In the cruise mode, communication S-band low-gain antennas are provided. One is mounted to the S-band high-gain antenna feed and the other on the aeroshell behind an rf transparent window, thus providing complete visibility. The spacecraft cruises with the high-gain S-band antenna pointed at the sun. The cruise solar power array is attached to the base cover and is approximately 15° from the sun line. Approximately 55 ft^2 of projected area is provided. Cruise attitude control is provided by a cold gas system integrated into the aeroshell assembly, with a completely balanced system of 12 nozzles spaced around the aeroshell.

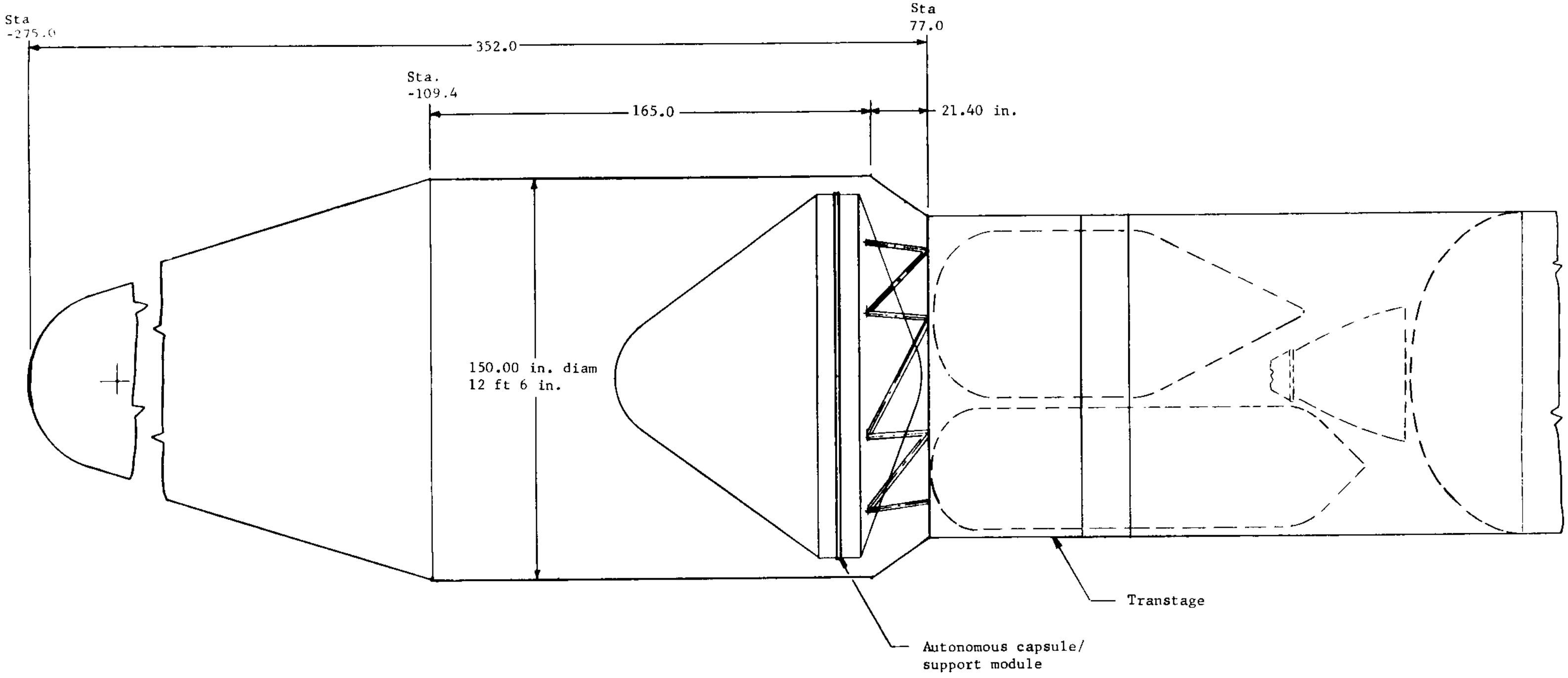
Sta
-275.0
352.0
Sta
77.0
Sta.
-109.4
165.0
21.40 in.
150.00 in. diam
12 ft 6 in.
Transtage
Autonomous capsule/
support module

Figure 26.- Integration Sketch, Autonomous Capsule/Support Module
(All Sterilized)

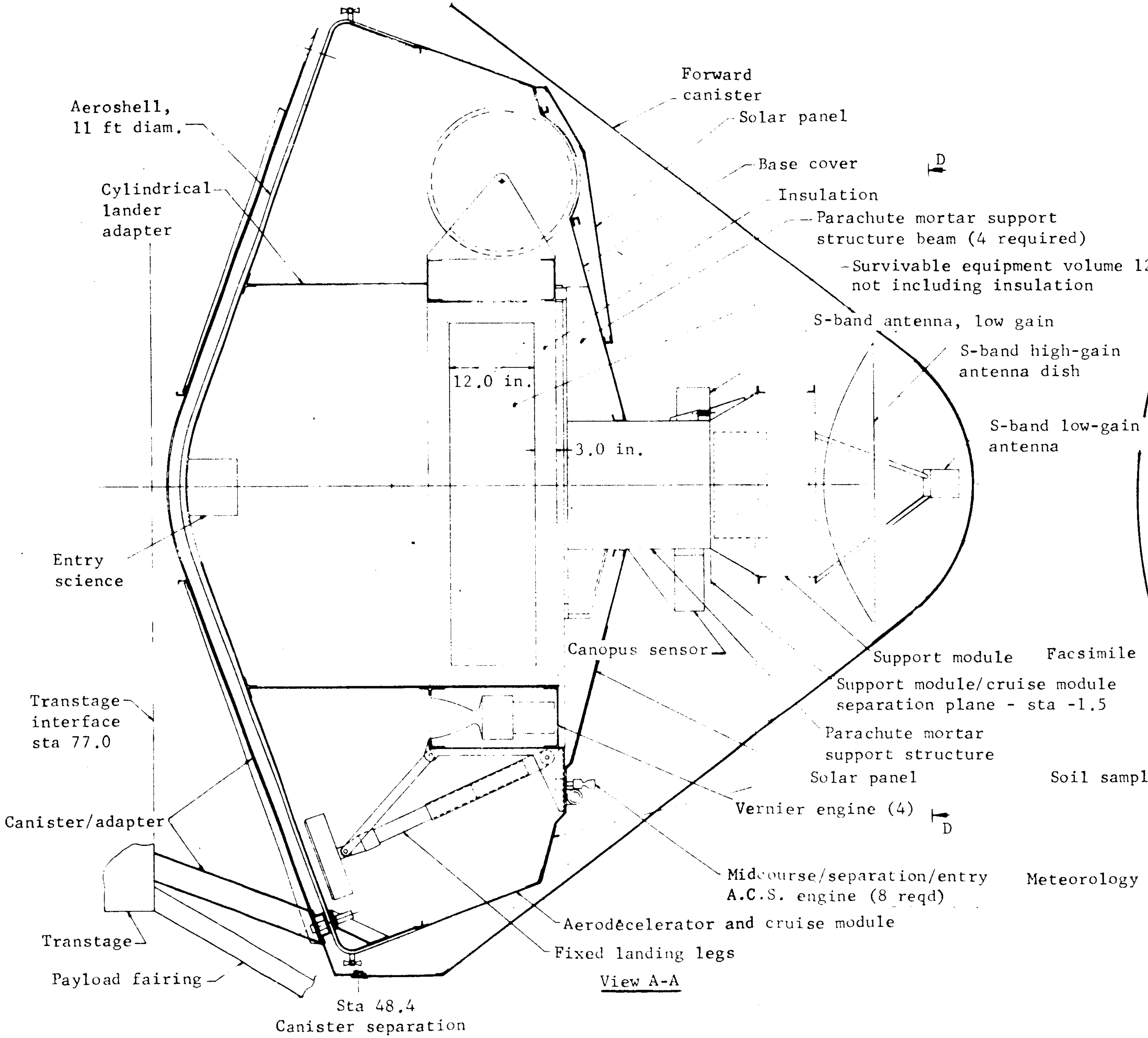
Aeroshell, 11 ft diam.
Cylindrical lander adapter
Entry science
Transtage interface sta 77.0
Canister/adapter
Transtage
Payload fairing
Sta 48.4 Canister separation
Forward canister
Solar panel
Base cover
D
Insulation
Parachute mortar support structure beam (4 required)
Survivable equipment volume 12 cu ft not including insulation
12.0 in.
3.0 in.
S-band antenna, low gain
S-band high-gain antenna dish
S-band low-gain antenna
Canopus sensor
Support module
Support module/cruise module separation plane - sta -1.5
Parachute mortar support structure
Solar panel
Vernier engine (4)
D
Midcourse/separation/entry A.C.S. engine (8 reqd)
Aerodecelerator and cruise module
Fixed landing legs

View A-A

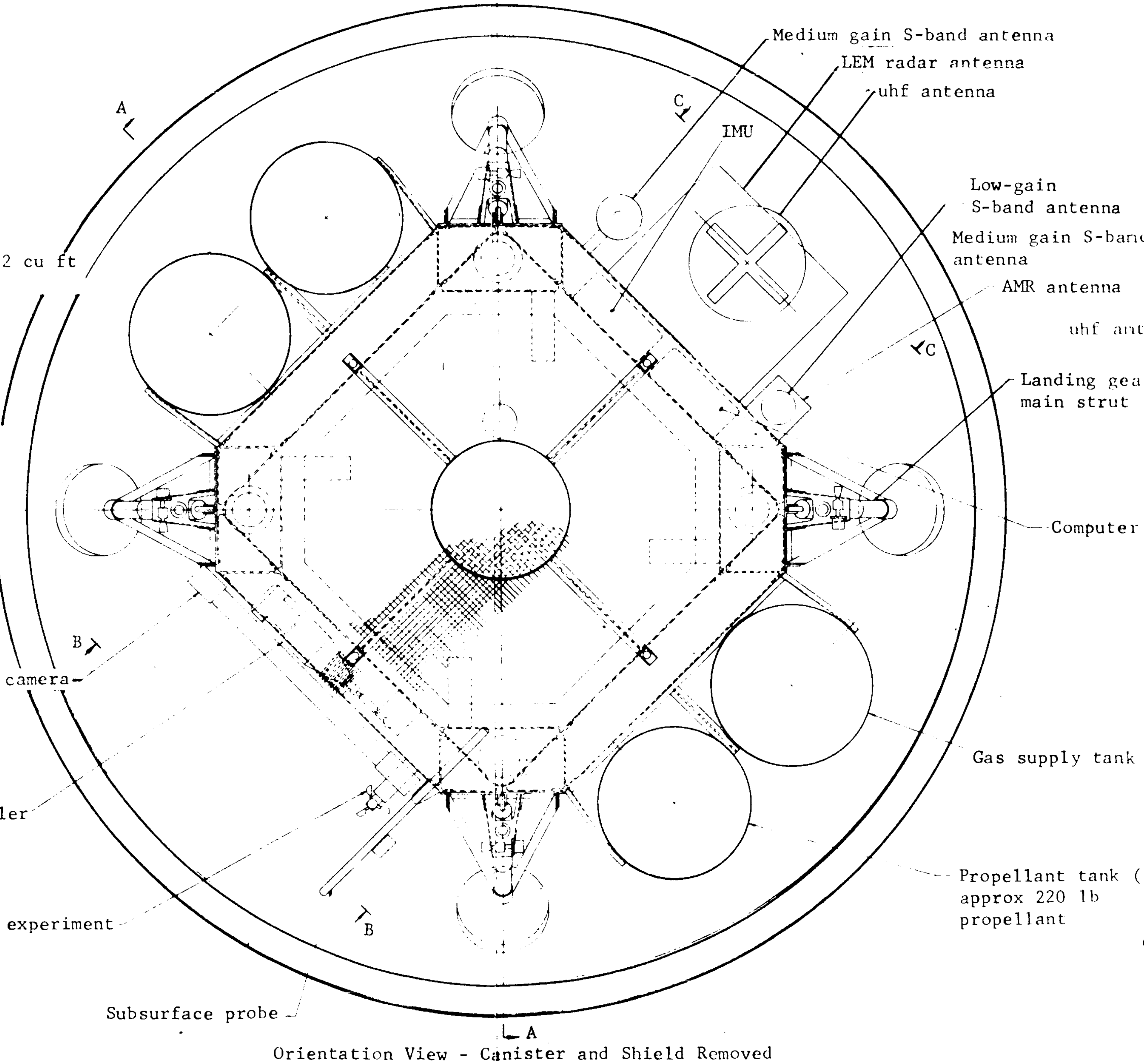
Medium gain S-band antenna
LEM radar antenna
uhf antenna
A
C
IMU
C
Landing gear main strut
Computer
B
Facsimile camera
Soil sampler
Meteorology experiment
B
Subsurface probe
A
Gas supply tank (2)
Propellant tank (2) approx 220 lb propellant

Orientation View - Canister and Shield Removed

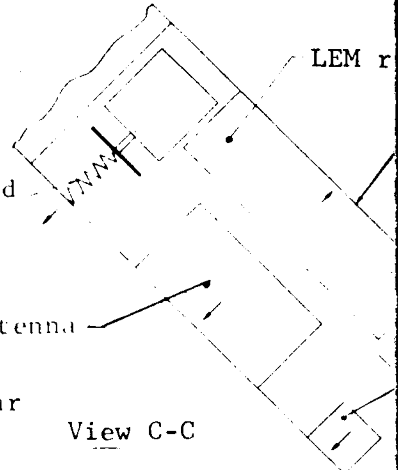
LEM r
Low-gain S-band antenna
Medium gain S-band antenna
AMR antenna
uhf antenna

View C-C

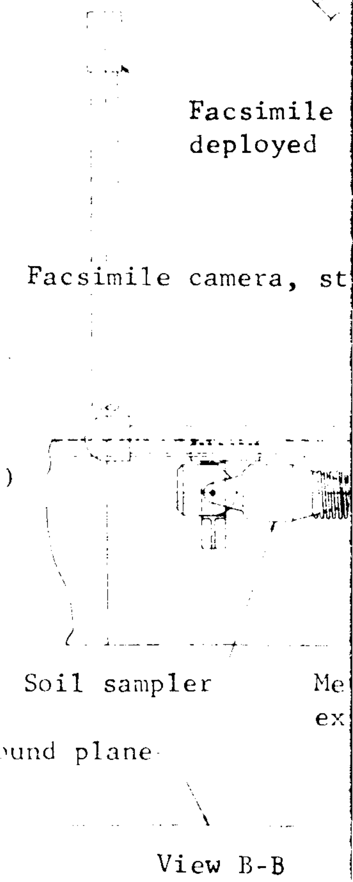
Facsimile deployed
Facsimile camera, st
Soil sampler
Me ex
Ground plane

View B-B rotated 45°

Part 1

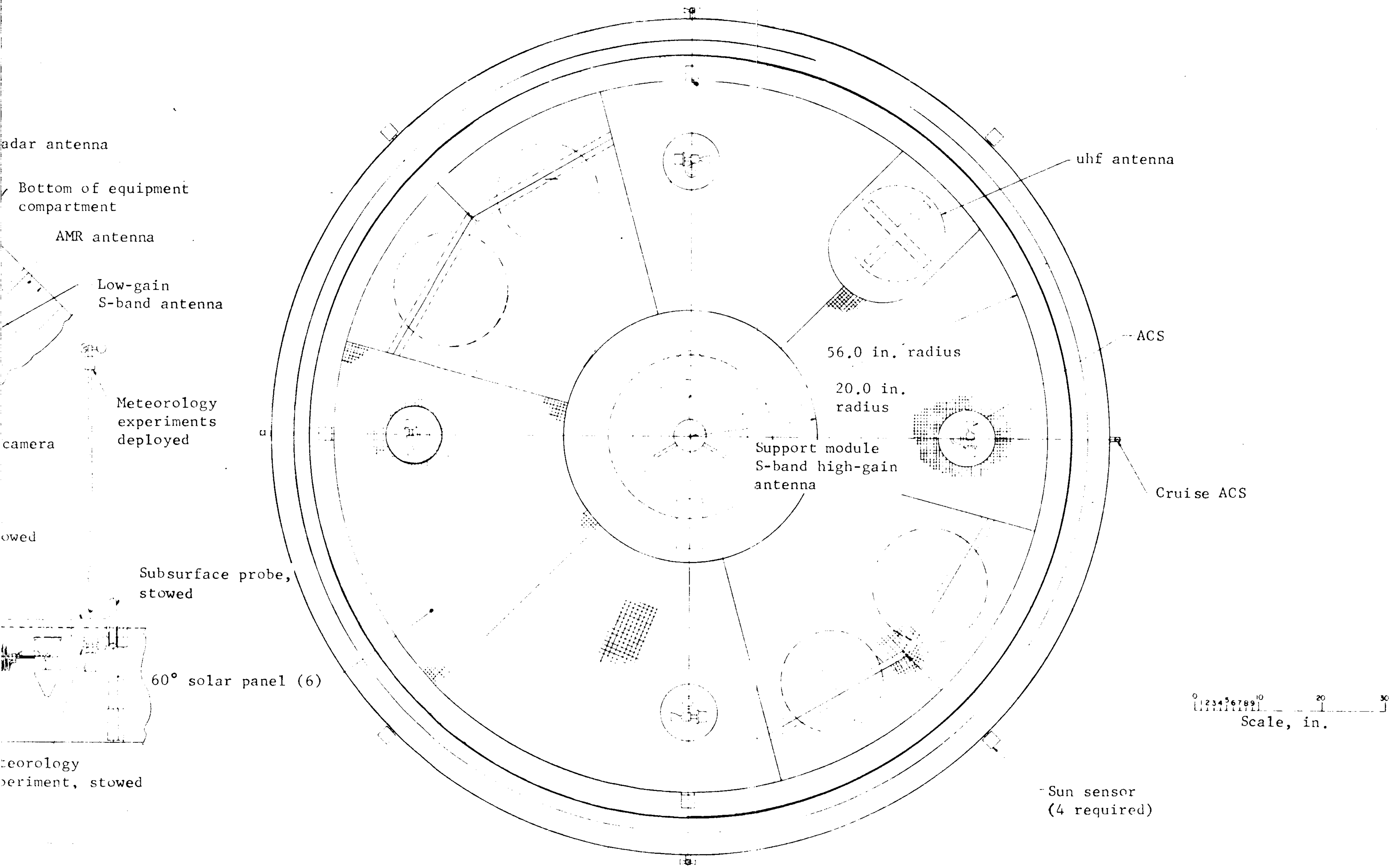
adar antenna
Bottom of equipment compartment
AMR antenna
Low-gain S-band antenna
Meteorology experiments deployed
camera
owed
Subsurface probe, stowed
60° solar panel (6)
teorology
periment, stowed
CCW
uhf antenna
56.0 in. radius
20.0 in. radius
Support module S-band high-gain antenna
ACS
Cruise ACS
Sun sensor (4 required)
0 1 2 3 4 5 6 7 8 9 10 20 30
Scale, in.

View D-D
Solar panel array - canister removed
55 sq ft projected

Part 2

Figure 27.- All-Sterilized Autonomous Capsule and Support Module

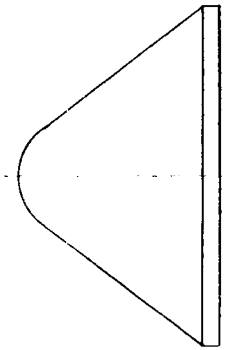	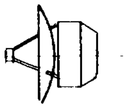	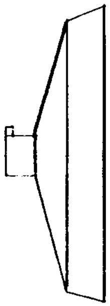	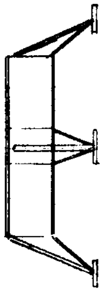	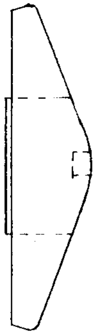	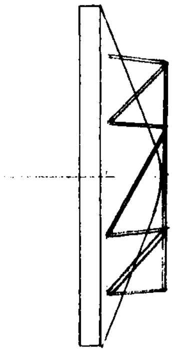
Forward canister	Support module	Aerodecelerator cruise module	Lander	Aeroshell assembly	Canister/adapter
Canister skin	S-band low gain S-band high gain UHF low gain Spin rockets Nutation damper Thermal insulation S-band transmitter uhf receiver Storage batteries	Parachute Mortar Mortar reaction Energy absorber Mortar support structure Base cover Cruise solar array S-band low gain antenna Canopus sensor Separation systems Thermal insulation	Lander structure Legs Vernier propulsion Hot gas ACS Landed science Guidance and control Insulation Isotope heaters Landed solar array Communication equipment Storage batteries Separation systems Data acquisition system	Aeroshell Heat shield Entry science Cruise ACS Sun sensors Lander adapter S-band antenna AMR antenna	Canister skin Biovent Truss Canister seal Canister separation

Figure 28.- Six Major Assemblies and Associated Subsystems

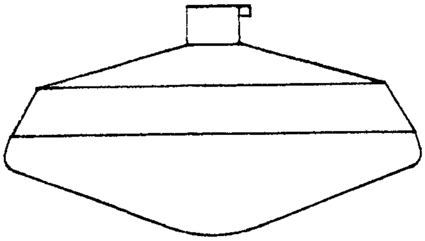

Entry mode

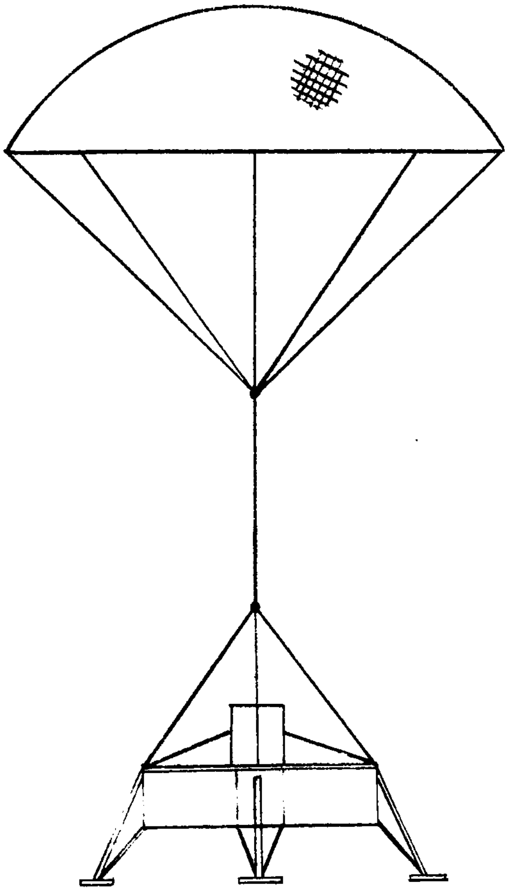

Parachute mode

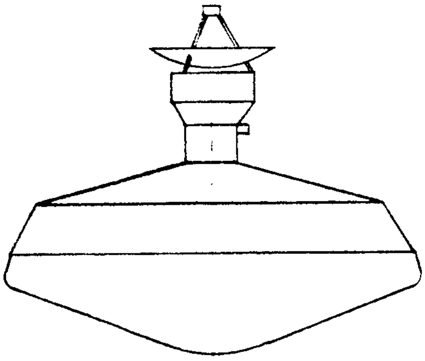

Cruise mode

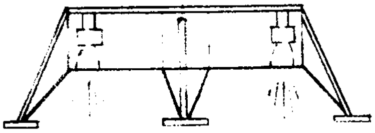

Landing mode

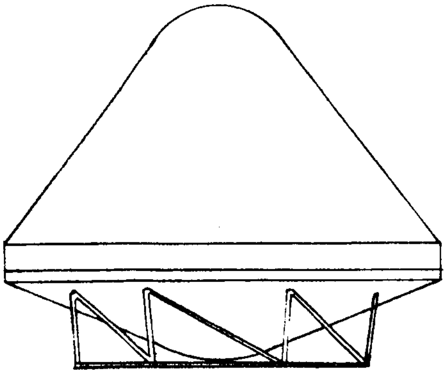

Launch mode

Figure 29.- Autonomous Capsule/Support Module (Alternative Configuration) Configuration Modes

Four sun sensors are also mounted around the periphery of the aeroshell, providing a view in the antisolar direction to aid in sun acquisition. A sun gate and a pair of sun sensors are mounted to the base cover. The Canopus sensor is attached to the support module support structure. Midcourse ΔV propulsion is provided by the 5-lb thrust hot gas system of eight nozzles that are attached to the lander and project through the base cover.

Near Mars the entire spacecraft is oriented to point the high-gain S-band antenna at Earth. Using springs the support module is then structurally separated and accelerated from the aerodecelerator/cruise module. When clearance is achieved four small solid rockets spin the support module. The entry capsule is then realigned for the trajectory deflection burn and again reoriented for entry attitude after the burn.

During entry the uhf link is maintained from entry capsule to support module. The uhf antenna on the lander transmits through an rf transparent window on the base cover and a hole in the cruise solar array. At Mach 2.0 the parachute is deployed and when subsonic velocity is achieved the aeroshell is separated. At approximately 5300-ft altitude, the aerodecelerator/cruise module is separated from the lander, and the lander descends using the vernier propulsion system for energy management. Kinetic energy at impact is absorbed by four liquid spring landing gear main struts. After landing, the medium gain S-band antenna is erected to the local vertical and the science instruments are deployed.

Canister/Adapter

The canister/adapter (fig. 27), which encloses approximately half of the sterilized hardware, is an aluminum shell structure combined with an adaptor truss that attaches the spacecraft to the booster. At its maximum diameter (Sta 48.4) the canister/adapter mates with and is sealed to the closure frame of the forward canister. The forward canister is separated from the canister/adapter by a linear charge that shears many pins and imparts a separating velocity to the forward canister. Sealing is accomplished by a large diameter elastomeric band stretched over the canister/adapter and forward canister mating flanges. Internal pressure is limited to 1 psi or less during launch by venting through biovents. The adapter truss transmits launch loads through the canister skin into the closure frame of the aeroshell.

Aerodecelerator/Cruise Module

The aerodecelerator consists of the parachute mortar support structure, base cover, separation systems, and mounting provisions for the cruise solar array, S-band low-gain antenna, Canopus sensor, and thermal insulation.

The parachute mortar support structure is a cylinder that attaches to the lander through four radial beams. At the tip of each beam is a fitting that mates with the lander and contains inflight separation provisions. At the forward end, the cylinder adapts to the support module by providing two tension separation bolt ties and four separation springs. The Canopus sensor and S-band low-gain antenna are mounted to the cylinder at the forward end by brackets.

The base cover consists of two cone frustums of different angles joined in tandem. At the large-diameter end the base cover seats against the aeroshell base ring. At the small-diameter end the base cover is attached to the parachute mortar support structure. The solar panels attach to the base cover and are penetrated by four engine clusters and the uhf antenna rf transparent window. Two of the solar panels are raised to clear the lander propellant tanks as shown in figure 27, View A-A.

Lander

The lander (fig. 27) is composed of aluminum/magnesium body assembly, aluminum landing legs, and miscellaneous brackets.

The lander body is square in planform with the corners truncated to produce 16-in. flats that form a base for landing leg attachment. The structure consists of two 6-in. deep, eight-sided frames at the upper and lower levels of the 18-in. deep body structure. Vertical corner fittings span the 18-in. height joining the upper and lower level frame providing landing leg attachment fittings, and supports for the four vernier engines and the survivable equipment pallet. Transverse shear loads are carried by sheet metal webs between the upper and lower level frames.

Survivable equipment is packaged on a pallet (46-in. square with clipped corners) that is attached 3-in. above the lower level frame to the vertical corner fittings. The equipment is enclosed inside 3-in. of thermal insulation. Approximately 12 ft^3 of survivable equipment compartment volume is provided.

The landing legs consist of a main strut, a bipod, and a foot pad assembly. The main strut contains a liquid spring shock attenuator similar to the type used on Surveyor. The bipod is a fixed structure with no energy absorbing capability. The foot pad assembly is equipped with crushable energy absorbing material. The lateral shear strength of the foot pad is designed to limit the bipod axial loads in the event of high lateral friction forces between the Mars surface and the foot pad. The landing legs are attached to the lander in a fixed position, therefore requiring no deployment.

Items requiring mechanical design are the medium-gain S-band antenna, science experiments, and the isotope heaters. The S-band antenna requires erection to the local gravity vector.

The science instruments requiring mechanization are the facimile camera, the weather sensor mast, the digger, the sample distribution system, and the subsurface probe (see fig. 27, - View B-B).

During transit and landing the facsimile camera is stowed against the lander body upper level frame. The camera is attached to the frame by a simple pivot fitting which is spring driven 90° to the erected position when released. The camera is located so that it can survey the area of operation of the digger and the subsurface probe.

The weather mast is a "jack in the box" type of tape mast. A restraining cover must be released to deploy this device.

The soil sampler is an extendable and retractable tape mast equipped with articulated spoons at the tip and a two-axis drive at the base. The soil sampler places soil in the distribution system, which delivers small samples to the direct biology experiment and the pyrolosis unit.

The subsurface probe is a small-diameter tube (approximately 0.10 in. diam.) that is inserted to a depth of about 1 ft in the soil. The 0.10-in. insertion tube is supported inside a larger-diameter tube that is attached to the lander via a deployment arm.

The four 50 W isotope heaters are mounted at each corner of the survivable equipment compartment, near the landing leg. During cruise these heaters must be outside of the survivable compartment to allow the heat to be rejected to space. After landing, the heaters are positioned either in or out of the compartment, depending on the internal temperature.

Aeroshell Assembly

The aeroshell (fig. 27) is an aluminum skin/aluminum frame shell 11 ft in diameter. The lander adapter structure is a part of the aeroshell assembly and is composed of forward and aft frames and a 56-in.-diam. stiffened cylinder. Attachment to the lander is made by four bolts and separation nuts.

Forward Canister

This assembly (fig. 27) consists of aluminum skin, closure, and stabilization frames. Ejection occurs in Earth orbit.

Support Module

The support module for the alternative configuration is identical to the selected configuration except for slightly larger batteries and a slight relocation of the uhf antenna. Sterilization requires that the cells be lengthened from 2.75 in. to 5.50 in. The uhf antenna must be moved aft 1.0 in. to accomodate the larger cells.

The support module consists of an aluminum cylinder and disc-shaped floor. A 26-in. diam. by 8-in.-long cylinder forms the body and also serves as the radiator for thermal control. The cylinder is equipped with ring frames at each end to attach the S-band high-gain antenna and to mate with the cruise module.

All equipment is mounted on the disc-shaped floor fabricated of aluminum alloy, approximately 0.125 in. effective thickness. The floor beams component loads to the cylindrical body and also serves to transmit heat from the equipment to the cylindrical body which acts as a radiator.

3. PROPULSION

This section presents detailed descriptions of the candidate hardware in the preferred propulsion subsystems and the data on which the hardware selections were made. Also presented is a weight summary of the preferred design.

The results of testing performed on the candidate landing engine throttle valve is presented along with a summary of a test program in which this valve and the landing engine will be combined and tested to further reduce the program risk and cost.

Landing Engine Selection

From parametric data derived for the Mars Mission Modes Study (Contract NAS1-7976), the required thrust range for the monopropellant landing engines was determined to be between 300 and 650 lb, depending on capsule weight and parachute terminal velocity conditions.

The results of a survey of the monopropellant engine manufacturers are shown in table 18.

TABLE 18.- ENGINE MANUFACTURER SURVEY

Manufacturer	Thrust level, lb	Weight	Status
Walter Kidde	300 to 100	49 lb	Qual 3/69 for AF program
TRW	300 to 15	Work horse	In-house development
Rocket Research	400 to 100	Work horse	In-house development
Marquardt	300 to 30	Work horse	In-house development

The table shows that the Walter Kidde 300-lb-thrust engine is the only engine that has been developed past the conceptual phase. Therefore, this engine was selected for the preferred propulsion subsystem design.

A sketch of this engine and its performance capability are shown in figure 30. The dashed outline of the engine represents the present configuration while the solid line depicts the engine as modified for the Mars lander. The modifications to the engine are:

1) Modify expansion section of the nozzle from an ϵ of 85.5:1 to 20:1;

2) Add parallel throttle valves to provide variable thrust.

Neither of these modifications affects the thrust chamber of the engine. Therefore, the amount of requalification testing for the Mars lander is minimized to engine/valve qualification.

Four landing engines are necessary to provide the thrust-to-weight ratio required for the preferred design. As shown in table 19, the four-engine configuration has a thrust-to-weight ratio of 2.224 compared with 1.668 for the three-engine case. The four-engine system requires 160.8 lb of propellant and 5298 ft of altitude to perform the landing while 213.4 lb of propellant and 9381 ft are needed with three engines. From a weight standpoint, the four-engine system has an advantage of approximately 20 lb. The lower altitude and higher thrust-to-weight ratio are advantageous from a guidance and control point of view in that these parameters are compatible with the LM radar.

As shown in table 19, the three-engine case has a system reliability of 0.970 compared to 0.954 for four engines.

TABLE 19.- COMPARISON OF THREE-ENGINE AND FOUR-ENGINE CONFIGURATIONS

Parameter	Three-engine configuration	Four-engine configuration
Propellant weight, lb	213.4	160.8
Engine weight, lb	105	140
Thrust-to-weight ratio	1.665	2.224
Height, ft	9381	5298
Reliability	0.970	0.954

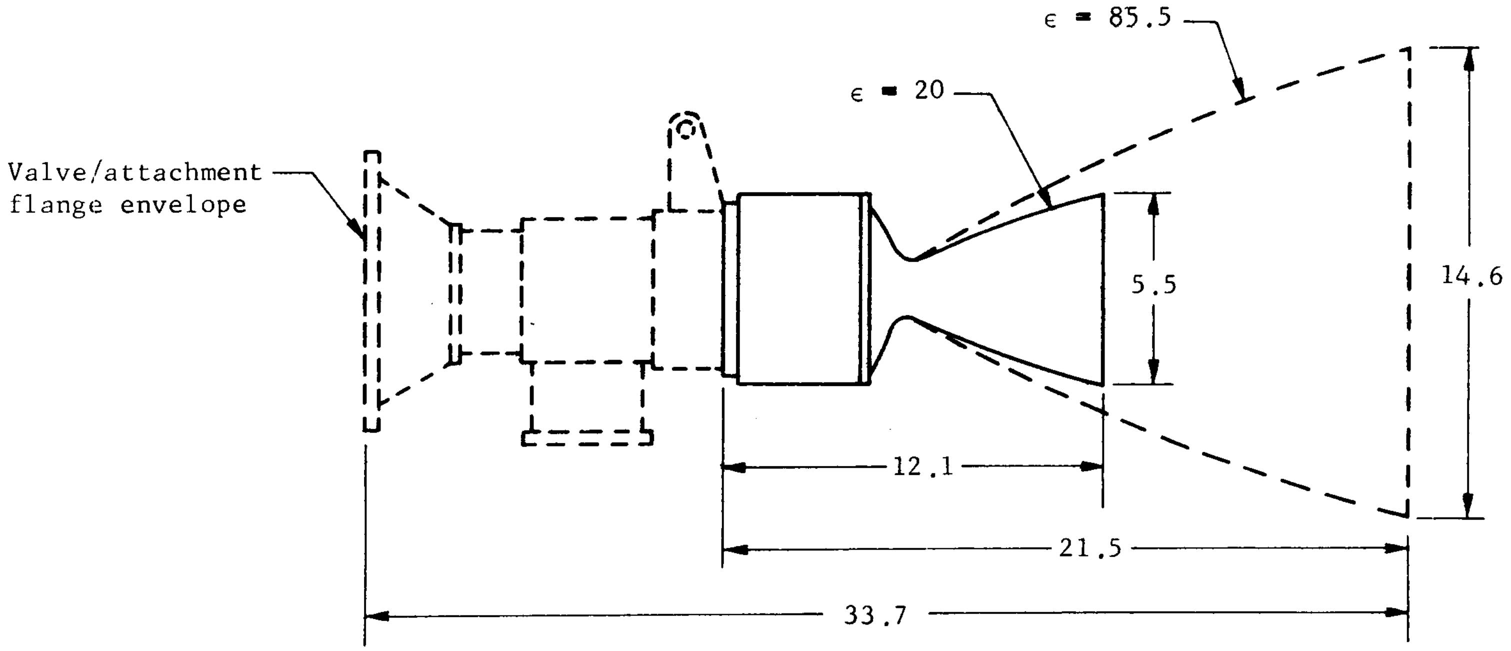
Valve/attachment flange envelope
ϵ = 85.5
ϵ = 20
5.5
14.6
12.1
21.5
33.7

Characteristics	Present	Mars '73
Thrust, lb	300 to 100	300 to 100
Specific impulse, sec	240 max., 230 min.	228 max., 219 min.
Expansion ratio	85.5:1	20:1
Chamber pressure, psia	100 to 33	100 to 33
Weight, lb	49	35 (incl throttle valves)
Propellant	Hydrazine	Hydrazine

Figure 30.- Walter Kidde 300-lb_f Monopropellant Engine

Although the three-engine configuration has a reliability advantage, the capability of the four-engine case to satisfy mission requirements at a lower weight determined final configuration selection.

Valve Selection

The candidate engine throttle valve was selected in a manner similar to that used in selecting the landing engine in that an industry survey was conducted.

The only valve with continuous throttling capability that is developed and qualified is the LTV Electrosystems Minuteman III liquid injection thrust vector control valve shown in figure 31. The figure also presents the existing valve characteristics and those required for the lander engine. Figure 32 shows the valve as it has been modified and tested for the landing engine application.

The valve pintle and seat were modified to provide the pressure drop and flow rate shown in table 20. No other components of the valve were changed.

TABLE 20.- PRESSURE DROP AND FLOW RATE

$\dot{w}$, lb/sec	ΔP, psi	Inlet pressure, psia
1.295	50	250
0.885	136	250
0.495	197	250
0.272	219	250

Figure 33 presents the flow rate versus differential pressure test. Each curve represents the flow of the valve at an input voltage (position) with a varying downstream pressure. The intersection of these curves with the required curve demonstrates the satisfactory operation of the throttle valve at the particular position.

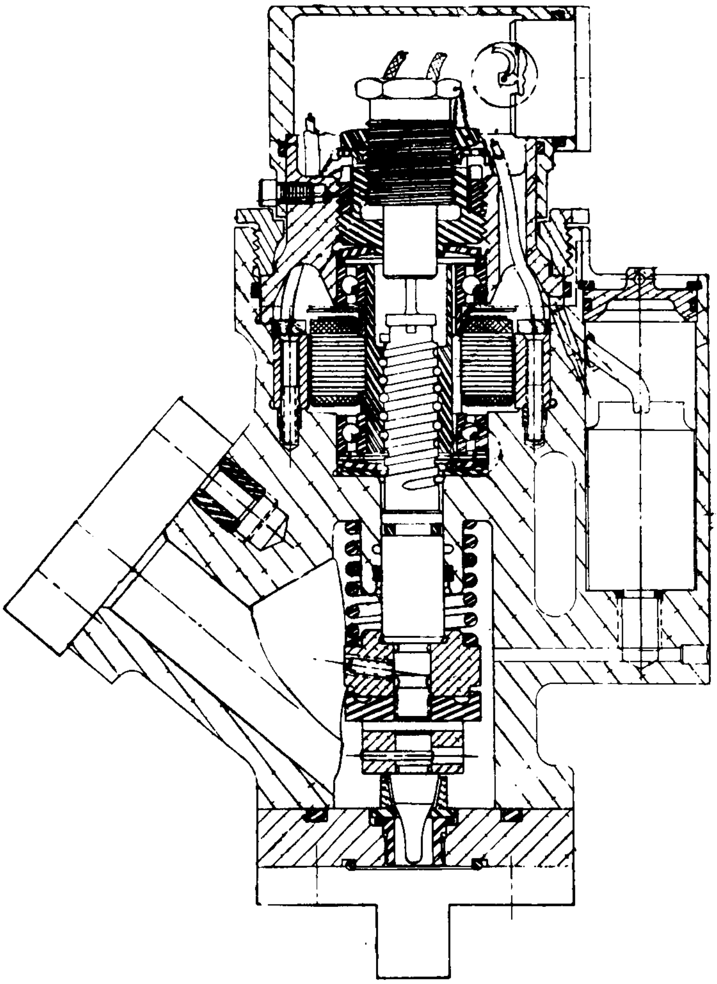

Valve characteristics

Parameter	Present	Required for Mars '73
Design inlet pressure (max.), psia	750 psia	300 psia
Valve pressure drop (at max. flow), psi	472 psi	50 psi
Flow rate (max.), lb/sec	12.5 $SR(ClO_4)_2$	1.295 N_2H_4
Bandwidth, Hz	8	5

Figure 31.- Minuteman III TVC Valve

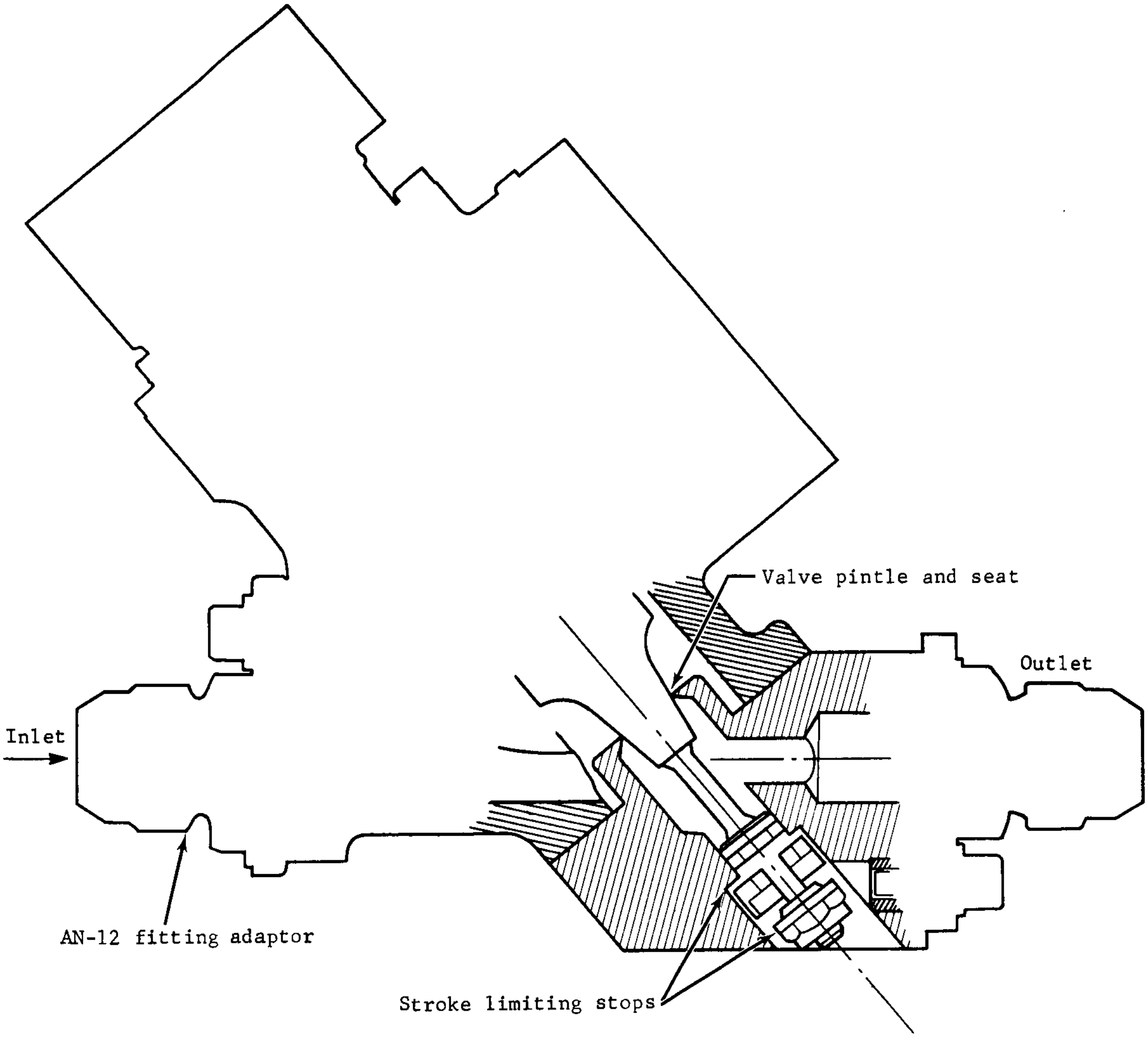
Valve pintle and seat
Outlet
Inlet
AN-12 fitting adaptor
Stroke limiting stops

Figure 32.- Mars Lander Valve

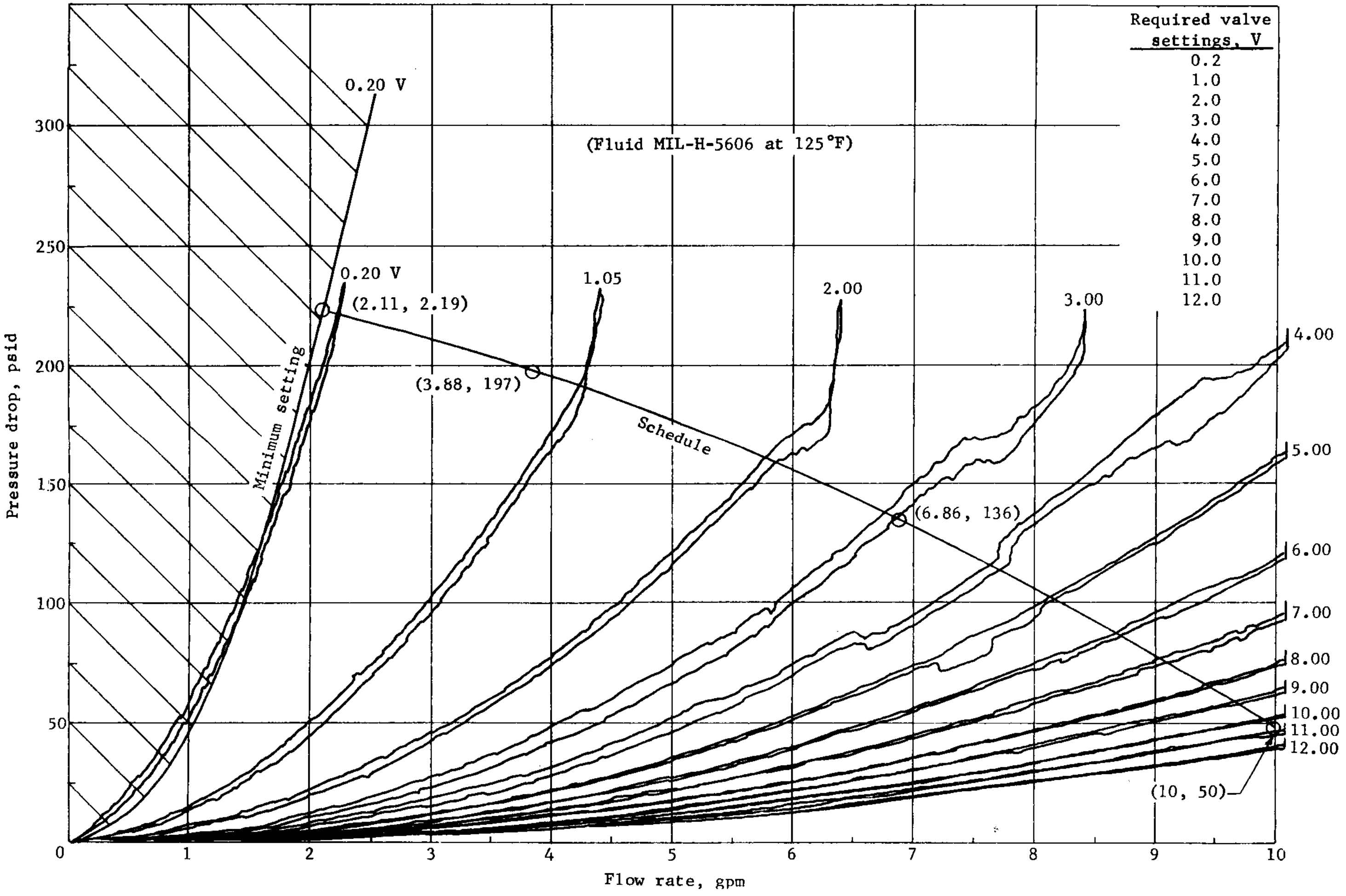

Figure 33.- Flow Rate vs Pressure Drop

Control system studies have shown that a valve that has dominant poles greater than 30 rad/sec and a damping ratio greater than 0.7 will provide sufficient stability margin when used in the control system. The results of frequency response testing on the LTV valve are shown in figure 34. These data show a flat response out to nearly 60 rad/sec, which is more than adequate. Results of the tests conducted at LTV indicate the throttle valve is compatible with the Kidde engine.

Sterilization testing on a Minuteman III valve was performed at Martin Marietta Corporation to determine if any of the internal components of the valve were not sterilizable. The results of this testing indicate that the O-ring seals are susceptible to deformation during sterilization and that a shift in torque motor resistance occurred. Seal changes were observed by visual inspection and the motor performance shift was noted by comparing pretest and posttest hysterisis data.

The seals will be replaced with sterilizable units and the torque motor will be replaced with a high temperature (500°F) component for the flight valve.

The midcourse/deflection/entry ACS engine is shown in figure 35. This engine is currently under development by Rocket Research Corporation for an Air Force Program and will be qualified by 12/31/68. This engine was selected on the basis of its stage of development and its ability to perform the midcourse, deflection, and entry attitude control maneuvers. Selection of this approach eliminates the need for a separate propulsion system to perform these functions and reduces system weight, as shown in table 21.

TABLE 21.- SYSTEM WEIGHTS

Parameter	Total weight, lb	
	Separate system	Combined system
Total propulsion subsystem	555.3	521.4
Adapter and canister	194.0	179.0
Structure	239.0	209.0
Total	988.3	909.4

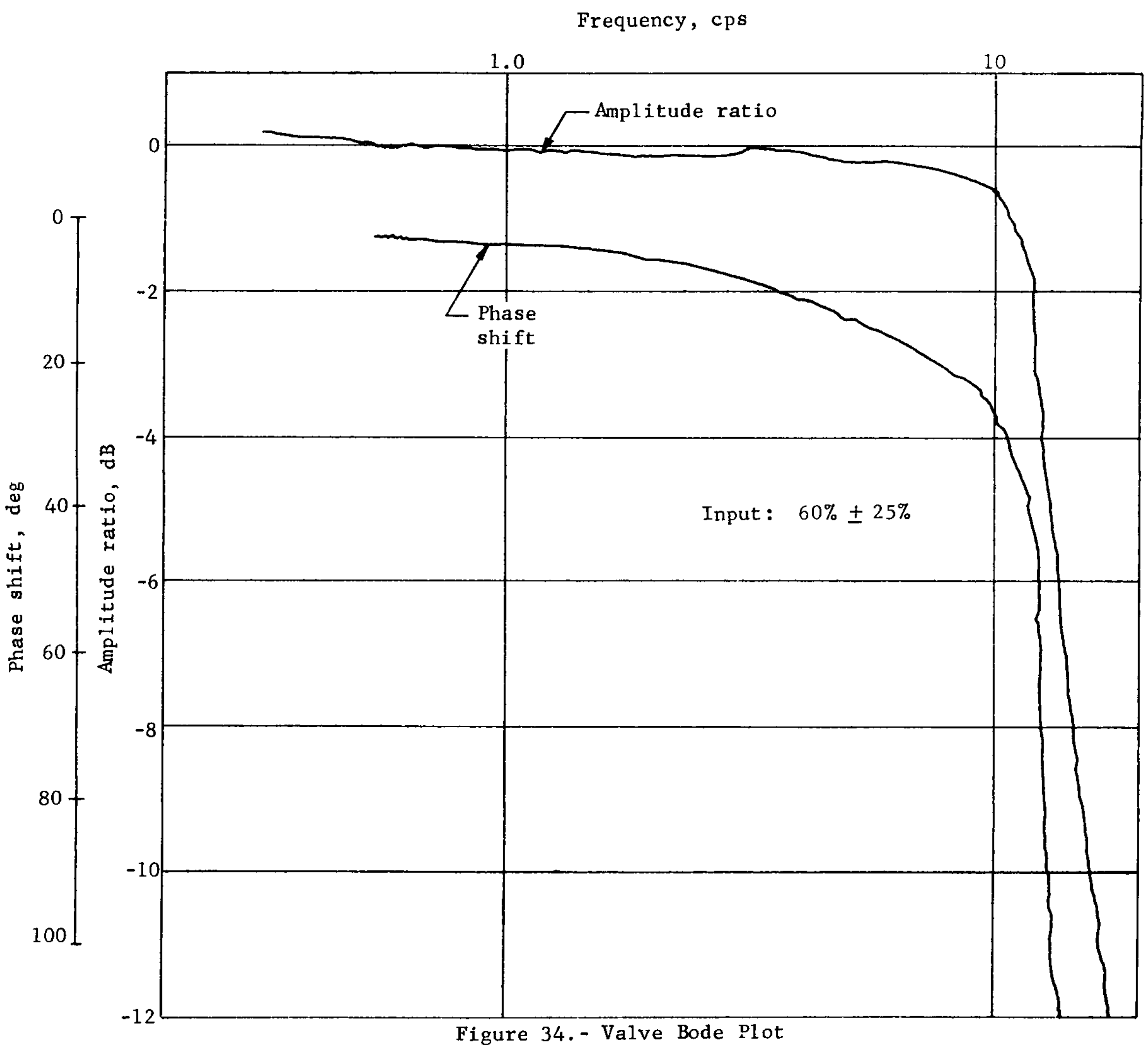

Figure 34.- Valve Bode Plot

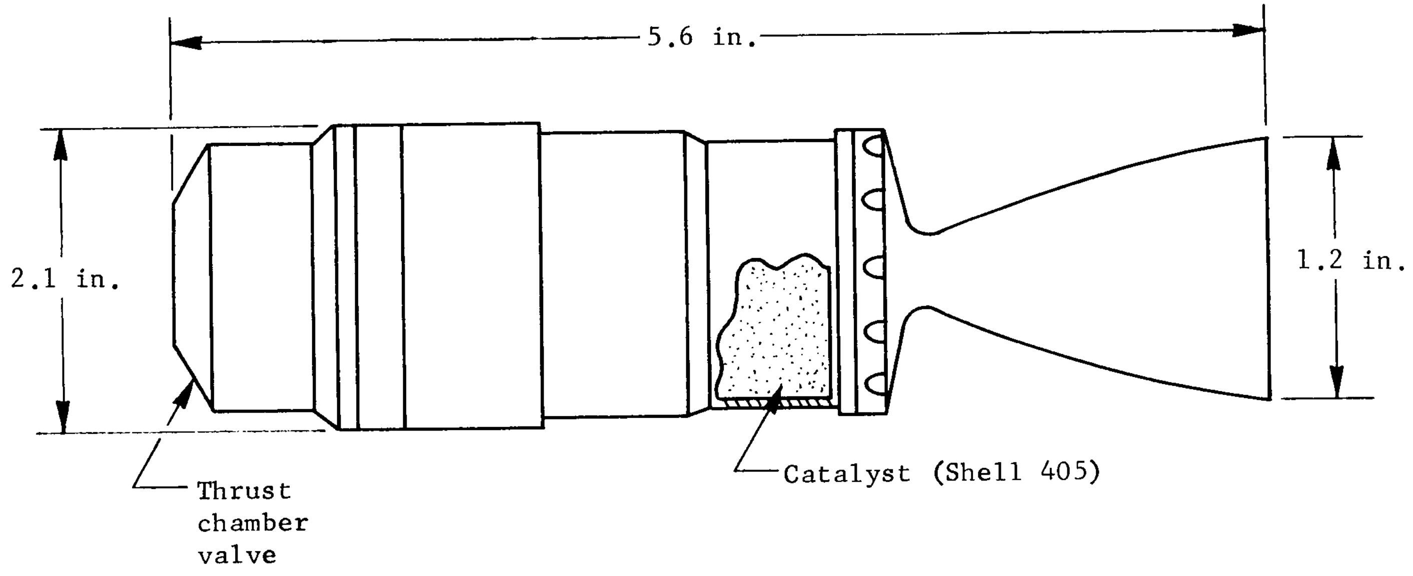
5.6 in.
2.1 in.
1.2 in.
Thrust chamber valve
Catalyst (Shell 405)

Characteristics

Thrust, lb_f	5.3 to 2.6
Chamber pressure, psia	101 to 50
Feed pressure, psia	216 to 85
Minimum pulse width, msec	20
Steady-state burn (max. per burn), sec	1200
Weight, lb	1.1

Figure 35.- Midcourse/Deflection/ACS Engine

The engines and valve selected for the preferred design were used in determining a propulsion subsystem that satisfies the following requirements:

Midcourse ΔV, 30 m/sec;

Deflection ΔV, 75 m/sec;

ACS total impulse, 244 lb-sec;

Landing total impulse 36 180 lb-sec.

A total weight statement and a schematic for this subsystem are shown in figure 36.

The Mariner '69 propulsion systems were examined during this study to determine the applicability of the hardware to the autonomous capsule design.

The requirements for the cruise mode attitude control system are as follows:

Thrust, 0.006-lb pitch and yaw, 0.0085-lb roll;

Angular acceleration, 0.225 mrad/sec^2;

Minimum on time, 20 msec;

Limit cycle, 8 mrad (pitch and yaw), 4 mrad (roll).

Based on these requirements, the Mariner '69 attitude control thruster valves, regulator, and ordnance valves were selected to perform similar functions on the autonomous capsule.

The preferred design differs from that used on Mariner in that completely redundant systems were not included due to a weight penalty of approximately 25 lb associated with the dual system design.

The preferred design includes series solenoid valves on each thruster to protect against a valve failure in the open position. Failure in the closed position does not constitute a mission failure in that control in all three axes is available with one thruster closed.

The preferred cruise mode ACS configuration is shown in figure 37. It features 12 thrusters -- four pitch, four yaw, and four roll -- to provide pure couples in the three control axes.

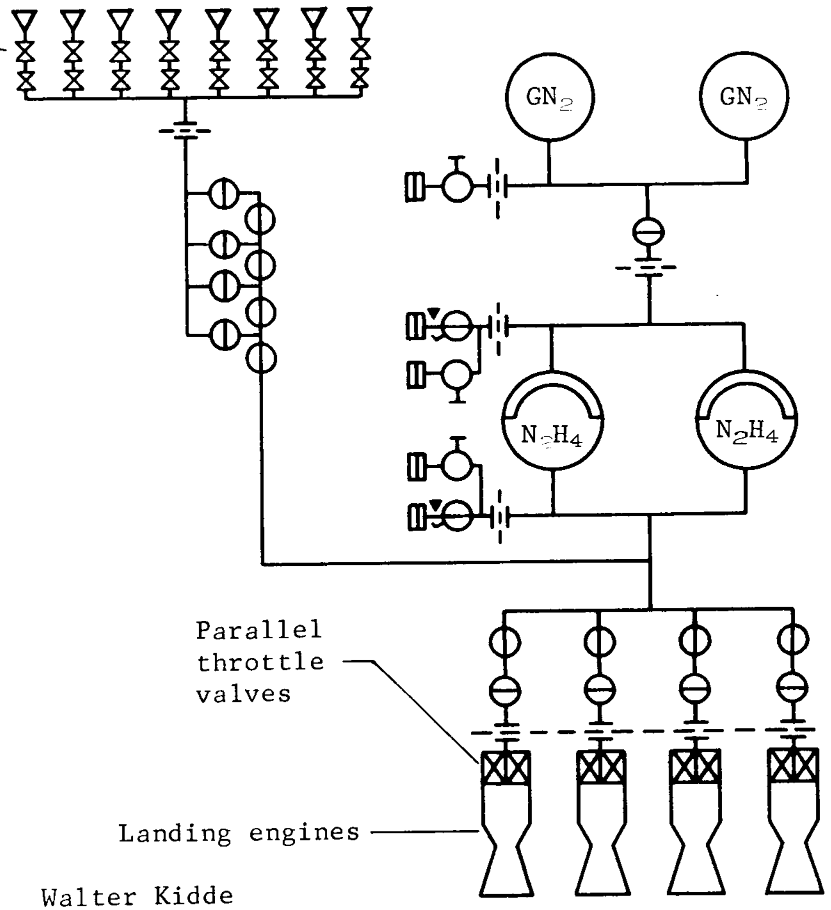
Midcourse/deflection/ACS engines
GN$_2$
GN$_2$
N$_2$H$_4$
N$_2$H$_4$
Parallel throttle valves
Landing engines

Midcourse/deflection/ACS engines

Rocket Research
$F = 5.3$ to 2.6 lb
$P_c = 101$ to 50 psia
$I_{sp} = 228$ to 222 sec
$\epsilon = 40:1$
Weight = 1.1 lb

Weight statement

Propellant		272.7
Midcourse	32.1	
Deflection	64.4	
ACS	2.4	
Landing	160.8	
Residual	13.0	
Fuel tanks		12.1
Nitrogen		10.6
Nitrogen tanks		12.0
Landing engines		140.0
Midcourse/deflection/ ACS engines		8.8
Components and lines		26.0
Supports		39.2
Total		521.4

Landing engines

Walter Kidde
$F = 300$ to 100 lb
$P_c = 100$ to 33 psia
$I_{sp} = 228$ to 219 sec
$\epsilon = 20:1$
Weight = 35 lb

Figure 36.- Propulsion Subsystem Preferred Design

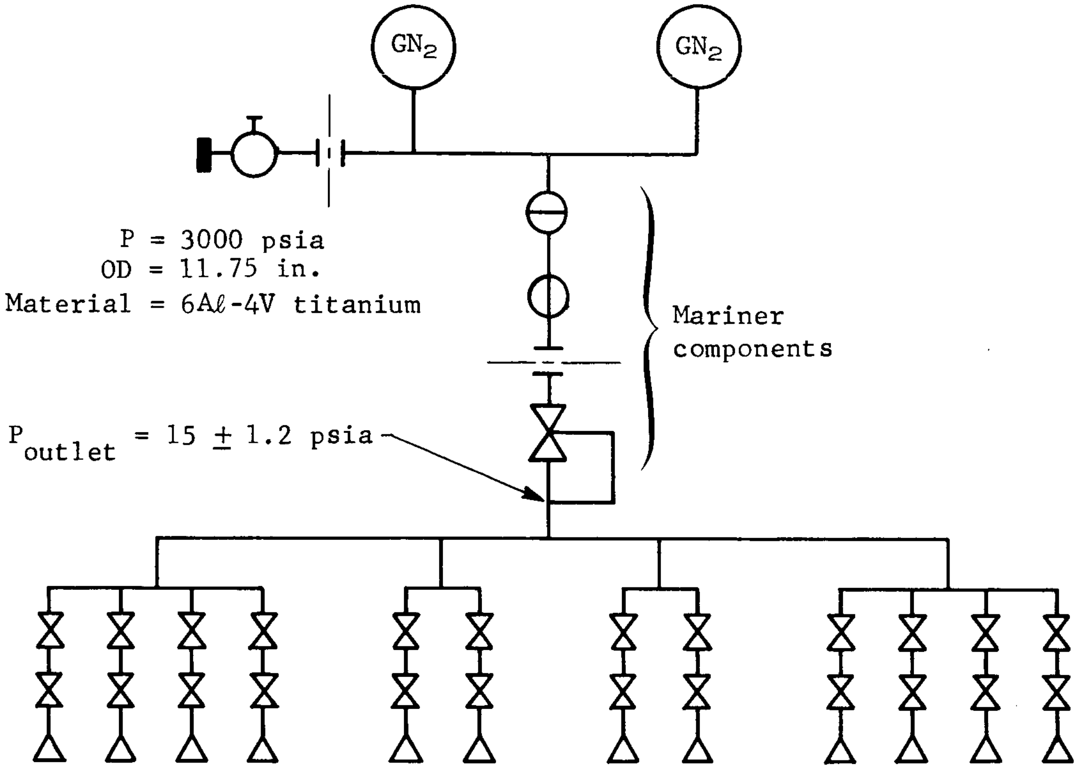
GN2
GN2
P = 3000 psia
OD = 11.75 in.
Material = 6Aℓ-4V titanium
Mariner components
P outlet = 15 ± 1.2 psia

Mariner thrusters

Thrust

Pitch, yaw = 0.006 lb
Roll = 0.0085 lb

I_{sp}

Pulse mode = 35 sec
Steady state = 60 sec

Minimum impulse bit

Pitch, yaw = 0.00012 lb/sec
Roll = 0.00017 lb/sec

Weights

Propellant		14.0
Required	6.85	
Margin	6.85	
Residual	0.3	
Tank		18.4
Thrusters		6.0
Components and lines		4.8
Supports		8.0
Total		51.2

Figure 37.- Cruise Attitude Control System

Solid rocket motors were selected for the support module spin system. This decision was based on availability of the hardware, weight advantage, and impulse accuracy and predictability. A support module spin rocket and its characteristics are shown in figure 38.

The preferred propulsion subsystem design determined by this study has produced a landing engine/throttle valve combination that significantly reduces Mars soft lander program development cost and risk. To further prove that this configuration is feasible, Martin Marietta Corporation is proposing a test program that will integrate these two pieces of hardware and will demonstrate their compatibility and ability to satisfy the lander requirements discussed in this report.

In summary, the test program consists of procuring the hardware, mating parallel valves to the engine, and performing tests to determine their performance.

The testing consists of a series of firings at various throttle settings to determine engine/valve flow characteristics at nominal inlet conditions; another series to determine performance at expected extreme inlet conditions; and a third series in which engine/valve dynamic response will be determined.

Successful completion of this program will clearly indicate the extent of engine/valve development required for the Mars soft lander program.

The salient points of the test program are summarized in figure 39.

Manufacturer	Atlantic Research Corporation
Designation	0.3-KS-5.0
Application	Tiros
Status	Qualified 1960
Average thrust	5.0 lb
Burntime	0.3 sec
Total impulse	1.5 lb-sec
Specific impulse	175 sec
Weight	0.085 lb

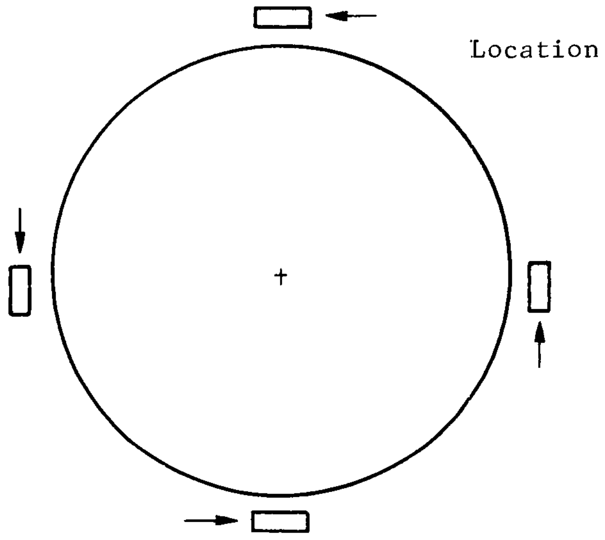

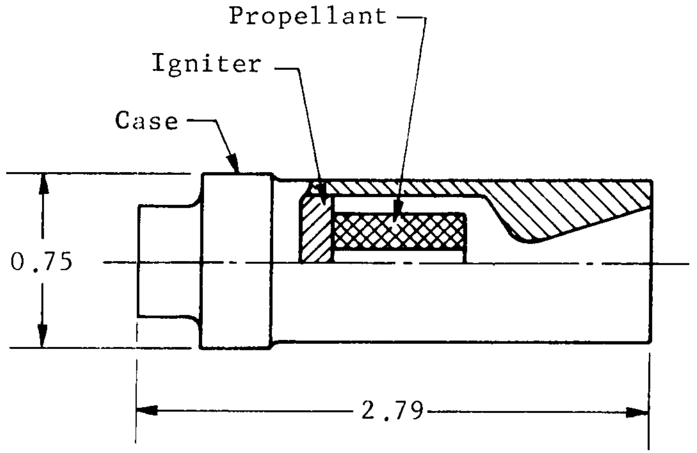
Propellant
Igniter
Case
0.75
2.79

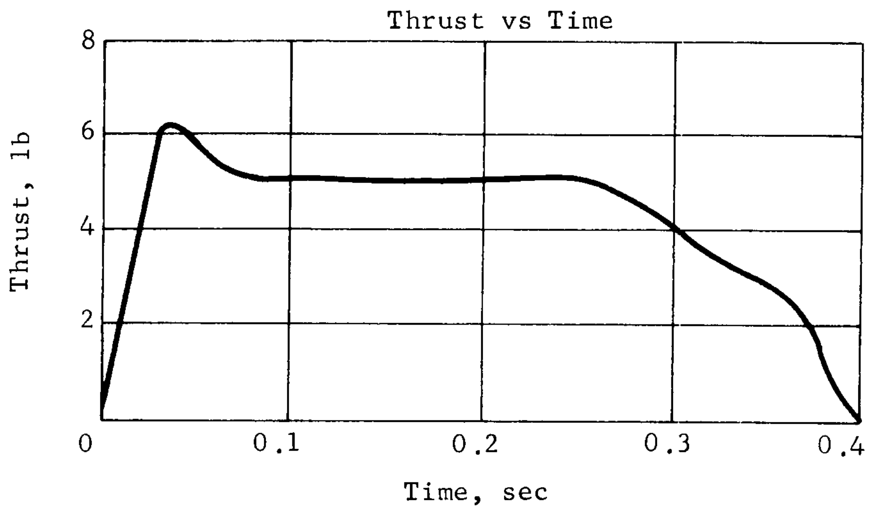

Figure 38.- Support Module Spin Rocket

Objective: To verify that the performance of the LTV valve and Walter Kidde engine combination meets the requirements of the Mars '73 lander and to define any problems associated with the use of this combination

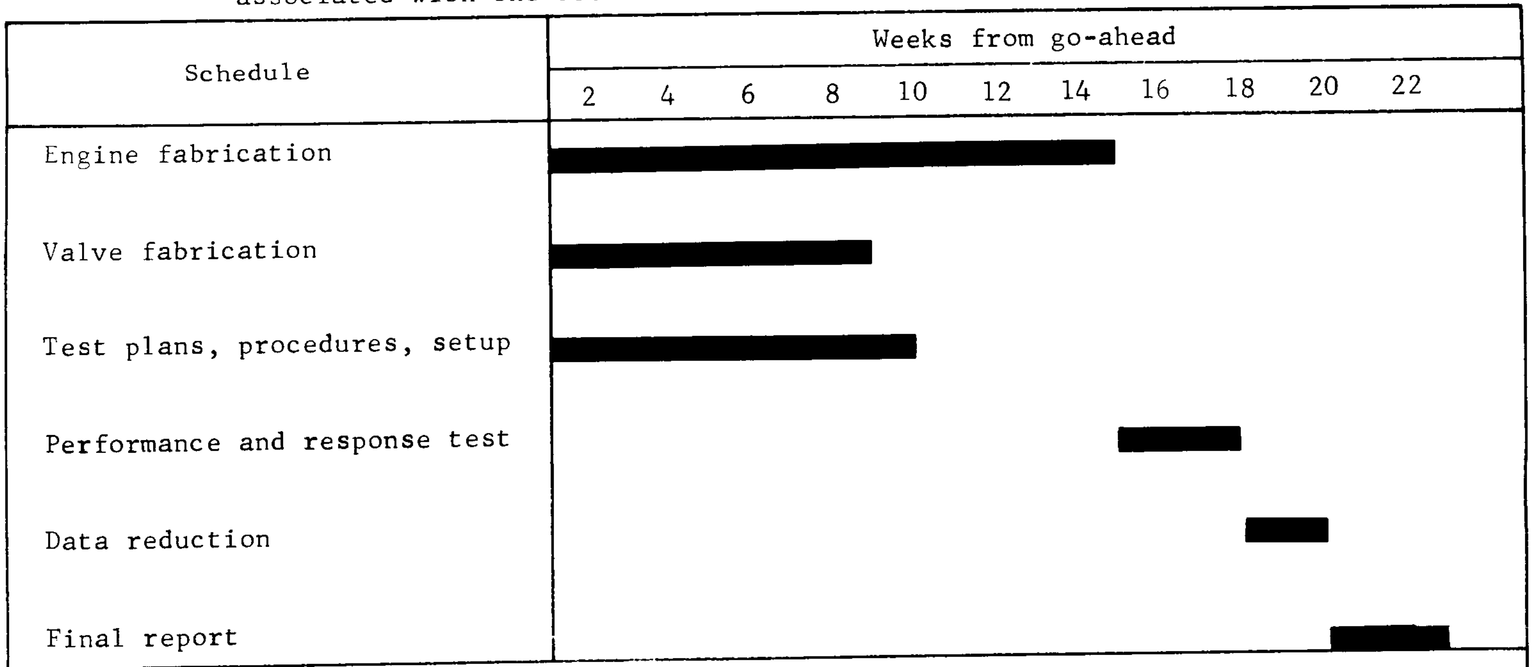

Results:
- Engine performance vs flow rate
- Start and shutdown characteristics
- Flow rate vs valve position
- Engine thermal data
- Engine/valve response
- Engine performance and response at extreme inlet conditions

Figure 39.- Throttle Valve/Engine Test Program

4. GUIDANCE AND CONTROL SYSTEM

The results of the guidance and control study for the soft lander/support module are presented in this section. The design ground rules were to select a guidance and control reference system by using existing or developed equipment [in particular Mariner components and the lunar module (LM) radar] where possible.

The study considered sensor requirements and control modes from booster separation through the terminal descent and landing phases. Volume IV of this report includes the results of the LM radar analysis performed by the Martin Marietta Corporation with the cooperation of Ryan Aeronautical Company.

Preferred Configuration

The preferred guidance and control configuration for the autonomous capsule consists of Mariner '69 sun and Canopus sensors, a three-gyro, three-accelerometer strapdown inertial measurement unit, a modified LM radar, and a high- and a low-altitude radar altimeter, all outputs being processed by a central digital computer. Signals from the computer are fed to the valve drive amplifiers, which in turn drives the attitude control jets and the vernier engines (fig. 40). The computer also performs the sequencing and ground command decoding function.

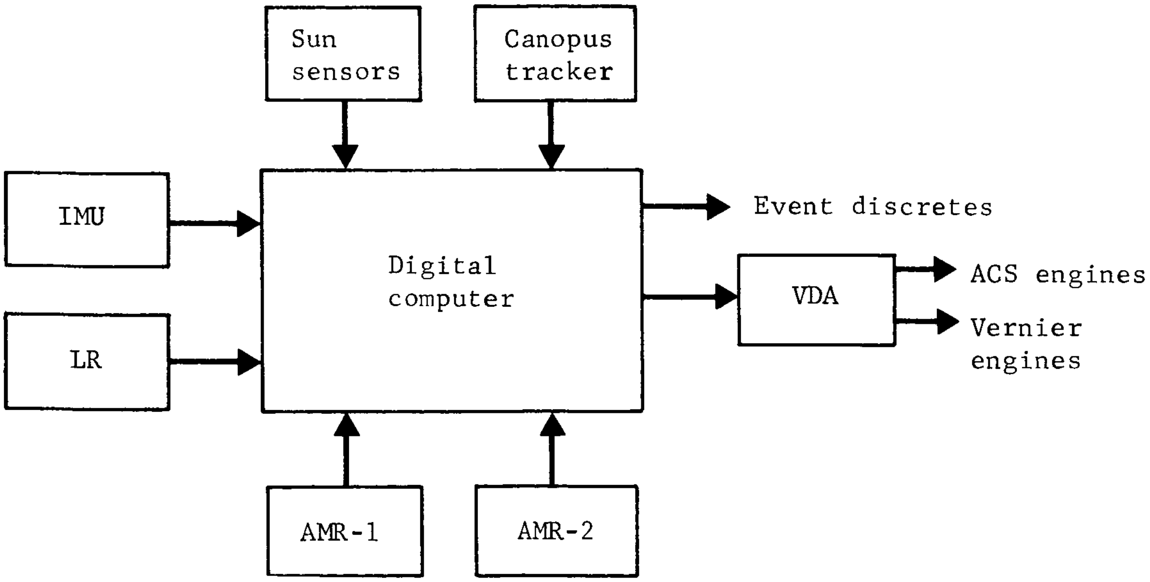

Figure 40.- Guidance and Control System Block Diagram

Criteria

The criteria for successfully performing the soft lander/ support module guidance and control function was arrived at by investigating the results of the Phase B Voyager study, the Mission Mode studies, and by considering performance capability of existing equipment, such as stellar sensors and inertial components. The range of existing sensors available is limited due to the environmental requirements. As a result of this effort, the performance requirements listed in table 22 evolved.

TABLE 22.- GUIDANCE AND CONTROL PERFORMANCE REQUIREMENTS (3σ)

Maintain attitude hold at booster separation . . .	±2°
Automatic stellar acquisition	from any orientation
Cruise control	±0.5° sun and Canopus LOS
Midcourse maneuver	±0.2° pointing, ±0.5% impulse
Orient for support module release	0.5°
Spinup and stabilize support module	2.0°
Deflection maneuver	±0.2° pointing, ±0.5% impulse
Control entry angle of attack	±5°
Control parachute sequence	±200-ft deployment, ±50-ft jettison
Achieve soft landing	$V_V < 25$ fps, $V_H < 10$ fps

Functional Description and Sequence

Prelaunch.- Before launch the guidance and control system is not powered except for the gyros that are spun up and the accelerometers that are electrically caged to withstand the launch and separation environment. Just before separation the Titan III transtage orients the spacecraft roll axis toward the sun and close to the precomputed Canopus roll reference position.

Separation and acquisition.- At separation, the spacecraft enters an attitude hold mode. This orientation is maintained until the sun is no longer shaded and acquisition can begin. At this time the celestial reference acquisition mode is initiated. Sun acquisition will almost be instantaneous because the spacecraft will be prealigned in pitch and yaw to the sun line-of-sight and Canopus in roll. Rotation rates are sensed by the three gyros. The cruise ACS then reduces the initial rates to deadband values of ±4 mrad and orients the spacecraft solar panels with respect to the line-of-sight (LOS) to the sun through the use of six coarse and fine sun sensor assemblies. These sensors provide the pitch and yaw cruise reference. When within ±5° in pitch and yaw of the sun LOS, the sun gate provides a signal that deenergizes the Canopus sun shutter, and a roll search is initiated for the star Canopus. The capsule will then roll at a controlled rate (0.116°/sec) in search of Canopus, discriminating against other stars on the basis of brightness gate settings in the Canopus sensor acquisition logic. The cone angle field of view is limited to ±5.5° from the nominal setting, which is based on seasonal variations of the Canopus cone angle. This setting is controlled by the computer with ground command backup. When a star satisfying these criteria is acquired, roll search is terminated, and the roll error signal from the Canopus tracker is switched into the control loop. At this time three-axis cruise orientation is established and a timer is initiated to turn off the gyros. The gyros remain off until 1 hr before a maneuver.

Cruise.- A stellar reference is maintained throughout the cruise mode by providing the required error signals for attitude control. The spacecraft will maintain its orientation to ±8 mrad with respect to the LOS to the sun and Canopus. This includes ±4 mrad for the pitch, yaw, and roll deadband size. Automatic reacquisition of the sun and Canopus references will occur if either or both of these references is lost due to external disturbances.

Midcourse maneuvers.- In response to ground commands to the computer, the cruise attitude control system will orient the spacecraft to any attitude for a trajectory correction maneuver. This orientation is accomplished by a pitch-roll sequence of magnitude-controlled turns. The angular rotation is controlled by the duration of the command at a constant rate of turn (0.116°/sec). At 1 hr before performing a maneuver the IMU is activated and, during a maneuver, attitude is controlled according to rate signals from three gyros in the IMU. The Canopus tracker remains on but the sun shutter is activated by a signal from the sun gate, thereby protecting the photomultiplier tube in the tracker from the sun's rays.

Thrust vector control.- After the turn sequence is completed, the cruise ACS holds the attitude until the midcourse correction thrust phase is initiated. This thrust is provided by firing the entry ACS pitch and yaw thrusters simultaneously. The cruise ACS does not have the torque capability to maintain attitude control while the entry ACS thrusters are on. Therefore, the entry ACS maintains control by pulsing off the appropriate nozzle in pitch and yaw. This is identical to the operation of the propellant settling mode used on the Titan III transtage. Roll control is maintained by the entry ACS roll jets in the normal manner. The 4 mrad deadband is maintained.

Rate and angular position signals for attitude control during thrusting are obtained from the gyros, and the acceleration and velocity signals are measured by the three single-axis accelerometers along three orthogonal vehicle axis. The outputs from the accelerometers are used in a closed loop configuration to compensate for thrust axis misalignment. At the termination of attitude hold for thrusting, the entry ACS is turned off, and the cruise ACS will reorient the spacecraft for stellar reacquisition.

Reacquisition and cruise.- After completing the correction maneuver sequence, the computer issues a command to start acquisition of the sun and Canopus references as previously stated in the separation and acquisition discussion.

Backup modes (during cruise).-

Automatic stellar reacquisition: If the stellar reference is lost during cruise, the computer will initiate an automatic acquisition sequence as described previously.

Roll override: Ground control will be capable of overriding the automatic acquisition system and commanding the Canopus tracker to initiate a roll search and acquire the next star satisfying the acquisition criteria.

Inertial control: Should there be a malfunction in the stellar equipment, the gyros will be spun up and used to provide attitude hold signals to the cruise ACS jets.

Support module separation and control.- Before the support module separates, a maneuver sequence will be initiated as previously described under midcourse maneuvers. When the spacecraft is positioned in the required orientation for separation, the spring release system is enabled, separating the support module with a ΔV of 1.0 ft/sec and tip off rates not exceeding 0.5°/sec. At 1.0 sec after separation the support module is spun up via four spin rockets positioned on its perimeter. Because of the unbalanced moment disturbances during the separation process and misalignments of the spin rockets, nutation of the support module in free flight may result. This motion could result in undesirable relay link signal fluctuations. The complexity and weight penalty of adding an active control system to remove this coning dictates the need for passive devices such as sliding masses or liquid filled toruses for nutation dampers. Therefore a passive spring mass damper (as used on OSO) was selected to remove residual nutations. Based on the analysis presented below, the support module antenna assembly will maintain its inertial orientation to less than 2° (3σ) for the duration of the mission.

The following error sources were assumed for the purpose of computing the pointing error of the support module:

1) Pointing error of capsule prior to separation, 0.5°;
2) Alignment of module within capsule, 0.5°;
3) Tip-off rates at separation, 0.5°/sec;
4) Spin up rocket misalignment within module, 0.25°;
5) Thrust axis misalignment of the spin rockets, 0.125°.

A three-degree-of-freedom digital simulation was performed on the separation, spin-up, and nutation decay phases of the support module. The worst-case model for total error was used for errors 3), 4), and 5) listed above. That is, the total misalignment of the spin rockets was postulated to be in a direction that produced a transverse body velocity that directly added to the initial tip off rate. Figure 41 shows the results of the separation and spin up phases, and shows the angular error of the module at the end of spin up as 0.81°. Figure 42 shows the resulting coning motion and the nutation decay when using an inverted pendulum-type damper for time running from 6 to 100 sec after separation. The center of the cone is the final error of 0.72° that would exist after denutation.

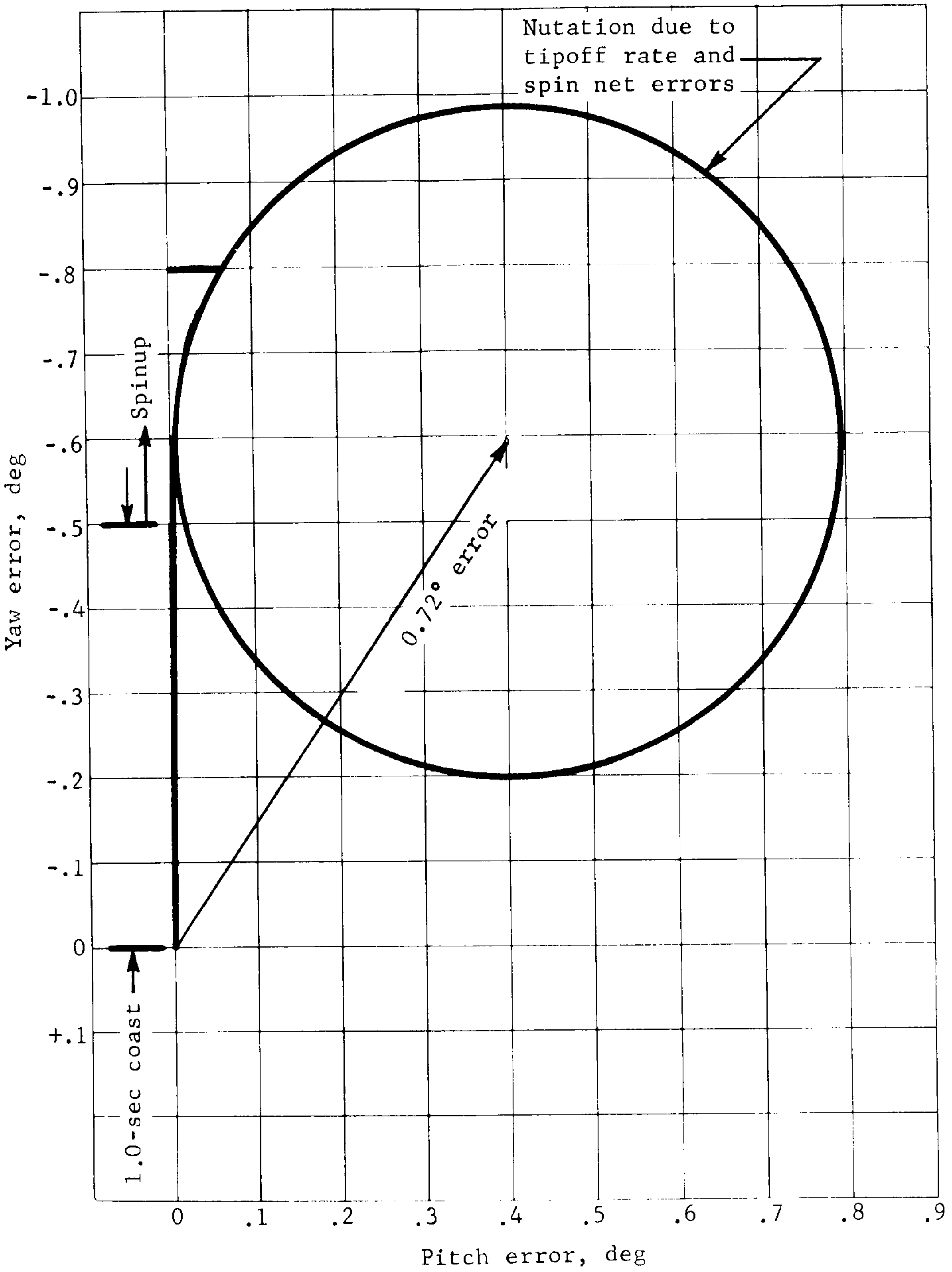

Figure 41.- Errors Due to Tipoff Rate and Spinup

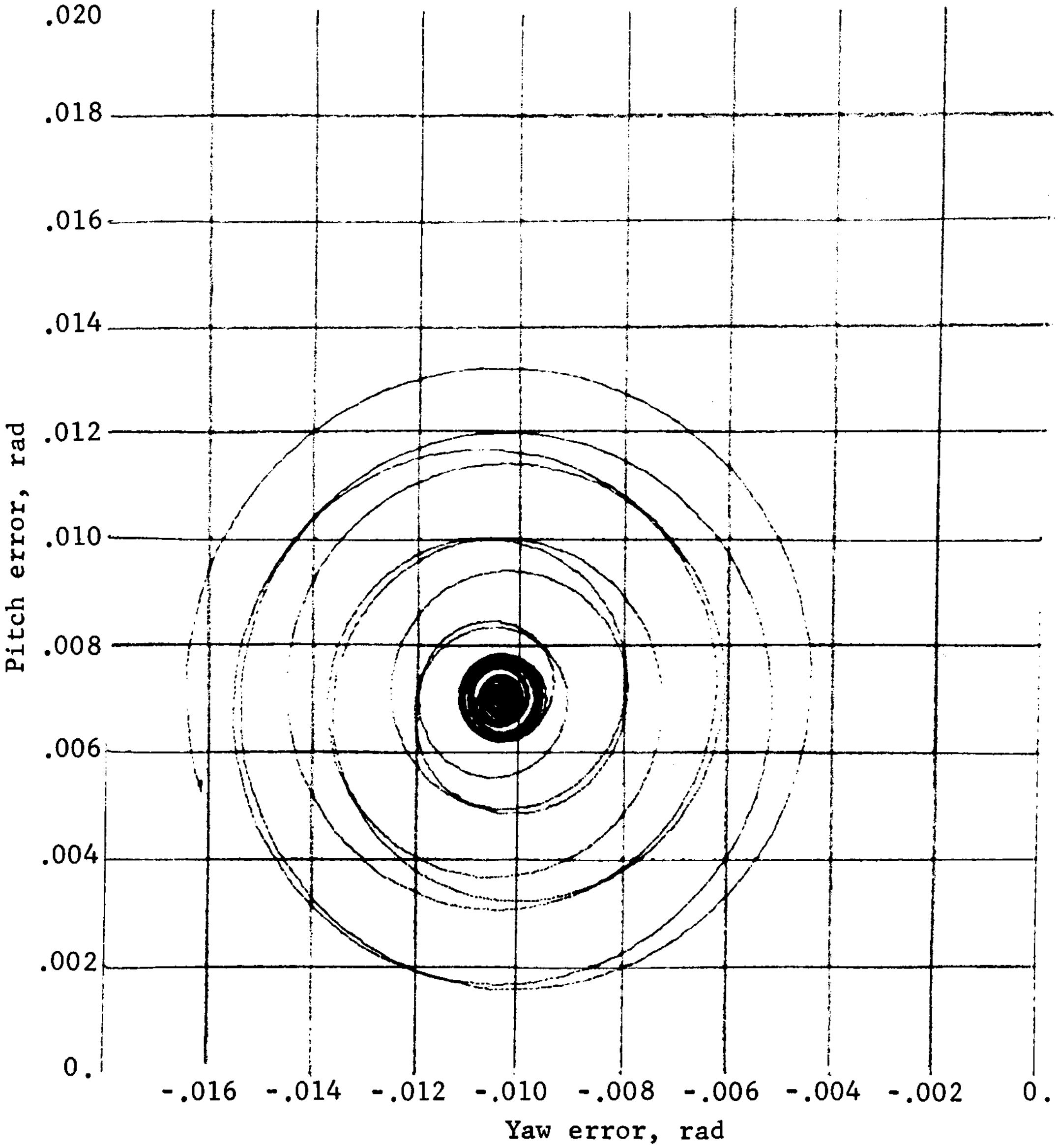

Figure 42.- Denutation of Support Module with Pendulum Damper from Time = 6 to 100 sec

An inverted pendulum is a pendulum with the hinge joint at a greater radius from the spacecraft center of gravity than the pendulum mass (see fig. 43). This is done to enable tuning of the damper to the body fixed nutation rate, thereby permitting maximum energy exchange between body and damper. The body fixed nutation rate is given by:

$$\omega_{nut.} = \frac{\left(I_S - I_T\right)}{I_T}\,\omega_Z = \frac{(2.5 - 1.7)}{1.7}\,2.8 = 1.32\ \frac{\text{rad}}{\text{sec}}$$

where

I_S = spin inertia,

I_T = transverse inertia,

ω_Z = spin rate.

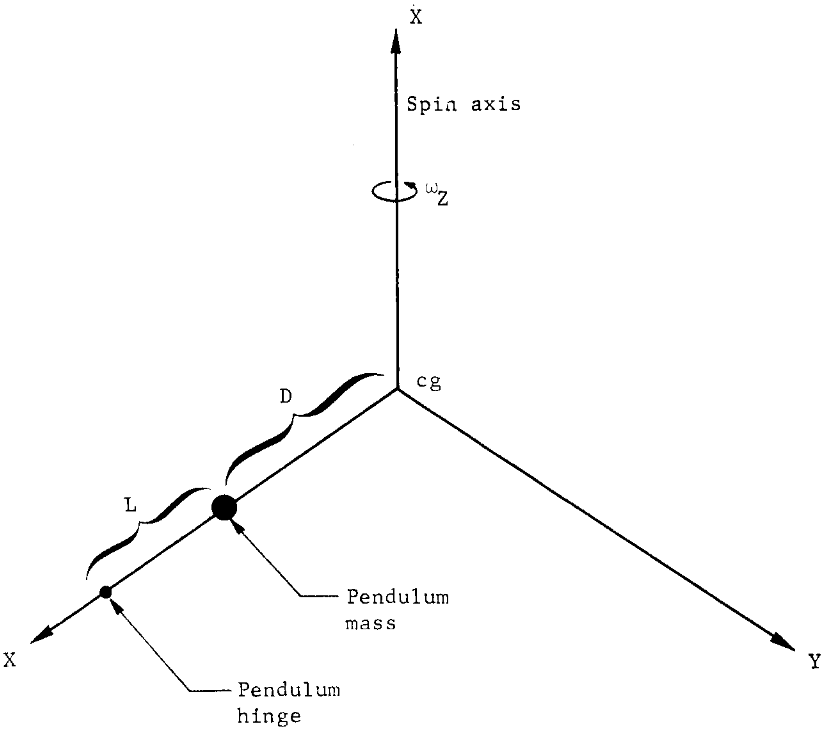

Figure 43.- Pendulum Damper Schematic

The pendulum natural frequency is given by (assuming the pendulum degree of freedom is in the X - Z plane):

$$\omega_N^2 = \left(\frac{k}{mL^2} - \omega_Z^2 \frac{D}{L}\right)$$

where

k = pendulum spring rate,

m = pendulum mass,

L = pendulum arm,

D = distance to mass from center of gravity.

Since the pendulum must be located at a positive distance, D, the only way to make the natural frequency equal to the nutation frequency is to have the centrifugal force "spring constant" subtract from the real spring constant (in other words, invert the pendulum).

A pendulum damper with a 1-lb bob mass and a pendulum arm length of 3-in. gives a denutation time constant of 16 sec. This damper is more than adequate to completely remove the nutation in the allotted time of 16 hr.

If the error resulting from the worst-case spin up assuming that denutation has occurred is added to errors 1) and 2), the resulting total worst-case error is 1.72°.

Canister separation.- About halfway through the reorientation maneuver for deflection, the canister is separated from the lander and allowed to continue on a flyby trajectory. The stellar sensors and entry ACS jets are located on this canister.

Deflection maneuver.- At separation from the support module the IMU provides the required attitude reference to the capsule.

Attitude control is maintained by the entry ACS. About 30 minutes after support module and canister separation the capsule orientation to the correct attitude for the deflection velocity change is complete. The velocity is changed by firing the entry ACS thrusters. Attitude control is maintained by pulsing off the appropriate thruster using a ±4 mrad limit cycle.

The velocity is metered by the accelerometer data. Closed-loop lateral velocity steering is used to improve the accuracy.

After the deflection thrust burn the capsule is reoriented to the attitude desired for atmospheric entry. The limit cycle used during coast is opened to ±5° to conserve ACS propellant.

Atmospheric entry.- Entry into the atmosphere is sensed by the IMU accelerometer package as 0.1 g. At this point the capsule entry ACS is switched by the computer to a rate damping mode in pitch and yaw. Roll attitude hold (±5°) is maintained so that the high-altitude altimeter antenna is oriented to the planet surface. During entry the rate damping system attempts to maintain vehicle rates less than 0.5°/sec.

Parachute descent.- At a preset altitude, measured by the high altitude radar altimeter, the computer initiates the parachute deployment sequence. The high-altitude altimeter is jettisoned with the aeroshell and pitch and yaw attitude control channels are disabled.

The low-altitude altimeter and the terminal descent radar are then turned on. Updating of the inertial navigation equations to local vertical reference begins as soon as valid radar lock on any beam is achieved. Complete inertial navigation updating can be achieved with valid data from two velocity beams and the altimeter beam. At a preset altitude, as measured by the low-altitude altimeter, the vernier engines are ignited. Two seconds after vernier ignition, the parachute is released if all engines are functioning properly.

Vernier descent and landing.- The first action of the computer after release of the parachute is to close the lateral velocity steering loops. This causes the lander to orient the thrust axis directly along the velocity vector. The velocity data are provided by the landing radar or by the inertial navigator if the radar data are incomplete. Three seconds are allowed to perform this attitude maneuver, after which the axial velocity control loop is closed. The vehicle then descends at 40% of full thrust (3:1 throttle ratio) until the range decreases below a value defined by a preprogramed range-velocity descent contour as indicated in figure 44. The engines are then throttled up to the setting (40→90%) required to follow the descent contour to a range of 60 ft above the surface and a velocity of 10 ft/sec.

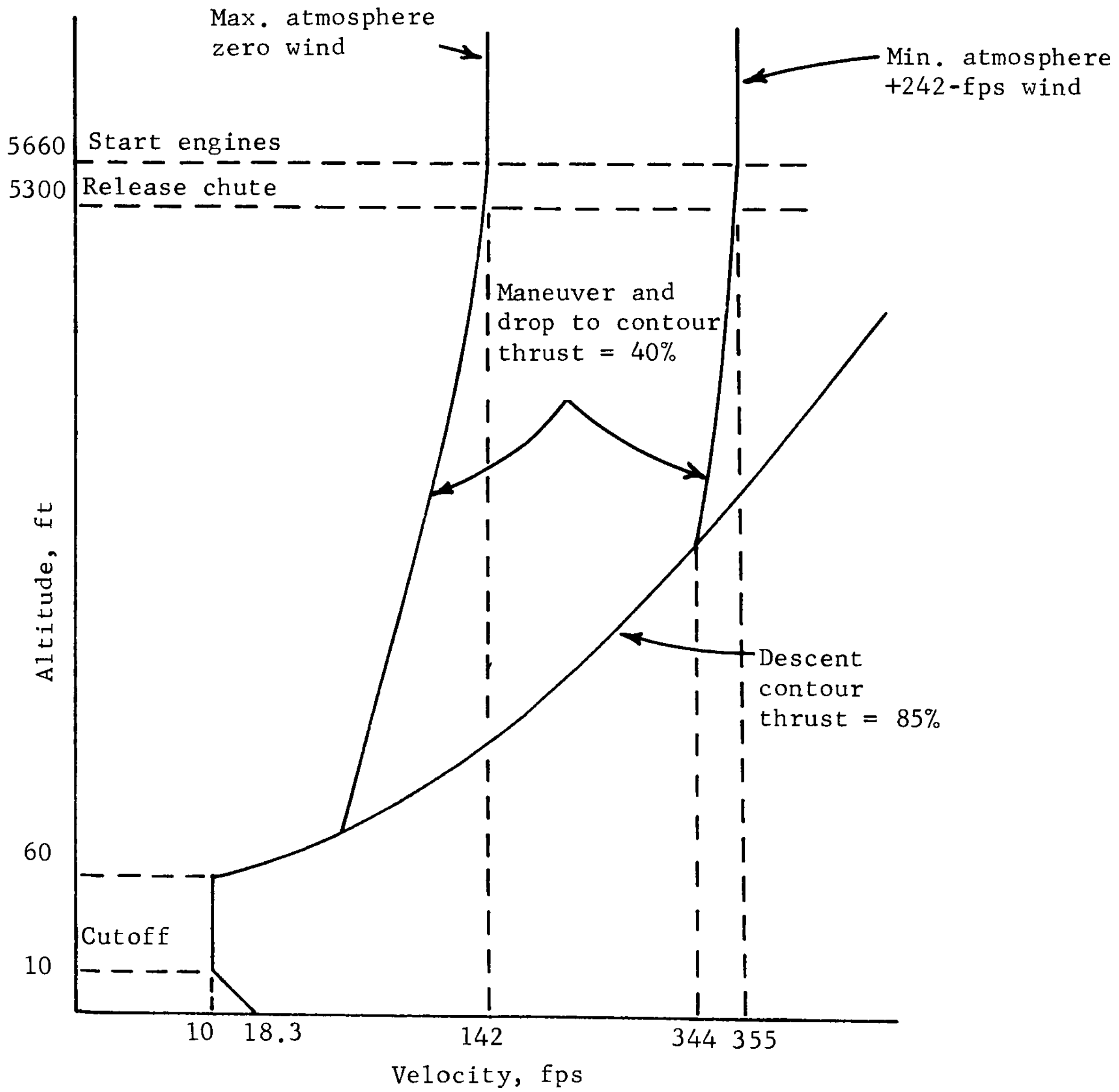

Figure 44.- Terminal Descent Axial Control Plan

From that point the lander descends at 10 ft/sec to an altitude (or range) of 10 ft. At 10 ft the vernier engines are shut down and the lander descends to the surface. The nominal impact velocity is 18.3 ft/sec vertical, 0 ft/sec horizontal. During the descent, the landing radar is used as the primary guidance sensor when all radar beams are locked. During beam unlock periods the inertial navigator data are used. Whenever the radar data are good, the inertial navigator is slaved to the radar data. Altimeter data are always provided to the navigator for updating in case of a zero Doppler or high incidence angle condition.

Physical Description

This section presents a physical description of the required guidance and control subsystems for the soft lander/support module. A number of component manufacturers were contacted as indicated in table 23 and the requirements discussed. This was done so that existing or qualified equipment such as the Mariner '69 stellar sensors and the LM radar could be used.

TABLE 23.- GUIDANCE AND CONTROL SYSTEM COMPONENT SOURCES

Component	Genesis	Potential sources
IMU	PRIME Lunar Module	Honeywell United Aircraft Autonetics
Computer	Centaur Mariner '69	Teledyne Litton Autonetics
Canopus tracker	Mariner '69	Honeywell
Sun sensors	Mariner '69	Honeywell
Radar altimeter 1	Saturn Space probe studies	Ryan Texas Instrument Westinghouse
Radar altimeter 2	Aircraft programs Space probe studies	Honeywell Texas Instrument Westinghouse
LR	Lunar Module Aircraft dopplers	Ryan Autonetics

Stellar sensors.- A solar reference for pitch and yaw was chosen because of solar power requirements. Also by using relatively simple devices, i.e., sun sensors, the sun can easily be identified and tracked. Having chosen the sun as a primary reference, and with the capsule trajectory near the ecliptic plane, a roll reference star, Canopus, near the ecliptic South Pole was chosen.

Also since the hardware, i.e. sun sensors and Canopus tracker, have already been developed and flown on previous programs, such as Mariner, it is logical to take advantage of the cost savings by using the same sensors for the soft lander/support module application.

Sun sensors: The basic function of the sun sensors is to provide error signals to the cruise attitude control system to attain sun acquisition and to maintain sun lock after acquisition during the cruise phase. The sun sensors selected for this application are basically the same as used on the Ranger and Mariner programs. The primary difference is in the mounting locations on the capsule, required to provide a 4π steradian field of view.

The sun sensor detectors consist of cadmium sulfide photoconductive cells where resistance of the detector varies as a function of light intensity. The primary detectors have a null uncertainty of ±20 arc-sec. The demonstrated accuracy of detecting an angular rotation is ±0.25°. This is accomplished by nulling the shadow position between two opposing primary detectors. The shadows are created by the sun impinging across the edge of a masking block onto the detector. The field of view of the primary detectors about the sensitive axis is 85°. The secondary detectors have a 95° field of view about the sensitive axes and are used for coarse acquisition.

Two primary two-axis sun sensor assemblies, each containing two primary detectors and two secondary detectors, are mounted on the sunlit side 180° apart. Four secondary single-axis sun sensor assemblies are mounted on the perimeter of the unsterilized canister, 90° apart, looking out from the dark side of the capsule. The location and field of view for these sensors is illustrated in figure 45. All five sun sensor assemblies and the sun gate are shown in figure 46.

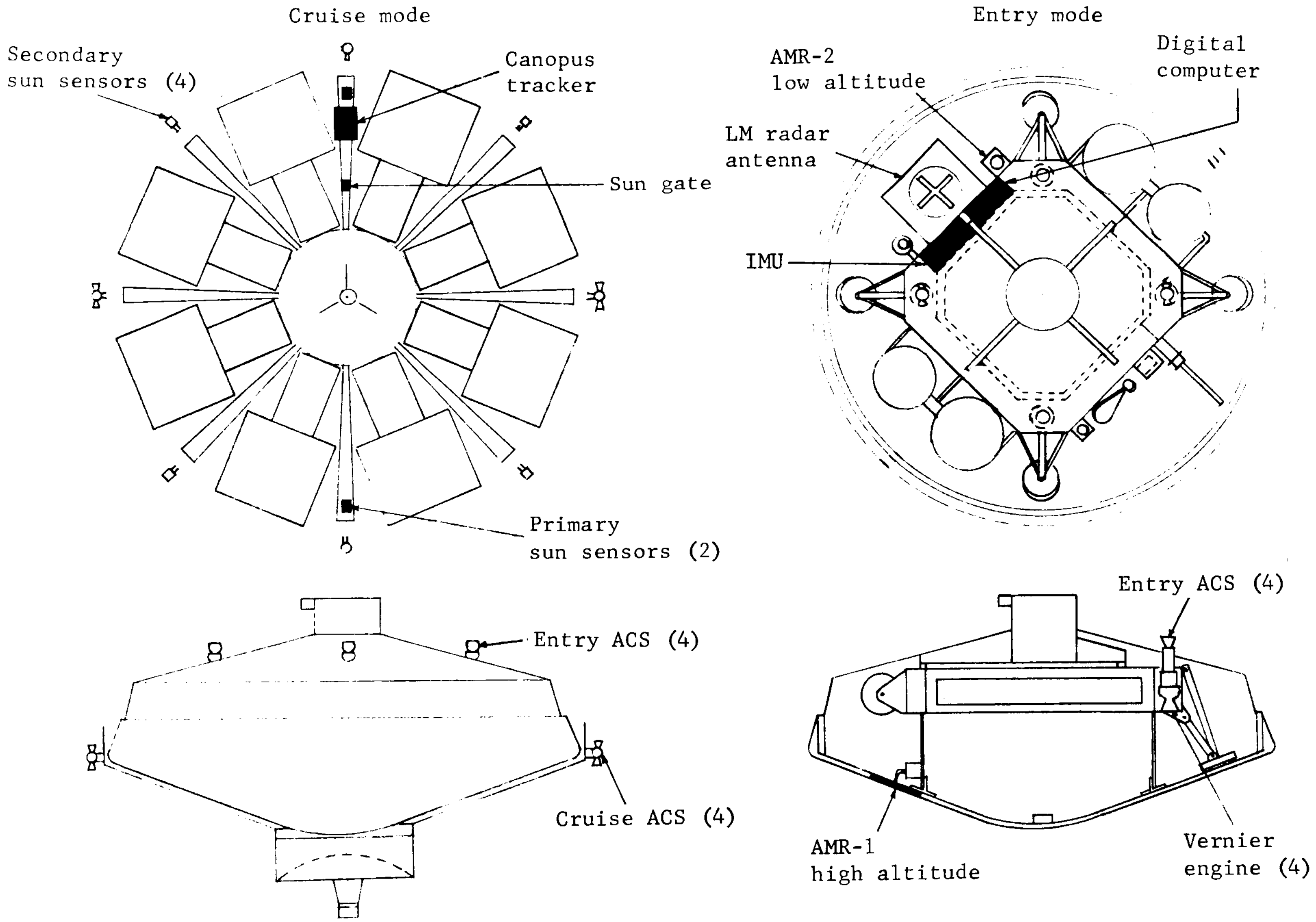
Cruise mode
Secondary sun sensors (4)
Canopus tracker
Sun gate
Primary sun sensors (2)
Entry ACS (4)
Cruise ACS (4)
Entry mode
AMR-2 low altitude
Digital computer
LM radar antenna
IMU
Entry ACS (4)
AMR-1 high altitude
Vernier engine (4)

Figure 45.- Guidance and Control Hardware Configuration

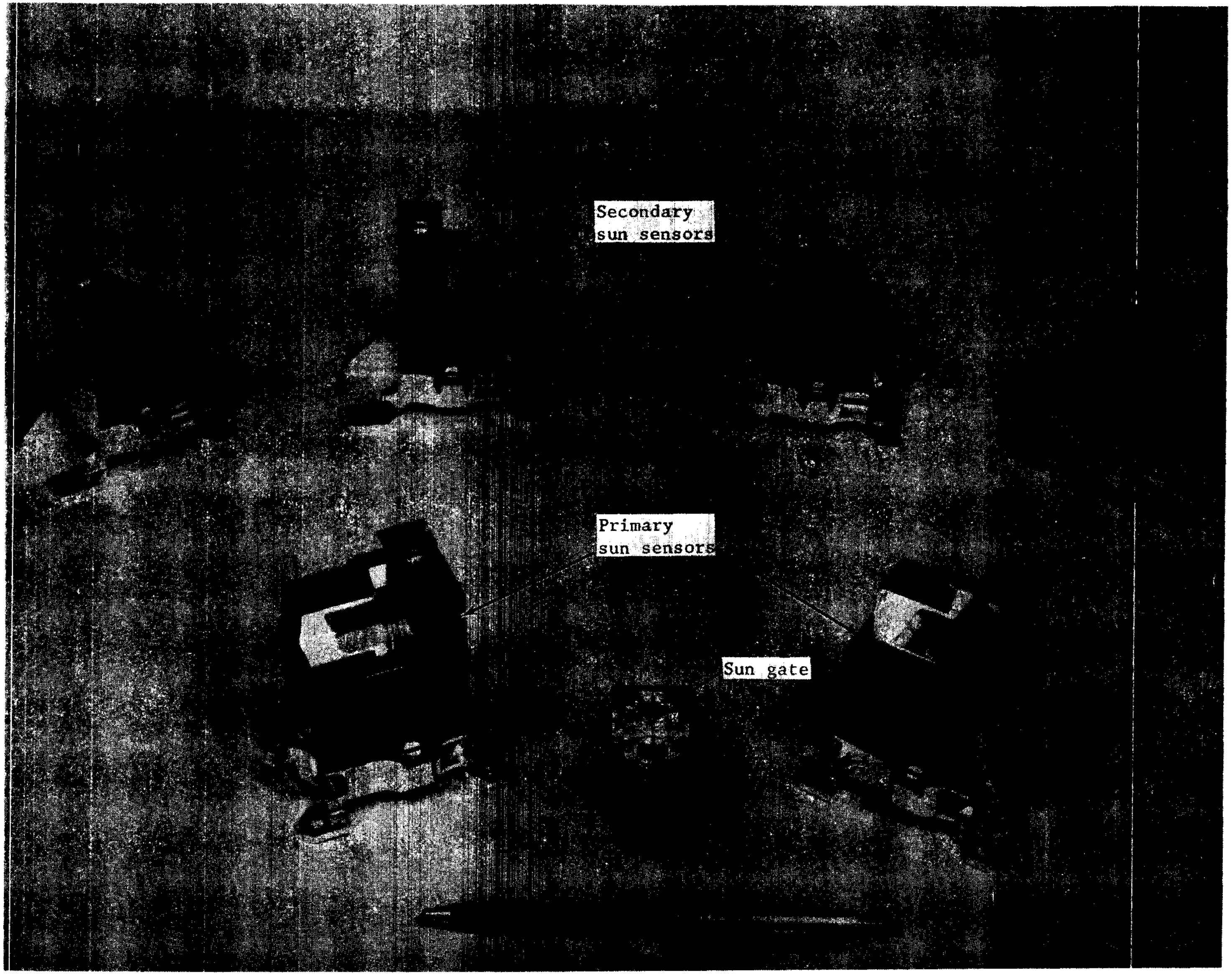
Secondary
sun sensors
Primary
sun sensors
Sun gate

Figure 46.- Sun Sensor Assemblies

The basic functional requirement for the sun gate is to provide an indication of sun acquisition. The sun gate performs the following functions. It holds power on to the acquisition sun sensors and to the Canopus sun shutter, and keeps the Canopus tracker electronics off, thereby protecting the photomultiplier tube from the damaging effects of the sun when the capsule is not sun oriented. When the capsule roll axis is oriented within ±5° of the sun line, the sun gate signal disappears and power is switched from the acquisition sun sensors to roll-search logic. The signal holding the Canopus sensor power off is also removed and the sun shutter is opened.

The detectors used in the sun gate are identical to those used in the sun sensors. The sun gate consists of an aluminum housing containing two separate cadmium sulfide photocells, associated light baffles and apertures, plus a terminal board. The photocells, or photoresistors, are masked so that they are sensitive to spacecraft cone angle, but insensitive to clock angle. Each photocell provides output signals for pitch and yaw errors. Because they are connected in parallel, redundancy is achieved.

The primary sun sensor and the sun gate assemblies each weigh 0.13 lb, and the secondary sun sensors each weigh 0.10 lb. All sensors contain similar detectors that require 100 mW per detector.

Since the sun sensors are mounted on the canister, there is no requirement to sterilize them. Consequently they will be identical to the Mariner '69 sensors, and no development effort is required.

Canopus tracker: The Canopus tracker is the position sensor in the roll attitude control loop during the cruise phase. The tracker is an electro-optical device that provides a single axis error signal proportional to the angle between the line of sight to the star and a reference axis in the mounting plane of the tracker. Table 24 summarizes the performance and physical characteristics of the Canopus tracker, which is identical to the Mariner '69 tracker.

The roll control system is capable of searching through the entire 2π radians of roll angle at 0.2°/sec or greater, rejecting objects that differ markedly from Canopus brightness. The acquisition signal is controlled by the upper and lower brightness gates, i.e., 0.04 to 3.0 x Canopus brightness.

TABLE 24.- CANOPUS TRACKER PERFORMANCE SUMMARY

Tracking accuracy	
Short term	0.002° (single axis sens. only)
Long term	0.05° (single axis sens. only)
Tracking star brightness range	0.04 to 3.0 x Canopus brightness
Field of view	
Instantaneous	1.05 x 11°
Scanned	3 x 11°
Acquisition (electrically gimbaled)	9 x 35.8°
Electronic gimbal authority	
Sensitive axis (roll)	±3° from null axis
Nonsensitive axis	±17.9° from tracker axis
Size	
Tracker	11.5x5.0x4.3 in.
Baffle	12.25x7.2x5.3 in.
Weight, tracker and baffles	8.0 lb
Power	
Tracker	5.5 W
Sun shutter (only when activated)	6.5 W
Modes of operation	
Acquisition	Automatic or commanded
Star brightness selection for acquisition	Commanded
Electronic gimbal position	Commanded
Override acquired star	Commanded

Tracker outputs:

1) Roll error signal (attitude reference and sensitive axis gimbal position);
2) Adaptive gate setting (acquisition star brightness gate);
3) Acquisition output;
4) Star brightness output;
5) Cone angle setting (nonsensitive axis gimbal position);
6) Temperature (tracker internal temperature).

Tracker inputs:

1) Input power;
2) Acquisition bias disable command (disable automatic acquisition);
3) Adaptive gate step command (controls star brightness to be acquired);
4) Roll override (overrides star being tracked);
5) Cone angle step command (controls nonsensitive axis gimbal position).

The position of the spacecraft in the solar system will be known by ground trackers computing trajectory parameters in a ground-based computer. Since the capsule is sun oriented about the pitch and yaw axes, and the Canopus sensor cone angle field of view is known, it can be predicted as to which celestial objects will pass through or near the field of view as a 360-degree roll search is performed at any given time. Therefore the acquisition of Canopus can be verified on the ground. Should the tracker lock on to another object in spite of its rejection capability, ground control will issue roll override commands and the tracker will proceed to acquire Canopus.

The Canopus tracker has five modes of operation:

1) The scanning field of view is biased to the negative edge of the tracker look angle giving a negative roll error signal until the spacecraft roll search brings Canopus into view;
2) The tracker identifies the star Canopus and the scanning field of view is released to track star position and provide a normal roll error signal;
3) If the acquired star is lost, a single roll sweep search of the full tracker look angle is made to reacquire, without initiating a spacecraft roll search;
4) If an acquisition signal cannot be obtained under all conditions, the acquisition bias can be inhibited on command so that the tracker will track any star of intensity greater than 0.04 x Canopus that enters the field of view and provide a proportional roll error signal;
5) Under any of the preceding operating modes, the tracker field of view may be momentarily reset to the acquisition bias position by command, thus releasing any star being tracked until a new star enters the field of view.

The instantaneous field of view of the star tracker is $1.05 \pm 0.05°$ by $11.0 \pm 0.1°$ in the roll and cone directions, respectively. This field of view is automatically scanned in the roll direction over a range of $\pm 1.0°$ at a rate of 1200 Hz for signal modulation and is capable of a minimum field of view center roll angle of $\pm 3°$. The instantaneous field of view center is capable of being stepped over a minimum range of $\pm 12.4°$ in the cone direction. The star tracker, therefore, has a total unvignetted field of view of 9° by 35.7° minimum in the roll and cone directions, respectively.

Since the Canopus tracker is physically located on the unsterilized canister, there is no sterilization requirement, and therefore the Mariner '69 Canopus tracker has been selected for this application.

Inertial measurement unit.- The inertial measurement unit (IMU) required for the soft lander/support module application provides three-axis attitude rate information and three-axis acceleration data. The sensor outputs are processed through a pulse rebalance mechanization whose output signals are synchronized pulse trains with frequencies proportional to attitude rates and linear acceleration, respectively. The pulse count changes are accumulated in external registers located in the digital computer. The basic IMU requirements are indicated in table 25.

TABLE 25.- IMU REQUIREMENTS

Rate channel and gyros	
Range	0 to ±35°/sec
Scale factor	1 arc sec/pulse from zero to 8°/sec
Scale factor accuracy	.2%
Long-term drift	.25°/hr
Acceleration sensitivity	2°/hr/g^2
Alignment to case reference	2 mrad/axis
Accelerometers	
Range	0 to 2 g (operating)
Scale factor	.05 fps/pulse
Scale factor accuracy	.2%
Bias	10 µg (compensated)
Axis alignment to case	1 mrad
Nonlinearity	200 ppm/g
IMU power	30 W 28 ± 6 Vdc, exclusive of heater power
IMU weight	20 lb

As a result of previous studies performed on gimbaled versus strapdown platforms (ref. 22), the gimbaled system was eliminated as a practical contender due to reliability and sterilization problems. The gyroscopes considered (ref. 28) were further limited to those capable of being torqued at reasonable rates in a strapdown mode of operation. The gyroscopes are compared in table 26.

An initial examination of a wide field of accelerometers resulted in limiting the candidates to simple force balance sensors using jewel and pivot or flexure proof mass support because of their simplicity, performance, and reliability predictions. The accelerometers that appear in table 27 were chosen for these reasons and also for their sterilization potential.

Computer.- The digital computer is required to convert sensor outputs into commands to the active attitude control and propulsion subsystems, and to generate time- and event-dependent discrete signals.

To meet the computational requirements, a general purpose digital computer with a minimum memory requirement of 4000 18-bit words (expandable to 8000 words) is used. Basic inputs will be pulse trains from sensors, as well as status discretes. All necessary input/output equipment required to interface with the sensors and computer will be a part of the digital computer. This includes the counter registers required to process the inertial sensor and radar outputs. The computer also contains required power supplies.

The computer input requirements are as follows:

Pulse train signals, 12;

Status discretes, 12;

Event discretes, 6;

Audio frequency, 5.

The output requirements are:

Proportional analog commands, 9;

On-off discrete commands, 12;

Memory discrete sequence signals, 100;

Clock signals, 3;

Pulse train commands, 4.

TABLE 26.- GYROSCOPE COMPARISON

	United Aircraft RI1139 GB	Honeywell GG 334S	Autonetics G10B
Physical characteristics			
Type	Rate integrating SDF	RI-SDF	Free Rotor-2DF
Size, in.	3 in. max. diam by 3.7 in. long	2.20 in. diam by 3.00 in. length	5.3 in. diam by 3.5 in.
Weight, lb	1.5	1.0	1.6
Angular momentum, g-cm/sec^2	$.5 \times 10^6$	1×10^5	2.4×10^5
Torquing rates, deg/sec			
Max. continuous	6	10	8
Short duration	35	35	35
Spin motor power, W Start/run	4.1/3.0	8.0/3.5	50/1.2
Torquer power (continuous), W	1.64	170 Ω dc res.	2.1 at 8°/sec
Control heater power/gyro, W max.	6.8	32 V, 140Ω(control)	----
Operating temperature range, °F	160 ± .2	180 ± 2	-30 to 150
G-capability (spunup), g	40	35	±25
Storage temperature range, °F	-65 to 275	+50 to 280	-65 to 165
Pulse torquing mech	Pulse width modulation (PWM)	Pulse on demand	PWM
Experience	Developed for SPARS	Deliv 5 units, JPL	Prototype
Sterilization potential	In-house effort RI1139GB materials through steril	JPL funded. Sterilized one unit	In-house effort materials sterilized
Performance parameters[a]			
Bias, deg/hr	.03 (1σ)	0.5	----
Random drift, deg/hr	.04 (1σ)	.01	.03
G-sensitive drift, deg/hr/g	1.5	.5	0 ± 1.5
G^2-sensitive drift, deg/hr/g^2	.3	.04	-2.0 ± 2
Torquer scale factor, deg/hr/ma	----	360	360
Accuracy, %	.3	----	----
Linearity, %	1	.01	±.6
Temperature sensitivity, ppm/°F	25	----	30
Long-term stability, ppm	20	----	300
Alignment to case ref., sec	±60	----	±4 min.
Long-term stability, sec	±5 (120 days)	----	±1.5 min.
Temperature sensitivity, sec/°F	----	----	7.5

[a] All performance parameters are 3σ numbers unless otherwise noted.

TABLE 27.- CANDIDATE ACCELEROMETERS

Characteristics	Bell model VII	Autonetics EMA-100
Scale factor		
Range, g	±50	±10
Accuracy	2:10 000	1:2000
Stability, ppm	100 (180 day)	100 (180 day)
Linearity, ppm/g	< 100	50
Temperature coefficient, ppm/°F	25	50 (100 to 185°F)
Cross axis sens., ppm/g	5	10
Bias		
Magnitude, μg	100	2000
Magnitude (comp), μg	5	< 10
Stability, μg	200 (300 day)	50 (180 day rms)
Temperature coefficient, μg/°F	< 5 (-40 to 180°F)	2 (100 to 185°F)
Noise (referred to input), μg	----	10
Axis		
Alignment, arc min	2	3
Stability, arc sec	10 (180 day)	20 (180 day)
Temperature coefficient	< .1 arc sec/°F (-40 to 180°F)	1 μrad/°F (100 to 180°F)
Electronics		
Scale factor value	$SF = \frac{\text{acceleration range, ft/sec}^2}{\text{clock frequency, Hz}}$ Typical clock frequency 5000 Hz	
Size	Sensor: 1-3/4-in. diam by 1 in. length. Analog electronics 1-3/4-in. diam by 1½ in. length. Pulse rate converter (PRC): 3x2x1½ in.	1.25 in. diam by 1.85 in. length-total
Weight	Sensor: 6.4 oz Analog electronics: 6.4 oz PRC 1 lb	3.5 oz total
Power	Sensor and electronics < 1 W PRC < 2 W	2.7 W total
Suspension	Metal flexure	Quartz flexure
Fluid medium	Gas	Gas
Sterilization	Cycled two units: at JPL and one at Bell	Cycled one unit at Autonetics
Linear acceleration	Model VII - Flight tested on Minuteman re-entry program by AVCO to measure reentry profile at 125 g linear acceleration. A-100 - 100 g projected (nonoperating).	

The computational requirements for a typical planetary lander mission are as follows:

1) Guidance and control -
    IMU initialization,
    Guidance maneuvers,
    Attitude hold,
    Rate damping,
    Throttable engine attitude control,
    Inertial navigation;
2) Sequencing -
    Preseparation update,
    Attitude commands,
    Time- and event-dependent discretes;
3) Coordinate conversion, direction cosine transformation matrix;
4) Sensor bias computation and insertion;
5) Sensor failure detection and mode switching;
6) Power strobing during cruise - memory, input/output, and processor shutdown;
7) Computer self-test;
8) Ground command decoding.

The general problem of power strobing or programed power shutdown during minimum computational periods has been investigated by Litton Inc. This concept would result in a substantial power savings for the major portion of the cruise phase. This technique must not destroy data in the memory in the event of a power transient or during power turn on or turn off. The timing requirements are such that various read/write currents must be turned on or off in specific time sequences. The required circuitry has been developed to accommodate these requirements and can easily be adopted to allow a "power strobing," which will effectively reduce the average system power.

An existing concept of power strobing can be extended from the memory to other portions of the computer system if the power saving warrants it. For example, during interplanetary cruise, when there are minimal computational requirements on the computer, all power to the memory and most of the power to the processor and input/output can be turned off with the exception of that portion of the computer required for ACS logic computations. There need be only enough circuitry active to recognize and implement a request to turn on.

The use of such power strobing techniques should result in the following types of power savings. If the memory runs at a slower cycle time, average power will be considerably less. During complete memory shutdown, standby power can be reduced to zero. The processor and input/output during shutdown (cruise) can be reduced to below 2 W average power.

As a result of the above study, the reference computer will have a maximum power requirement of 100 W at 28 ± 6 Vdc under full computational conditions, and a powered-down mode during cruise at a maximum of 25 W.

Table 28 lists the parameters of three computers potentially acceptable for this application with minimum modifications.

Radar altimeter (high altitude).- The high-altitude altimeter (AMR-1), a wide-beam pulse radar, is used during entry into the Martian atmosphere from an altitude of approximately 200 000 ft to 15 000 ft. Blackout will occur at the higher altitudes of this range but will not affect its inflight guidance and control function, i.e., chute deployment. The altimeter antenna is built into the heat shield. The performance and physical characteristics of the high-altitude altimeter are given in table 29.

The uhf altimeter chosen during the Voyager Phase B study is the basis for the parameters shown. The altimeter is fully within the state of art and entirely solid state for high reliability.

Because this altimeter will be jettisoned with the aeroshell following parachute deployment, there is no requirement for a mode change to allow low altitude use. The mechanization is a simple pulse altimeter with no requirements for "chirp" or pulse comparison techniques.

The 15 000-ft minimum altitude requirement allows the use of relatively long pulses with correspondingly narrow receiver bandwidth for better power efficiency.

TABLE 28.- CANDIDATE DIGITAL COMPUTERS

Parameter	Teledyne Centaur	Litton LC-728 with SCORS memory	Honeywell SDC-III
Type	General purpose	General purpose	General purpose
Operation	Parallel	Serial parallel	Parallel
Memory	Random access DRO core 8192 words	Random access DRO (SCORS) 4096 (exp to 32 768)	Plated wire memory NDRO 2048 words (exp to 16 384)
Clock frequency	----	2 MHz	----
Word size	24 bits including sign	28 bits	16 bits, two's complement
Instructions	29	50	51
Addressing	26 single address instructions, direct addressing 8192 words	Indirect addressing	Multilevel indirect addressing and indexing
Indexing	3 hardware index registers	----	2 registers
Add time	6 μsec	6 μsec	8 μsec
Multiply time	22½ μsec	57.0 μsec	72 μsec
Memory cycle time	3 μsec	3.5 μsec	4 μsec
Size	3.5x7.5x12 in.	----	300 cu in.
Weight	30 lb	29.4 lb	13 lb
Power	96 W	150 W	11.5 W
Cooling	Conduction to outer case	Thermal conduction to mounting	Thermal conduction to mounting
Status	Prototype for Centaur production	Production with CORCT memory	Prototype

TABLE 29.- AMR-1 RADAR ALTIMETER CHARACTERISTICS

Tracking rate, ft/sec	13 000
Operating range, ft	200 000 to 15 000
Accuracy, %	±1
Weight, lb	12
Power, W	7.2

Two possible configurations of X-band altimeters are considered as alternatives to the uhf altimeter chosen for this configuration. These are the results of the Space Probe Radar Altimeter Studies performed by Westinghouse and Texas Instruments under Contracts NAS1-5953 and NAS1-5954. In both cases a larger aperature than shown in studies is required to allow for higher altitude required. Both X-band radars use phased array-electronically steered antennas and require an rf transparent section in the heat shield.

The uhf antenna is integral to the heat shield and does not require structural modification (honeycomb, frames, etc) to the aeroshell structure. The only connection through the shell is the coaxial feed to the driven elements of the stripline array.

Possible vendors are Ryan Aeronautical Co., Texas Instrument, Autonetics, and Westinghouse.

Antenna design considerations are a beam pattern that will give adequate coverage compatible to heat shield cone angle, vehicle entry angle, and the change in entry angle during the gravity turn (from 200 000 ft to 15 000 ft). In addition, the ablative material used in the heat shield must be compatible with respect to attenuation of transmitted and received signal frequencies.

Radar altimeter (low altitude).- The low-altitude radar altimeter (AMR-2) is required to measure the range from 15 000 to 10 ft of the planet surface. The radar altimeter consists of an electronics unit containing a transmitter, modulator, receiver, power supplies, and data conversion circuitry. It will operate with a 3 dB gain antenna and accept basic inputs of 28 Vdc power and computer clock signal. The output data signal will be a clock-synchronized pulse train whose average frequency is proportional to altitude (range). Status discretes will be provided to indicate reliability of output and scale factor (if required).

The radar altimeter will satisfy the following performance requirements and conditions:

Altitude (maximum), 15 000 ft;

Altitude (minimum), 10 ft;

Altitude rate (maximum), 3000 ft/sec;

Accuracy, ±1%.

The weight and power requirements are 10 lb and 30 W at 28 ± 6 Vdc, respectively.

Minneapolis Honeywell and Westinghouse were contacted during this study to provide fully developed hardware for this application. The Honeywell system parameters and required modifications are outlined in table 30.

Two other radars are candidates for the AMR-2. Both are electronically steered narrow beam pulse radars examined in the Space Probe Radar Altimeter Studies by Westinghouse (table 31) and Texas Instruments under Contracts NAS1-5953 and NAS1-5954.

In both cases, the low altitude limit is 1000 ft so that a mode switch would be required, either to a narrower pulse or to FM-CW to extend the lower limit of capability.

Landing Radar.- The landing radar (LR) selected for the soft lander/support module application is a modified LM radar. The LR measures velocity relative to the planet surface using a three-beam doppler velocity sensor. The LR measures range to the surface with a single beam altimeter (slant range).

The LR is composed of two assemblies -- the antenna assembly and the electronics assembly -- illustrated in figures 47 and 48. The antenna assembly contains one CW transmitter, three velocity receivers, one FM/CW transmitter, one range receiver, and the cluster of phased array antennas. One component of velocity, after conversion from beam velocity to body axis components, is used to correct the range measurement of the altimeter beam for the velocity error inherent in the linear FM/CW modulation used in this radar.

TABLE 30.- HONEYWELL MICRO-MIN RADAR ALTIMETER

Characteristic	Basic altimeter	Honeywell options
System type	Pulsed radar, leading edge tracking	----
Number of units	One transmitter/receiver, two identical antennas	Single antenna
Volume	T/R: 160 in.^3 max.	----
Weight	T/R 7.5 lb, antennas 1.2 lb each	----
Operating frequency	4.3 GHz	----
Tracking rate	±2000 ft/sec	----
Search rate	15 000 ft/sec min.	----
Maneuverability, pitch and yaw	±35°	±45° to 50°
System sensitivity	-83 dBm	----
Altitude	0 to 5000 ft	----
Receiver transmitter output linear analog	0 to -40 Vdc	Digital output
Static accuracy H_R	±(5 ft + 3% of actual range) 3σ (analog)	±(2 ft + 0.2% of actual range) 3σ (digital)
Range memory (from loss of track)	1 sec	----
Dynamic accuracy	Static + 5% of range rate	Static + 1.5% of range rate (digital)
Rate of change of altitude H_R	±(5 ft + 10% of actual rate) 3σ	----
Performance monitor type	Manual, simulated altitude, 100 ft	Automatic
Sample rate	0.25 cps	----
Power consumption	28 Vdc, 30 W	115 V, 400 cps
Mounting requirements	Hard mounting	----
Warm-up time	1 min	----
Reliability	5600 hr	----
Development status	Prototype	----

TABLE 31.- WESTINGHOUSE ALTIMETER PARAMETERS

Frequency, GHz	8
Peak power, W	500
Average power, W	
Search	0.244
Track	0.122
Pulsewidth, μsec	1.067
PRF, Hz	
Search	457.4
Track	228.7
Antenna gain, dB	
Broadside	19
At 60°	16
Antenna coverage, deg	±60, 2 axes
Antenna steering	Discrete, 64 steps
Maximum altitude, km	20.47
IF noise bandwidth, MHz	1
Noise figure, dB	8.5
Reflection coefficient, dB	-30
RF losses, dB	5.1
Minimum signal to noise at 15.5 km, dB	2.2
Pulses integrated	
Detection threshold	10
Acquisition threshold	64
Range sweep time, sec	2.8
Acquisition probability, %	90
False alarm time (detection threshold), sec	3
False alarm number, (acquisition threshold)	10^{10}
Altitude noise error, %	±0.3
Altitude quantization, meters	10

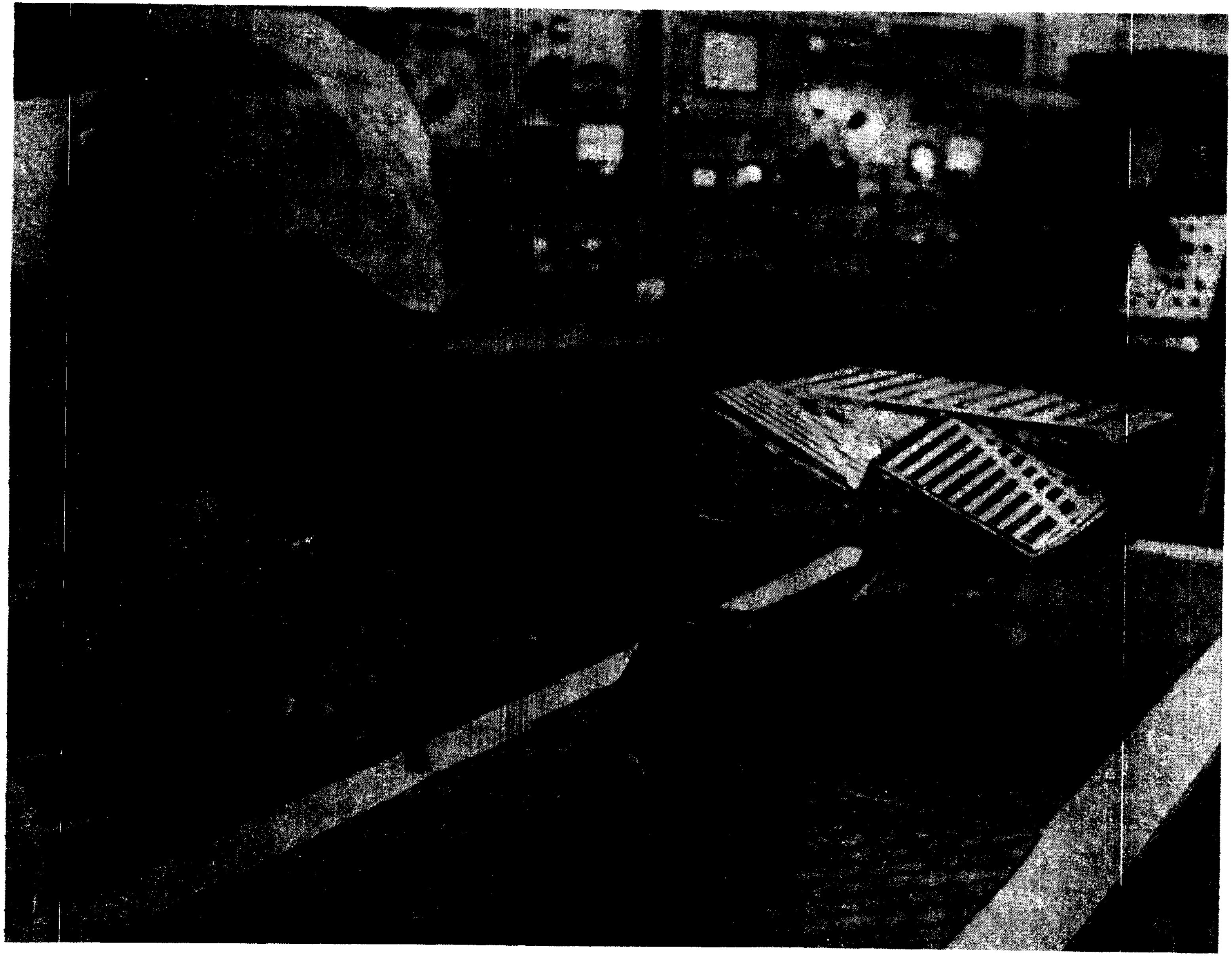

Figure 47.- LM Radar Electronics and Antenna Assembly

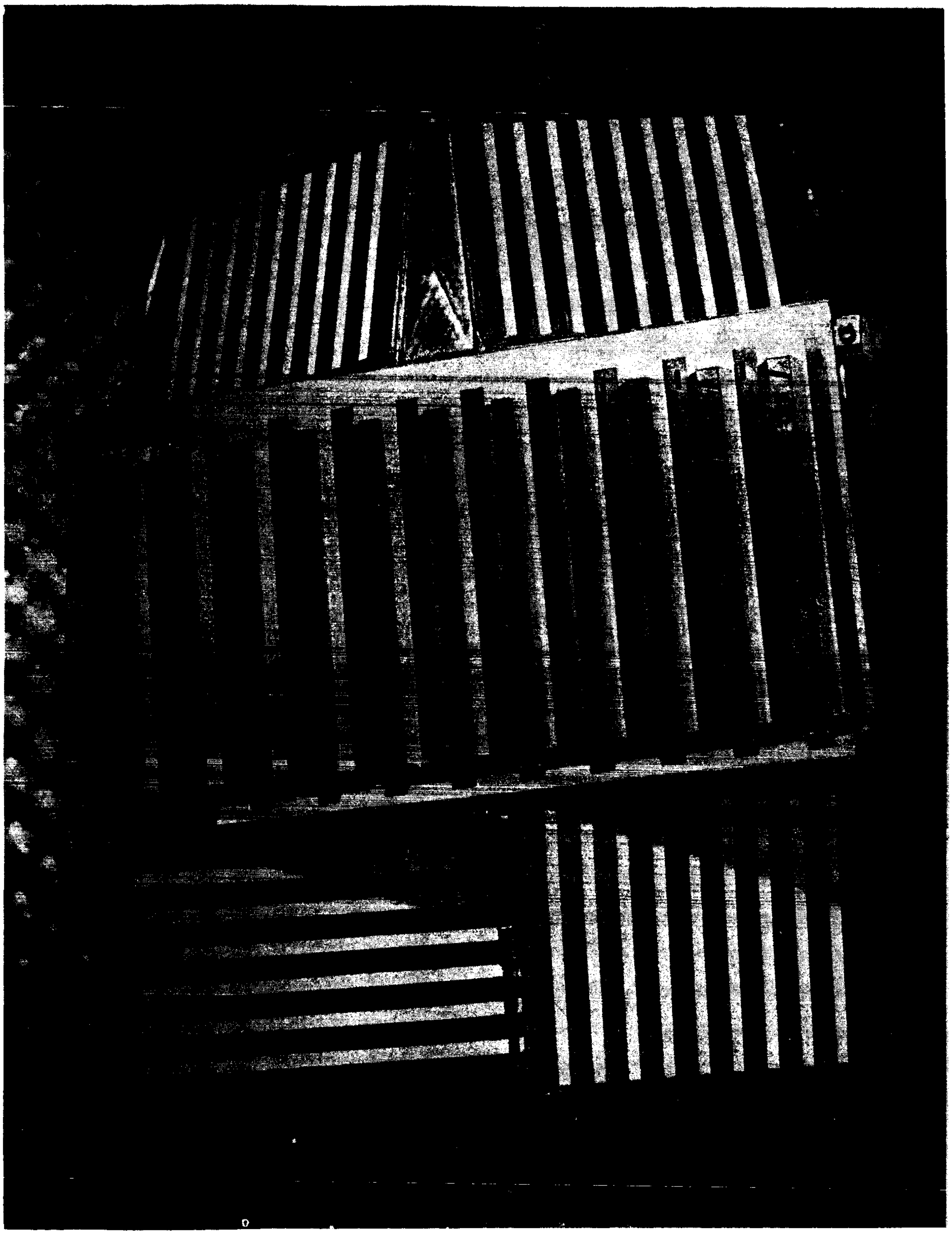

Figure 48.- LM Radar Antenna Assembly

The worst-case performance characteristics of the LM radar are listed in table 32, as published in Ryan document titled Description of the Landing Radar for the Apollo Lunar Module. These accuracies were found to be adequate with respect to the terminal descent and landing requirements. Four points in a terminal descent trajectory were given to Ryan for purposes of defining the three-sigma parameter errors via their error analysis program (see Volume IV, Appendixes). The results for that trajectory were compatible with the accuracies found in table 32.

TABLE 32.- LM RADAR SPECIFIED ACCURACIES

Parameter	Altitude, ft	Accuracy
Range (digital and pulse train)	10 to 2000 2000 to 25 000	±(1.4% + 5 ft) ±(1.4% + 15 ft)
Velocity V_{xa} (digital) V_{ya} (digital)	5 to 25 000 5 to 200 200 to 2000 2000 to 25 000	±1.5% or ±1.5 fps ±2% or ±1.5 fps ±3.5% or ±3.5 fps ±2% or ±2 fps
V_{za} (digital)	5 to 200 200 to 2000 2000 to 25 000	±2% or ±1.5 fps ±3% or ±3 fps ±2% or ±2 fps
Velocity V_{xa} (pulse train)	5 to 50 50 to 200 200 to 2000 2000 to 25 000	±0.6 fps ±0.7 fps ±1.4% or ±1.4 fps ±1.3%
V_{ya} (analog)	5 to 50 50 to 200 200 to 2000 2000 to 25 000	±1.2 fps ±1.6 fps ±2.8% or ±2.8 fps ±1.7%
V_{za} (analog)	5 to 50 50 to 200 200 to 2000 2000 to 25 000	±1.0 fps ±1.3 fps 3.0% or ±3.0 fps 3%

Recommended modifications to the LM radar are summarized in table 33. The modifications are recommended as a result of the investigation described in detail in Volume IV.

TABLE 33.- RECOMMENDED LM RADAR MODIFICATIONS

Modification description	Modification	Hardware change
Relocate the range antenna pointing direction	See fig. 49	Change the pointing direction of the range receiving antenna and phase compensation in the range transmitter antenna.
Tracker acquisition search time	From 6 sec to 3 sec, all channels	Changes in selected parts (resistors and capacitors).
Tracker acquisition search range	All modes and channels (see table 34)	Changes in selected parts (resistors and capacitors).
Tracker acquisition search rates	All modes and channels (see table 34)	Changes in selected parts (resistors and capacitors).
Tracker step low pass filter bandwidths	High mode velocity channel from 2800 to 600 Hz	Changes in selected parts (resistors and capacitors).
Delete the LM coordinate transformation	Parallel per beam output	Circuit deletion.
Mode switching criteria	From 2500 to 1250 ft	Changes in selected parts (resistors and capacitors).
Discretes	Parallel per channel discretes indicating tracker lock	Discretes exist; requires interface to bring them out.
Radar data	Parallel digital output or convert to analog format for per channel parallel analog output	Add three counter-registers or add two analog converters and modify two.
Radar/vehicle mechanical interface	Remove antenna tilt mechanization	New interface bracket.
Sterilization requirements	----	Change 51 of 124 materials. Change 24 of 4970 parts.

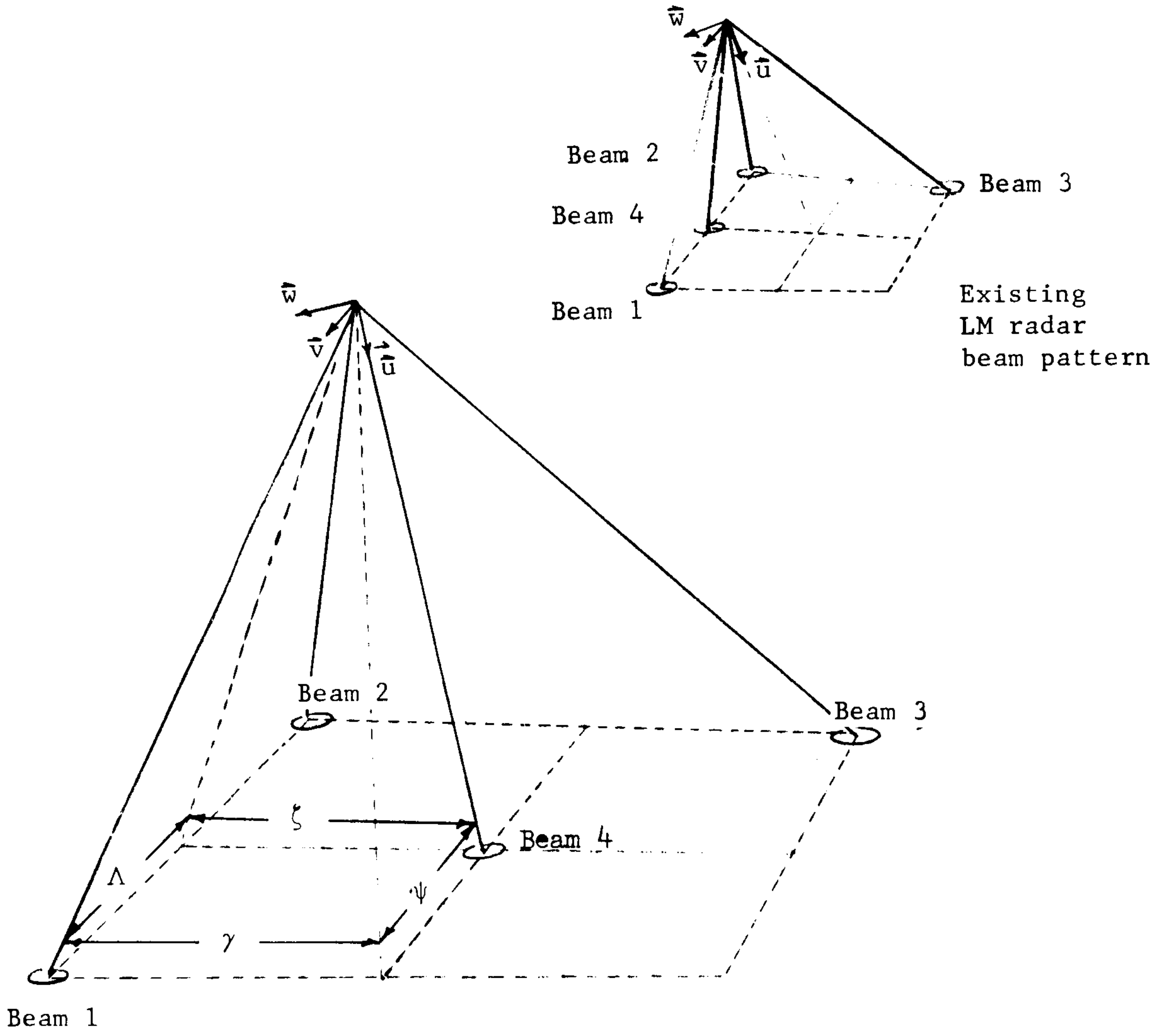
$\vec{w}$
$\vec{v}$
$\vec{u}$
Beam 2
Beam 4
Beam 1
Beam 3
Existing LM radar beam pattern
$\vec{w}$
$\vec{v}$
$\vec{u}$
Beam 2
Beam 3
ζ
Beam 4
Λ
ψ
γ
Beam 1

Note: Beam 4 is the range beam.

Figure 49.- Recommended Beam Pattern for the LM Radar (Modify Pointing Direction for Beam 4)

TABLE 34.- TRACKER MODIFICATIONS FOR SEARCH LIMITS AND SEARCH RATES

	High Mode		Low Mode	
	LM	M-73	LM	M-73
Velocity beam search range	-41. to 52. kHz[a] -20. to 77. kHz[b]	0. to 12. kHz	-5.24 to 7.4 kHz	0. to 6. kHz
Velocity beam search rates	27.4 kHz/sec[a] except 2.3 kHz/sec for -1.44 kHz $< f <$ 1.44 kHz and 26.4 kHz/sec[b] except 2.3 kHz/sec for -1.44 kHz $< f <$ 1.44 kHz	2.3 kHz/sec for $f <$ 1.44 kHz 6.6 kHz/sec for 1.4 kHz $< f <$ 12. kHz	2.3 kHz/sec	2.14 kHz/sec
Range beam search range	1. to 141. kHz	1. to 66. kHz	1. to 38. kHz	1. to 19. kHz
Range beam search rates	25.6 kHz/sec	23.2 kHz/sec	6.85 kHz/sec	6.4 kHz/sec

[a] Beams 1 and 2.

[b] Beam 3.

Valve drive amplifier (VDA) unit.- The VDA is the electrical power interface between the digital computer and the engine valves. Discrete commands for ACS control and proportional commands for vernier control are generated by the computer as shown in figure 50. Steering is accomplished by the VDA for ACS control in accordance with polarity and mode status generated by the computer. Throttle level and attitude commands are mixed in the VDA for vernier engine control. Throttle control valves are the flow rate control type with position feedback linear differential transformers.

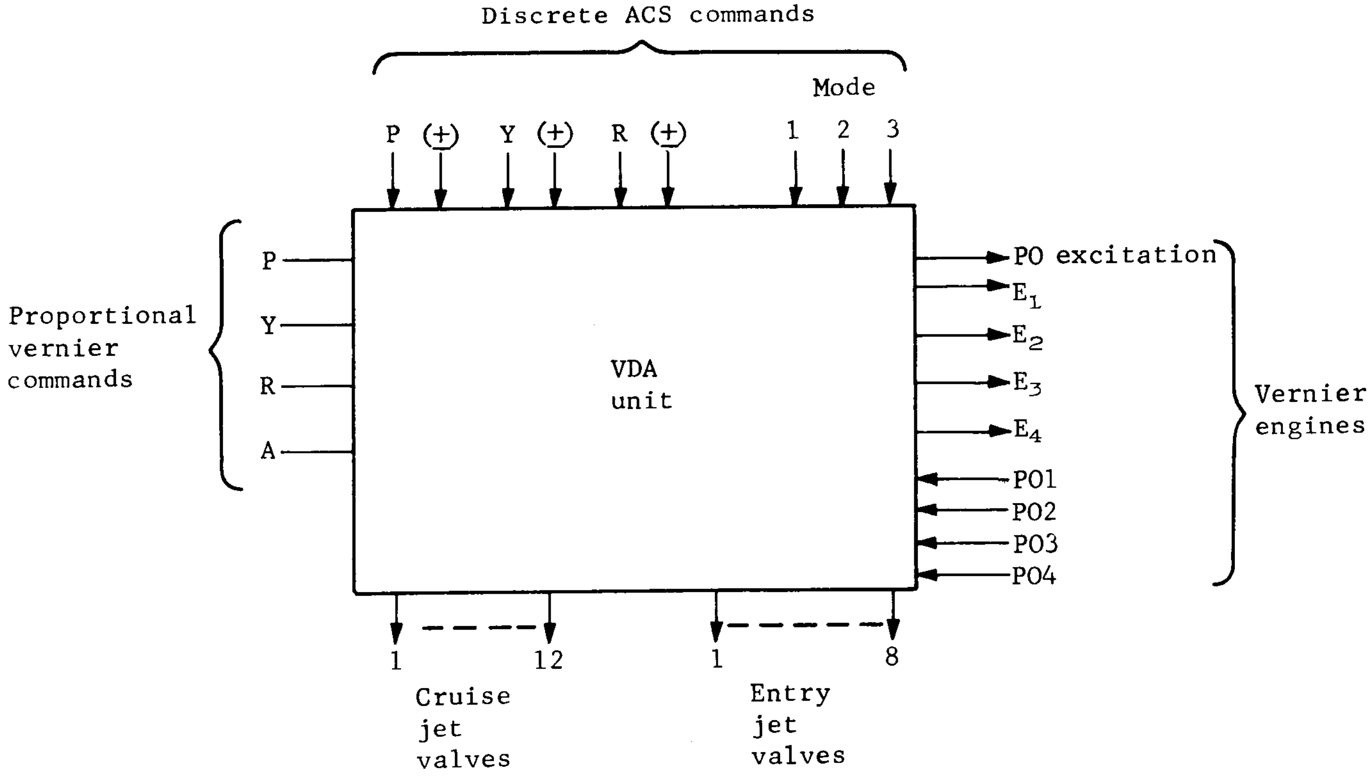
Discrete ACS commands
Mode
P
(±)
Y
(±)
R
(±)
1
2
3
Proportional vernier commands
P
Y
R
A
VDA unit
PO excitation
E_1
E_2
E_3
E_4
PO1
PO2
PO3
PO4
Vernier engines
1
12
Cruise jet valves
1
8
Entry jet valves

Figure 50.- VDA Inputs and Outputs

Error Budget

The results of the guidance and control error estimates for cruise and maneuver phases are presented in this section. Briefly, these estimates were made to assist in establishing the requirements for the sensors and active control systems used from booster separation to entry. The calculations produced estimates of midcourse ΔV errors, cruise and entry attitude control system errors, and gyro and accelerometer accuracy requirements.

Cruise orientation errors.- At booster separation an attitude error of ±2° (3σ) will have accrued due to launch geodetic and gravitational uncertainties, vehicle alignment, boost vehicle platform errors, and transfer alignment errors. Shortly after separation stellar acquisition will commence and attitude errors will be maintained to less than ±0.5° (3σ). This is due to the sun sensor resolution of ±0.25° and the dead band rectangular probability distribution of 4 mrad (0.23°) about a nominal zero point. A summary of the cruise orientation errors is as follows for the pitch and yaw axes:

Sensor alignment error (7.5 $\overset{\frown}{\text{min}}$)	0.125°
Null offsets (20 $\overset{\frown}{\text{sec}}$)	0.006°
Sensor drift (±1 $\overset{\frown}{\text{min}}$)	0.003°
Detector resolution	0.25°
	0.28° RSS (3σ) per axis
Rectangular deadband error (4 mrad)	0.23°
Total attitude deviation	0.51°

Before performing a midcourse attitude maneuver, a zero crossing detector mechanization in the computer could be used to minimize the limit cycle error resulting in an RSS (3σ) attitude uncertainty of less than ±0.28°.

Maneuver error.- The RSS (3σ) error at the end of a maximum maneuver consisting of a 180° pitch and a 90° roll maneuver is as follows:

Cruise orientation error	0.28°
Gyro alignment	0.11°
Gyro drift contribution	0.11°
Torquer scale factor	0.03°
Maneuver error	0.32°

Assumptions: Maneuver rate = 3.14 mrad/sec
Total angular rotation = 180° P + 90° R = 270°
Gyro drift = 0.25°/hr

Thrust misalignment errors.- The error in performing a midcourse velocity change and the entry deflection velocity change is presented in table 35. The values for representative parameters are based on mission requirements and typical instrument capabilities.

In the calculation of these errors, it was assumed that the lateral accelerometer data would be used to steer out thrust misalignment due to mechanical mounting of the engines, thrust magnitude differences between engines, and the control limit cycle. Consequently, the accelerometer bias produces an angular error. The velocity magnitude is measured by the thrust axis accelerometer, rather than using a thrust timer. The timer approach would produce 5 to 10% errors in velocity magnitude due to uncertainties in the nonregulated propulsion system.

Future Studies

Alternative radar approaches.- In Volume IV of this report, a detailed study of the application of the LM Radar to the Mars Soft Lander mission has been documented. Several modifications to the radar and guidance system changes are recommended to improve the confidence in achieving a soft landing. Although the LM radar with the system proposed appears to adequately perform the mission, several alternatives should be considered.

Bessel sideband radar: Previous Martin Marietta configurations have proposed use of a five-beam Bessel-sideband radar, providing range and velocity on each beam as proposed for Voyager Phase B by Autonetics. The probability of mission success is improved by this design primarily because of the redundancy provided by the five beams. Detailed simulations of this radar have not been conducted as was done for the LM radar because, until recently, the Bessel sideband approach was only a design. A detailed simulation study should be done if this radar is a serious candidate for the Mars Soft Lander mission. Another approach is a three-beam Bessel sideband radar with three velocity channels and one range channel. It would have less problems with unlocked beams than the LM radar. Each transmitter should be on a separate frequency. Alternate 3, 4, and 5 beam geometry should also be considered.

TABLE 35.- MIDCOURSE AND DEFLECTION ERROR BUDGET

Error sources	Representative parameters	Midcourse maneuver errors		Entry deflection errors	
		Magnitude, %	Direction/axis, deg	Magnitude, %	Direction/axis, deg
Cruise errors					
Stellar sensor alignment	7.5 arc min	----	0.125	----	0.125
Null offsets	20.0 arc sec	----	0.006	----	0.006
Sensor drift	±1.0 arc min	----	0.003	----	0.003
Detector resolution	0.25°	----	0.25	----	0.25
Attitude reference gyros					
Alignment	2 mrad/axis	----	0.11°	----	0.11°
Drift rate	0.25°/hr for 25 min	----	0.11°	----	0.11°
Torquer scale factor	0.01%	----	0.03°	----	0.03°
Acceleration induced	Negligible error	----	----	----	----
Accelerometers					
Bias	10 μg (compensated)	0.12	0.07	0.09	0.05
Scale factor	0.1%	0.1	----	0.1	----
Input axis alignment	70 sec	----	0.02	----	0.02
S.F. non-linearity	200 ppm/g	----	----	----	----
Output quantization	0.05 fps/pulse	0.08	0.04	0.08	0.04
Thrust cutoff approximation	0.05 sec	----	----	----	----
ACS jet misalignment	0.25° (no effect)	----	----	----	----
Thrust vector misalignment	0.125° (no effect)	----	----	----	----
RSS total		0.18	0.33	0.16	0.33

Three-beam doppler plus altimeter: The simplest complete nonredundant radar approach for the vernier descent phase is to use a low altitude altimeter (10 000 to 10 ft) with a separate three-beam doppler radar and strapdown inertial navigator. The LM radar simulations have shown that functionally, this approach is adequate. It promises to be the least expensive and the altimeter and the doppler radar need not be obtained from the same supplier. A thorough survey and analysis of alternative candidates should be undertaken.

Digital control analysis.- A study is recommended to further define the digital computer effects on the various control systems used on the soft lander. Because of the depth and difficulty of such a study, time has not permitted a thorough undertaking of it. A digital computer can have a profound effect on system stability and sensor noise problems. An early preliminary study of these potential problems can reduce the likelihood of problems occurring in these areas during hardware testing later in the program.

Parachute phase radar operation.- For the LM radar or any other candidate terminal descent radar, a critical problem area in the descent is the parachute phase. The parachute dynamics cannot be thoroughly analyzed without a six degree of freedom simulation. The resulting radar track and lock problems can only be approximated in a less complete simulation. Work should proceed in simulating the radar-parachute phase, including wind and gust effects. In conjunction with this simulation, work should proceed on defining the best approach to initializing the inertial navigator during the parachute phase even though one or more radar beams may be unlocked. "Best" in this sense does not necessarily mean "optimum" (such as a Kalman filter) but represents a tradeoff between rapid reduction of the navigator error and mechanization difficulty.

5. TELECOMMUNICATIONS

Direct Link S-Band Analyses

The soft lander/support module configuration for the Mars 1973 mission must provide the functions of command, tracking, and telemetry, as applicable, throughout the mission. These functions are to be implemented with S-band radio subsystems in conjunction with the deep space information facility/deep space network (DSIF/DSN). For this study, the DSN was assumed to consist of a network of three 85-ft antennas, and a second network of two 210-ft antennas. The 85-ft stations and one 210-ft station at Goldstone are operational sites. The other 210-ft station will be located near Canberra and will support the 1973 mission.

The nominal operating frequencies compatible with the DSIF frequency allocation will be 2295 MHz for downlink communications and 2115 MHz on the uplinks. Microwave characteristics and receiver characteristics for the standard receiver implementation and the proposed planetary receiver implementation are described in JPL document EPD-283, Revision 2, dated January 1, 1967. These characteristics will not be summarized or detailed here.

Cruise communications geometry.- A typical band of launch dates selected for the 1973 mission is from 7/13/73 to 8/12/73 based on the criterion of maximum injected weight for Type I transfer trajectories. Arrival at the target planet occurs between 1/25/74 and 2/22/74 with flight durations of 196 and 194 days, respectively. The cone angle of Earth and the distance to Earth from 9 days into the mission to planetary encounter is shown in figure 51 for the selected launch window. It is evident from this figure that, for the earliest launch date, Earth does not stay within one hemisphere. For launches near the end of the window, Earth will be within one hemisphere from injection to planetary encounter.

Soft lander/support module cruise functions and requirements.- This mission phase begins at the termination of the near-Earth phase when separation, orientation, midcourse maneuvers, and midcourse correction have been accomplished. Typically, the midcourse correction is applied at 5 days into the mission at the latest. By 9 days into the mission, the soft lander/support module will be properly aimed for a planetary encounter and locked to its celestial references. The functions to be provided during cruise by a radio subsystem are command, tracking, and telemetry.

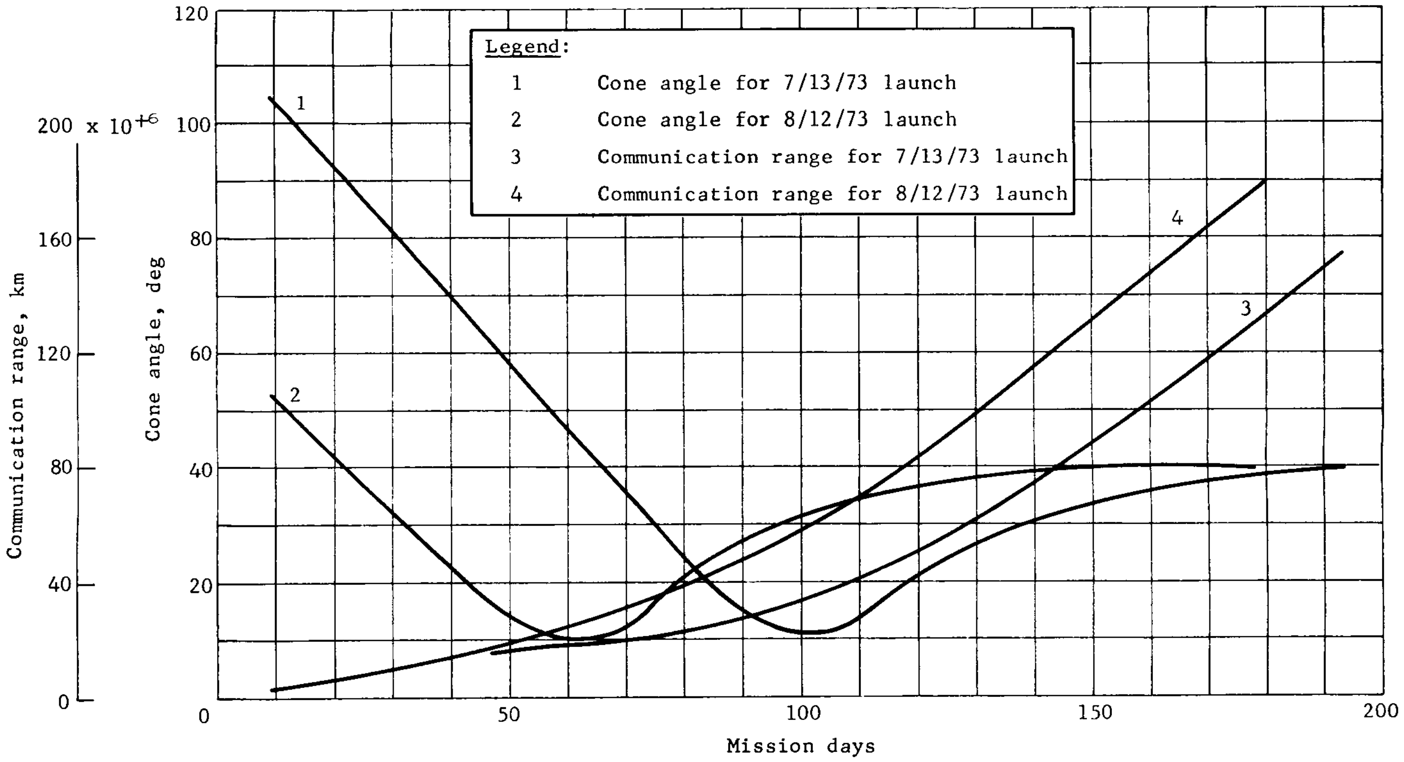

Figure 51.- Cone Angle and Communication Range

Uplink command communications will be accommodated by a low-gain, nonsteerable antenna. Since no requirement has been identified for rapid range updates during cruise, the tracking function will be limited to doppler tracking. Downlink telemetry will be required within the view capability of the DSN.

The soft lander/support module cruise radio subsystem must receive commands at a data rate of 1 bps with a BER of 1×10^{-5} or less and transmit telemetry data at a rate of 8-1/3 bps with a BER of 5×10^{-3} or less on DSN reception. Both of these functions are to be provided with a low-gain, nonsteerable antenna that is diplexed for simultaneous transmission and reception.

The data presented in figure 51 do not represent maximum values. The cruise radio subsystem will be required to operate out to 210×10^6 km corresponding to arrival at 3/2/74. The maximum cone angle will be greater than 40° due to a maneuver requirement on the support module at encounter. Thus, the subsystem parameters must be selected to provide a small performance margin above adverse tolerances to accommodate a maneuver at encounter.

Cruise radio subsystem parameters and performance.- The low-gain, nonsteerable antenna selected to accommodate the reception and transmission of data consists of a cavity-backed, crossed-slot with a helical feed. This antenna configuration is characterized by a peak gain of 5 dB and a half-power beamwidth of 130°. The gain pattern of this antenna is shown in figure 52. Pattern rolloff is slow and the gain is greater than 0 dB over 160°.

The modulation technique for telemetry transmission will be single-channel PSK/PM with the PCM data stream uncoded. This system requires an allocation of sufficient power to phase lock the S-band carrier at the ground station. For effective radiated power (ERP) of approximately 50 dBm, analyses show that a 210-ft antenna in a listen-only mode with a 5 Hz two-sided receiver APC loop is required to support the data link.

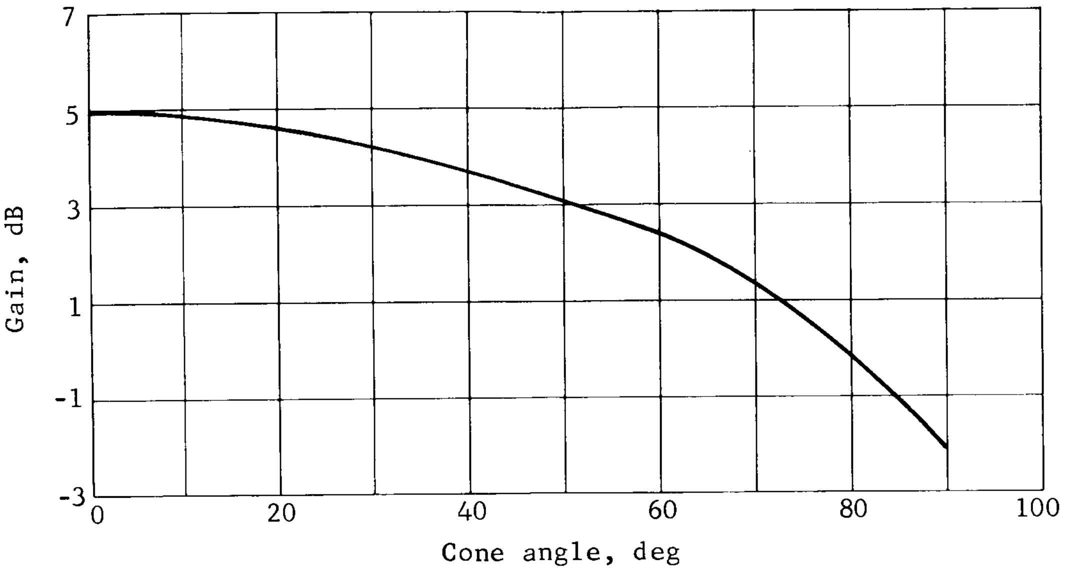

Figure 52.- Low-Gain Antenna Radiation Pattern

The performance capability of the telemetry downlink with a 25-W output power transmitter for an uncoded data rate of 8-1/3 bps is presented in table 36. The required ST/N_o of 6.8 dB for a BER of 5×10^{-3} includes a degradation of 1.5 dB from theoretical to account for IF phase error degradation, bit sync timing error, and bit detection process degradation. The tolerances in table 36 have been assigned in such a manner that tolerances appearing in the negative column always denote a decrease in SNR, and those appearing in the positive column denote an increase. Performance margin above worst-case tolerances exists at the maximum range to allow for the degrading effects of a maneuver at encounter and other unidentified system degradations.

Performance predictions for this subsystem with an ERP of 49 dBm as a function of days into the mission are shown in figure 53 for the selected launch date window. For launch on the first day of the window, telemetry transmission can be received with the diplexed 85-ft stations for 136 days. At 136 days, the carrier channel greys out and switchover to a nondiplexed 210-ft antenna is required. With a launch on the last day of the window, the diplexed 85-ft sites can be used for telemetry reception 105 days into the mission before switchover is required.

TABLE 36.- TELECOMMUNICATION DESIGN CONTROL TABLE; SUPPORT MODULE:
8-1/3 BPS DATA CHANNEL, LOW-GAIN ANTENNA, CRUISE

Parameter	Value	Tolerance, dB +	Tolerance, dB -	Notes
Total transmitter power	+44.0 dBm	1.0	0.0	25 W min.
Transmitting circuit loss	-1.5 dB	0.5	0.5	
Transmitting antenna gain	+5.0 dB	0.5	0.5	
Transmitting antenna point loss	-3.0 dB	0.0	0.0	±65°
Space loss, F = 2295 MHz, R = 210 x 10^6 km	-266.1 dB	0.0	0.0	Maximum
Polarization loss	-0.6 dB	0.0	0.0	Maximum
Receiving antenna gain	+61.0 dB	0.0	0.0	210-ft dish
Receiving antenna pointing loss	-0.0 dB	0.0	0.0	
Receiving circuit loss	-0.2 dB	0.0	0.0	
Net circuit loss	-205.4 dB	1.0	1.0	
Total received power	-161.4 dBm	2.0	1.0	
Receiver noise spectral density, T_{sys} = 25°K	-184.6 dBm	0.0	0.0	Listen only
Carrier modulation loss	-3.1 dB	0.3	0.5	θ = 0.80 rad ± 5%
Received carrier power	-164.5 dBm	2.3	1.5	
Carrier APC noise BW, $2B_{LO}$ = 5 Hz	+7.0 dB	0.5	0.0	
Carrier performance, telemetry				
Carrier threshold SNR in $2B_{LO}$	+10.0 dB	0.0	0.0	
Threshold carrier power	-167.6 dBm	0.5	0.0	
Performance margin	+3.1 dB	2.8	1.5	+1.7 dB worst case
Data channel performance				
Modulation loss	-2.9 dB	0.3	0.3	θ = 0.80 rad ± 5%
Received data subcarrier power	-164.3 dBm	2.3	1.3	
Bit rate (T^{-1} = 8-1/3 bps)	+9.2 dB	0.0	0.0	
Required ST/N_o for 5 x 10^{-3} BER	+6.8 dB	0.5	0.5	Uncoded channel
Threshold subcarrier power	-168.6 dBm	0.5	0.5	
Performance margin	+4.3 dB	2.8	1.8	+2.5 dB worst case

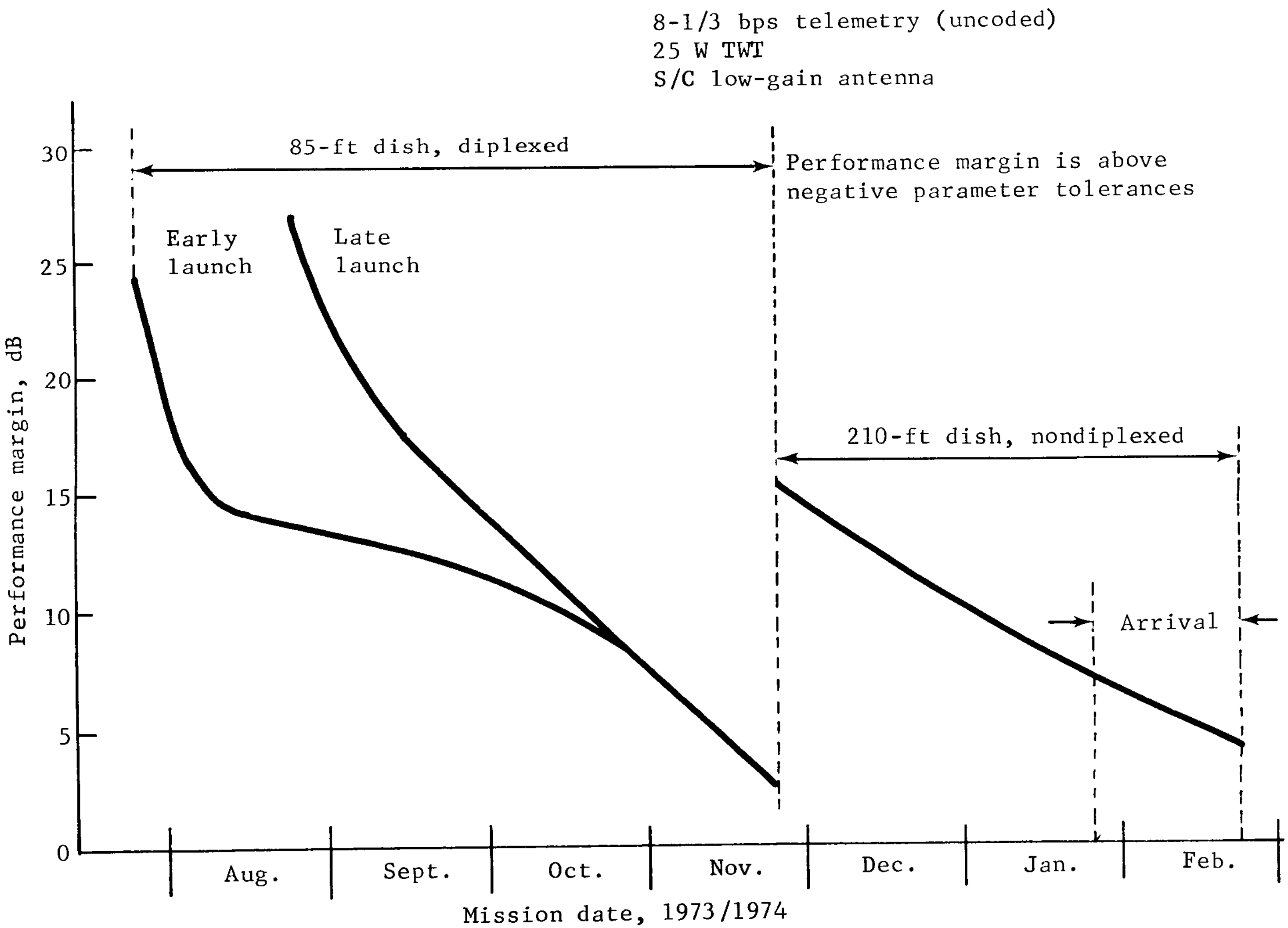

Figure 53.- Telecommunications Performance Predictions, Interplanetary Cruise

The command receiver selected for the cruise radio subsystem is characterized by a system noise temperature of 1750°K as measured at the mixer-preamplifier input, a two-sided carrier tracking loop bandwidth of 20 Hz, and a predetection bandwidth of 4.5 kHz. For an antenna temperature of 20°K and a loss of 1.5 dB, the noise temperature of 1750°K corresponds to a noise figure of 8.3 dB. This noise figure is conservative for receivers under development.

Performance capability of the command uplink is given in table 37 for the maximum range condition and isotropic receiving antenna gain. The command function can be supported by the 85-ft antenna sites out to a maximum range of 264×10^6 km, at which point the carrier tracking loop greys out. This capability of using the 85-ft antennas for the command function allows the 210-ft antennas to be operated in a receive-only mode for telemetry reception during the latter portion of the cruise mission.

During that portion of the cruise phase where the command function is provided by an 85-ft antenna and the telemetry function is accommodated by a 210-ft antenna, two-way doppler tracking can still be obtained. The mode of operation is a two-way, two-station coherent mode where the transmitter's VCO frequency is sent over a microwave link to the receiver station. The received VCO frequency is multiplied by the appropriate factor and mixed with the received downlink carrier to derive the doppler frequency.

Support module entry phase functions and requirements.- This mission phase begins at planetary encounter. The support module is separated, its roll axis oriented to Earth, and spun up. The support module then is on a flyby trajectory with its spin axis aligned to the vector to Earth. The primary function to be provided by a radio subsystem during this phase is telemetry transmission of entry science data which is relayed to the support module by the soft lander capsule. A design requirement is to provide the soft lander capsule entry science to the DSN in essentially real time, i.e., no delayed transmission of data relayed to the support module. Thus, the support module must be capable of telemetry transmission at a data rate of 2400 bps compatible with the soft lander capsule relay link data rate.

TABLE 37.- TELECOMMUNICATION DESIGN CONTROL TABLE; COMMAND UPLINK: EARTH TO SUPPORT MODULE

Parameter	Value	Tolerance, dB		Notes
		+	-	
Total transmitter power	+80.0 dBm	0.0	0.0	100 kw
Transmitting circuit loss	-0.4 dB	0.1	0.1	
Transmitting antenna gain	+51.0 dB	1.0	0.5	
Transmitting antenna pointing loss	-0.0 dB	0.0	0.0	
Space loss, F = 2115 MHz, R = 210×10^6 km	-265.5 dB	0.0	0.0	
Polarization loss	-0.6 dB	0.0	0.0	Maximum
Receiving antenna gain	+5.0 dB	0.5	0.5	
Receiving antenna pointing loss	-5.0 dB	5.0	0.0	±80°
Receiving circuit loss	-1.5 dB	0.2	0.2	
Net circuit loss	-217.0 dB	6.8	1.3	
Total received power	-137.0 dBm	6.8	1.3	
Receiver noise spectral density, T_{sys} = 1750°K	-166.2 dBm	1.1	1.1	
Carrier modulation loss	-2.2 dB	0.2	0.2	θ_D = 0.50 rad ± 5% θ_s = 0.60 rad ± 5%
Received carrier power	-139.2 dBm	7.0	1.5	
Carrier APC noise BW, $2B_{LO}$ = 20 Hz	+13.0 dB	0.5	0.4	
Carrier performance, two-way tracking				
Threshold SNR in $2B_{LO}$	+3.8 dB	0.0	0.0	
Threshold carrier power	-149.4 dBm	1.6	1.5	
Performance margin	+10.2 dB	8.6	3.0	+7.2 dB worst case
Carrier performance, command				
Threshold SNR in $2B_{LO}$	+8.0 dB	1.0	1.0	
Threshold carrier power	-145.2 dBm	2.6	2.5	
Performance margin	+6.0 dB	9.6	4.0	+2.0 dB worst case
Data channel performance				
Modulation loss	-11.0 dB	0.5	0.5	θ_D = 0.50 rad ± 5%
Received data subcarrier power	-148.0 dBm	7.3	1.8	
Bit rate (T^{-1} = 1 bps)	+0.0 dB	0.0	0.0	
Required ST/N_o for 1×10^{-5} BER	+12.1 dB	1.0	1.0	
Threshold subcarrier power	-154.1 dBm	2.1	2.1	
Performance margin	+6.1 dB	9.4	3.9	+2.2 db worst case
Sync channel performance				
Modulation loss	-5.5 dB	0.4	0.4	θ_s = 0.60 rad ± 5%
Received sync subcarrier power	-142.5 dBm	7.2	1.7	
Sync APC noise BW, $2B_{LO}$ = 2.0 Hz	+3.0 dB	1.0	0.8	
Threshold SNR in $2B_{LO}$	+13.7 dB	1.0	1.0	
Threshold subcarrier power	-149.5 dBm	3.1	2.9	
Performance margin	+7.0	10.3	4.6	+2.4 dB worst case

Support module entry radio subsystem parameters and performance.- To support the high data rate requirement of 2400 bps at the maximum encounter range, an ERP in the region of 74 dBm is required. Reduction of ERP requirements by using 210-ft antennas in a listen-only mode and the incorporation of coding in the PCM data stream was investigated. Nondiplexed operation of the 210-ft antennas provides a system gain of about 3.4 dB. The use of a (32,6) biorthogonal code with a WER of 1×10^{-2} will provide a system gain of 2.2 dB relative to an uncoded PCM data stream with a BER of 5×10^{-3}. This last advantage is gained with coherent modulation techniques.

The antenna aperture requirements are in part dictated by the accuracy to which the spin axis of the support module can be aligned to Earth. Analyses of spin attitude control techniques result in a 3-sigma alignment accuracy of ±2° as feasible for the duration of this mission phase. Thus, half-power beamwidths of 4° or greater will satisfy the alignment accuracy of the antenna rf axis to the Earth vector. The wider beamwidths are more desirable from a communications viewpoint to reduce the sensitivity of the link to the pointing error angle.

The antenna selected to accommodate the telemetry downlink rate of 2400 information bps is a 40-in. circular aperture parabolic reflector. This antenna is characterized by an on-axis gain of 25.6 dB and a half-power beamwidth of 9°. With the incorporation of biorthogonal coding and operation of the 210-ft antenna in a nondiplexed mode, an ERP of 69.6 dBm is required to support the information rate. For the selected antenna gain of 25.6 dB, the transmitter output power requirement is 25 W minimum. The performance capability of this telemetry downlink is given in table 38 for the selected and derived radio subsystem parameters. A worst-case performance margin of +3.0 dB exists in the data channel with 3 dB of antenna pointing loss to allow for unidentified system degradations due to increased system noise temperature, receiving antenna gain loss, propagation path attenuation, etc. The required ST/N_0 of 4.6 dB for a WER of 1×10^{-2} includes a degradation of 1.6 dB from theoretical to account for IF phase error degradation, bit sync timing error, and bit detection process degradation. The received carrier power is well above the threshold level for a 12 Hz tracking loop receiver bandwidth.

TABLE 38.- TELECOMMUNICATION DESIGN CONTROL TABLE; SUPPORT MODULE: 2400 BPS ENTRY SCIENCE DATA CHANNEL

Parameter	Value	Tolerance, dB		Notes
		+	-	
Total transmitter power	+44.0 dB	1.0	0.0	25 W min.
Transmitting circuit loss	-1.5 dB	0.5	0.5	
Transmitting antenna gain	+25.6 dB	0.5	0.5	40-in. dish
Transmitting antenna pointing loss	-3.0 dB	3.0	0.0	±4.5°
Space loss, F = 2295 MHz, R = 2.0×10^8 km	-266.1 dB	0.0	0.0	Maximum
Polarization loss	-0.6 dB	0.0	0.0	Maximum
Receiving antenna gain	+61.0 dB	0.0	0.0	210-ft dish
Receiving antenna pointing loss	-0.0 dB	0.0	0.0	
Receiving circuit loss	-0.2 dB	0.0	0.0	
Net circuit loss	-184.8 dB	4.0	1.0	
Total received power	-140.8 dBm	5.0	1.0	
Receiver noise spectral density, T_{sys} = 25°K	-184.6 dBm	0.0	0.0	Listen only
Carrier modulation loss	-8.6 dB	1.2	1.4	θ = 1.19 rad ± 5%
Received carrier power	-149.4 dBm	6.2	2.4	
Carrier APC noise BW, $2B_{LO}$ = 12 Hz	+10.8 dB	0.5	0.0	
Carrier performance, telemetry				
Carrier threshold SNR in $2B_{LO}$	+10.0 dB	0.0	0.0	
Threshold carrier power	-163.8 dBm	0.5	0.0	
Performance Margin	+14.4 dB	6.7	2.4	+12.0 dB worst case
Data channel performance				
Modulation loss	-0.6 dB	0.1	0.3	θ = 1.19 rad ± 5%
Received data subcarrier power	-141.4 dBm	5.1	1.3	
Bit rate (T^{-1} = 2400 bps)	+33.8 dB	0.0	0.0	
Required ST/N_o for $1 \times 10^{-[illegible]}$ WER	+4.6 dB	0.5	0.5	Coded channel
Threshold subcarrier power	-146.2 dBm	0.5	0.5	
Performance margin	+4.8 dB	5.6	1.8	+3.0 dB worst case

Postland communications geometry.- The Mars-Earth communication distance for the earliest arrival date of 1/25/74 is 160 x 10^6 km and increases with time at a rate of about 1.5 x 10^6 km/day. The position of Earth with respect to the Martian equator is 18° south at the above date and ascending northward with time at a rate of about 0.25°/day.

The contact time with Earth depends on the latitude of the landing site. Initially, southern latitudes are favored and provide longer view times. As time increases, contact time in the southern latitudes decreases with the northern latitudes increasing in viewing capability.

Soft lander telecommunications functions and requirements.- The soft lander radio subsystem design is to provide the capability of transmitting 10^7 bits of science data under the constraint of a 3-day minimum lifetime on the surface of the planet. The radio subsystem will also provide the function of command reception. Uplink command communications will be accommodated by a low-gain, nonsteerable antenna.

For the minimum 3-day life requirement, the radio subsystem must be capable of transferring 0.33 x 10^7 bits of science data per day at a maximum communication range of 210 x 10^6 km. A minimal cost constraint requires a subsystem implementation with a nonarticulated transmitting antenna that provides maximum reliability.

For this study, a 90-day design goal for the lander lifetime on the surface exists. Secondary data transfer requirements for life expectancy over and above the 3-day minimum are to be satisfied by the daily transmission of 5000 bits of meteorological data at a rate of 8-1/3 bps. The maximum communication range for the extended life will be 330 x 10^6 km for the last arrival date plus 90 days.

Soft lander radio subsystem parameters and performance.- The radio subsystem utilizes a nonarticulated antenna to provide a data rate capability and a view time that are compatible with the primary science data volume requirements. The antenna gain and beamwidth coverage are interrelated and must be adjusted to satisfy the daily data volume requirements. Larger view times are obtained by increasing the antenna beamwidth. However, the antenna gain is reduced, resulting in a reduction of the data rate for a fixed transmitter output power and communication range. The sensitivity of view time to antenna beamwidth is shown in the figures in the Missions Analysis section, Volume I. These curves were derived by assuming local vertical orientation of the antenna at the latitudes shown with Earth passing through the half-power beamwidth. The maximum of these curves occur on the dates for which the declination of Earth coincides with the latitude. At a maximum, the daily data volume capability for a fixed transmitter output power with a 60° beamwidth antenna is (46/60) of the capability with a 46° beamwidth antenna, neglecting rf carrier acquisition time.

The antenna parameters of gain and beamwidth were selected on the basis of matching the daily data volume requirement with a 50-W transmitter. At this power output level, an on-axis gain of 12.5 dB and a half-power beamwidth of 46.5° is required to support the data link. The data transmission capability with these subsystem parameters is 353 information bits per sec at the maximum range of 210 x 10^6 km. As shown in table 39, this capability exists with a 210-ft nondiplexed receiving antenna with a 12 Hz design point two-sided carrier tracking loop bandwidth. With an effective data transmission time of 2.8 hr/day, allowing 0.5 hr for carrier acquisition, the data rate of 353 bps provides 0.36 x 10^7 bits of data per day.

The S-band transmitting antenna selected consists of a 7-in. helix mounted on a 5-in. ground plane that is gravity oriented to local vertical by a counterweight. A helix was chosen on the basis that it automatically produces about the highest directivity possible for an antenna of its size over a considerable beamwidth. It is also a simple antenna to manufacture and is capable of handling 50 W of rf power in the Martian environment without breakdown.

The proposed antenna configuration will provide a minimum Earth view time of 1 hr within the 4-dB beamwidth at the end of a 90-day mission. The maximum range to be encountered for the extended lifetime is 330 x 10^6 km. With 59.5 dBm of effective radiated power, the data transfer capability of the proposed subsystem design is 80 bps (uncoded) at the end of the mission. This capability exists with a 210-ft nondiplexed receiving antenna with a 12 Hz receiver loop bandwidth as shown in table 40. The incorporation of a dual-power traveling wave tube amplifier (TWTA) with the capability of 50 W output in a high-power mode to satisfy the primary data transfer requirements and 25 W output in a low-power mode to satisfy the meteorological data transfer requirements is advocated to reduce the transmitter Watt-hour drain on the power subsystem after the primary 3-day mission. The low-power mode will provide an uncoded data rate of 40 bps at the end of the mission. This capability exists with a 210-ft nondiplexed,

TABLE 39.- TELECOMMUNICATION DESIGN CONTROL TABLE; LANDED MODULE: 353 BPS PRIMARY SCIENCE DATA CHANNEL

Parameter	Value	Tolerance, dB +	Tolerance, dB -	Notes
Total transmitter power	+47.0 dBm	1.0	0.0	50 W min.
Transmitting circuit loss	-1.5 dB	0.5	0.5	
Transmitting antenna gain	+12.5 dB	0.5	0.5	
Transmitting antenna pointing loss	-3.0 dB	3.0	0.0	±23.2°
Space loss, F = 2295 MHz, R = 210 x 10^6 km	-266.1 dB	0.0	0.0	Maximum
Polarization loss	-0.6 dB	0.0	0.0	Maximum
Receiving antenna gain	+61.0 dB	0.0	0.0	210-ft dish
Receiving antenna pointing loss	-0.0 dB	0.0	0.0	
Receiving circuit loss	-0.2 dB	0.0	0.0	
Net circuit loss	-197.9 dB	4.0	1.0	
Total received power	-150.9 dBm	5.0	1.0	
Receiver noise spectral density, T_{sys} = 25°K	-184.6 dBm	0.0	0.0	Listen only
Carrier modulation loss	-5.3 dB	0.6	0.8	θ = 1.0 rad ± 5%
Received carrier power	-156.2 dBm	5.6	1.8	
Carrier APC noise BW, $2B_{LO}$ = 12 Hz	+10.8 dB	0.5	0.0	
Carrier performance, telemetry				
Carrier threshold SNR in $2B_{LO}$	+10.0 dB	0.0	0.0	
Threshold carrier power	-163.8 dBm	0.5	0.0	
Performance margin	+7.6 dB	6.1	1.8	+5.8 dB worst case
Data channel performance				
Modulation loss	-1.5 dB	0.3	0.3	θ = 1.0 rad ± 5%
Received data subcarrier power	-152.4 dBm	5.3	1.3	
Bit rate (T^{-1} = 353 bps)	+25.5 dB	0.0	0.0	
Required ST/N_o for 1 x 10^{-2} WER	+4.6 dB	0.5	0.5	Coded channel
Threshold subcarrier power	-154.5 dBm	0.5	0.5	
Performance margin	+2.1 dB	5.8	1.8	+0.3 dB worst case

TABLE 40.- TELECOMMUNICATION DESIGN CONTROL TABLE; LANDED MODULE: 80 BPS TERTIARY SCIENCE DATA CHANNEL

Parameter	Value	Tolerance, dB		Notes
		+	-	
Total transmitter power	+47.0 dBm	1.0	0.0	50 W min.
Transmitting circuit loss	-1.5 dB	0.5	0.5	
Transmitting antenna gain	+12.5 dB	0.5	0.5	
Transmitting antenna pointing loss	-4.0 dB	4.0	0.0	±26.4°
Space loss, F = 2295 MHz, R = 330 x 10^6 km	-270.0 dB	0.0	0.0	Maximum
Polarization loss	-0.6 dB	0.0	0.0	Maximum
Receiving antenna gain	+61.0 dB	0.0	0.0	
Receiving antenna pointing loss	-0.0 dB	0.0	0.0	
Receiving circuit loss	-0.2 dB	0.0	0.0	
Net circuit loss	-202.8 dB	5.0	1.0	
Total received power	-155.8 dBm	6.0	1.0	
Receiver noise spectral density, T_{sys} = 25°K	-184.6 dBm	0.0	0.0	Listen only
Carrier modulation loss	-5.3 dB	0.6	0.8	θ = 1.0 rad ± 5%
Received carrier power	-161.1 dBm	6.6	1.8	
Carrier APC Noise BW, $2B_{LO}$ = 12 Hz	+10.8 dB	0.5	0.0	
Carrier performance, telemetry				
Carrier threshold SNR in $2B_{LO}$	+10.0 dB	0.0	0.0	
Threshold carrier power	-163.8 dBm	0.5	0.0	
Performance margin	+2.7 dB	7.1	1.8	+0.9 dB worst case
Data channel performance				
Modulation loss	-1.5 dB	0.3	0.3	θ = 1.0 rad ± 5%
Received data subcarrier power	-157.3 dBm	6.3	1.3	
Bit rate (T^{-1} = 80 bps)	+19.0 dB	0.0	0.0	
Required ST/N_o for 5 x 10^{-3} BER	+6.8 dB	0.5	0.5	Uncoded channel
Threshold subcarrier power	-158.8 dBm	0.5	0.5	
Performance margin	+1.5 dB	6.8	1.8	-0.3 dB worst case

receiving antenna with a 5 Hz tracking receiver. Thus, at the end of the mission, the low-power output mode of operation of the TWTA provides a data transmission rate capability which is 4.8 times greater than that required for the transfer of meteorological data.

With the incorporation of a dual-power TWTA in the subsystem design, the transfer of data volumes in excess of the primary requirement of 10^7 bits total, in 3-days is possible. Increased data volumes are to be obtained by operating the subsystem in the high-power mode when there is sufficient energy in the power subsystem to support the operation. The postlanding Earth visibility for the selected antenna configuration is about 3 hr for 40 days after the first arrival date. Since the communication range is increasing at about 1.5×10^6 km/day, the maximum range based on the last date of arrival is 270×10^6 km. At this maximum range, the subsystem design is capable of providing a coded data transmission rate of 210 information bits per sec. An effective data transmission time of 2.5 hr will provide 0.19×10^7 bits per day at this rate. Thus, if energy is available to support the high-power mode for 40 days after the primary 3-day mission, an additional data volume of 7.6×10^7 bits can be obtained.

The following operating modes are suggested for this postland telecommunications subsystem. The TWTA will operate in the high-power mode, 50 W, providing 353 bps (coded) for the first 3 days after landing. After the primary mission, the TWTA will operate normally in the low-power mode, 25 W, transmitting data at 8-1/3 bps (uncoded) daily to the end of the mission. If telemetry data during the next 40 days indicate the availability of energy to support the high-power mode, the subsystem will be commanded to transmit data at the rate of 210 bps (coded) in the 50-W mode at the next daily contact. This mode of operation will be exercised on a day-to-day basis. For the time period of landing plus 43 days to the end of the mission, telemetry data will be used on a day-to-day basis to determine the availability of energy for high-power operation. If energy is available, the subsystem will be commanded to operate in the high-power mode to transmit data at 80 bps (uncoded). With these normal and commanded operating modes, data volumes in excess of 10^7 bits are achieved by completely using available energy. Telecommunications design control tables are presented (table 39 thru 43) showing the performance capability of the various data modes.

The command receiver parameters and low-gain, nonsteerable antenna characteristics selected for the command function are identical with those detailed previously. Command operations for the extended-life mission will be over the 210-ft antennas when the grey-out range of 264×10^6 km is reached on the 85-ft antennas.

TABLE 41.- TELECOMMUNICATIONS DESIGN CONTROL TABLE; LANDED MODULE: 210 BPS SECONDARY SCIENCE DATA CHANNEL

Parameter	Value	Tolerance, dB		Notes
		+	-	
Total transmitter power	+47.0 dBm	1.0	0.0	50 W min.
Transmitting circuit loss	-1.5 dB	0.5	0.5	
Transmitting antenna gain	+12.5 dB	0.5	0.5	
Transmitting antenna pointing loss	-3.0 dB	3.0	0.0	±23.2°
Space loss, F = 2295 MHz, R = 270 x 10^6 km	-268.3 dB	0.0	0.0	Maximum
Polarization loss	-0.6 dB	0.0	0.0	Maximum
Receiving antenna gain	+61.0 dB	0.0	0.0	
Receiving antenna pointing loss	-0.0 dB	0.0	0.0	
Receiving circuit loss	-0.2 dB	0.0	0.0	
Net circuit loss	-200.1 dB	4.0	1.0	
Total received power	-153.1 dBm	5.0	1.0	
Receiver noise spectral density, T_{sys} = 25°K	-184.6 dBm	0.0	0.0	Listen only
Carrier modulation loss	-5.3 dB	0.6	0.8	θ = 1.0 rad ± 5%
Received carrier power	-158.4 dBm	5.6	1.8	
Carrier APC noise BW, $2B_{LO}$ = 12 Hz	+10.8 dB	0.5	0.0	
Carrier performance, telemetry				
Carrier threshold SNR in $2B_{LO}$	+10.0 dB	0.0	0.0	
Threshold carrier power	-163.8 dBm	0.5	0.0	
Performance margin	+5.4 dB	6.1	1.8	+3.6 dB worst case
Data channel performance				
Modulation loss	-1.5 dB	0.3	0.3	θ = 1.0 rad ± 5%
Received data subcarrier power	-154.6 dBm	5.3	1.3	
Bit rate (T^{-1} = 210 bps)	+23.2 dB	0.0	0.0	
Required ST/N_o for 1 x 10^{-2} WER	+4.6 dB	0.5	0.5	Coded channel
Threshold subcarrier power	-156.8 dBm	0.5	0.5	
Performance margin	+2.2 dB	5.8	1.8	+0.4 dB worst case

TABLE 42.- TELECOMMUNICATION DESIGN CONTROL TABLE; LANDED MODULE: 8-1/3 BPS METEOROLOGY DATA CHANNEL

Parameter	Value	Tolerance, dB +	 -	Notes
Total transmitter power	+44.0 dBm	1.0	0.0	25 W min.
Transmitting circuit loss	-1.5 dB	0.5	0.5	
Transmitting antenna gain	+12.5 dB	0.5	0.5	
Transmitting antenna pointing loss	-4.0 dB	4.0	0.0	±26.4°
Space loss, F = 2295 MHz, R = 330 x 10^6 km	-270.0 dB	0.0	0.0	Maximum
Polarization loss	-0.6 dB	0.0	0.0	Maximum
Receiving antenna gain	+61.0 dB	0.0	0.0	210-ft dish
Receiving antenna pointing loss	-0.0 dB	0.0	0.0	
Receiving circuit loss	-0.2 dB	0.0	0.0	
Net circuit loss	-202.8 dB	5.0	1.0	
Total received power	-158.8 dBm	6.0	1.0	
Receiver noise spectral density, T_{sys} = 25°K	-184.6 dBm	0.0	0.0	Listen only
Carrier modulation loss	-2.8 dB	0.3	0.3	θ = 0.76 rad ± 5%
Received carrier power	-161.6 dBm	6.3	1.3	
Carrier APC noise BW, $2B_{LO}$ = 5 Hz	+7.0 dB	0.5	0.0	
Carrier performance, telemetry				
Carrier threshold SNR in $2B_{LO}$	+10.0 dB	0.0	0.0	
Threshold carrier power	-167.6 dBm	0.5	0.0	
Performance margin	+6.0 dB	6.8	1.3	+4.7 dB worst case
Data channel performance				
Modulation loss	-3.2 dB	0.3	0.4	θ = 0.76 rad ± 5%
Received data subcarrier power	-162.0 dBm	6.3	1.4	
Bit rate (T^{-1} = 8-1/3 bps)	+9.2 dB	0.0	0.0	
Required ST/N_o for 5 x 10^{-3} BER	+6.8 dB	0.5	0.5	
Threshold subcarrier power	-168.6 dBm	0.5	0.5	
Performance margin	+6.6 dB	6.8	1.9	+4.7 dB worst case

TABLE 43.- TELECOMMUNICATION DESIGN CONTROL TABLE; LANDED MODULE: 8-1/3 BPS METEOROLOGY DATA CHANNEL

Parameter	Value	Tolerance, dB +	Tolerance, dB -	Notes
Total transmitter power	+44.0 dBm	1.0	0.0	25 W min.
Transmitting circuit loss	-1.5 dB	0.5	0.5	
Transmitting antenna gain	+12.5 dB	0.5	0.5	
Transmitting antenna pointing loss	-4.0 dB	4.0	0.0	±26.4°
Space loss, F = 2295 MHz, R = 330 x 10^6 km	-270.0 dB	0.0	0.0	Maximum
Polarization loss	-0.6 dB	0.0	0.0	Maximum
Receiving antenna gain	+61.0 dB	0.0	0.0	210-ft dish
Receiving antenna pointing loss	-0.0 dB	0.0	0.0	
Receiving circuit loss	-0.2 dB	0.0	0.0	
Net circuit loss	-202.8 dB	5.0	1.0	
Total received power	-158.8 dBm	6.0	1.0	
Receiver noise spectral density, T_{sys} = 45 ± 10°K	-182.1 dBm	1.1	0.9	Diplexed
Carrier modulation loss	-2.8 dB	0.3	0.3	θ = 0.76 rad ± 5%
Received carrier power	-161.6 dBm	6.3	1.3	
Carrier APC noise BW, $2B_{LO}$ = 5 Hz	+7.0 dB	0.5	0.0	
Carrier performance, telemetry				
Carrier threshold SNR in $2B_{LO}$	+10.0 dB	0.0	0.0	
Threshold carrier power	-165.1 dBm	1.6	0.9	
Performance margin	+3.5 dB	7.9	2.2	+1.3 dB worst case
Data channel performance				
Modulation loss	-3.2 dB	0.3	0.4	θ = 0.76 rad ± 5%
Received data subcarrier power	-162.0 dBm	6.3	1.4	
Bit rate (T^{-1} = 8-1/3 bps)	+9.2 dB	0.0	0.0	
Required ST/N_0 for 5 x 10^{-3} BER	+6.8 dB	0.5	0.5	
Threshold subcarrier power	-166.1 dBm	1.6	1.4	
Performance margin	+4.1	7.9	2.8	+1.3 dB worst case

UHF Relay Link Analyses

The lander/capsule configuration for the Mars 1973 mission must provide the function of telemetry transmission to the support module during capsule coast, entry, and landing. The requirement for a relay communication technique during this phase of the mission is a derived one. A direct link capability for the capsule with a direct entry from a flyby trajectory requires steep flightpath angles resulting in payload penalties. The data transmission capability of a capsule/lander direct link for reasonable ERP levels also results in a data volume penalty.

Communications geometry.- The communications geometry must be consistent with providing, as a minimum, a postland view capability of 10 minutes. Nominal parameters selected to define the geometry are (1) 2500-km periapsis altitude; (2) -18° capsule entry flightpath angle, and (3) -26° support module lead angle at capsule entry. A summary of the communications geometry is shown in figures 54 thru 57, which contain time histories of support module and capsule antenna aspect angles and the communications range. Dispersions from the nominal conditions and the bounding atmosphere models considered are noted on the figures. Angle convention and trajectory parameters are defined in figure 58.

Functions and requirements.- The capsule/lander relay radio subsystem is required to relay all data collected during coast, entry, and landing in real time to the support module. All entry science data collected must be returned independent of landing success. This radio subsystem must be capable of transmitting 200 000 bits of entry science data redundantly before touchdown. The derived data transmission rate is 2400 bps.

Subsystem parameters and performance.- The modulation technique will be noncoherent FSK with a split-phase PCM data stream. The nominal operating frequency will be 400 MHz. Antenna gain and coverage requirements for both ends of the link will be met with body-mounted, fixed antennas. Of all alternative antenna configurations, a cavity-backed crossed-slot antenna has been selected for both ends of the link because of its greater pattern coverage and on-axis gain. A delayed transmission technique will be used to recover capsule data collected during the communications blackout period. Technical considerations governing the selection of operating frequency, modulation technique, and transmission technique are discussed in the telecommunications section of Appendix D to the Mars Mission Modes Final Report.

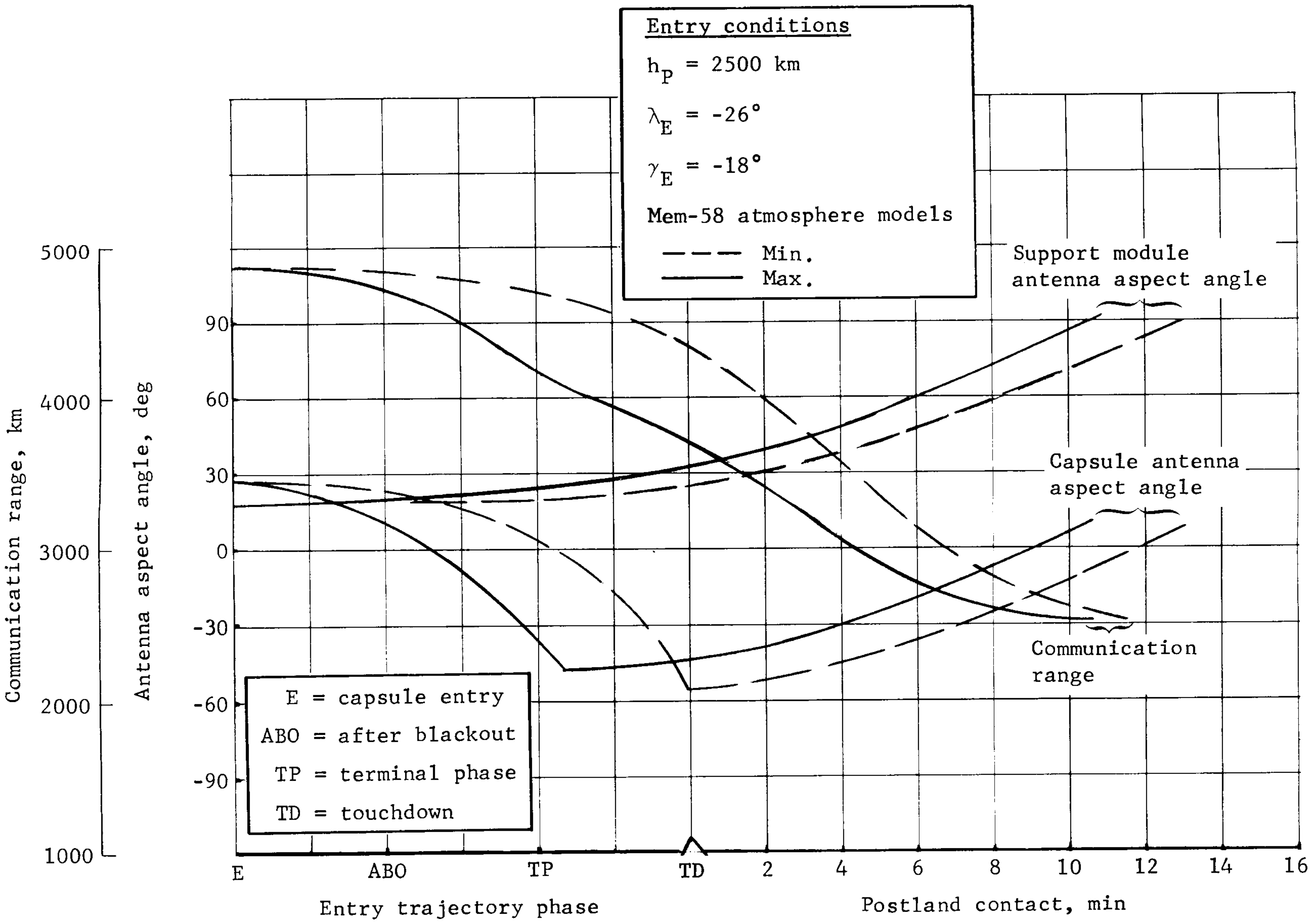

Figure 54.- Nominal Entry Geometry

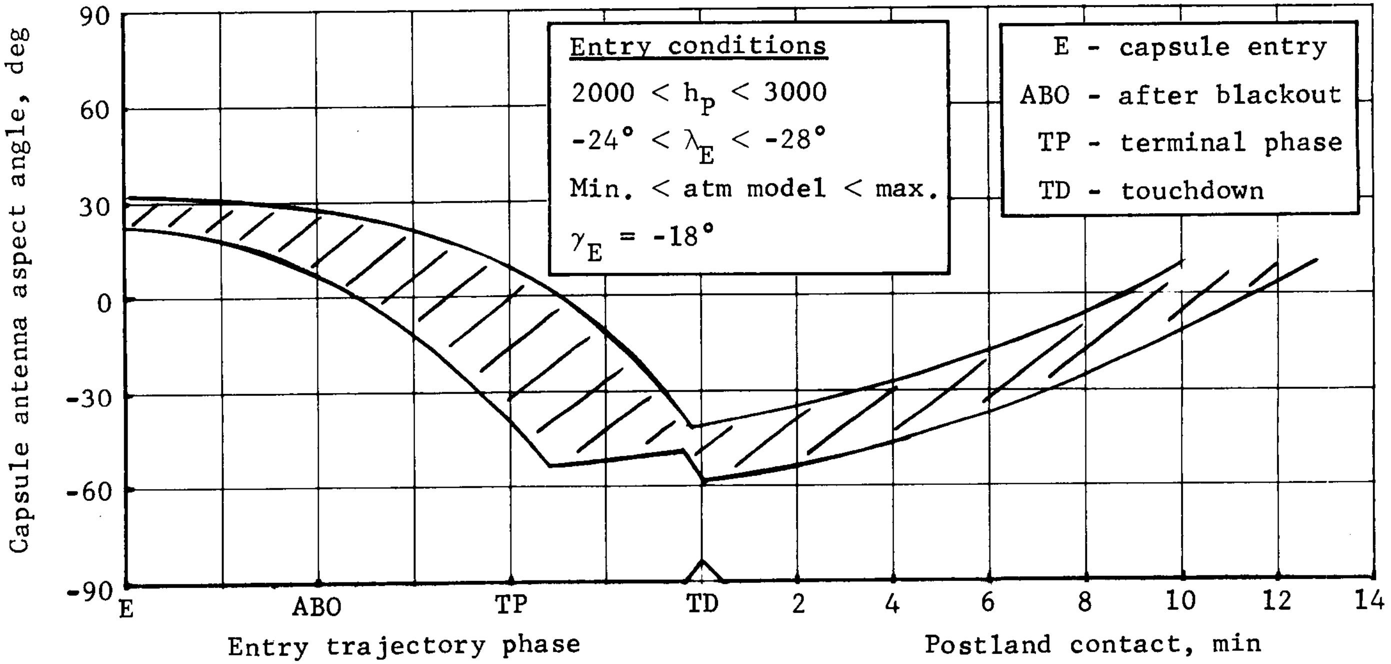

Figure 55.- Capsule Antenna Aspect Angle Dispersions

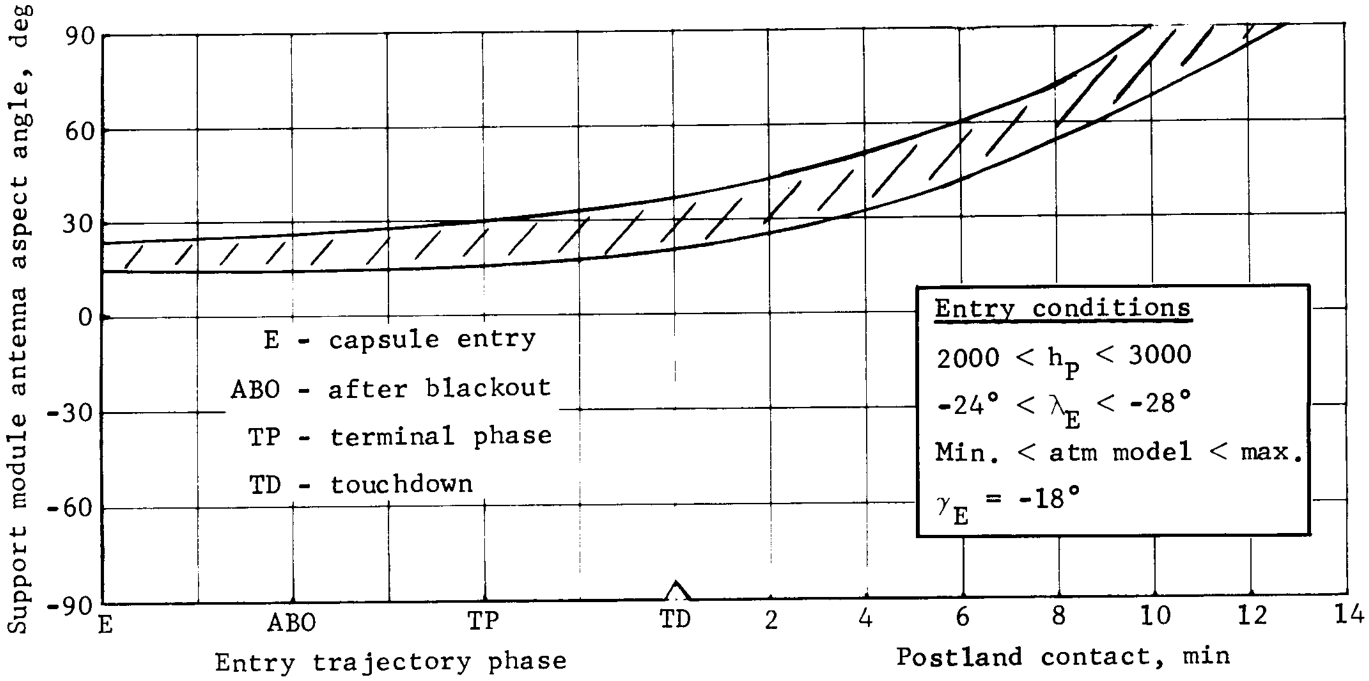

Figure 56.- Support Module Antenna Aspect Angle Dispersions

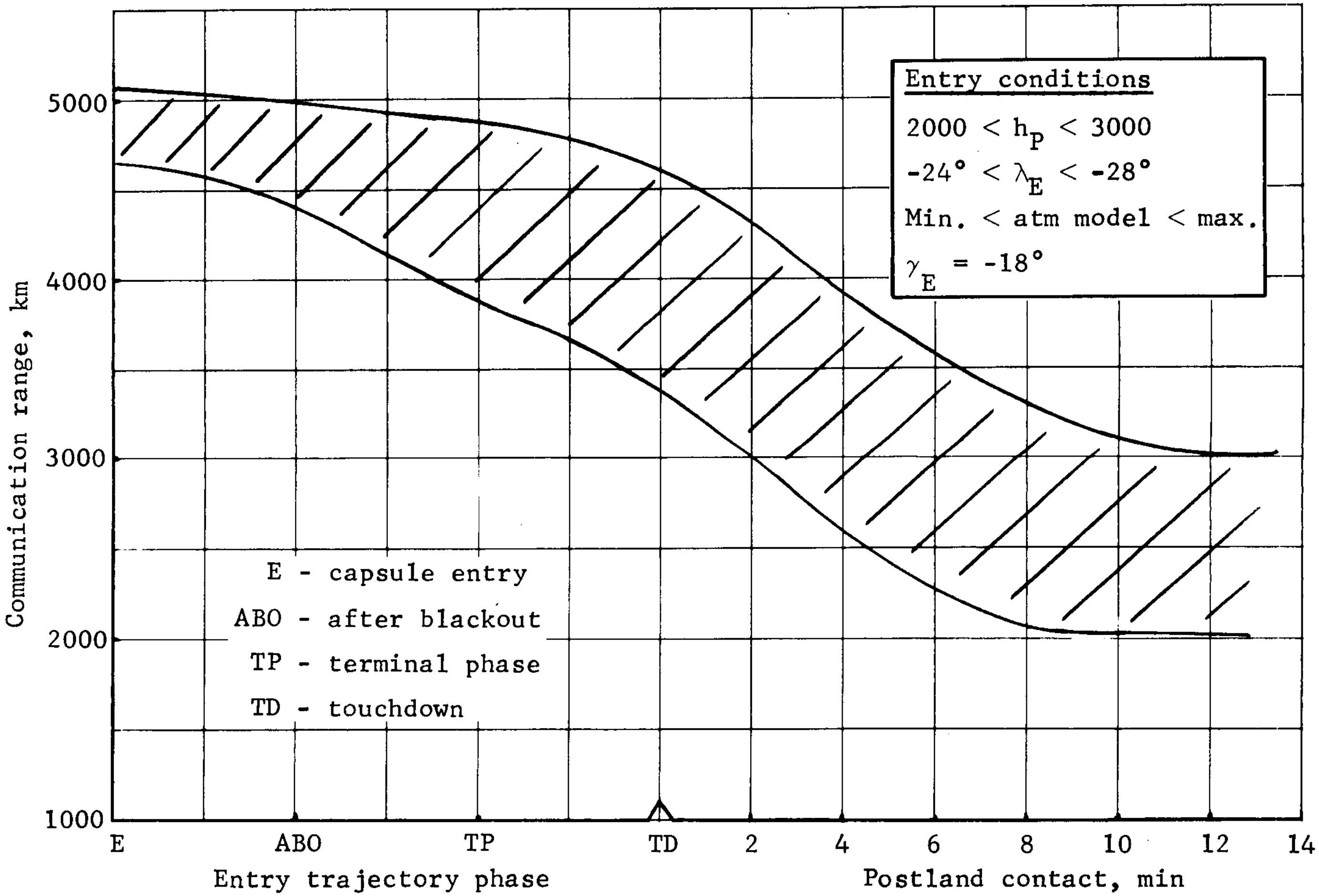

Figure 57.- Communication Range Dispersions

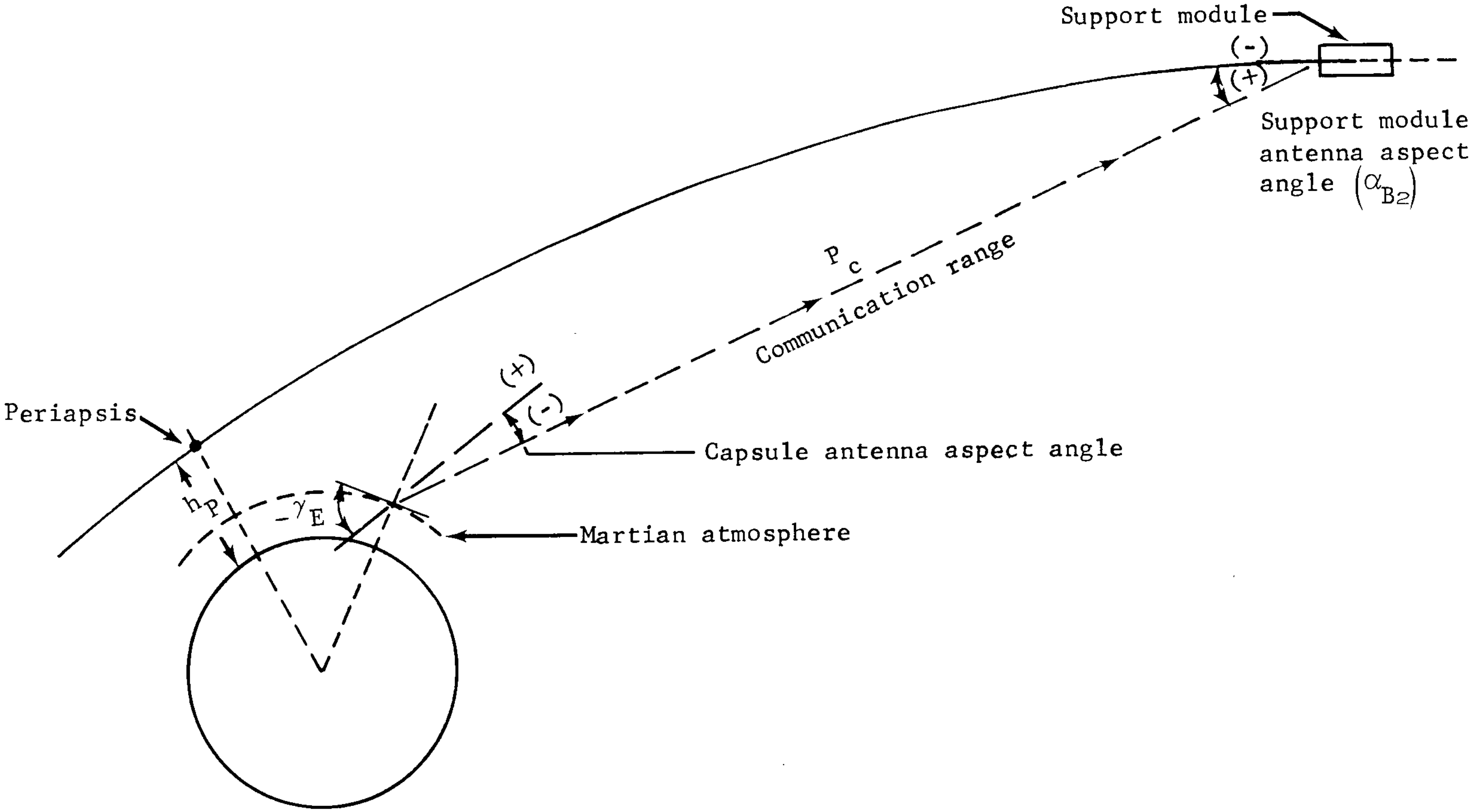
Support module
(-)
(+)
Support module antenna aspect angle (α_{B2})
P_c
Communication range
(+)
(-)
Periapsis
Capsule antenna aspect angle
h_P
$-\gamma_E$
Martian atmosphere

Figure 58.- Definition of Angle Convention and Trajectory Parameters

The relay link performance for a 10-W output transmitter, from entry through termination of the postland relay contact, is shown for nominal entry conditions and dispersions about the nominal in figures 59 and 60, respectively. During the entry phase, an allowance was made for fading to overcome the effects of a possible multipath environment. The fading margin is geometry dependent and requires that the electrical properties of the planet surface, front-to-back ratio of the transmitting antenna, the incident angle of the planet reflected signal, and the differential range of the direct and reflected signals be considered. For the postland contact, a 2-dB lobing loss is used to compensate for pattern nulls from ground reflections. The subsystem parameters used to derive figures 59 and 60 are presented in table 44. This telecommunication design control table contains nominal parameter values and tolerances for the geometry that occurs during the descent trajectory identified in figure 60 as point A. The performance figures show that the 2400 bps data rate can be supported over a range of atmospheres and a 22° adverse slope. Available link time after touchdown is greater than 10 min, which allows for the early transmission of imaging data.

The use of a simple receiving antenna on the spinning support module causes the steep loss of margin at the end of the postland contact. Use of a more complex receiving antenna implementation and increased transmitter output power could extend the communication time by another 8 min, if required. This problem is currently under investigation.

For checkout, the capsule/lander uhf transmitter will have a low-power output capability at the 1-W level. This power level will be used to transmit engineering data for a 1-hr period following the completion of separation and postseparation maneuvers. Moderate antenna aspect angles exist during this period of time allowing transmission of the required data over the relatively short ranges of less than 300 km with 1 W of transmitter power.

The relay link will be reactivated 1 hr before capsule entry with the transmitter at the 10-W level. The aspect angles are still moderate, however, the range is increasing and will reach a maximum value of approximately 500 km shortly after capsule entry. The minimum relay link performance occurring during this time will be near capsule entry and will be comparable to the entry margins shown in figures 59 and 60.

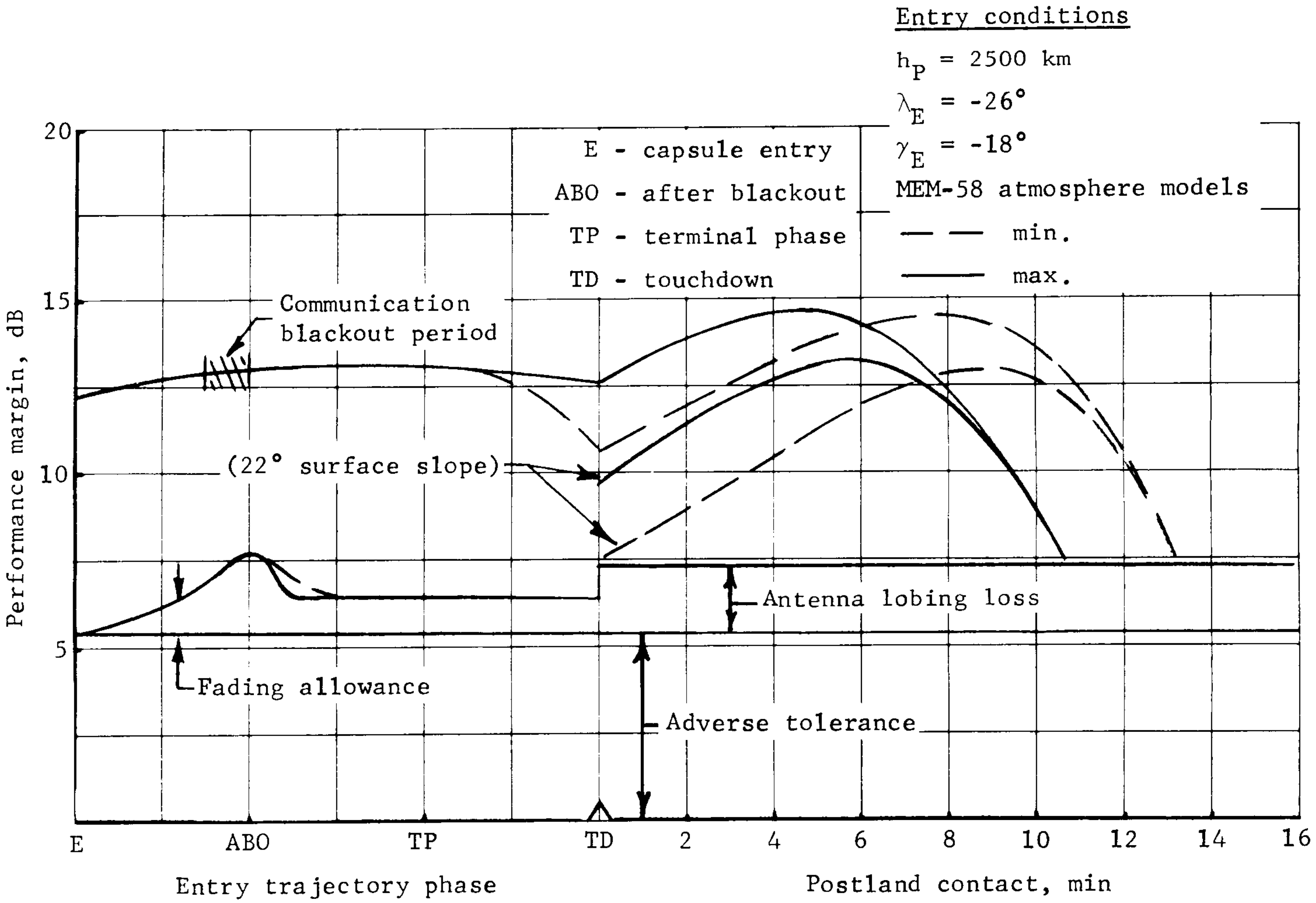

Figure 59.- Nominal Communication Profile

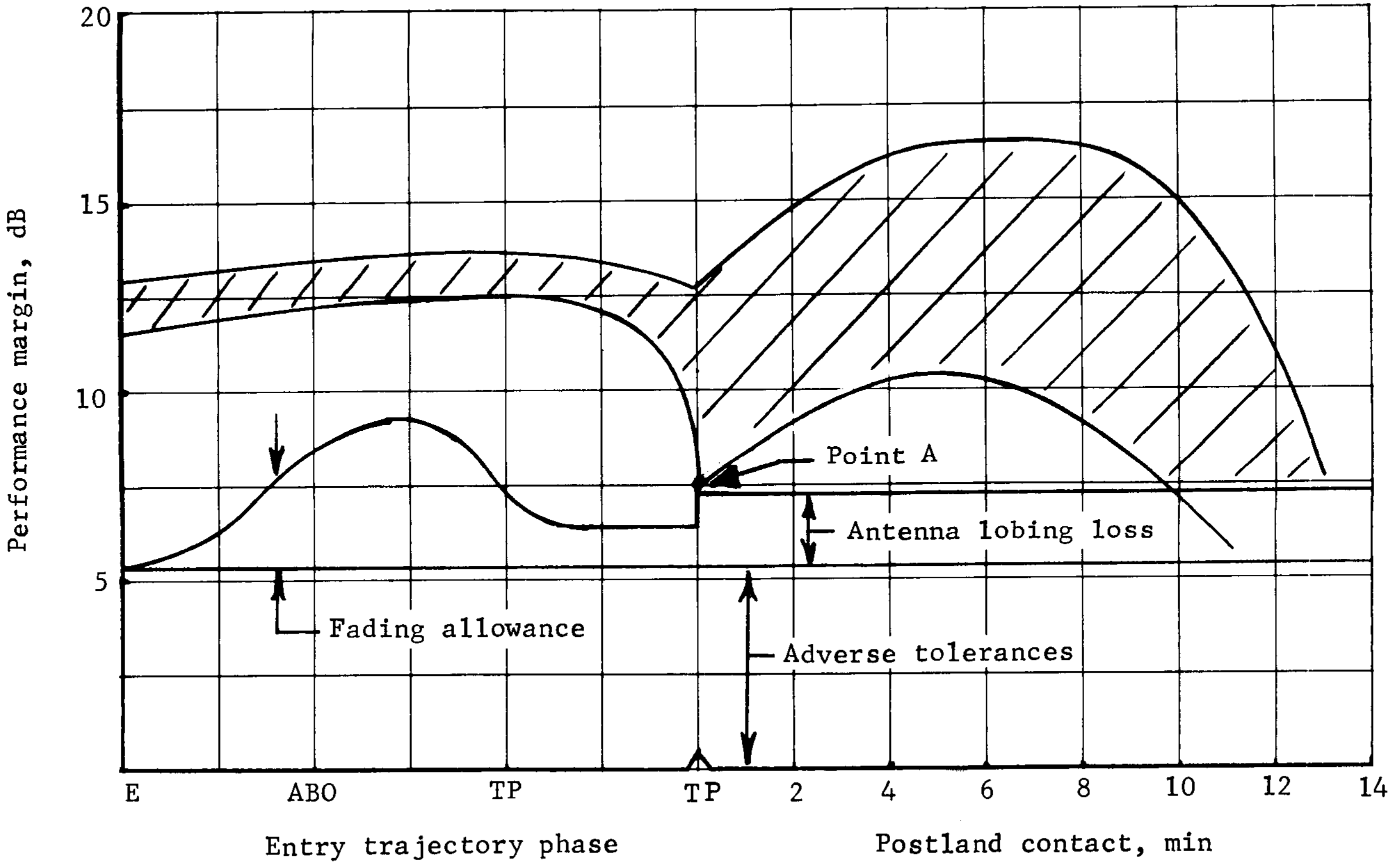

Entry conditions

$2000 < h_P < 3000$

$-24° < \lambda_E < -28°$

Min. < atm model < max.

$\gamma_E = -18°$

E - capsule entry

ABO - after blackout

TP - terminal phase

TD - touchdown

Figure 60.- Communication Profile (Dispersion from Nominal)

TABLE 44.- TELECOMMUNICATION DESIGN CONTROL TABLE

Parameter	Value	Tolerance, dB		Notes
		+	-	
Transmitter power	+40.0 dBm	1.0	0.0	10 W min.
Transmitting circuit loss	-1.0 dB	0.5	0.5	
Transmitting antenna gain	+5.0 dB	0.5	0.5	
Transmitting antenna pointing loss	-6.6 dB	0.0	0.0	α_C = -81°, incl 22° slope
Space loss, F = 400 MHz, R = 4170 km	-156.8 dB	0.0	0.0	
Polarization loss	-0.2 dB	0.2	0.3	
Receiving antenna gain	+5.0 dB	0.5	0.5	
Receiving antenna pointing loss	-0.2 dB	0.0	0.0	α_{B2} = +19°
Receiving circuit loss	-1.0 dB	0.5	0.5	
Net circuit loss	-155.8 dB	2.2	2.3	
Received carrier power	-115.8 dB	3.2	2.3	
Receiver noise spectral density	-170.6 dBm	1.0	2.0	T_S = 1000°K (max.)
Predetection noise bandwidth	+44.5 dB.Hz	0.0	0.0	28.4 kHz
Receiver noise power	-126.1 dBm	1.0	2.0	
Carrier-to-noise ratio	+10.3 dB	4.2	4.3	
Threshold carrier-to-noise ratio	+2.7 dB	1.0	1.0	$P_e^b = 4 \times 10^{-3}$
Performance margin	+7.6 dB	5.2	5.3	
Antenna lobing loss	-0.0 dB	2.0	2.0	
Worst-case margin	+0.3 dB	7.2	----	

Note: Sample design for point A, figure 60.

Preferred radio subsystem design.- The proposed radio subsystem design was evolved from an analysis of telecommunications requirements, functions, and parameters for the various mission phases. Support module rf transmitter requirements for cruise and entry relay are identical at the 25-W output power level. Command capability is required for the support module during cruise only. The soft lander requires a postland command capability. By the crossing of interfaces, an integrated design for telecommunications can be achieved, resulting in an economy of hardware.

The soft lander/support module telecommunications block diagram is shown in figure 61. The elements contained in the support module form a uhf receiving subsystem and an S-band radio subsystem. The S-band radio subsystem consists of a modulator-exciter, a 25-W TWTA with an integral power supply, two low-gain nonsteerable antennas, a fixed 40-in. circular aperture parabolic reflector, and a diplexer-rf switch assembly. Two low-gain antennas are required on the support module to provide spherical coverage since Earth is not within one hemisphere for the selected launch window. Engineering data are transmitted by the 25-W TWTA over one of the two low-gain antennas at a data rate of 33-1/3 bps (uncoded) up to the completion of the first midcourse maneuver, and at 8-1/3 bps (uncoded) up to planetary encounter. The command functions for the support module are provided by the command receiver and command detector that are located in the soft lander module. The requirements for near-Earth ranging and doppler tracking are provided by the hardwires crossing the interface.

The uhf receiving subsystem consists of an antenna, a receiver, a detector, and a (32,6) block encoder. Capsule entry data, transmitted at a rate of 2400 bps, are received by this support module subsystem and retransmitted to the DSIF in real time. During the entry relay phase, the 25-W TWTA is connected to the 40-in. antenna.

The elements contained in the lander form a uhf transmitting subsystem, an S-band radio subsystem, and a telemetry subsystem. The telemetry subsystem consists of signal conditioning, a data encoder, a static storage, a transducer power supply, and a sterilization battery measurement multiplexer. The uhf transmitting subsystem consists of a 10/1-W FSK transmitter (400 MHz) and a broadbeam, body-fixed, transmitting antenna. The low-power mode of the FSK transmitter is used for checkout and data transmission shortly after separation of the lander capsule from the support module.

The lander S-band radio subsystem consists of a modulator-exciter, a 50/25-W dual power mode TWTA and integral power supply, a command receiver and command detector, a body-fixed low-gain receiving antenna, and a medium gain transmitting antenna. The transmitting antenna is a 12.5 dB helix that is oriented to local vertical by a counterweight.

The proposed radio subsystem design for this configuration is nonredundant. Table 45 summarizes the weight, volume, and power requirements for this baseline design.

TABLE 45.- RADIO SUBSYSTEM WEIGHT, VOLUME, AND POWER SUMMARY

	Weight, lb	Power, W	Volume, in.^{3}
Support module			
uhf receiver	1.9	2.0	40
Bit detector and block encoder	3.6	2.5	50
uhf receiving antenna	4.0	----	7x24 d
Modulator-exciter	3.0	2.0	90
TWTA and power supply (25 W)	7.8	85	200
Diplexer and rf switch assembly	5.0	----	100
S-band low-gain antenna (2)	1.2	----	4x4 d (ea)
S-band high-gain antenna	6.0	----	40 in. diam
Lander/capsule			
uhf transmitter (10 W)	3.0	35	100
uhf transmitting antenna	4.0	----	7.5x15 d
Modulator-exciter	3.0	2.0	90
TWTA and power supply (50/25 W)	9.0	150/85	240
Command receiver	5.0	2.5	150
Command detector	4.0	1.5	40
rf switch assembly	1.0	----	10
S-band low-gain antenna	0.6	----	4x4 d
S-band medium-gain antenna	2.0	----	7x5 d

Note: Does not include packaging and internal cabling.

The radio subsystem parameters for the support module allow the 8-1/3 bps downlink telemetry channel to be supported entirely with the 85-ft antenna network until the end of November 1973. Beyond this date, the 210-ft antennas are required in a listen-only mode for downlink telemetry reception. Adequate margin exists in the downlink to support the near-Earth telemetry requirement of 33-1/3 bps and provide turnaround ranging for rapid range updates. The command function can be provided by the 85-ft network out to a range of 264 x 10^6 km.

In the high-power mode, the radio subsystem in the soft lander provides an initial telemetry downlink capability of 353 information bits per sec for the first 3 days on the planet surface. For the remainder of the mission, the subsystem operates in the low-power mode to provide a data rate of 8-1/3 bps (uncoded) for the transfer of meteorological data. The low-power mode data rate is capable of being detected by the 210-ft antenna stations operating in a diplexed mode at the end-of-mission life. Additional

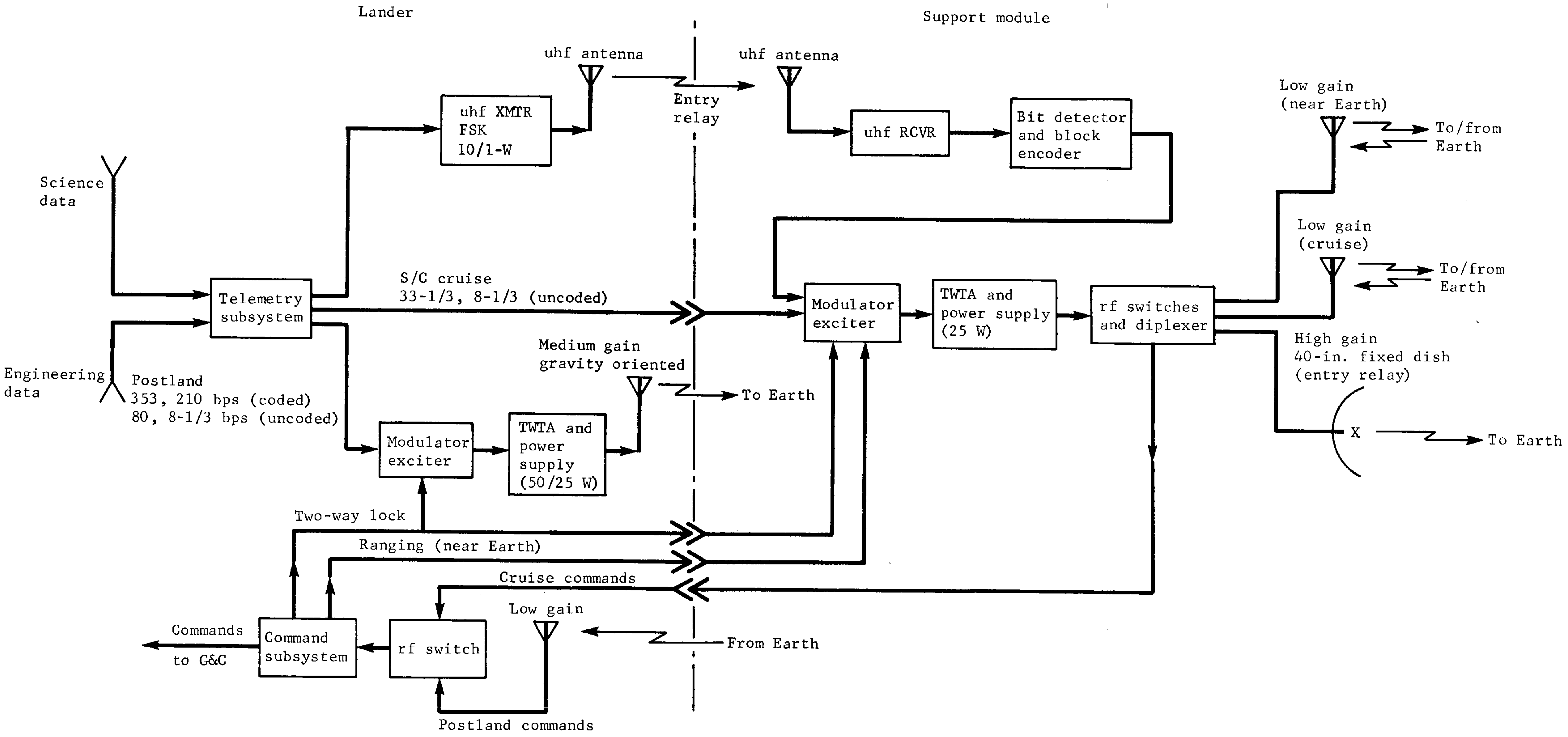
Lander
Support module
uhf antenna
uhf antenna
Entry relay
uhf XMTR FSK 10/1-W
uhf RCVR
Bit detector and block encoder
Low gain (near Earth)
To/from Earth
Science data
Low gain (cruise)
To/from Earth
Telemetry subsystem
S/C cruise
33-1/3, 8-1/3 (uncoded)
Modulator exciter
TWTA and power supply (25 W)
rf switches and diplexer
High gain
40-in. fixed dish
(entry relay)
Medium gain
gravity oriented
To Earth
Engineering data
Postland
353, 210 bps (coded)
80, 8-1/3 bps (uncoded)
Modulator exciter
TWTA and power supply (50/25 W)
X
To Earth
Two-way lock
Ranging (near Earth)
Cruise commands
Low gain
Commands
to G&C
Command subsystem
rf switch
From Earth
Postland commands

Figure 61.- Telecommunications Block Diagram

high rate telemetry channels at 210 information bits per sec and 80 bps (uncoded) are provided for the extended mission by the commanding of the high-power mode of operation whenever there is sufficient energy available to operate the TWTA at the 50-W level. Command capability for the soft lander extended mission is provided by the 210-ft DSIF stations. Postland data return capability for the minimum mission and under favorable conditions are given in tables 46 and 47.

TABLE 46.- POSTLAND DATA RETURN MINIMUM MISSION

Phase	Transmission time	Information rate, bps	Data volume, bits
After touchdown	10 min.	2400	1.44×10^6
Primary landed	2.62 hr/day for 3 days	353	10.00
Weather station	10 min./day for 87 days	8-1/3	.43
Total			11.87

TABLE 47.- POSTLAND DATA RETURN, FAVORABLE CONDITIONS

Phase	Transmission time	Information rate, bps	Data volume, bits
After touchdown	13.5 min.	2400	1.94×10^6
Primary landed	2.62 hr/day for 3 days	353	10.00
Extended life	2.5 hr/day for 24 of next 36 days	353	76.40
	2.5 hr/day for 20 of next 30 days	210	37.80
	1.5 hr/day for last 21 days	80	9.08
	10 min./day for 22 days	8-1/3	.11
Total			135.33

Conditions:

1/25/74 arrival
18° S lat
0° local slope
No clouds
90-day landed mission

6. POWER AND PYROTECHNIC SUBSYSTEMS

Power Subsystem Functional Description

The power subsystem is a 30 Vdc (nominal) system. Figure 62 is a block diagram identifying the configuration of the power subsystem and the location of the equipment.

During interplanetary cruise, power is furnished by an unsterilized solar array of silicon cells. The converter/regulator located in the lander provides a nominal 30 Vdc output to the subsystems operating during cruise. Power is also used for battery charging. The load control assemblies control distribution of power as commanded by the guidance computer or the command link.

Battery power is required during the boost phase and to support peak power demands during spacecraft maneuvers. The lander Ag-Zn batteries provide this power and are recharged after use.

The boost, cruise, and midcourse power requirements are shown in table 48. The cruise solar array was sized to provide the power required during cruise under the worst near-Mars conditions. Figure 63 shows the output of the cruise solar array.

At planetary encounter, the support module is separated and the cruise solar array (mounted on the cruise module) is staged. The support module uses battery power for 17 hr to accomplish its relay link mission. The load control assembly provides control of power to the support module equipment on command from the support module sequencer.

The battery selected for the support module uses the Mariner-type 50 A-h cells repackaged into single cell cases. This battery, although larger than required to meet the equipment (excluding thermal control) loads, was selected to minimize cost and risk by using a developed and proved cell. Much of the surplus energy was used to meet thermal control needs during the coast after support module separation. The support module power profile is shown in figure 64 and the required equipment operation times, loads and energies are listed in table 49.

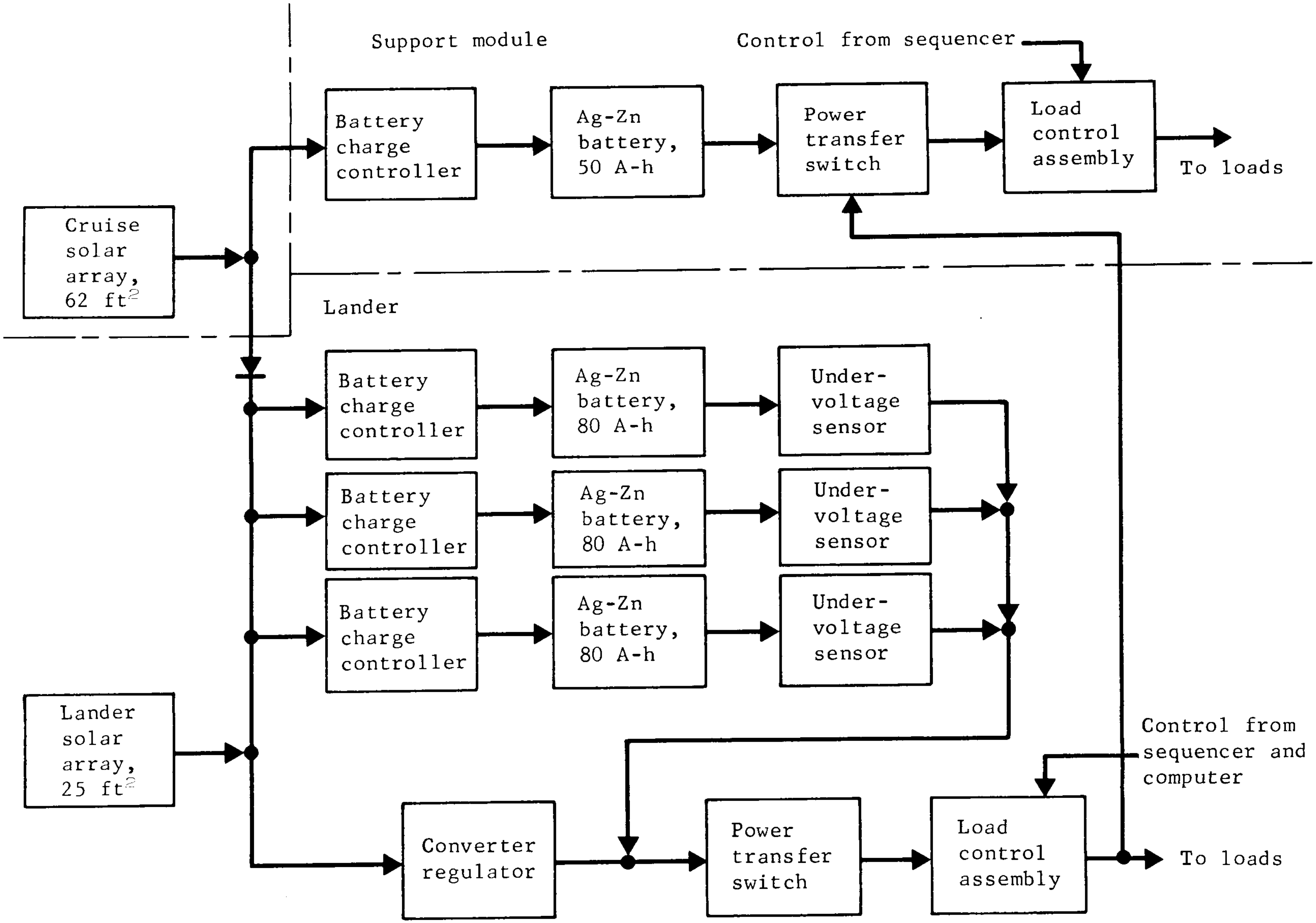
Support module
Control from sequencer
Battery charge controller
Ag-Zn battery, 50 A-h
Power transfer switch
Load control assembly
To loads
Cruise solar array, 62 ft^2
Lander
Battery charge controller
Ag-Zn battery, 80 A-h
Under-voltage sensor
Battery charge controller
Ag-Zn battery, 80 A-h
Under-voltage sensor
Battery charge controller
Ag-Zn battery, 80 A-h
Under-voltage sensor
Lander solar array, 25 ft^2
Control from sequencer and computer
Converter regulator
Power transfer switch
Load control assembly
To loads

Figure 62.- Power Subsystem Block Diagram

TABLE 48.- POWER REQUIREMENTS FOR BOOST, CRUISE, AND MIDCOURSE CORRECTION

Component	Load, W		
	Boost	Cruise	Midcourse
Modulator/exciter (SM)	----	2	2
TWTA and power supply (25 W rf)	----	85	85
Data encoder	15	15	15
Transducer power supply	2	2	2
Command receiver	----	2.5	2.5
Command detector	----	1.5	1.5
Command decoder	----	5.0	5.0
Computer	100	25	100
IMU	30	----	30
VDA	----	1	1
Canopus tracker	----	6.5	6.5
Sun sensor	----	4.7	4.7
Sun shutter	----	----	7.7
Battery charging	----	21	----
Subtotal	147	171.2	262.9
Loss (wiring)	4.5	5.3	8.1
Total	151.5	176.5	271.0

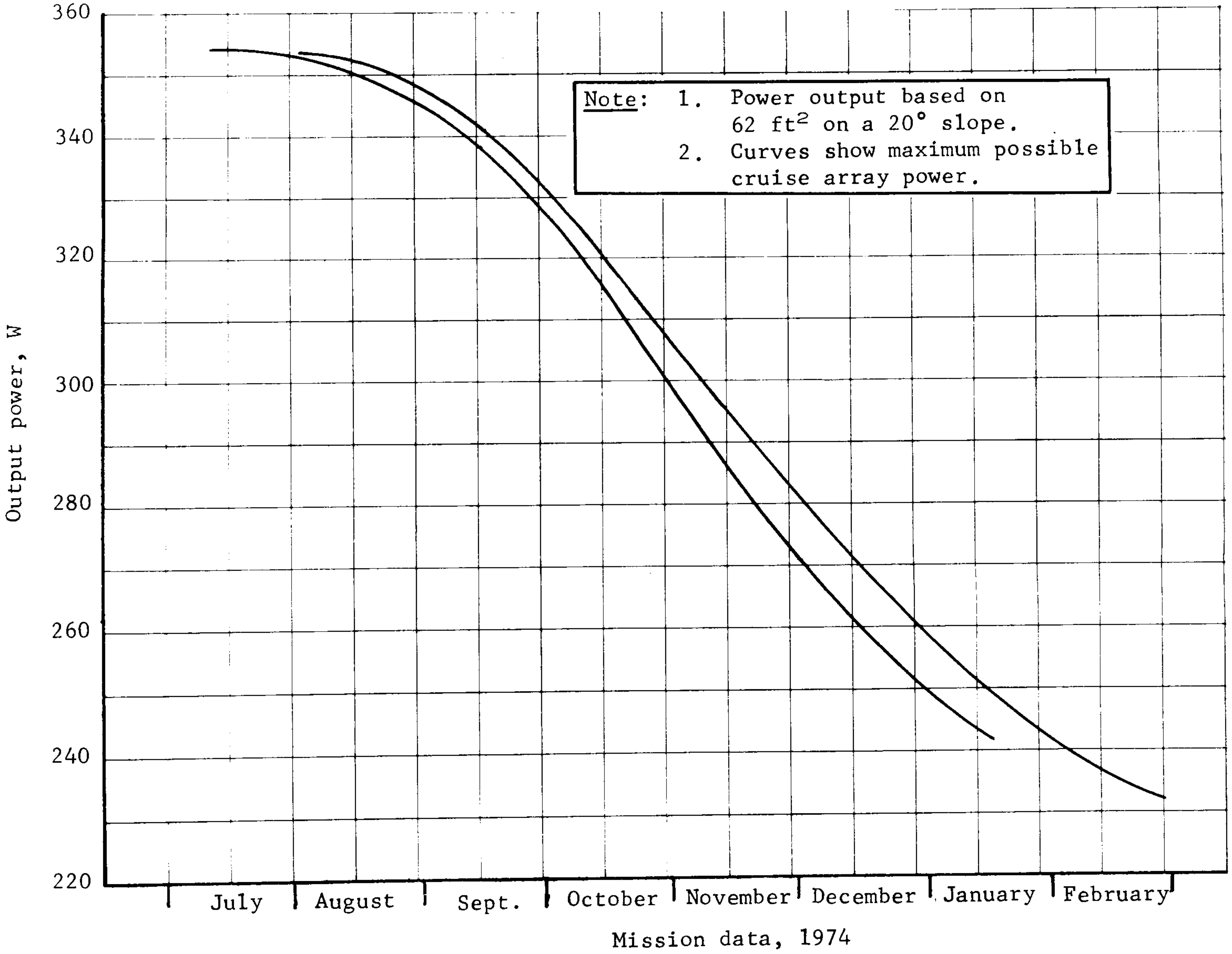

Figure 63.- Cruise Solar Array Output

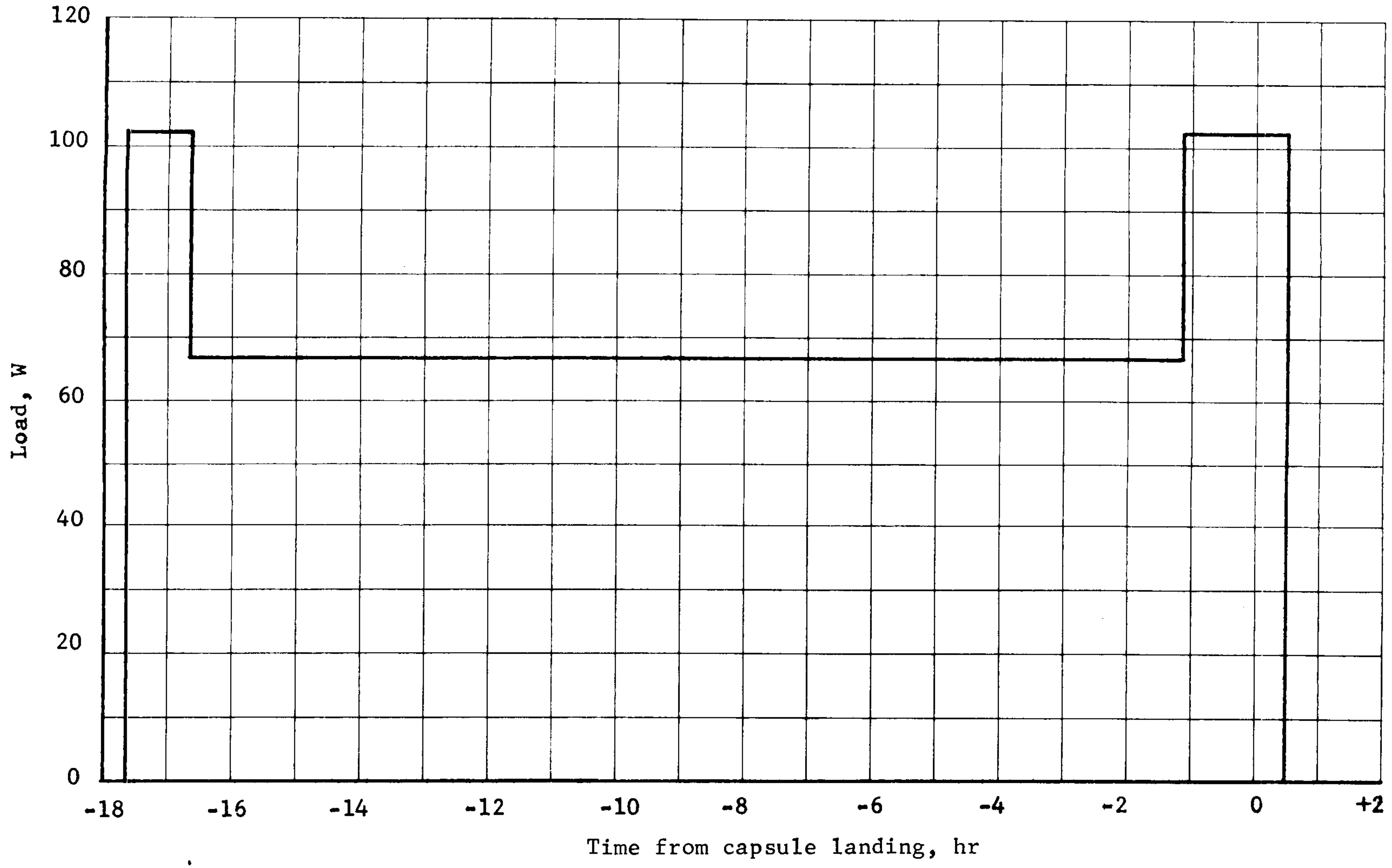

Figure 64.- Support Module Load Profile

TABLE 49.- SUPPORT MODULE EQUIPMENT OPERATING TIMES, LOADS, AND ENERGIES

Component	Time, hr	Load, W	Energy, W-h
Sequencer	17.7	2	35.4
UHF receiver and bit detector	2.7	6	16.2
Modulator/exciter	2.7	2	5.4
TWTA and power supply (25 W rf)	2.7	85	229.5
Heaters	15.0	60	900.0
Subtotal			1186.5
Losses (wiring)			36.7
Total			1223.2

After separation of the cruise solar array, the power required by the capsule during coast and entry is furnished by three sterilizable Ag-Zn batteries. Sufficient additional battery energy is provided to assure 3 days of landed operation independent of the lander solar array performance.

The required equipment operation times, loads, and energies for entry and the first three days are listed in table 50. To assure a minimum of 3 days operation after landing, the battery size required is based on no solar array energy being available during these 3 days. Figure 65 shows the lander power profile for entry and the first three days. The sequence of events after landing is based on the requirements of the science subsystem.

For long-term surface operations power is provided by a sterilizable solar array of silicon cells that are body mounted on the top surface of the lander. The Ag-Zn batteries used for boost, cruise, entry, and the first 3 days are used to provide night time and peak power requirements.

The minimum energy extended mission power requirements are based on a sequence of events required to meet the science requirements. Table 51 shows the equipment operation times, loads, and energy per day to meet the minimum requirements. The solar array size was determined by the minimum profile (fig. 66) and the energy required for the range of proposed landing site latitudes, and an adverse slope of 22° at the end of mission. The output of the 25 ft^2 solar array is shown in figure 67 along with the energy required to meet the minimum profile. The margin under the adverse conditions at the end of mission is about 15%.

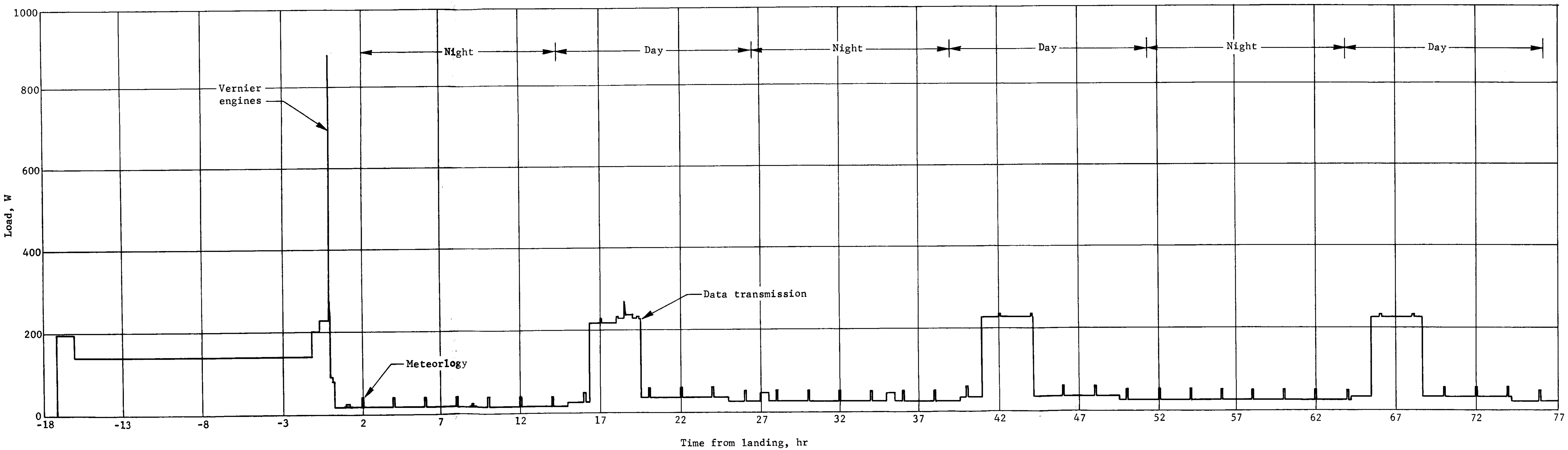

Figure 65.- Lander Power Profile, Encounter through Landing + 3 Days

TABLE 50.- LANDER PRIMARY MISSION EQUIPMENT OPERATING TIMES, LOADS, AND ENERGIES

Component	Time, hr	Load, W	Energy, W-h
Modulator/exciter	9.36	2	18.7
TWTA and power supply (50 W rf)	9.36	150	1404.0
uhf transmitter	2.70	35	94.5
Data encoder	15.06	15	225.9
Transducer power supply	15.06	2	30.1
Static storage	15.06	1	15.1
Command receiver	[a]30.00	2.5	75.0
Command detector	[a]30.00	1.5	45.0
Command decoder	[a]30.00	5	150.0
Sequencer	73.86	3	221.6
Computer	17.20	100	1720.0
IMU	17.20	30	516.0
AMR 1	.09	30	2.7
AMR 2	.02	27	0.5
TDLR	.02	130	2.6
VDA	.20	1	.2
Vernier engines	.01	560	5.6
Accelerometer triad	.60	4	2.4
Total temperature transducer	.60	1	.6
Stagnation pressure transducer	.60	3	1.8
Hygrometer-entry	.7	1	.7
Mass spectrometer	.7	8	5.6
Mass spectrometer pump	19.0	1	34.0
Facsimile camera	10.0	9.36	93.6
Gas chromatograph/mass spectrometer	20.0	1.5	30.0
Gas chromatograph/mass spectrometer pump	33.5	1	33.5
Biology	54.86	10	548.6
Soil sampler	10.0	1	10.0
Meterology	3.7	5.1	18.9
Subsurface probe	2.8	2.0	5.6
Data automation system	74.5	11	819.5
Subtotal			6132.3
Loss (wiring)			155.7
Total			6388.0

[a]The command link operates for 10 hr/day.

TABLE 51.- LANDER EXTENDED MISSION EQUIPMENT OPERATING TIMES, LOADS, AND ENERGIES

Component	Time, hr	Load, W	Energy, W-h
Modulator exciter	.67	2	1.3
TWTA and power supply (25 W rf)	.67	85	57.0
Data encoder	1.67	15	25.0
Transducer power supply	1.67	2	3.3
Static storage	1.67	1	1.7
Command receiver	[a]10	2.5	25.0
Command detector	[a]10	1.5	15.0
Command decoder	[a]10	5.0	50.0
Sequencer	24.62	3	73.9
Meterology	1.0	5.1	5.1
Subsurface probe	1.0	2	2.0
Subtotal			259.3
Losses (wiring)			8.0
Total			267.3

[a] Maximum times; command link operates from sunrise to sunset.

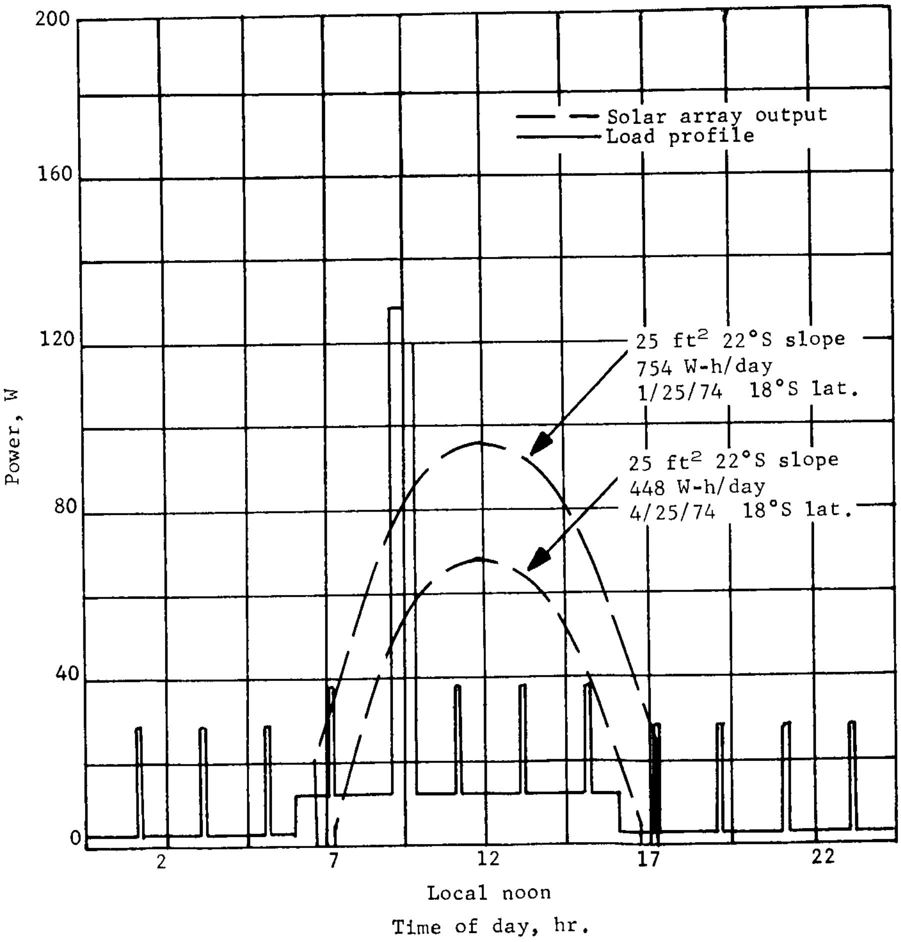

Figure 66.- Extended Mission Power Profile and Solar Array Power

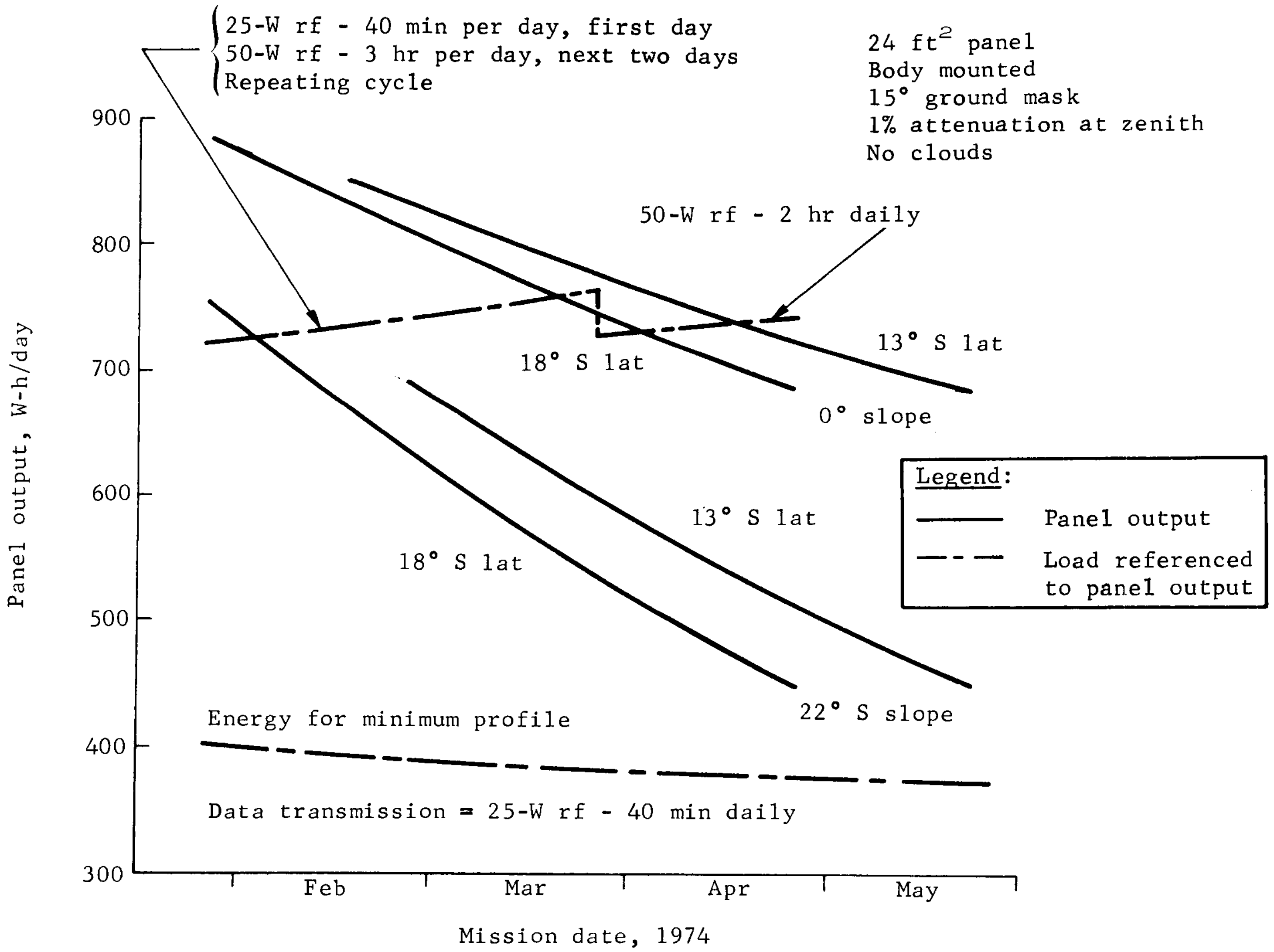

Figure 67.- Lander Solar Panel Performance

The probability of encountering these adverse conditions, however, is very low. Based on the probability density distribution for surface slopes on Mars (ref. 24, fig. III.C-4) and assuming a linear distribution of slope azimuths, the probability of landing on slopes greater than or equal to 22° with an azimuth of 135° to 225° is only 0.5%. The probability of landing on a slope of 8° or less with any azimuth is 67%. Therefore, mission capabilities based on near-zero slopes have been investigated.

For the more favorable ground slopes much more margin is available. The energy available with 0° ground slope and sunny skies during the entire mission would permit operation of the data link, facsimile camera, and data automation system for 3 hr on 2 out of 3 days during the early part of the mission and 2 hr every day during most of the remainder of the mission. The energies required for this improved mode of operation, are also shown in figure 67. The available battery energy with the above favorable conditions is shown in figure 68. This curve is based on having power available from the solar array during the first 3 days, thereby reducing the energy required from the batteries. The data transmission cycle shown leaves approximately 3500 W-h in the batteries at the end of the mission. This energy could be used to provide additional data transmission capability.

The undervoltage sensor with an enable signal from the sequencer is used to keep any or all batteries isolated from the loads when they are not required. Battery and solar array power is provided through the power transfer switch and the load control unit to the subsystems. The load control units contain one mag-latch relay for each load. This permits sequencer (computer) control of the loads with a minimum energy loss. The power subsystem weights are shown in table 52.

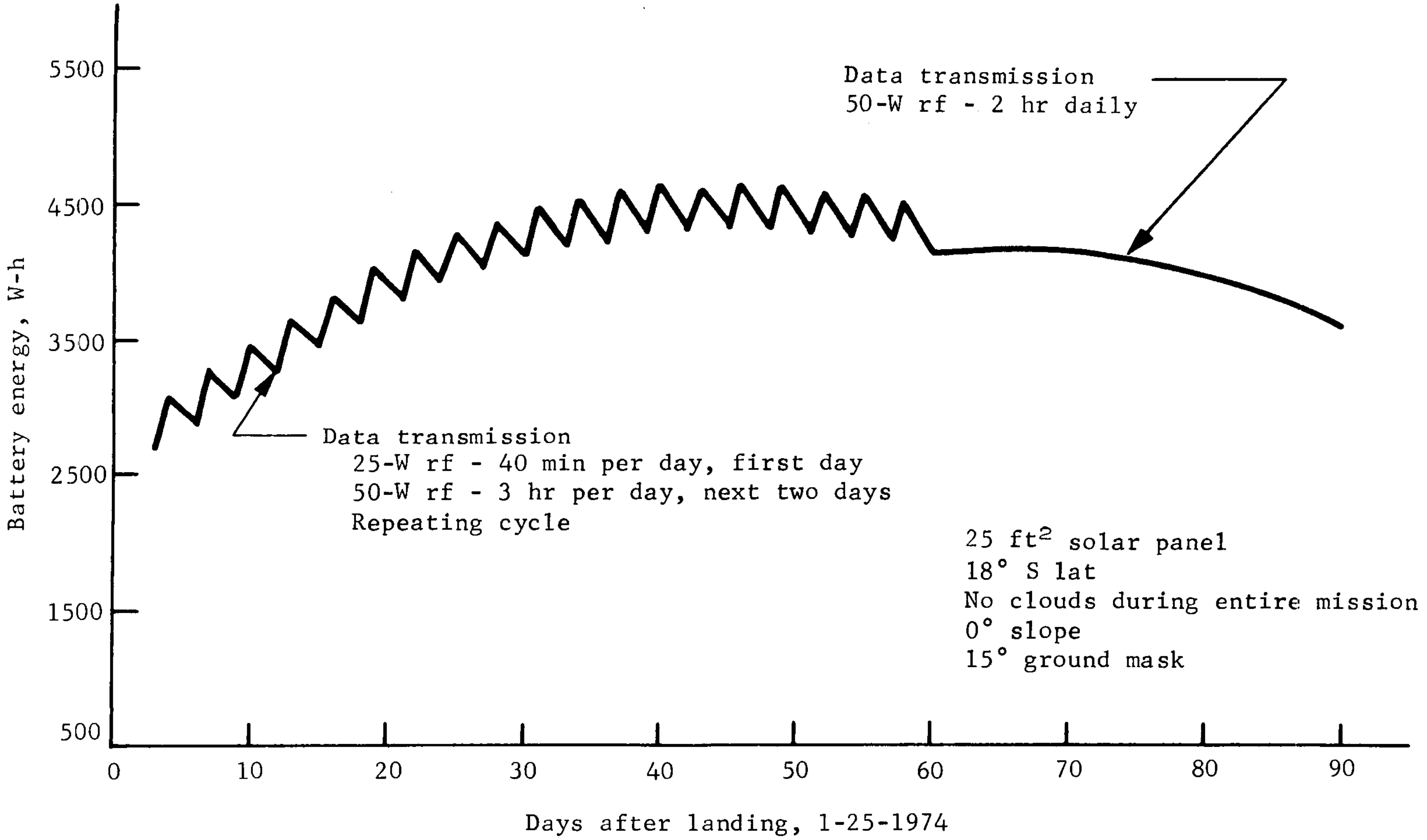

Figure 68.- Available Battery Energy Profile

TABLE 52.- POWER SUBSYSTEM WEIGHTS[a]

Item	Quantity	Weight each, lb	Weight total, lb
Support module			
Power transfer switch	1	2.5	2.5
Battery charger	1	3.0	3.0
Load control assembly	1	2.0	2.0
Diodes, shunts, and isolation assemblies	1	1.5	1.5
Ag-Zn battery (50 A-h)	1	34.0	34.0
Support module total			43.0
Canister-mounted equipment			
Cruise solar array (62 ft^2)	1	62.0	62.0
Canister-mounted equipment, total			62.0
Lander			
Ag-Zn batteries (80 A-h)	3	62.0	186.0
Solar array (25 ft^2)	1	17.0	17.0
Battery chargers	3	3.0	9.0
Converter/regulator	1	7.0	7.0
Power transfer switch	1	2.0	2.0
Load control assembly	1	4.0	4.0
Shunts and isolation assemblies	1	2.0	2.0
Diode assemblies	1	2.0	2.0
Undervoltage sensors	3	2.0	6.0
Lander total			235.0

[a] Does not include external cabling and supports. These items are tabulated in the sequential weight statement, volume 1.

Pyrotechnic Subsystem Functional Description

The pyrotechnic subsystem consists of the equipment shown in the block diagram (fig. 69). Power to the pyrotechnic subsystem is provided from the power subsystem, and control signals are received from the guidance and control computer and the postland sequencer.

Fourteen capacitor assemblies in the lander and three capacitor assemblies in the support module provide energy storage for firing the bridgewires at the prescribed time. Capacitor assembly charging is initiated as required during the mission, and within 12 sec the capacitors are ready for use. A minimum of 12 sec between subsequent events allows the capacitor assemblies to be recharged and used again. Time-critical functions are grouped into events with sufficient time between events to allow the capacitor assemblies to be recharged. Each capacitor assembly provides the required energy to fire one bridgewire in a given event. The number of capacitor assemblies required is established by the maximum number of bridgewires required in an event.

The pyrotechnic subsystem size for the lander is based on a total of 88 bridgewires with a maximum of 14 bridgewires fired in a 12-sec period and for the support module a total of six bridgewires all fired within a 12-sec period.

The use of a small capacitor assembly to fire each bridgewire instead of a larger capacitor bank to fire all bridgewires in a given event eliminated the need for current-limiting resistors in each bridgewire circuit and resultant larger capacitor bank to provide for resistor losses. A minimum firing energy of approximately 0.150 J per bridgewire is provided to ensure firing within an allowable time period.

A safe/arm switch provides arming and safing of each pyrotechnic circuit. The events are arranged so that no function is armed more than one minute before firing. After all pyrotechnic functions in an event are fired, the switches are reset to the safe position, thus opening the power circuit and removing any load caused by a bridgewire short.

The safe/arm switch contains a 100 000-ohm resistor connected from the negative bridgewire lead to structure. This provides a ground reference for the bridgewires to prevent a static charge build up before firing the bridgewire.

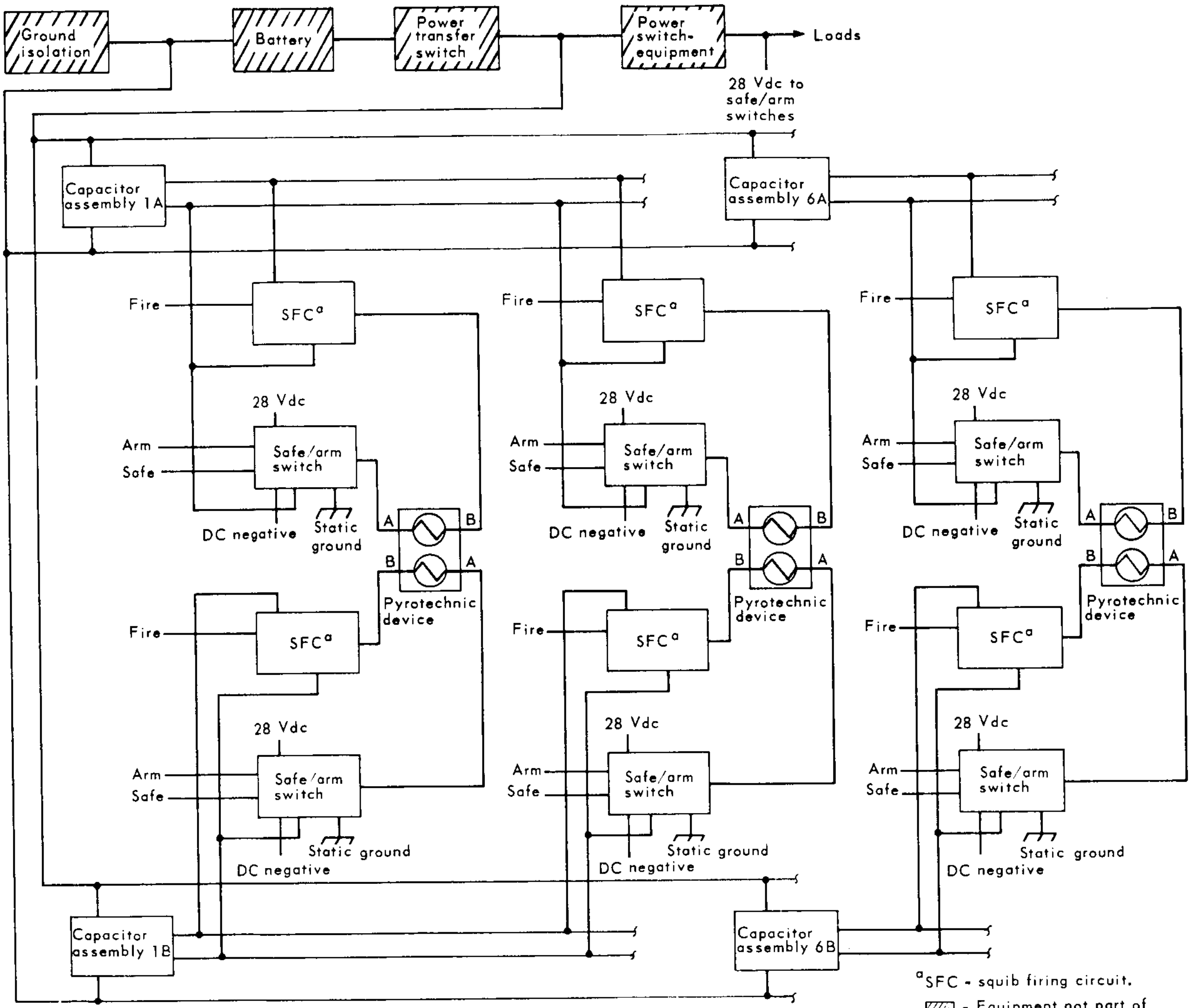
Ground isolation
Battery
Power transfer switch
Power switch-equipment
Loads
28 Vdc to safe/arm switches
Capacitor assembly 1A
Capacitor assembly 6A
Capacitor assembly 1B
Capacitor assembly 6B
Fire
SFC^a
28 Vdc
Arm
Safe
Safe/arm switch
DC negative
Static ground
A
B
Pyrotechnic device

Figure 69.- Simplified Block Diagram, Lander Pyrotechnic Subsystem

[a] SFC - squib firing circuit.

▨ - Equipment not part of pyrotechnic subsystem

The final switch between the energy source and the squib is the solid-state squib firing circuit (SFC), which receives its fire control signal from the sequencing subsystem.

The squibs provide gas pressure to operate valves, cable cutter, and separation nuts or initiate linear-shaped charges for canister separation.

The block diagram (fig. 69) shows the typical redundancy provided for each function. Parallel circuits are provided from the power subsystem through redundant capacitor assemblies, safe/arm switches, squib firing circuits and to one of two squibs in each pyrotechnic device. Two squibs with one bridgewire each are used for each function. With this design, the proper functioning of either circuit branch will fire all associated pyrotechnic devices.

The pyrotechnic subsystem weights are shown in table 53.

TABLE 53.- PYROTECHNIC SUBSYSTEM WEIGHTS[a]

Item	Quantity	Weight each, lb	Total weight, lb	
Support module				
Capacitor assembly	6	0.16	1.0	
Safe/arm switch	6	0.19	1.1	
Squib fire switch	6	0.06	0.4	
Internal cabling and connectors	----	----	1.3	
Packaging	----	----	2.0	
Support module total				5.8
Lander				
Capacitor assembly	14	0.16	2.2	
Safe/arm switch	88	0.19	16.7	
Squib fire switch	88	0.06	5.4	
Internal cabling and connectors	----	----	1.8	
Packaging	----	----	5.5	
Lander total				31.6

[a] Does not include external cabling and supports. These items are tabulated in the sequential weight statement, volume 1.

7. THERMAL CONTROL

During the initial Mars Mission Mode study, primary emphasis was placed on thermal control on the Mars surface because of the wide range of possible environments and thermal design options. Based on those studies, we recommend the use of radioisotope heaters, because such a system will provide a long life on the Mars surface over a very wide range of possible environments at an acceptable weight.

The primary emphasis in this study is the thermal design of the capsule and support module during the cruise and postseparation phases of the mission. The Mars surface thermal control remains basically the same as for other configurations considered during the initial Mission Mode study. The main difference in the capsule is that some of the lander equipment is powered up during the cruise phase of the mission to perform basic spacecraft functions.

Unsterilized Support Module Configuration

Requirements.- The thermal control subsystem must be able to maintain temperatures within acceptable limits while the capsule and support module are subjected to a wide range of environmental conditions throughout the various phases of the mission.

Space environment: During the entire interplanetary mission, some parts of the vehicle are exposed to solar radiation while the entire vehicle radiates to space. The solar flux on the vehicle varies from 442 Btu/hr ft^2 near Earth to about 180 Btu/hr ft^2 near Mars.

During most of the cruise phase, the vehicle is oriented so that the solar flux is on the aeroshell side. During the postseparation phase, the capsule orientation is reversed so the solar flux is on the opposite side. During the launch, initial acquisition, midcourse correction, and deflection maneuver, the vehicle orientation varies from the normal cruise phase position for a maximum of 2 hr at a time, with the solar flux impingement varying accordingly.

Mars surface environment: The Mars surface environment was considered in considerable detail in connection with previous Mission Mode studies. This environment exhibits wide variations as shown in table 54. The solar flux may vary from near zero on an overcast day to a maximum of 232 Btu/hr ft^2 on a clear day with Mars at its perihelion. The atmospheric temperatures may vary from -190°F on an overcast day to over 100°F on a hot day. Other pertinent parameters also vary widely or have a high degree of uncertainty.

TABLE 54.- MARS THERMAL ENVIRONMENT PARAMETERS

Environmental parameter	Nominal	Range
Solar flux, Btu/hr ft^2	180	160 to 232
Atmospheric solar transmissivity	----	0 to 0.99
Surface solar absorptivity, α	0.80	0.65 to 0.95
Surface emissivity, ϵ	0.80	0.60 to 1.0
Surface density, ρ, lb/ft^3	62.4	----
Surface heat capacity, C, Btu/lb °F	0.17	----
Surface thermal conductivity, k, Btu/hr ft °F	0.145	0.0242 to 0.242
Surface thermal inertia, $\sqrt{k\rho C}$, Btu/hr ft °R hr$^{\frac{1}{2}}$	1.24	0.51 to 1.6
Surface temperature, T_g, °F	----	-190 minimum
Atmospheric temperature, T_a, °F	----	-190 minimum
Atmospheric pressure, mb	9	6 to 20
Wind velocity at 1 meter, ft/sec	----	44 to 148
Atmospheric composition, mol %		
CO_2	68.5	19 to 100
N_2	18.5	60 to 0
A	13.0	21 to 0

Electrical equipment heating: The electrical equipment in the different compartments will be operated at various times and levels. Equipment inside the heavily insulated survivable equipment compartment is powered with 28 W throughout the cruise phase, but is shut down after the deflection maneuver. After landing, this equipment is again powered up to a level that varies with time, as shown in figure 70.

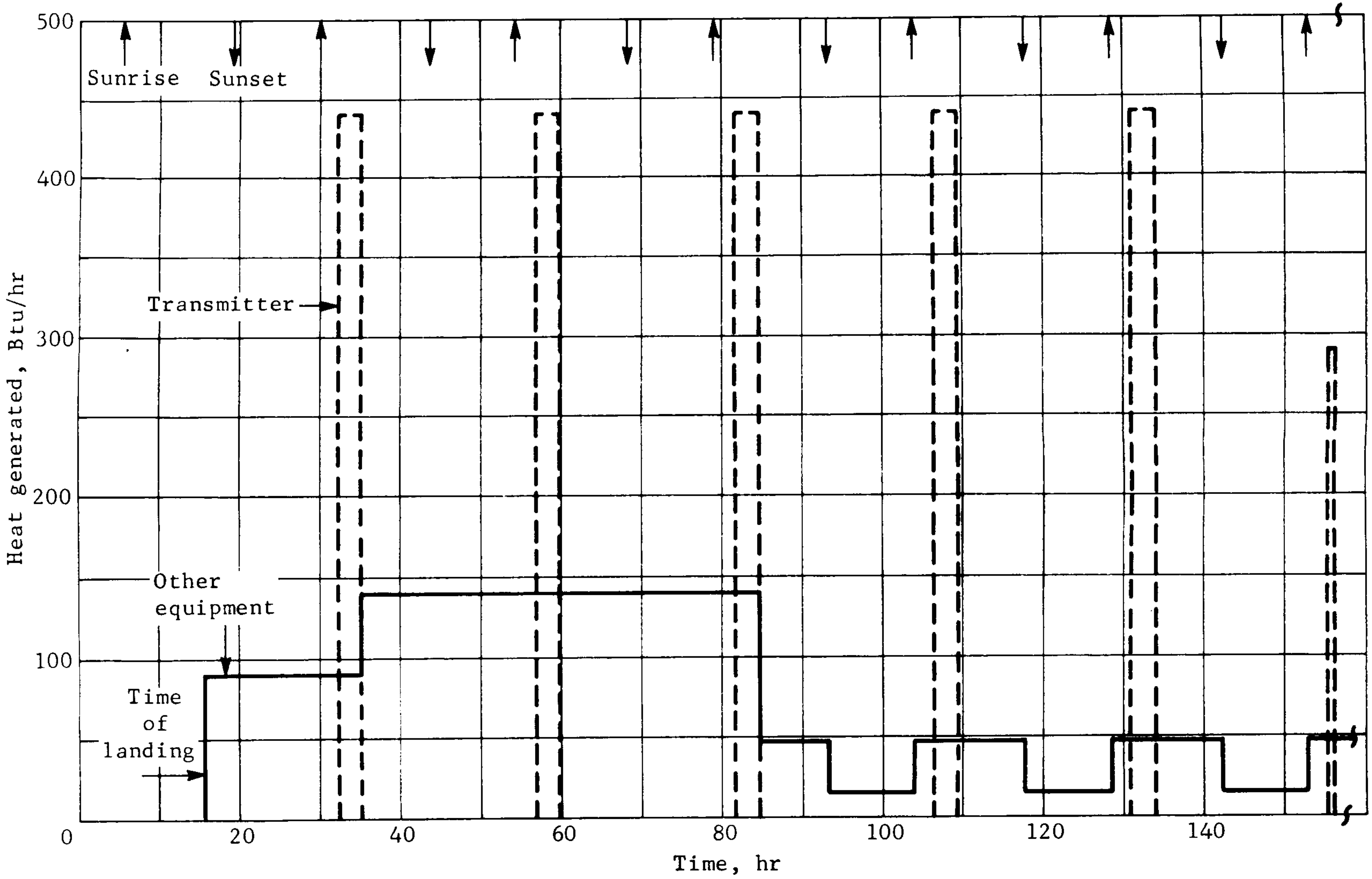

Figure 70.- Equipment Heat Output after Landing

The transmitter is operated for 3 hr each of the first three days. It is operated thereafter either for 2 hr each day, or with a 3-day repeating cycle of 3 hr for 2 days, and 40 minutes at reduced level for the third day, depending on the time of year. The other equipment is operated at a high level the first three days and then reduced to a daily cycle at a low level.

The computer is operated at 100 W during the midcourse corrections and the postseparation phase, and 25 W during the remainder of the cruise phase. The IMU is powered with 30 W during launch through initial sun acquisition, during midcourse maneuvers, and during the postseparation phase, but is shut down at all other times.

The transmitter in the support module is powered up during the cruise phase, and for the first and last hour of the 17-hr postseparation phase.

Equipment temperature limits: The more important limits are:

Batteries, 40 to 100°F;

Electronics, 35 to 125°F;

Propellants, 45 to 100°F.

Thermal control system description.- The thermal control techniques were established after performing detailed thermal analyses for the three basic phases of the mission.

Cruise: The cruise mode thermal control system is shown in figure 71.

Capsule: Gold-plated, crinkled Mylar (multilayer) insulation is used to thermally isolate the internal equipment from solar radiation so that equipment temperatures will not change appreciably between Earth and Mars. Twenty layers of this insulation are used under the solar panels to minimize the effect of the solar flux, which varies during cruise from 442 Btu/hr ft^2 at Earth to 180 Btu/hr ft^2 at Mars. Similar insulation is also used on the opposite side of the capsule, because the sun is on that side following separation.

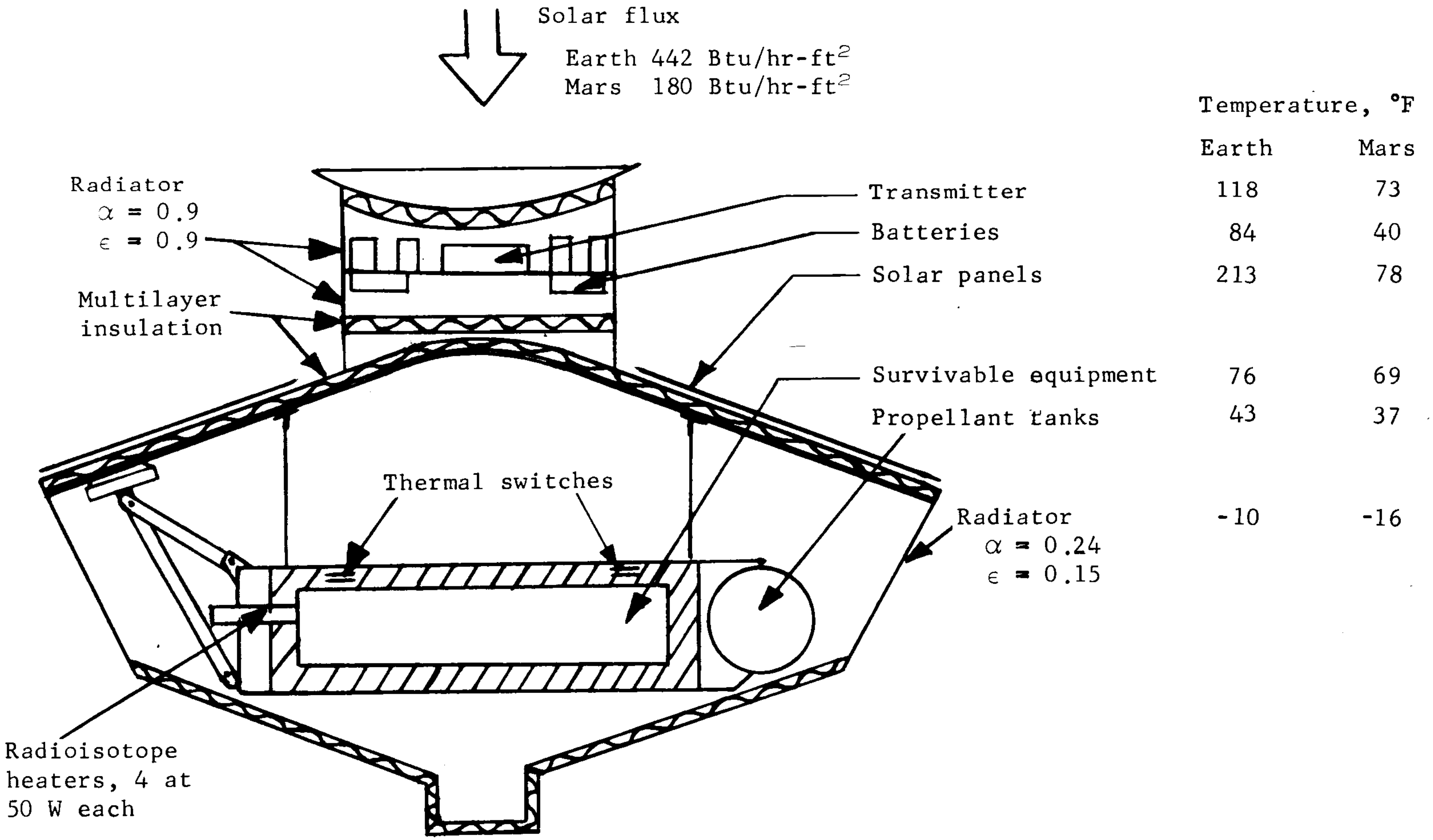
Solar flux
Earth 442 Btu/hr-ft^2
Mars 180 Btu/hr-ft^2
Temperature, °F
Earth Mars
Radiator
$\alpha = 0.9$
$\epsilon = 0.9$
Transmitter 118 73
Batteries 84 40
Solar panels 213 78
Multilayer insulation
Survivable equipment 76 69
Propellant tanks 43 37
Thermal switches
Radiator -10 -16
$\alpha = 0.24$
$\epsilon = 0.15$
Radioisotope heaters, 4 at 50 W each

Figure 71.- Cruise Mode Thermal Control System

During cruise 253 W of heat is generated inside the capsule. This includes 50 W from each of the four radioisotope heaters, 25 W from the computer, and 28 W from equipment inside the lander's survivable equipment compartment. The heat inside the heavily insulated survivable equipment compartment is conducted out through normally-closed thermal switches in the bottom of the compartment. These switches are opened at or shortly after landing. The heat is radiated from the compartment bottom to the concial (side) surface of the capsule where all of the internal heat is radiated to space. A coating with radiation properties of $\alpha = 0.24$ and $\epsilon = 0.15$ is used on the outside of the conical surface.

Additional heat is required for the propellant tank bays to augment the heat available from existing heat sources. A combination of about 5 W of heat and six layers of multilayer insulation is used for these bays.

Support module: Multilayer insulation is used on the sun side of the support module under the high-gain antenna to minimize the effect of solar radiation on internal temperatures. The opposite side of the module is also covered with multilayer insulation to minimize the heat loss to space following separation.

The structural support tray to which all the equipment and batteries are attached is used to conduct the thermal energy from each component to the outside cylindrical surface of the module where it is radiated to space. During cruise the transmitter, which is located at the center of the tray, generates 60 W of thermal energy, and each of the four groups of batteries generates 1 W. The outside radiating surface is coated with a black paint with $\alpha = \epsilon = 0.9$.

Postseparation:

Capsule: The capsule postseparation thermal control system is shown in figure 72. Twenty layers of multilayer insulation are used on the side opposite the solar panels, because this surface is exposed to solar radiation following separation. Again the insulation serves to thermally isolate the internal equipment from the Mars solar flux of 180 Btu/hr ft^2. The insulation on the aeroshell is jettisoned along with the solar panels before the deflection maneuver. The guidance computer and IMU are operating, adding 105 W of heat to the system. The coatings on the aeroshell and side surfaces are as shown to obtain a thermal balance during this phase of the mission.

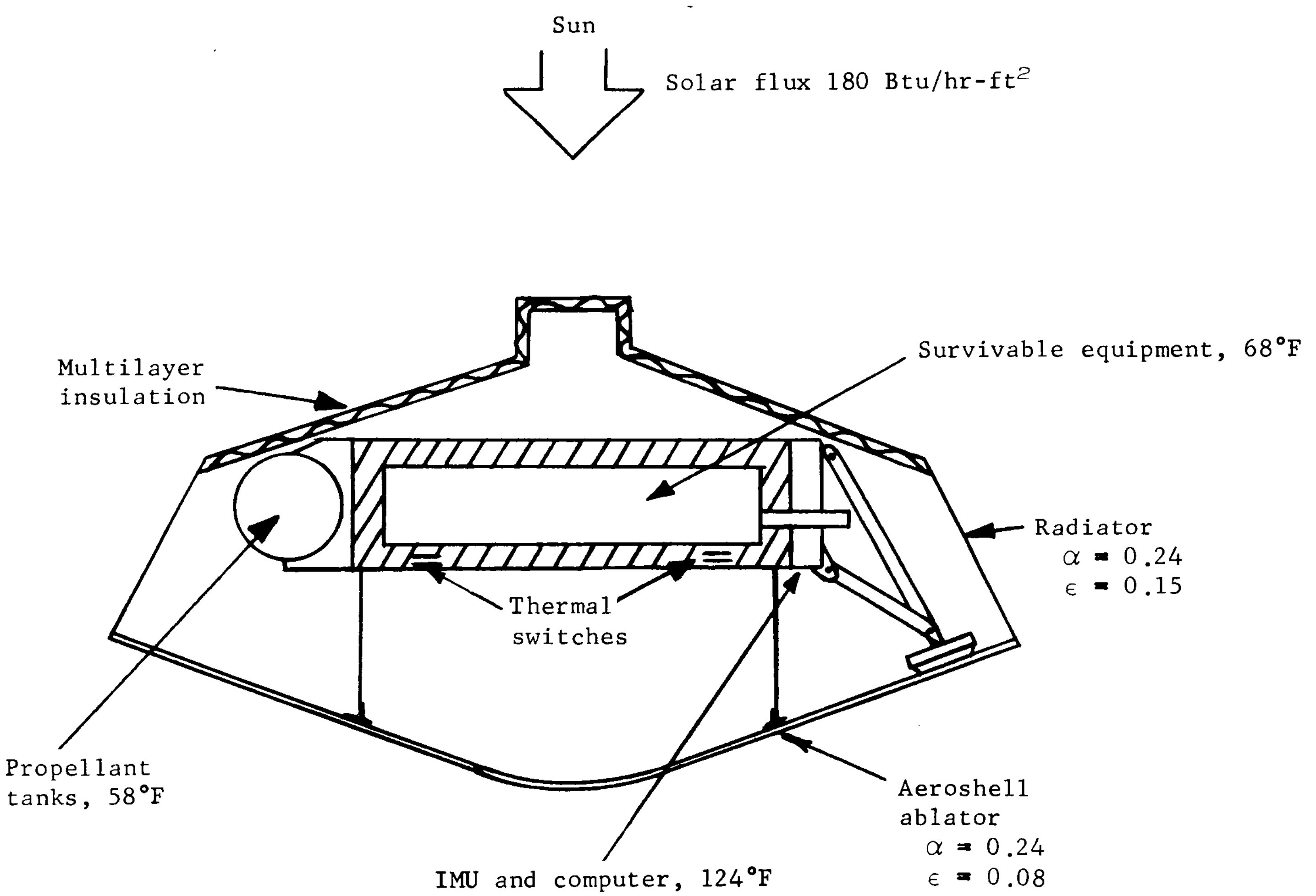
Sun
Solar flux 180 Btu/hr-ft^2
Multilayer insulation
Survivable equipment, 68°F
Radiator
$\alpha = 0.24$
$\epsilon = 0.15$
Thermal switches
Propellant tanks, 58°F
Aeroshell ablator
$\alpha = 0.24$
$\epsilon = 0.08$
IMU and computer, 124°F

Figure 72.- Capsule Postseparation Thermal Control System

Support module: The support module is spin stabilized with the high-gain antenna pointed toward Earth as shown in figure 73. As a result, the angle between the spin axis and the sun line is 40°. During the 17-hr postseparation phase, the transmitter is on for only the first and last hour.

Thermostatically controlled heaters are attached to each battery group to provide heat during the postseparation phase when the transmitter is shut down for 15 hr. No additional battery weight is required because an existing battery will be used that has enough extra capacity to provide the necessary energy for thermal control.

Additionally, a standoff is located between each battery group and the support tray to maintain the battery temperatures within acceptable limits during the period when the transmitter is shut down. Each of the standoffs has an equivalent thermal conductance of 2.5 Btu/hr °F.

Mars surface: The thermal control system used for the survivable equipment compartment while on the Mars surface is basically the same as that used for Configuration 1B in the initial Mars Mission Mode Study. This consists of a 3-in.- thick layer of insulation, radioisotope heaters of about 200 W total power and phase change material for peak power loads as shown in figure 74. Thermal control is obtained by moving the heaters, which are insulated on the ends, in and out of the insulated compartment as the internal temperature varies. The requirements for this configuration differ from those for 1B primarily in the difference in power duty cycle and in the addition of the thermal switches that produce additional heat leak penetrations.

Analysis.- Detailed thermal analyses were performed for steady-state conditions during cruise near Earth and near Mars and post-separation phases, and transient conditions during the midcourse maneuver. Martin Marietta's CDC computer program WD-201, "Thermal Analysis for Space Vehicles" was used to perform the analyses. Two separate analytical models were used: one representing the capsule and the other representing the support module. These models and the results of their respective analyses are described in the following paragraphs.

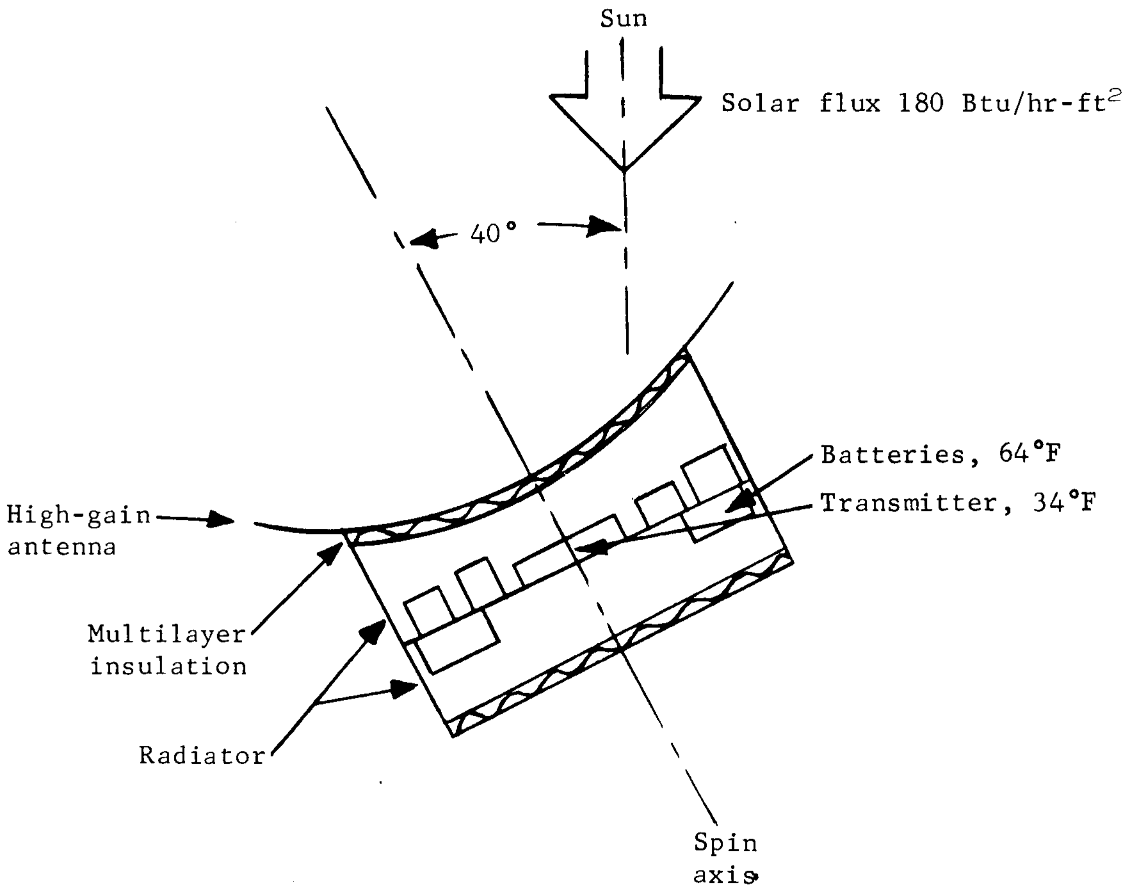
Sun
Solar flux 180 Btu/hr-ft^2
40°
Batteries, 64°F
Transmitter, 34°F
High-gain antenna
Multilayer insulation
Radiator
Spin axis

Figure 73.- Support Module Postseparation Thermal Control System

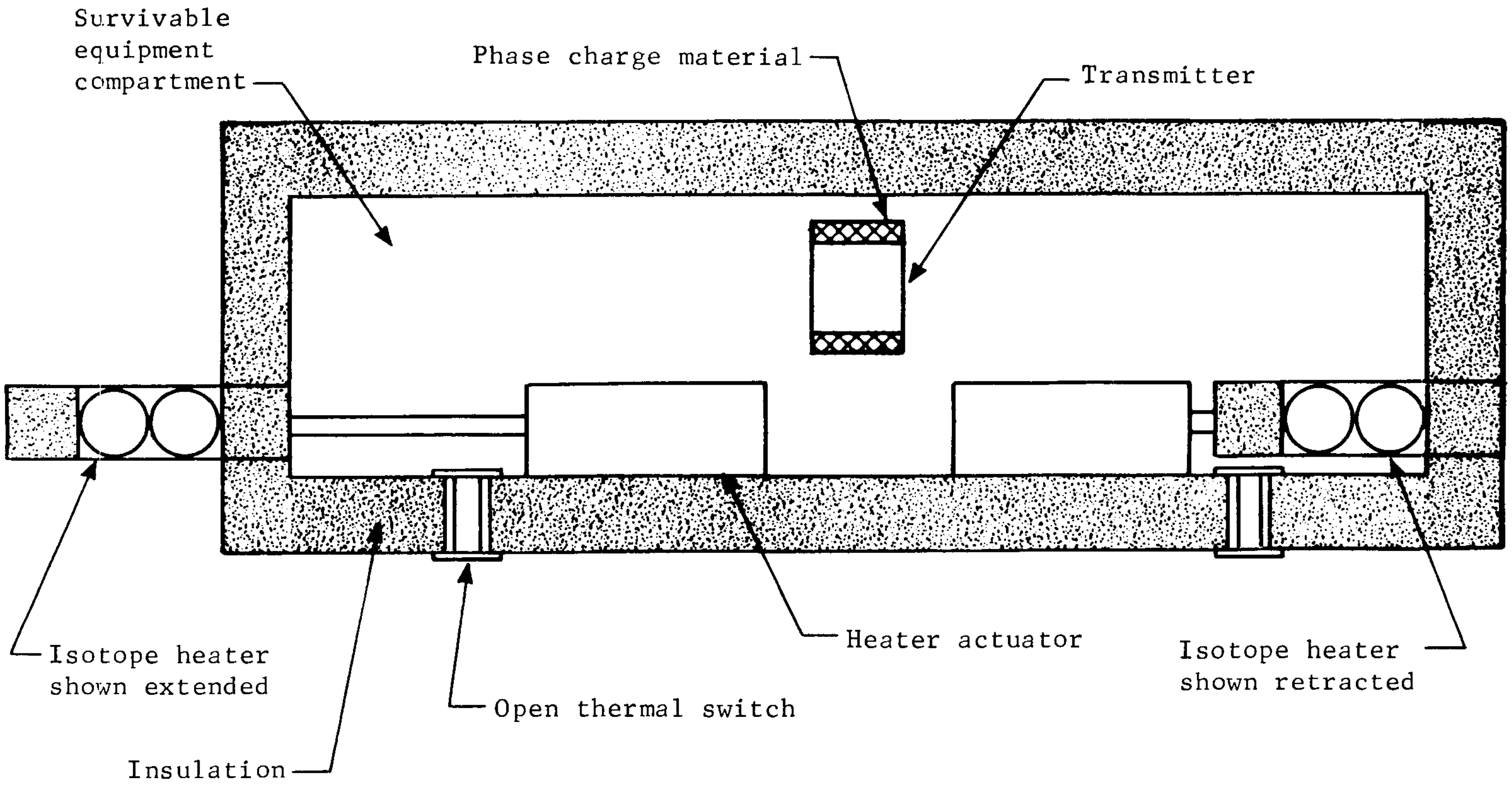
Survivable equipment compartment
Phase charge material
Transmitter
Isotope heater shown extended
Heater actuator
Isotope heater shown retracted
Open thermal switch
Insulation

Figure 74.- Mars Surface Thermal Control System

Capsule: A 60-node computer model of the capsule was developed. The nodal breakdown is shown in figure 75 and the nodes are described in table 55. As shown in the nodal diagram, symmetry about a plane through the center of the capsule was assumed. The same model was used to calculate steady-state temperatures during cruise at Earth and at Mars with only the incident solar flux changed. Some of the more important temperatures are shown in figure 75. Earth cruise temperatures are designated EC, and Mars cruise temperatures are designated MC. Between Earth and Mars the temperatures inside the capsule do not change significantly, as a result of the multilayer insulation, but the solar panel temperature changes significantly. The solar cell efficiency is reduced at Earth due to its relatively high temperature, but the solar array is sized by the conditions at Mars where the solar flux is much lower. Six layers of multilayer insulation are used in the propellant bays, and less than 5W of energy is added by thermostatically-controlled heaters to maintain the propellant temperatures at 50°F.

The program was used to calculate transient temperatures for 2 hr (maximum midcourse correction time) with the sun (Earth solar flux) in the worst position as shown in figure 75. This position for the sun was selected because it is normal to the radiator surface and on the side nearest the guidance computer and IMU, which are powered up during the transient. The response of some of the more critical components is shown in figure 76. All temperatures remain within acceptable limits.

The post separation capsule thermal control system described in figure 72 was also analyzed using the same computer model described above with the following changes:

1) The multilayer insulation was removed from the aeroshell side;
2) The sun was on the side opposite the aeroshell as shown in figure 75.
3) The equipment power duty cycle was changed.

Steady-state postseparation temperatures were calculated and are shown in figure 75 designated PS. All temperatures are within acceptable limits.

	Earth cruise (EC)	Mars cruise (MC)	Postseparation (PS)
Solar flux, Btu/hr-ft^2	442	180	180
Internal thermal energy, W			
Radioisotope heaters	200	200	200
Survivable equipment	28	28	0
Computer	25	25	100
IMU	0	0	30

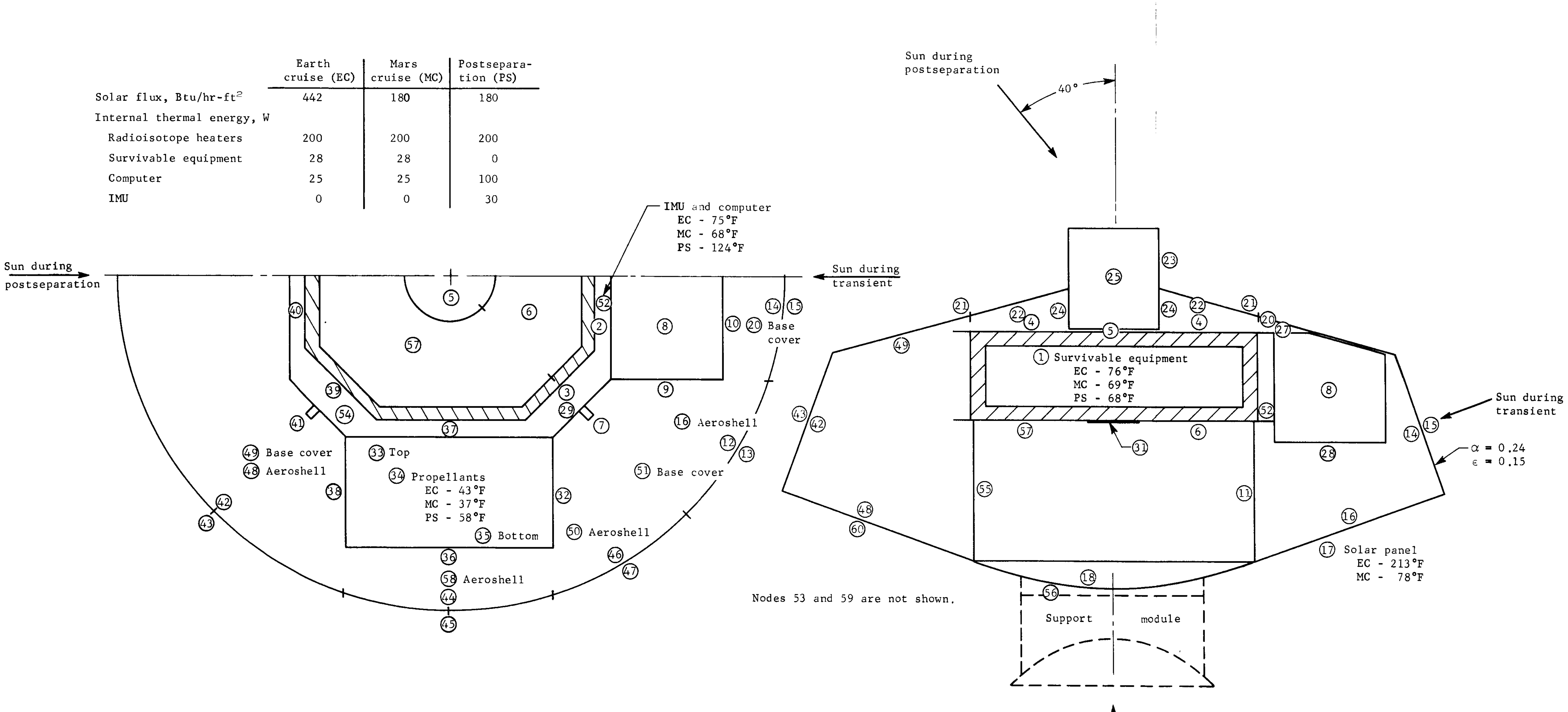

Sun during postseparation
IMU and computer
EC - 75°F
MC - 68°F
PS - 124°F
Sun during transient
⑤ ⑥ ㊵ ㊷ ② ⑧ ⑩ ⑳ Base cover
⑭ ⑮
57
㊴ ③ ㉙ ⑨
㊶ ㊹ ⑦
⑯ Aeroshell
⑫ ⑬
㊾ Base cover
㊽ Aeroshell
㉝ Top
㉞ Propellants
EC - 43°F
MC - 37°F
PS - 58°F
㉟ Bottom
㊳ ㉜ ㉛ Base cover
㊷ ㊸
㊿ Aeroshell
㊻ ㊼
㊱
58 Aeroshell
㊹ ㊺
Nodes 53 and 59 are not shown.
Sun during postseparation
40°
㉕ ㉓
㉑ ㉒ ④ ㉔ ⑤ ㉔ ㉒ ④ ㉑ ⑳ ㉗
㊾
① Survivable equipment
EC - 76°F
MC - 69°F
PS - 68°F
⑧
㊸ ㊷
57 ⑥ ㉛ ㊷
Sun during transient
⑭ ⑮
㉘
α = 0.24
ε = 0.15
55 ⑪
㊽ 60
⑯
⑰ Solar panel
EC - 213°F
MC - 78°F
⑱ 56
Support module
Sun during cruise

Figure 75.- Capsule Nodal Diagram

TABLE 55.- CAPSULE NODAL DESCRIPTION

No.	Node description
1	Survivable equipment compartment, interior
2	Survivable equipment compartment side, outside
3	Survivable equipment compartment side, outside
4	Survivable equipment compartment top, outside
5	Survivable equipment compartment top, outside
6	Survivable equipment compartment bottom, outside
7	Radioisotope heater
8	Antenna, interior
9	Antenna side, outside
10	Antenna side, outside
11	Structural ring
12	Conical side, inside
13	Conical side, outside
14	Conical side, inside
15	Conical side, outside
16	Aeroshell, inside
17	Solar panel[a]
18	Aeroshell, inside
19	Dummy
20	Aeroshell, inside
21	Aeroshell, outside
22	Aeroshell, inside
23	Parachute mortar side, outside
24	Parachute mortar side, outside
25	Parachute mortar, interior
26	Dummy
27	Antenna bay top, outside
28	Antenna bay bottom, outside
29	Bottom flange
30	Dummy
31	Survivable equipment compartment bottom, outside
32	Tankage bay side, outside
33	Tankage bay top, outside
34	Tankage bay, interior
35	Tankage bay bottom, outside
36	Tankage bay side, outside
37	Survivable equipment compartment side, outside
38	Tankage bay side, outside
39	Survivable equipment compartment side, outside
40	Survivable equipment compartment side, outside
41	Radioisotope heater
42	Conical side, inside
43	Conical side, outside
44	Conical side, inside
45	Conical side, outside
46	Conical side, inside
47	Conical side, outside
48	Aeroshell, inside
49	Aeroshell, inside
50	Aeroshell, inside
51	Aeroshell, inside
52	Bottom flange, IMU and computer
53	Structural ring
54	Bottom flange
55	Structural ring
56	Aeroshell, outside
57	Survivable equipment compartment bottom, outside
58	Aeroshell, inside
59	Solar panel[a]
60	Solar panel[a]

[a] These nodes represent the "Aeroshell, outside" following separation.

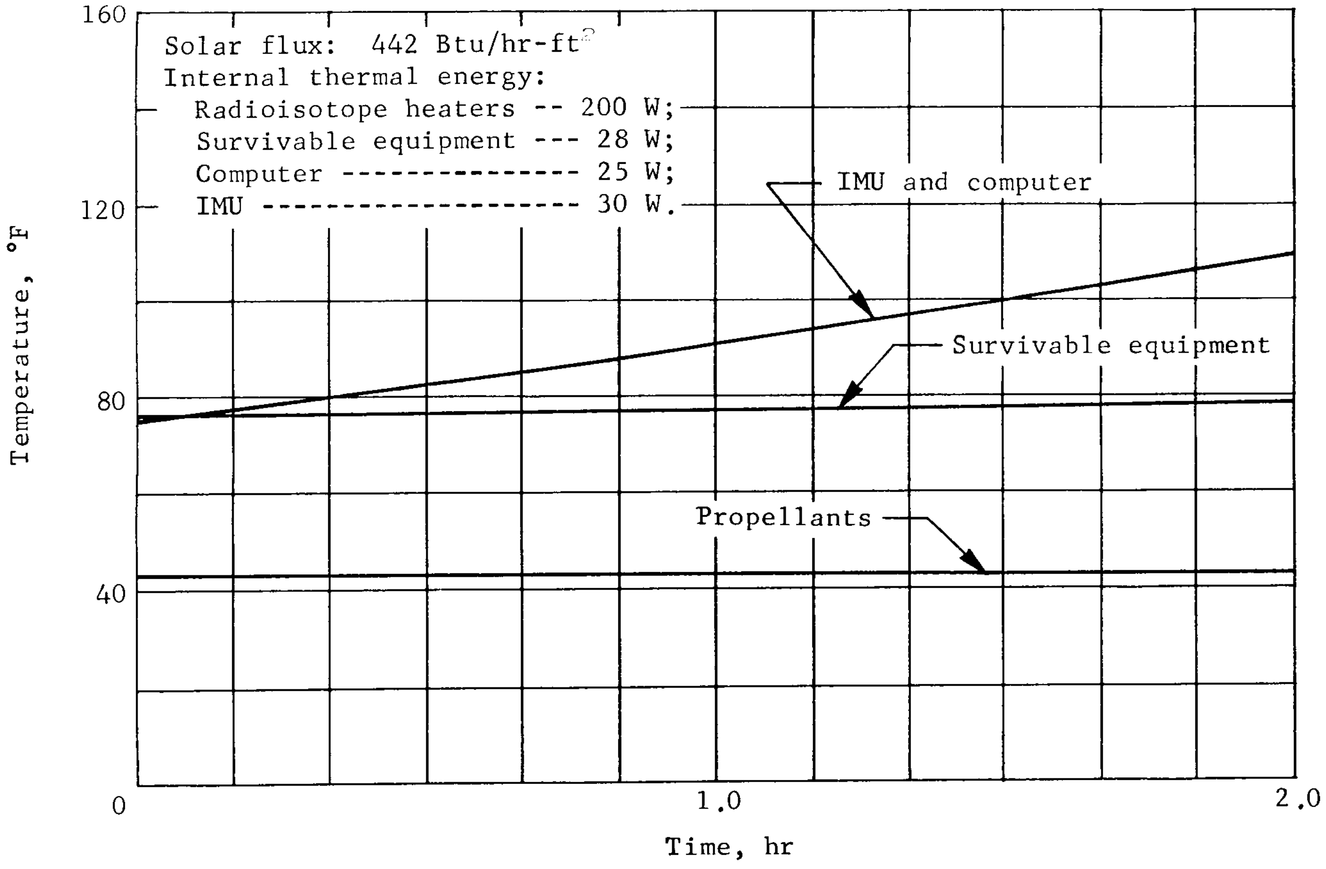

Figure 76.- Capsule Transient Temperatures

Support module: The analytical model for the support module shown in figure 77 consists of 50 nodes. The nodes are described in table 56. Fifteen of these nodes are attached to the support tray (fig. 77). Nodes 1 thru 10 represent the electronics; node 11 represents the transmitter, and nodes 46 thru 49 represent the batteries. The remaining 35 nodes represent the outer surfaces of the module.

Steady-state temperatures of the transmitter, electronics and the batteries are presented in figure 77 for Earth cruise (EC), Mars cruise (MC), and postseparation (PS). These temperatures are for a radiator with $\alpha = \varepsilon = 0.9$. During postseparation the support module is spin-stabilized with the sun angle as shown in figure 73. The temperatures are well within allowable limits.

Temperatures of these same components during midcourse maneuver are presented in figure 78. The maximum temperature changes range between 15 and 25°F. The temperature of the transmitter after 2 hr is approximately 140°F, which is near its maximum qualification limit. However, this temperature represents the very worst condition, with the solar flux at its maximum near-Earth value of 442 Btu/hr ft^2, with the sun normal to the radiator, and with a maneuver period of 2 hr. These conditions are not expected to be this severe.

Mars surface: The performance of the thermal control system on the landed capsule is very similar to that reported previously for other configurations. The differences are due to the different power duty cycle and the additional penetrations from the added thermal switches. The conductance of the open thermal switches is estimated to be 0.003 Btu/hr-ft-°R.

The heat required to maintain 40°F in the capsule is 594 Btu/hr or 174 W under the extreme cold conditions of no electrical power with -190°F external surface temperature and including this added penetration loss. To cover the possibility of higher science penetration losses and variations in heater output with time, 200 W total heater output was used for the other analyses. The corresponding maximum temperatures occurring with a 90°F landing temperature, the extreme hot day and normal power duty cycle are shown in figure 79 to be within acceptable limits.

TABLE 56.- SUPPORT MODULE NODAL DESCRIPTION

No.	Node description	No.	Node description
①	Shunt, capacitor assembly and squib fire circuitry	㉖	Radiator, upper sector
②	Exciter	㉗	
③	Gyro capacitor assembly and power transfer switch	㉘	
④	Battery charger	㉙	Radiator, lower sector
⑤	UHF receiver	㉚	
⑥	Diplexer	㉛	
⑦	UHF receiver	㉜	
⑧	Diplexer	㉝	
⑨	Load control	㉞	
⑩	RF switch	㉟	
⑪	TWTA transmitter	㊱	Upper flange
⑫	Radiator, middle sector	㊲	Lower flange
⑬		㊳	Antenna bottom side, outside module
⑭		㊴	Antenna ring, outside insulation
⑮		㊵	Adapter ring
⑯		㊶	Solar panel, under atnenna
⑰		㊷	Solar panel, outside antenna
⑱		㊸	Top, inside insulation
⑲		㊹	Side, inside insulation below support tray
⑳		㊺	Bottom, inside insulation
㉑		㊻	Batteries
㉒		㊼	
㉓	Radiator, upper sector	㊽	
㉔		㊾	
㉕		㊿	Antenna top side

	Earth cruise (EC)	Mars cruise (MC)	Postseparation (PS)
Solar flux, Btu/hr-ft^2	442	180	180
Internal thermal energy, W			
Transmitter	60	60	0
Batteries	4	4	4
Battery heaters	0	0	56

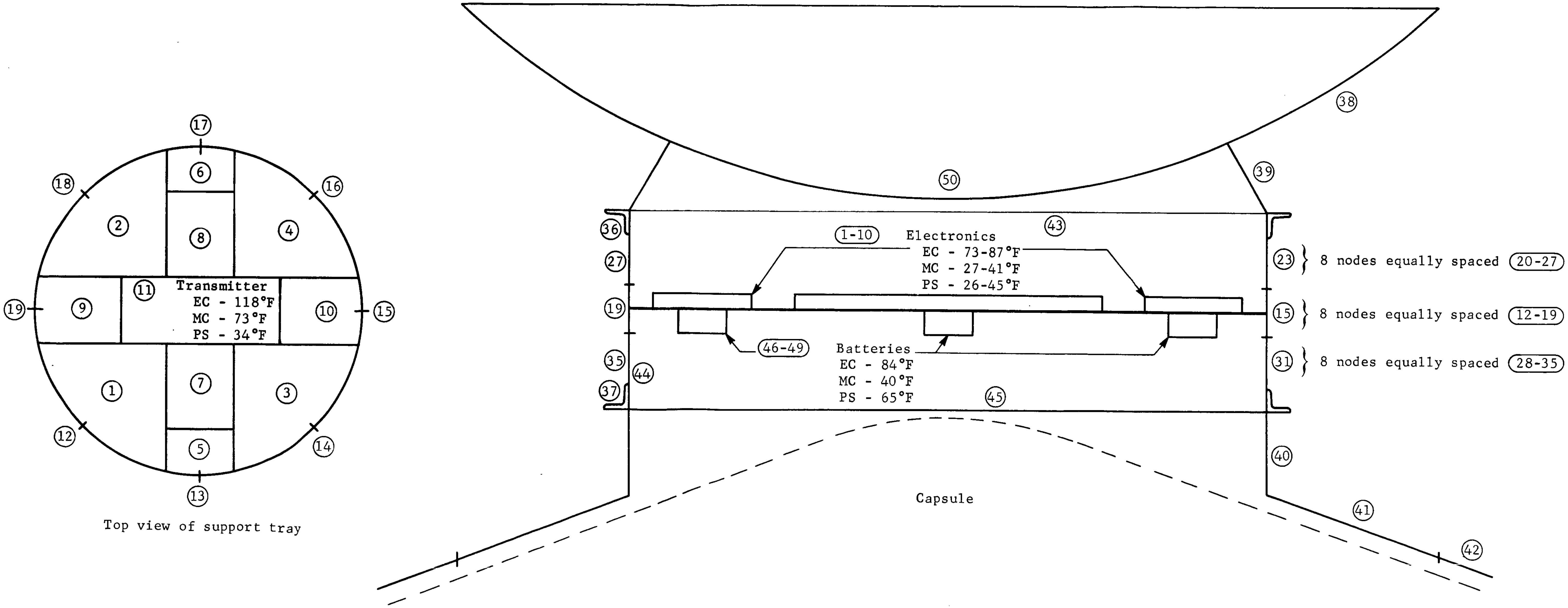
Top view of support tray

(1) (2) (3) (4) (5) (6) (7) (8) (9) (10) (11)
(12) (13) (14) (15) (16) (17) (18) (19)
Transmitter
EC - 118°F
MC - 73°F
PS - 34°F
(1-10) Electronics
EC - 73-87°F
MC - 27-41°F
PS - 26-45°F
(46-49)
Batteries
EC - 84°F
MC - 40°F
PS - 65°F
(23) 8 nodes equally spaced (20-27)
(15) 8 nodes equally spaced (12-19)
(31) 8 nodes equally spaced (28-35)
(27) (19) (35) (36) (37) (38) (39) (40) (41) (42) (43) (44) (45) (50)
Capsule

Figure 77.- Support Module Nodal Diagram

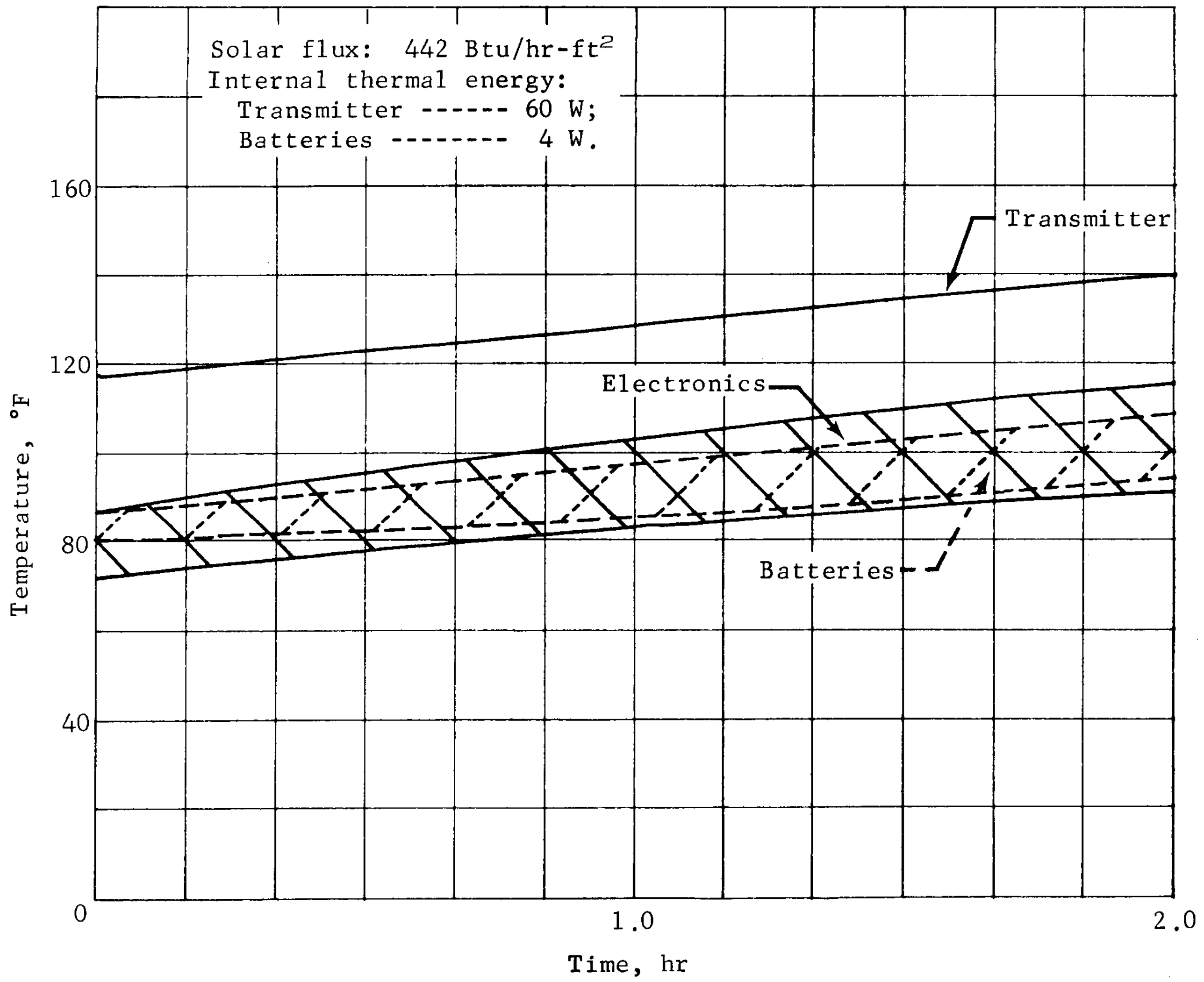

Figure 78.- Support Module Transient Temperatures

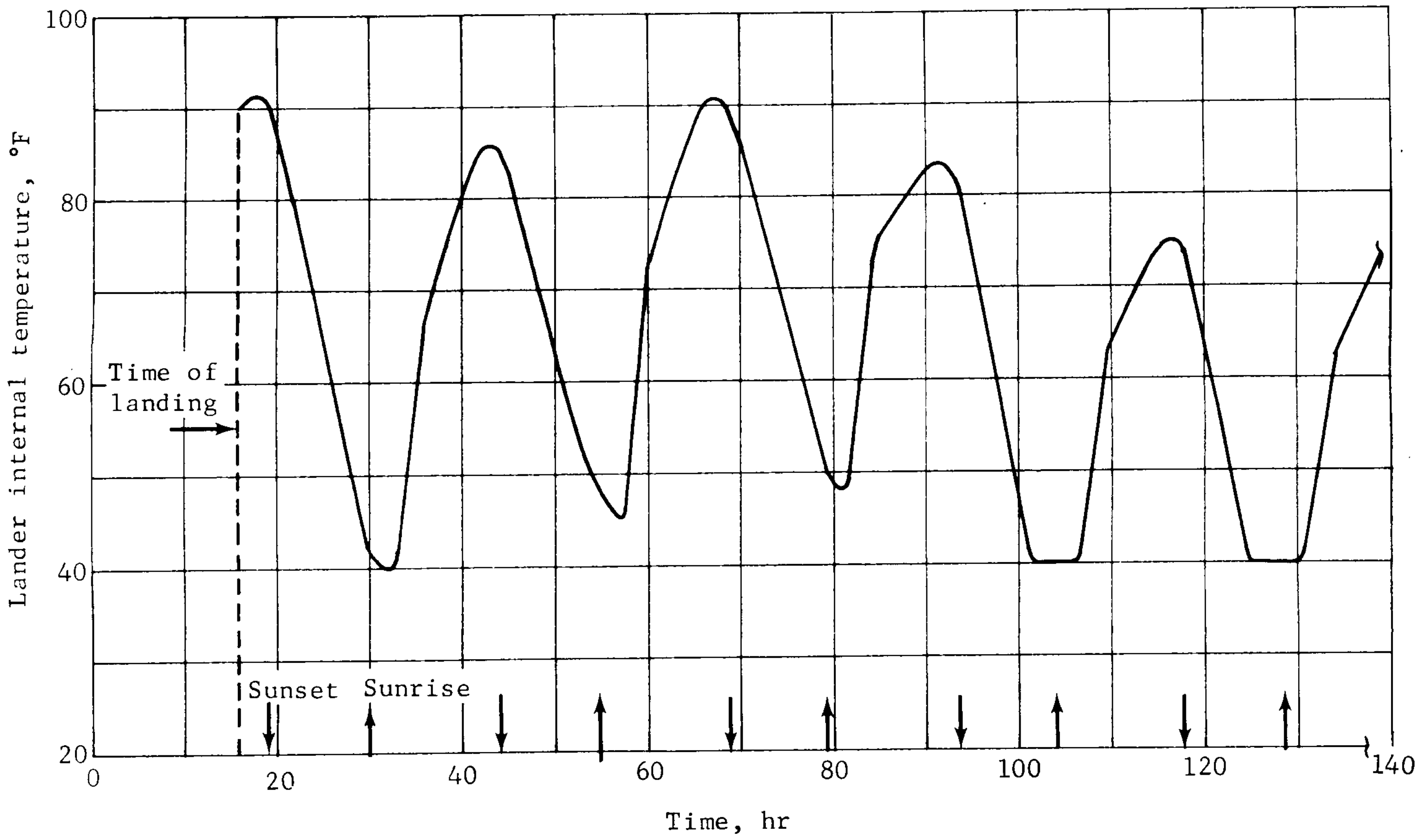

Figure 79.- Lander Temperature, Hot Environment

When the heaters are retracted into the capsule, the equipment closest to the heaters reach higher temperatures than the equipment farther away. For a typical structure with the equipment grounded to the structure and having black radiating surfaces, the equipment adjacent to the heaters could reach 110 to 120°F when the average internal temperature is only 50°F. Suitable surface coatings or radiation shields and insulated mounts can reduce this temperature gradient to less than 10°F.

Components.- A summary of all of the components used in the thermal control system including their development status is presented in table 57. None of these items require long lead program funding. However, it must be emphasized that completion of the R&D effort on Mars surface insulation to be conducted by JPL, and the effort on radioisotope heaters being conducted by NASA Houston, are required for the Mars lander thermal control system.

Multilayer insulation: JPL has recently completed an extensive development program on insulation for sterilizable spacecraft (ref. 25). This work included sterilization, vibration, rapid depressurization, and full-scale thermal tests. The insulation system developed consists of 1/4-mil deep-crinkled Mylar, gold plated on one side without separators. A single step joint is used. Plastic posts attached to the vehicle with Velcro are used to attach the insulation. Little development effort would be required to apply this insulation to the present configuration.

Thermal switch: A thermal switch concept proposed to conduct heat out of the heavily insulated survivable equipment compartment during the cruise phase of the mission is shown in figure 80. It consists of an aluminum stud attached to the lander by a conventional ordnance-operated separation nut. The nut is fired at or shortly after landing, forcing the stud out. A plastic (typically phenolic-filled fiberglas) sleeve is used to minimize the penetration loss. Four switches with 1 1/4-in. studs are capable of conducting the 28 W of internal heat to the external surface with a temperature difference of 10°F. It may be possible to use one of the separation nuts specified for the structure and avoid the need to develop an additional separation nut.

TABLE 57.- THERMAL CONTROL SYSTEM COMPONENT SUMMARY

Component	Development status
Multilayer insulation - Crinkled gold-plated Mylar.	JPL development program complete. Included sterilization, vibration, and full-scale thermal testing.
Mars surface insulation candidate - Lightweight fiberglas with gold-plated Kapton shields.	JPL development program has been started to provide the required design data before Phase C.
Thermal switch - Aluminum stud ejected after landing by an ordnance operated separation nut.	Ordnance-operated separation nuts commonly used in space vehicles. May be possible to use one of the nuts used in the structure and avoid an additional development.
Radioisotope heater - Fuel enclosed in an ablative covered structure.	NASA Houston Phase I (study) to be complete by May 1969. Qualified units scheduled for July 1970. This program must be directed to meet the requirements for a Mars lander.
Isotope heater control - Thermostatically controlled linear actuator to move heaters in and out of lander.	Candidates are thermostatically controlled electrical actuators and a phase change material contained in a bellows. Similar type devices have been used extensively.
Mars surface coatings compatible with dust accumulation and erosion, candidate - flame sprayed coatings.	LRC research program presently in progress.
Thermal control coatings - black, aluminum, white, combinations.	Thermal control coatings commonly used on spacecraft. Preliminary JPL sterilization work indicates no problem with sterilization compatibility.

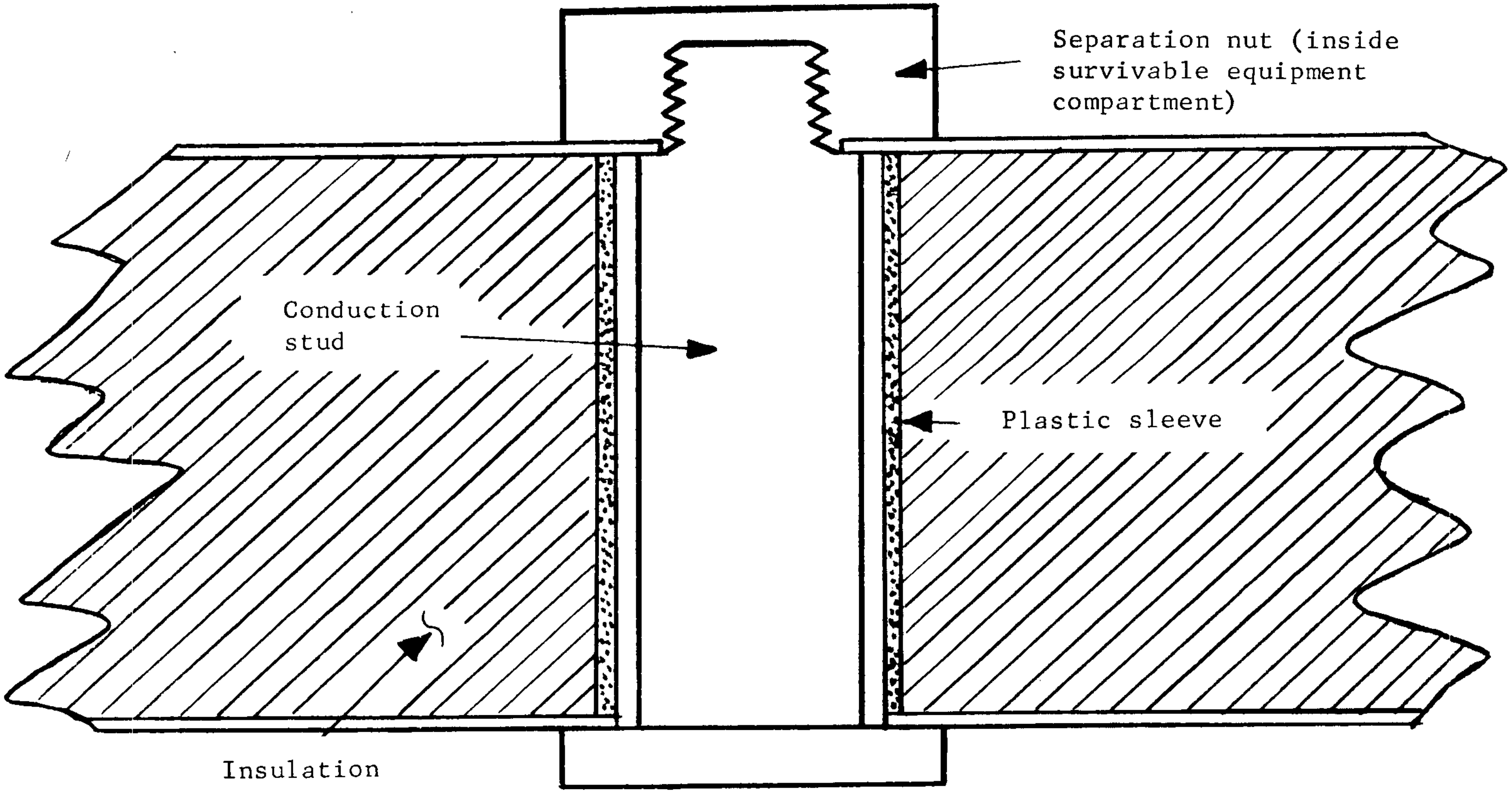
Separation nut (inside survivable equipment compartment)
Conduction stud
Plastic sleeve
Insulation

Figure 80.- Thermal Switch

Mars surface insulation: The performance of sterilizable insulation systems in the wide range of possible Mars surface environments can only be estimated at this time. Therefore, it is very important to the program that the JPL insulation program be completed as soon as possible. The analysis and design presented in this report are based on the use of the insulation described and analyzed in detail in the initial Mars Mission Mode Study. It consists of lightweight fiberglas with gold-plated Kapton shields at 1-in. spacing.

Radioisotope heater: Meeting the safety requirements for intact impact in the event of a booster failure is the primary heater development problem. We strongly recommend that LRC take the necessary action to ensure that the technical and schedule requirements for a Mars lander are included in the NASA Houston contract in progress. A preliminary nuclear radiation analysis has been completed that shows no significant interference problems with science or other electronic equipment (see science subsystem).

Isotope heater control: Temperature control of the lander is achieved by moving the four 50-W isotope heater assemblies in and out with a thermostatically controlled linear actuator as described in the initial Mission Mode study report. Possible approaches include electrical actuators and phase change materials contained in a bellows. Similar type devices are commonly used on spacecraft, such as the STEM (Storable Tubular Extendible Member) devices used on Mercury and Gemini and the louver actuators used on Nimbus. A tradeoff study must be conducted before a final choice is made.

Mars surface thermal control coating compatible with dust accumulation and erosion: The lander thermal control surface must have reasonably predictable optical properties in a clean condition, dust covered, new, or eroded. One of the more promising approaches is the use of flame-sprayed coatings. This approach is being evaluated in a development program at LRC.

Thermal control coatings: Preliminary sterilization testing of the commonly used coatings was conducted by JPL. No problems were found although qualification testing remains to be done. A coating with an $\alpha = 0.24$, $\epsilon = 0.15$ is used in the design, which is not attainable with a single coating. One approach to the problem is to use an aluminum paint ($\alpha = \epsilon = 0.24$) covered with a perforated gold-plated Mylar sheet. The size and spacing of the perforations would be adjusted to achieve the required properties.

Alternatives Considered

One of the basic system alternatives studied is the sterilized support module described in the Structures and Mechanisms section. From a thermal control standpoint the primary differences between this configuration and the unsterilized support module are as follows:

1) The support module is moved to the side opposite the aeroshell and is sun-oriented during cruise. As a result, the capsule sun orientation is the same during cruise and after separation;
2) The support module is separated 48 hr before entry.

The thermal designs for the capsule and support module are shown in figure 81. The capsule thermal design is the same as for the unsterilized support module case except that the side (conical) surfaces are insulated and the aeroshell is not. The emissivity of the aeroshell is selected to achieve a thermal balance when radiating the entire external energy including the 200 W from the isotope heaters. It is necessary to add louvers to the support module, because there is not enough energy in the batteries to maintain temperatures during the 48-hr postseparation phase of the mission.

Conclusions

The following conclusions regarding the thermal control system were reached:

1) Thermal control of both the unsterilized and sterilized support module system designs can be achieved by relatively simple passive means;
2) The sterilized support module requires louvers;
3) No long lead items are required for the thermal control system design if the following action is taken,
    a) The Mars surface insulation R&D work planned by JPL is done,
    b) The radioisotope heater development program in progress by NASA Houston continues and meets the technical requirements for the Mars lander mission.

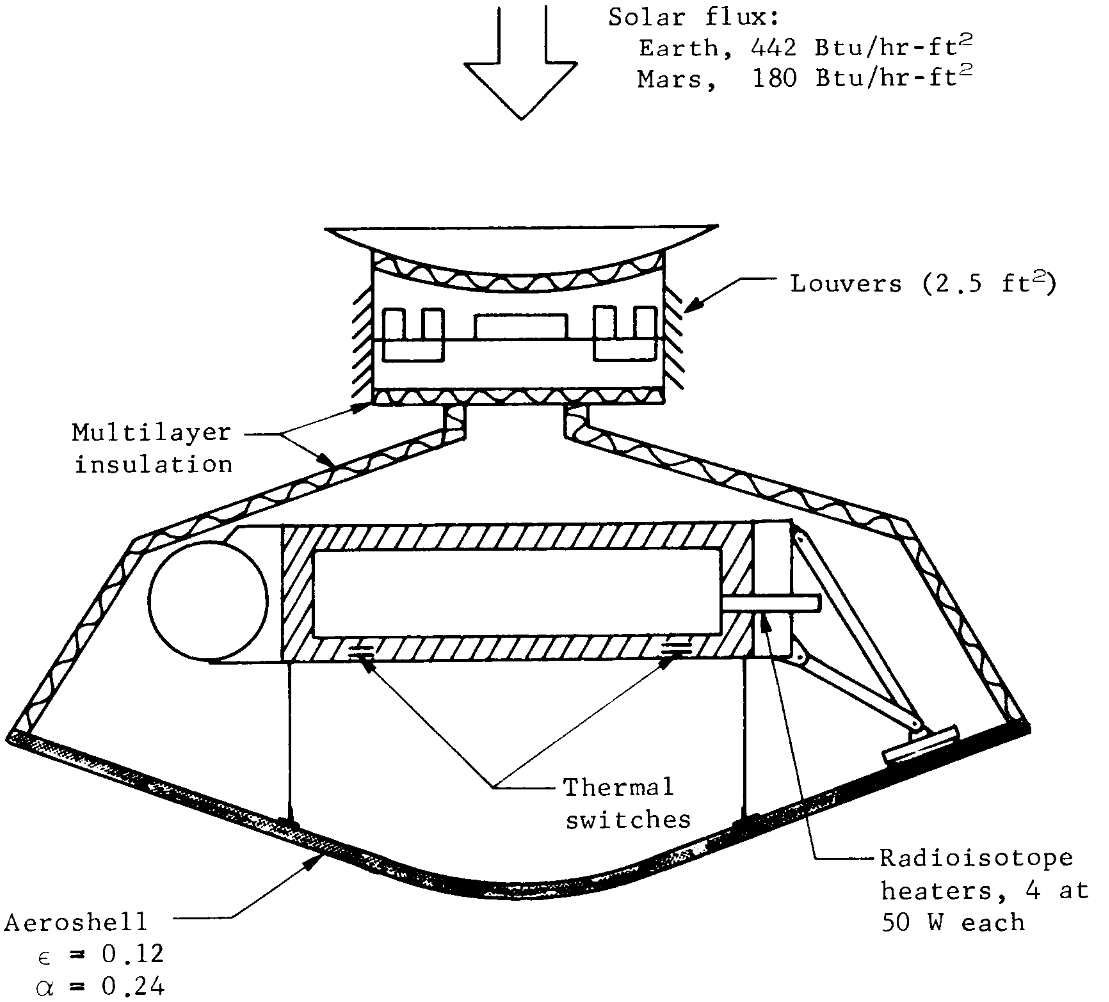
Solar flux:
Earth, 442 Btu/hr-ft^2
Mars, 180 Btu/hr-ft^2
Louvers (2.5 ft^2)
Multilayer insulation
Thermal switches
Radioisotope heaters, 4 at 50 W each
Aeroshell
$\epsilon = 0.12$
$\alpha = 0.24$

Figure 81.- Sterilized Support Module Thermal Control

REFERENCES

1. Anon.: Titan Mars '73 Mission Definition. M73-101-2, NASA Langley Research Center.

2. Anon.: Planetary Exploration 1968-75, Report of a Study of the Space Science Board. National Academy of Sciences, Washington, D. C., July 1968.

3. Leighton, R. B.; Murray, B. C. et al.: Mariner Mars 1964 Project Report: Television Experiment, Part I. Investigators' Report NASA JPL TR32-884, December 1967.

4. Scott, R. F. and Roberson, F. I.: Soil Mechanics Surface Sampler: Lunar Surface Tests, Results and Analysis. (Chapter IV of Surveyor III Mission Report, Part II. Scientific Results), NASA JPL TR32-1177, June 1967.

5. MacNaughton, J. D.: Unfurlable Metal Structures for Spacecraft. Canadian Aeron. and Space J., No. 4, April 1963, pp 103-116.

6. Anon.: Drum Rolled Space Tubes. Experimental Mech., October 1966, p 64.

7. Lachenbruch, A. H.: A Probe for Measurement of Thermal Conductivity of Frozen Soils in Place. Trans. A. G. U., 38, 1957, pp 691-697.

8. Kersten, M. S.: Laboratory Research for the Determination of the Thermal Properties of Soils. Final Report to Corps of Engineers, U. S. Army, St. Paul District, 1949.

9. Carslaw, H. S. and Jaeger, J. C.: Conduction of Heat in Solids. 2nd Edition, Clarendon Press, Oxford, 1959.

10. Russell, E. J. and Appleyard, A.: The Classic Reference on Soil Atmospheres. 1915.

11. Anon.: The Atmosphere of the Soil, Its Composition, and the Causes of Variations. J. of Agricultural Sciences. 7:1-48.

12. Boynton, D. and Reuther, W.: A Way of Sampling Soil Gases in Dense Subsoil and Some of Its Advantages and Limitations. Soil Sciences Society of America Proceedings, 3:37-42, 1938.

13. Lemon, E. R. and Erickson, A. E.: The Measurement of Oxygen Diffusion in the Soil with a Platinum Microelectrode. Soil Sciences Proceedings, vol. 16, no. 2, April 1952, pp 160-163.

14. Levin, G. V. and Horowitz, N. H.: Fifth Annual Progress Report; Radioisotopic Biochemical Probe for Extraterrestrial Life. NASA Contract No. NASr-10, 1966.

15. Vishniac, W.: The Wolf Trap, Life Sciences and Space Research II. (M Florkin, ed.), North Holland Publishing Co., Amsterdam, 1964.

16. Anon.: Unmanned Exploration of the Solar System, vol. 19, Advances in the Astronautical Sciences. (Morgenthaler, G. W. and R. G. Morra, eds.), Parts 5 and 6, 1965.

17. Levinthal, E.: Multivator-A Biochemical Laboratory for Martian Experiments. Life Sciences and Space Research II, (M. Florkin, ed.), North Holland Publishing Co., Amsterdam, 1964.

18. Lederberg, J. and Levinthal, E.: Cytochemical Studies of Planetary Microorganisms. Report to NASA, October 1966.

19. Levin, G. V. and Perez, G. R.: Life Detection by Means of Metabolic Experiments, in The Search for Extraterrestrial Life. vol. 22, Advances in the Astronautical Sciences Series, 1967.

20. Levin, G. V. et al.: Gulliver, An Instrument for Extraterrestrial Life Detection, in Life Sciences and Space Research II. (M. Florkin, ed.), North Holland Publishing Co., Amsterdam, 1964.

21. Stoddard, D. H. and Albenesius, E. L.: Radiation Properties of ^{238}Pu Produced for Isotopic Power Generators. duPont Savannah River Laboratory, N65-20895, July 1965.

22. Anon.: Trade Study for Inertial Sensor Mechanization, DRL-3f. Autonetics C7-1481.3/060, Sept. 1967.

23. Anon.: Guidance Sensor Technology Survey. TM 8400-68-1, Martin Marietta Corporation, January 1968.

24. Anon.: Engineering Model Parameters for Mission and Design Studies 1968. Langley Research Center, May 1968.

25. Anon.: Planetary Vehicle Thermal Insulation Systems. General Electric Co., (JPL Contract 951537), 3 June 1968.

NASA CR-66728-1, 2 and 3

National Aeronautics and Space Administration
FINAL SUMMARY REPORT, STUDY OF A SOFT LANDER/
SUPPORT MODULE FOR MARS MISSIONS, Raymond S.
Wiltshire, Hugh E. Craig, et al.

(NASA CONTRACTOR REPORT NASA CR-66728-1, 2 & 3)

This is the final summary report of the work accomplished by Martin Marietta Corporation for the Langley Research Center under Modification 3 to Contract NAS1-7976, Study of Direct Versus Orbital Entry for Mars Missions. The objective of this study was to determine the conceptual design of an altitude stabilized soft lander capsule and to obtain solutions in the areas of communication, data handling, cost, reliability (in general sense), weight, program implementation of long lead items, and affective use of existing equipment.

I. Wiltshire, Raymond S.; Craig, Hugh E.; et al.

II. NASA CR-66728-1, 2 & 3

NASA

NASA CR-66728-1, 2 and 3

National Aeronautics and Space Administration
FINAL SUMMARY REPORT, STUDY OF A SOFT LANDER/
SUPPORT MODULE FOR MARS MISSIONS, Raymond S.
Wiltshire, Hugh E. Craig, et al.

(NASA CONTRACTOR REPORT NASA CR-66728-1, 2 & 3)

This is the final summary report of the work accomplished by Martin Marietta Corporation for the Langley Research Center under Modification 3 to Contract NAS1-7976, Study of Direct Versus Orbital Entry for Mars Missions. The objective of this study was to determine the conceptual design of an altitude stabilized soft lander capsule and to obtain solutions in the areas of communication, data handling, cost, reliability (in general sense), weight, program implementation of long lead items, and affective use of existing equipment.

I. Wiltshire, Raymond S.; Craig, Hugh E.; et al.

II. NASA CR-66728-1, 2 & 3

NASA

NASA

This report is presented in the following three volumes;

NASA CR-66728-1 - Volume I - Summary
NASA CR-66728-2 - Volume II - Subsystem Studies
NASA CR-66728-3 - Volume III - Appendixes

NASA

This report is presented in the following three volumes;

NASA CR-66728-1 - Volume I - Summary
NASA CR-66728-2 - Volume II - Subsystem Studies
NASA CR-66728-3 - Volume III - Appendixes